Inhibition of monoamine oxidase by selected 8-[(phenylsulfanyl)methyl]caffeine derivatives

Thokozile Okaecwe

B.Pharm

Dissertation submitted in partial fulfillment of the requirements for the degree Magister Scientiae in Pharmaceutical Chemistry at the North-West University, Potchefstroom Campus

Supervisor: **Prof. J.P. Petzer**

Co-supervisor: **Prof. J.J. Bergh**

Potchefstroom

2012

TABLE OF CONTENTS

ABSTRACT

Title

Inhibition of monoamine oxidase by selected 8-[(phenylsulfanyl)methyl]caffeine derivatives.

Keywords

Parkinson's disease, monoamine oxidase, substantia nigra, caffeine, (E)-8-(3-chlorostyryl)caffeine, 8-(phenoxymethyl)caffeine, 8-[(phenylsulfanyl)methyl]caffeine, 8-[(phenylsulfanyl)ethyl]caffeine.

Purpose

Monoamine oxidase (MAO) consists of two isoforms, namely MAO-A and MAO-B. Both these isoforms are involved in the oxidation of dopamine. In Parkinson's disease (PD) therapy, the inhibition of the oxidation of dopamine by MAO may elevate the levels of dopamine in the brain and prevent the generation of toxic by-products such as hydrogen peroxide. MAO-B inhibitors have found application as monotherapy in PD and it has been shown that MAO-B inhibitors may also be useful as adjuvants to L-dopa in PD therapy. For example, an earlier study has shown that the combination of L-dopa with (R)-deprenyl (a selective MAO-B inhibitor), may lead to a reduction of the dose of L-dopa required for alleviating the motor symptoms in PD patients. However, older MAO inhibitors may possess adverse side effects such as psychotoxicity, liver toxicity and cardiovascular effects. The irreversible mode of inhibition of the older MAO-B inhibitors, such as (R)-deprenyl, may also be considered as less desirable. After the use of irreversible inhibitors, it may require several weeks for the MAO enzyme to recover activity. In contrast, after administration of a reversible inhibitor, enzyme activity is recovered as soon as the inhibitor is cleared form the tissues. The adverse effects and disadvantages of the older MAO-B inhibitors prompted us to undertake the discovery of safer and reversible inhibitors of MAO-B. Such compounds may find application in the treatment of PD.

Rationale

It was recently discovered that (E)-8-(3-chlorostyryl)caffeine (CSC) is a potent inhibitor of MAO-B, with an IC_{50} value of 0.128 μM. CSC has a caffeine moiety, which is thought to be

essential for MAO-B inhibition. It was also reported that a related series of 8-(phenoxymethyl)caffeine derivatives are potent and reversible inhibitors of MAO-A and –B. The IC_{50} values of the 8-(phenoxymethyl)caffeines ranged from 0.148–5.78 μM for the inhibition of MAO-B. For the purpose of this study the phenoxymethyl side-chain was replaced with a phenylsulfanyl moiety at C8. The aim of this study was therefore to synthesize a series of 8-[(phenylsulfanyl)methyl]caffeine analogues and to compare their MAO-B inhibition potencies to the previously synthesised 8-(phenoxymethyl)caffeine derivatives. A series of five 8-[(phenylsulfanyl)ethyl]caffeine analogues was also synthesized in order to determine the effect of carbon chain elongation on the potency of MAO inhibition.

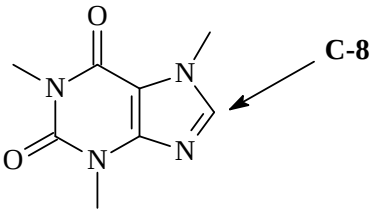

Caffeine

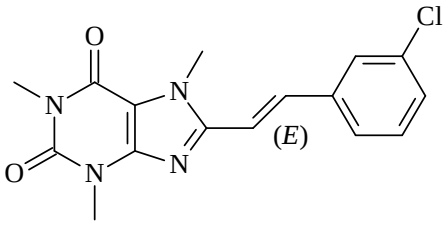

CSC

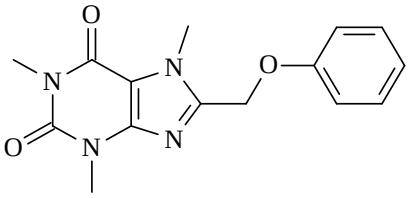

8-(Phenoxymethyl)caffeine

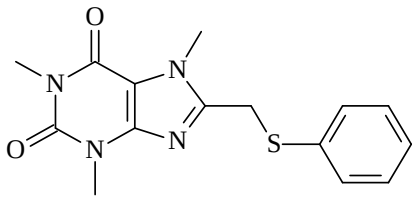

8-[(Phenylsulfanyl)methyl]caffeine

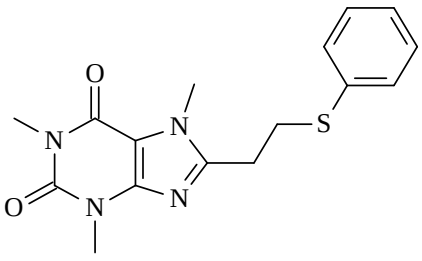

8-[(Phenylsulfanyl)ethyl]caffeine

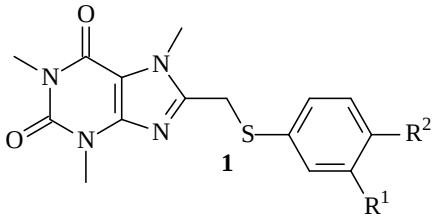

1

Compound	R^1	R^2
1a	H	H
1b	Cl	H
1c	Br	H
1d	F	H
1e	CH_3	H
1f	OCH_3	H
1g	OCH_2CH_3	H
1h	H	Cl
1i	H	Br

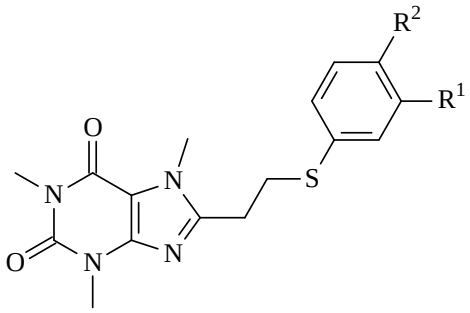

Compound	R^1	R^2
2a	H	H
2b	Cl	H
2c	Br	H
2d	H	Cl
2e	H	Br

Methods

The C8 substituted caffeine analogues were synthesised by reacting 1,3-dimethyl-5,6-diaminouracil with an appropriately substituted 2-(phenylsulfanyl)acetic acid or 3-(phenylsulfanyl)propanoic acid in the presence of a carbodiimide activating reagent, N-(3-dimethylaminopropyl)-N'-ethylcarbodiimide hydrochloride (EDAC). Ring closure of the intermediary amide was effected by reaction with sodium hydroxide. The resulting

theophylline analogues were subsequently methylated in the presence of iodomethane to yield the target compounds. The structures of the C8 substituted caffeine analogues were verified by NMR and MS analysis. The purities thereof were subsequently estimated by HPLC analysis.

The 8-[(phenylsulfanyl)methyl]caffeine and 8-[(phenylsulfanyl)ethyl]caffeine analogues were evaluated as MAO-A and –B inhibitors. The recombinant human enzymes were used as enzyme sources. The inhibitory potencies of the caffeine derivatives were expressed as IC_{50} values (the concentration of a drug that is required for 50% inhibition *in vitro*). The time-dependency of inhibition of MAO-B by the most potent inhibitor was also evaluated in order to determine the reversibility of inhibition of the test compound. A study was also conducted to determine the inhibition mode of the most potent test compound, by constructing a set of Lineweaver Burk plots.

Results

The results showed that the 8-[(phenylsulfanyl)methyl]caffeine analogues were inhibitors of MAO-A and –B. The most potent inhibitor in the first series (**1a**–**i**) of this study were 8-[(3-bromophenylsulfanyl)methyl]caffeine and 8-[(4-bromophenylsulfanyl)methyl]caffeine with IC_{50} values of 4.90 and 4.05 μM, respectively. When these results were compared to those of the previously studied 8-(phenoxymethyl)caffeine derivatives it was found that, for these compounds, the bromine substituted homologues were also the most potent MAO-B inhibitors. The bromine substituted 8-(phenoxymethyl)caffeine derivatives exhibited IC_{50} values of 0.148 and 0.189 μM for those homologues containing bromine on the *meta* and *para* positions of the phenoxy side chain, respectively. In general, the 8-[(phenylsulfanyl)methyl]caffeine derivatives were found to be less potent MAO-B inhibitors than the 8-(phenoxymethyl)caffeine derivatives. The 8-[(phenylsulfanyl)methyl]caffeine derivatives also did not show as high a degree of selectivity for MAO-B (compared to MAO-A) as did the 8-(phenoxymethyl)caffeines. Similar to the 8-(phenoxymethyl)caffeines, the 8-[(phenylsulfanyl)methyl]caffeines also proved to be weak MAO-A inhibitors. The most potent inhibitor of MAO-A among the test compounds exhibited an IC_{50} value of 19.4 μM. The most potent MAO-A inhibitor among the previously studied 8-(phenoxymethyl)caffeines was more potent with an IC_{50} value of 4.59 μM. From these results it may be concluded that the phenoxy side chain is more suited for the design of caffeine derived MAO inhibitors than the phenylsulfanyl side chain.

The results for the second series investigated in this study, the 8-[(phenylsulfanyl)ethyl]caffeines (**2a**–**e**), revealed the chlorine substituted derivatives to be the most potent MAO-B inhibitors. The *meta* and *para* chlorine substituted derivatives exhibited IC_{50} values of 5.67 and 7.79 µM, respectively, for the inhibition of MAO-B. Interestingly, the *meta* substituted derivative exhibited no inhibition toward the MAO-A isoenzyme. However, the 8-[(phenylsulfanyl)ethyl]caffeine derivatives were found to be very weak inhibitors of both MAO-A and –B and may be considered as less potent than the 8-[(phenylsulfanyl)methyl]caffeine derivatives.

Since one of the aims of this study was to synthesise reversible MAO inhibitors, a time-dependency study was carried out with the best inhibitor (**1i**). The aim of this study was to determine the reversibility of inhibition by the 8-[(phenylsulfanyl)methyl]caffeine derivatives. From the results, it was concluded that the inhibition of MAO-B by compound **1i** is reversible. To determine the mode of inhibition, a set of Lineweaver-Burk plots was constructed and since the plots were linear and intersected on the y-axis, it was concluded that **1i** is a competitive inhibitor of MAO-B.

Conclusion

This study concludes that the phenoxymethyl side-chain is more suited for the design of caffeine derived MAO-B inhibitors than the (phenylsulfanyl)methyl side-chain.

OPSOMMING

Titel

Remming van monoamienoksidase deur geselekteerde 8-[(fenielsufaniel)metiel]kafeïenderivate.

Sleutelwoorde

Parkinson se siekte, monoamienoksidase, substantia nigra, kafeïen, (E)-8-(3-chlorostiriel)kafeïen, 8-(fenoksimetiel)kafeïen, 8-[(fenielsufaniel)metiel]kafeïen, 8-[(fenielsufaniel)etiel]kafeïen.

Doelwit

Monoamienoksidase (MAO) bestaan as twee isovorme, naamlik MAO-A en MAO-B. Beide hierdie isovorme is by die oksidasie van dopamien betrokke. Tydens die behandeling van Parkinson se siekte (PD), kan inhibisie van MAO die oksidasie van dopamien inhibeer, wat aanleiding sal gee tot verhoogde konsentrasies van dopamien in die brein, en vervolgens die vorming van toksiese produkte, soos waterstofperoksied, sal verhoed. MAO-B-remmers word gebruik vir die behandeling van PD en dit is aangetoon dat MAO-B-remmers bruikbaar mag wees as hulpmiddels vir L-dopa tydens PD-behandeling. Byvoorbeeld, 'n vroeëre studie het getoon dat die kombinasie van L-dopa met (R)-depreniel ('n selektiewe MAO-B-remmer), meebring dat die dosis van L-dopa, vir verligting van die motoriese simptome in PD-pasiënte, verminder kan word. Die ouer MAO-remmers kan egter aanleiding gee tot newe-effekte soos psigotoksisiteit, lewertoksisiteit en kardiovaskulêre gevolge. Die onomkeerbare remmingsmeganisme van die ouer MAO-B-remmers, soos (R)-depreniel, is ook minder aanvaarbaar. Na gebruik van onomkeerbare remmers, mag dit 'n aantal weke neem voordat die MAO-ensiemaktiwiteit herstel. In teenstelling hiermee, by die gebruik van omkeerbare remmers, herstel ensiemaktiwiteit sodra die remmer uit die weefsel opgeruim is. Die ongunstige newe-effekte en nadele van die ouer MAO-B-remmers het ons laat besluit om die ontwerp van veiliger en omkeerbare MAO-B-remmers te ondersoek. Hierdie verbindings mag moontlik aangewend word vir die behandeling van PD.

Rasionaal

Dit is onlangs bevind dat (E)-8-(3-chlorostiriel)kafeïen (CSC), met 'n IC_{50}-waarde van 0.128 µM, 'n kragtige remmer van MAO-B is. CSC beskik oor 'n kafeïengroep, wat as noodsaaklik vir MAO-B-remming beskou word. Verder is aangetoon dat 'n reeks 8-(fenoksimetiel)kafeïenderivate potente en omkeerbare remmers van MAO-A en -B is. Die IC_{50}-waardes van die 8-(fenoksimetiel)kafeïene, vir die remming van MAO-B, wissel van 0.148–5.78 µM. Vir die doeleindes van hierdie studie is die fenoksimetiel-syketting met 'n fenielsulfanielgroep by C8 vervang. Die doel van die studie was derhalwe om 'n reeks 8-[(fenielsufaniel)etiel]kafeïenanaloë te sintetiseer en hul potensie vir MAO-B-remming te vergelyk met dié van die 8-(fenoksimetiel)kafeïenderivate wat voorheen gesintetiseer is. 'n Reeks, bestaande uit vyf 8-[(fenielsulfaniel)etiel]kafeïenanaloë is ook gesintetiseer om vas te stel wat die effek van die verlenging van die koolstofketting op die potensie van MAO-remming is.

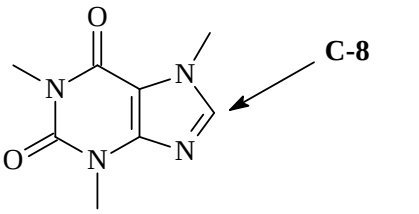

Kafeïen

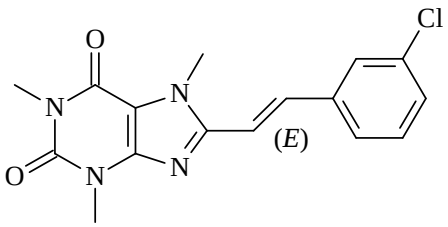

CSC

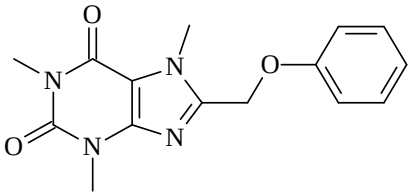

8-(Fenoksimetiel)kafeïen

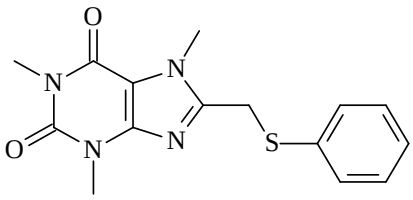

8-[(Fenielsulfaniel)metiel]kafeïen

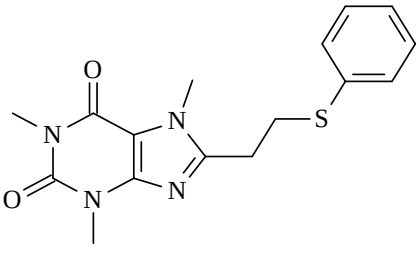

8-[(Fenielsulfaniel)etiel]kafeïen

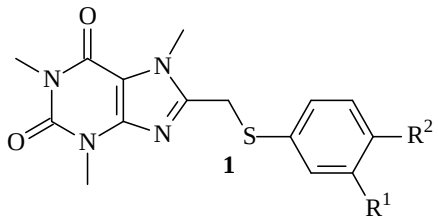

1

Verbinding	R^1	R^2
1a	H	H
1b	Cl	H
1c	Br	H
1d	F	H
1e	CH_3	H
1f	OCH_3	H
1g	OCH_2CH_3	H
1h	H	Cl
1i	H	Br

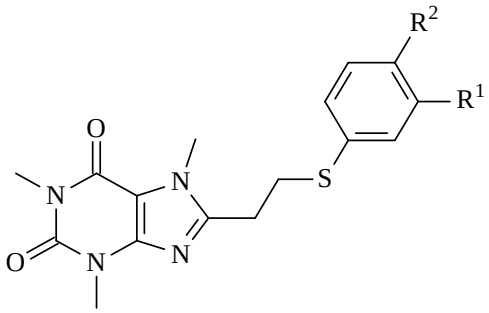

Verbinding	R^1	R^2
2a	H	H
2b	Cl	H
2c	Br	H
2d	H	Cl
2e	H	Br

Resultate

Die resultate toon dat die 8-[(fenielsufaniel)etiel]kafeïenanaloë remming van MAO-A en –B tot gevolg het. Die kragtigste remmers in die eerste reeks (**1a**–**i**) van hierdie studie was 8-[(3-bromofenielsulfaniel)metiel]kafeïen en 8-[(4-bromofenielsulfaniel)metiel] kafeïen met IC_{50}-

waardes van 4.90 en 4.05 µM, onderskeidelik. Indien hierdie resultate met dié van die 8-(fenoksimetiel)kafeïenderivate, wat voorheen bestudeer is, vergelyk word, is dit duidelik dat die broomgesubstitueerde homoloë, in beide reekse, die mees potente MAO-B-remmers is. Die broomgesubstitueerde 8-(fenoksimetiel)kafeïenderivate toon IC_{50}-waardes van 0.148 en 0.189 µM vir die homoloë wat broom, respektiewelik op die *meta*- en *para*-posisies, van die fenoksi-syketting bevat. Oor die algemeen is bevind dat die 8-[(fenielsufaniel)etiel]kafeïenderivate minder potente MAO-B-remmers as die 8-(fenoksimetiel)kafeïenderivate was. Die 8-[(fenielsufaniel)etiel]kafeïen-derivate se mate van selektiwiteit vir MAO-B (vergeleke met MAO-A) was ook nie so hoog as dié van die 8-(fenoksimetiel)kafeïene nie. Soortgelyk aan die 8-(fenoksimetiel)kafeïene, was die 8-[(fenielsulfaniel)metiel]kafeïene ook swak MAO-A-remmers. Die mees potente MAO-A-remmer van die toetsverbindings, het 'n IC_{50}-waarde van 19.4 µM gehad. Die kragtigste MAO-A-remmer in die 8-(fenoksimetiel)kafeïenreeks, wat voorheen bestudeer is, was meer potent, met 'n IC_{50}-waarde van 4.59 µM. Uit hierdie resultate kan afgelei word dat die fenoksi-syketting meer geskik is as die fenielsulfanielsyketting vir die ontwerp van kafeïen-afgeleide MAO-remmers.

By die tweede reeks verbindings wat in hierdie studie ondersoek is, die 8-[(fenielsufaniel)etiel]kafeïene (**2a**–**e**), is aangetoon dat die chloorgesubstitueerde verbindings die mees potente MAO-B-remmers was. Die *meta*- en *para*-gesubstitueerde derivate het respektiewelik IC_{50}-waardes van 5.67 en 7.79 µM vir die inhibisie van MAO-B vertoon. Dit is interessant dat die *meta*-gesubstitueerde derivaat geen inhibisie vir die MAO-A-isoensiem vertoon het nie. Dit is bevind dat die 8-[(fenielsufaniel)etiel]kafeïenderivate baie swak remmers van beide MAO-A en –B is en in hierdie opsig swakker inhibeerders as die 8-[(fenielsufaniel)metiel]kafeïenderivate is.

Aangesien een van die doelwitte van hierdie studie was om omkeerbare MAO-remmers te sintetiseer, is 'n tydsafhanklike studie op die beste inhibeerder, (**1i**), uitgevoer. Die doel van hierdie studie was om vas te stel of die remming van die 8-[(fenielsufaniel)etiel]kafeïenderivate omkeerbaar is. Die resultate het getoon dat verbinding **1i** MAO-B wel omkeerbaar rem. 'n Aantal Lineweaver-Burk-kurwes is opgestel om die werkingsmeganisme te bepaal en aangesien die grafieke reglynig was en die y-as op een punt gesny het, is tot die slotsom gekom dat **1i** 'n kompetitiewe remmer van MAO-B is.

Gevolgtrekking

Hierdie studie vind dat die fenoksimetiel-syketting meer geskik is as die (fenielsulfaniel)metiel-syketting vir die ontwerp van kafeïen-afgeleide MAO-B-remmers.

ABBREVIATIONS

5-HT	5-hydroxytryptamine
ACh	acetylcholine
ADH	aldehyde dehydrogenase
ADP	adenosine 5′-diphosphate
ATP	adenosine 5′-triphosphate
CSC	(E)-8-(3-chlorostyryl)caffeine
DA	dopamine
EDAC	N-(3-dimethylaminopropyl)-N'-ethylcarbodiimide hydrochloride
EI	electron ionization
FAD	flavin adenine dinucluetide
GSH	glutathione
HPLC	high performance liquid chromatography
HRMS	high resolution mass spectroscopy
IC_{50}	50% inhibitory concentration
MAO	monoamine oxidase
MPP^+	1-methyl-4-phenylpyridinium
MPTP	1-methyl-4-phenyl-1,2,3,6-tetrahydropyridine
NAD	nicotinamide adenine dinucleotide
NADH	reduced nicotinamide adenine dinucleotide
NSAIDs	non-steroidal anti-inflammatory drugs
PD	Parkinson’s disease
ppm	parts per million
ROS	reactive oxygen species
SEM	standard error of mean
SI	selective index
SNpc	substantia nigra pars compacta
TLC	thin layer chromatography
UV	ultraviolet

LIST OF FIGURES

CHAPTER 1

Introduction and rationale

1.1. Parkinson's disease

Parkinson's disease (PD) or *Paralysis Agitans* is a disease of the central nervous system. It affects 1 in every 100 persons aged 65 and older and it is considered to be the second most prevalent neurodegenerative disorder after Alzheimer's disease (Singh *et al*., 2007). The mean onset of the disease is 55 years of age and the risk of developing the disease increases 5-fold by the age of 70. There are two forms of this disease that have been identified thus far, namely the:

- sporadic form, which affects almost 90% of all patients of which the aetiology is unknown and
- familial form which affects close to 10% of all patients and which is linked to mutations in certain genes (Hald & Lotharius, 2005).

The clinical characteristics of PD include muscle rigidity, bradykinesia, resting tremor and postural instability. PD is a slow progressive disease and the patient rarely remembers the precise commencement of the symptoms (Alexi *et al*., 2000; Parkinson, 1817). The symptoms of PD are caused by the loss of dopaminergic neurons in the substantia nigra pars compacta (SNpc), which leads to the reduction of dopamine levels in the striatum. The loss of dopaminergic neurons occurs long before the patient experiences any symptoms. The mainstay of PD therapy is the dopamine precursor, L-dihydroxyphenylalanine (L-dopa). Unfortunately, as the disease progresses further, L-dopa loses its effectiveness (Hald & Lotharius, 2005; Alexi *et al*., 2000). Selegiline, a monoamine oxidase (MAO) inhibitor has been reported to potentiate the action of L-dopa (Foley *et al*., 2000). Based on the clinical effectiveness of MAO-B inhibitors in PD, this study will attempt to design novel reversible MAO inhibitors which may serve as therapy for PD.

PD can be classified as a syndrome rather than a single disorder, as several mechanisms have been shown to play a role in its pathogenesis (Yacoubian & Standaert, 2009). Intense research has been aimed at improving the quality of life of the patient and even delaying the progression of the disease. Strategies to improve the quality of life of a PD patient include neuroprotection and neurorescue. Neuroprotection refers to the protection of the remaining dopaminergic neurons and slowing down disease progression. Neurorescue refers to a disease-modifying intervention that converts "ailing" neurons into normally functioning cells (Lev *et al*., 2007). Table 1.1 depicts a number of PD mechanisms and targets for neuroprotective therapy.

Table 1.1: Mechanisms of PD pathogenesis and targets for therapy (Yacoubian & Standaert, 2009).

PD pathogenic mechanism	Targets for neuroprotection
Oxidative stress and mitochondrial dysfunction	Inhibitors of dopamine metabolism (MAO inhibitors, dopamine receptor agonists)
	Electron transport enhancers (CoQ10)
	Other antioxidants (Vitamin E, uric acid)
	Glutathione promoters (Selenium)
Protein aggregation and misfolding	Inhibitors of α-synuclein aggregation
	Agents that reduce α-synuclein protein levels
	Enhancers of parkin function
	Enhancers of UCH-L1 function
	Enhancers of proteosomal or lysosomal pathways
Neuroinflammation	Anti-inflammatory agents (NSAIDs, statins, minocycline)
Excitotoxicity	NMDA receptor antagonists
	Calcium channel antagonists
Apoptosis and cell death pathways	Anti-apoptotic agents
Loss of trophic factors	Neurotrophic factors (GDNF, neurturin)

1.2. Monoamine oxidase

In 1928, Hare discovered monoamine oxidase and named it tyramine oxidase, as it catalysed the oxidative deamination of tyramine. Later it was found that not only does tyramine oxidase oxidise tyramine, but it was also involved in the oxidation of other monoamines. It was thus called monoamine oxidase (Nagatsu, 2004). Johnston (1968) then discovered that there are two isoforms of this enzyme, monoamine oxidase A (MAO-A) and monoamine oxidase B (MAO-B). The two isoforms were distinguished from each other by their substrate preference and sensitivity to the inhibitor, clorgyline.

Monoamine oxidase is situated on the outer membrane of mitochondria and contains flavin adenine dinucleotide (FAD) as cofactor. It catalyses the following reaction:

$RCH_2NH_2 + H_2O + O_2 \rightarrow RCHO + NH_3 + H_2O_2$.

MAO has been implicated in neurodegenerative disorders such as PD due to the observation that toxic by-products such as hydrogen peroxide are generated in the catalytic

cycle of MAO. There is also an interesting correlation between the reduced MAO levels in the brains of smokers and the reduced risk of developing PD (Foley *et al*., 2000).

Currently there are 3 types of MAO inhibitors available:

- Older, irreversible nonselective drugs such as phenelzine and tranylcypromine
- Irreversible (suicide-type), selective drugs such as selegiline, rasagiline (MAO-B) and clorgyline (MAO-A)
- Reversible, selective drugs such as moclobemide (MAO-A) and safinamide (MAO-B)

Since irreversible inhibitors may have certain undesirable properties, selective reversible inhibitors were developed. For example, the reversible MAO inhibitor, moclobemide does not provoke the cheese reaction as reversibility allows competition and therefore dietary tyramine is able to displace the inhibitor from the enzyme and can be metabolised in its normal pathway. With the use of reversible, selective inhibitors, adverse effects such as liver toxicity, hypertensive crisis and even haemorrhage could be avoided (Youdim & Bakhle, 2006).

MAO inhibitors are effective in disorders such as PD, depression and psychiatric disorders (Riederer *et al*., 2004). Table 1.2 depicts examples of inhibitors and their clinical applications. As mentioned above, for the purpose of this study we will attempt to design new selective, reversible MAO inhibitors which may serve as adjunct or monotherapy for PD.

Table 1.2: MAO inhibitors and their main or potential therapeutic uses (Youdim *et al*., 2006).

Compound	**MAO selectivity**	**Inhibition type**	**Application**
Befloxatone	A	Reversible	Antidepressant
Brofaromine	A	Reversible	Antidepressant
Clorgyline	A	Irreversible	Antidepressant
(R)-Deprenyl (Selegiline)	B	Irreversible	Antiparkinson
2-HMP (and other aliphatic propargylamines)	B	Irreversible	Antiparkinson
Iproniazid	A & B	Irreversible	Antidepressant
Isocarboxazid	A & B	Irreversible	Antidepressant
Ladostigil	A & B	Irreversible	Antidepressant, antiparkinson and anti-Alzheimer
Lazabemide	B	Reversible	Antiparkinson

M30	A & B	Irreversible	Antidepressant, antiparkinson and anti-Alzheimer
Moclobemide	A	Reversible	Antidepressant
Nialamide	A & B	Irreversible	Antidepressant
PF 9601N	B	Irreversible	Antiparkinson
Phenelzine	A and B	Irreversible	Antidepressant
Rasagiline	B	Irreversible	Antiparkinson
Safinamide	B	Reversible	Antiparkinson
Toloxatone	A	Reversible	Antidepressant
Tranylcypromine	A and B	Irreversible	Antidepressant

Abbreviations→2-HMP, N-(2-heptyl)-N-methylpropargylamine; MAO, monoamine oxidase.

1.3. Rationale

Caffeine (Figure 1.1) may be considered as a lead compound for the design of new MAO-B inhibitors. Although caffeine is a weak MAO-B inhibitor, it has been previously reported that substitution on C8, with a variety of substituents, increases the MAO inhibition potency of caffeine to a large extent. (E)-8-(3-Chlorostyryl)caffeine (CSC, Figure 1.1), a potent inhibitor of MAO-B, which has an enzyme-inhibitor dissociation constant of 128 nM, is an example of this behaviour (Pretorius *et al*., 2008). There are a number of caffeine derived inhibitors that have been investigated thus far, which are more potent MAO-B inhibitors than caffeine. The recently synthesised 8-benzyloxycaffeinyl analogues (Figure 1.1) were found to inhibit both isoezymes of MAO reversibly. Inhibition potencies for MAO-A ranged from 0.14–1.30 μM and 0.023–0.59 μM for MAO-B (Strydom *et al*., 2010). It has also recently been shown that a series of 8-(phenoxymethyl)caffeine analogues are exceptionally potent reversible inhibitors of MAO-B (Swanepoel, 2010). These compounds are relatively weak inhibitors of MAO-A, and may therefore be classified as MAO-B selective. For these compounds, the inhibition potencies towards MAO-B ranged from 0.148 to 5.78 μM (Table 1.3), with the homologues, containing halogens on the phenyl ring, being the most potent. In this study we will expand on these results by synthesising a homologous series of 8-[(phenylsulfanyl)methyl]caffeines of which the C8 phenyl ring contains a variety of halogen and alkyl substituents. Subsequently, it will be determined if these derivatives are also inhibitors of human MAO-A and MAO-B.

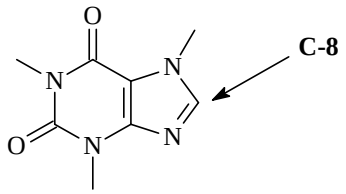

Caffeine

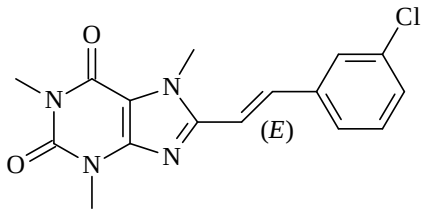

CSC

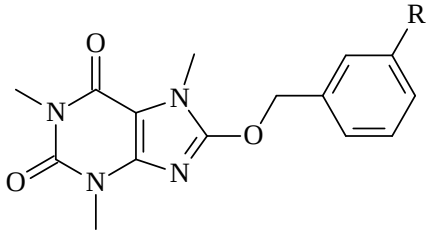

Benzyloxycaffeine

R= H, Cl, Br, F, CF_3, CH_3 and OCH_3

Figure 1.1: The chemical structures of caffeine, (E)-8-(3-chlorostyryl)caffeine (CSC) and 8-benzyloxycaffeinyl analogues.

Table 1.3: The IC_{50} values that were measured for the inhibition of recombinant human MAO-B by 8-(phenoxymethyl)caffeine analogues (Swanepoel, 2010).

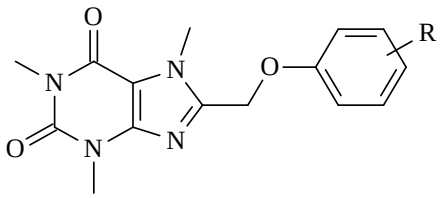

R	MAO-B IC_{50} (μM)
H	5.780
3-Cl	0.334
3-Br	0.148
3-F	1.610
3-CF_3	0.641
3-CH_3	1.230
3-OCH_3	1.960
4-Cl	0.250
4-Br	0.189

In this study seven 8-[(phenylsulfanyl)methyl]caffeine analogues (Table 1.4) will be synthesised and evaluated as inhibitors of recombinant human MAO-A and –B. The 8-phenylsulfanyl substituent is structurally related to the phenoxymethyl substituent and may thus produce similar or even better results than obtained with the phenoxymethyl moiety. The selected C8 substituents will differ by substitution on the *meta* position of the phenylsulfanyl phenyl ring. The MAO-A and –B inhibition potencies of the 8-[(phenylsulfanyl)methyl]caffeine analogues will then be compared to that of the previously studied 8-(phenoxymethyl)caffeine analogues. In addition, two 8-[(phenylsulfanyl) methyl]caffeine analogues containing substituents on the *para* position of the phenyl ring, structures **1h** and **1i**, will be synthesised and examined as MAO inhibitors. Also a series of five 8-[(phenylsulfanyl)ethyl]caffeine analogues (Table 1.5) will be synthesised to determine the effect that carbon chain elongation has on the potency of inhibition of MAO.

Table 1.4: The structures of the 8-[(phenylsulfanyl)methyl]caffeine analogues that will be synthesised, and examined in this study as MAO inhibitors

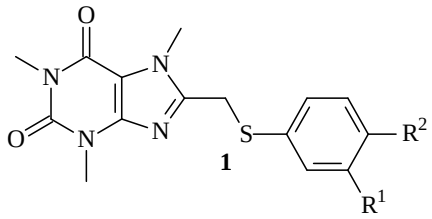

1

Compound	R^1	R^2
1a	H	H
1b	Cl	H
1c	Br	H
1d	F	H
1e	CH_3	H
1f	OCH_3	H
1g	OCH_2CH_3	H
1h	H	Cl
1i	H	Br

Table 1.5: The structures of the 8-[(phenylsulfanyl)ethyl]caffeine analogues that will be synthesised, and examined in this study as MAO inhibitors

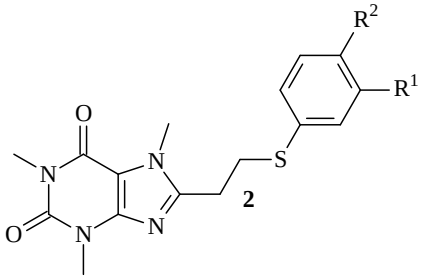

Compound	R^1	R^2
2a	H	H
2b	Cl	H
2c	Br	H
2d	H	Cl
2e	H	Br

1.4. Objectives

Based on the discussion above, the objectives of this study are as follows:

- Nine 8-[(phenylsulfanyl)methyl]caffeine analogues (**1a–i**) will be synthesised. An additional series of 8-[(phenylsulfanyl)ethyl]caffeine analogues (**2a–e**) will also be synthesised in this study. The key starting materials are 1,3-dimethyl-5,6-diaminouracil and the appropriately substituted phenylsulfanyl acetic acids and phenylsulfanyl propanionic acids. Most of the phenylsulfanyl acetic and propanionic acids are not commercially available and will thus be prepared from the corresponding thiophenols.
- The 8-[(phenylsulfanyl)methyl]caffeine and 8-[(phenylsulfanyl)ethyl]caffeine analogues will be evaluated as inhibitors of recombinant human MAO-A and –B. The commercially available human enzymes will be used. The inhibition potencies will be expressed as IC_{50} values. Fluorometric assays will be used to measure the enzyme activities. One of the assays is based on the detection of H_2O_2 in a horseradish peroxidase-coupled reaction using Amplex Red. The H_2O_2 formed during oxidation reacts with Amplex Red to form resorufin. The quantity of resorufin formed will subsequently be determined by measuring the fluorescence of the supernatant at excitation and emission wavelengths of 560 and 590 nm, respectively (Zhou & Panchuk-Voloshina, 1997). In the second fluorometric assay, kynuramine will be

used as substrate. Kynuramine is oxidized to yield 4-hydroxyquinoline, a fluorescent compound which is readily measurable in the presence of a non-fluorescent substrate. The quantity of 4-hydroxyquinoline formed will subsequently be determined by measuring the fluorescence of the supernatant at excitation and emission wavelengths of 310 and 400 nm, respectively.

- Studies to determine the reversibility of inhibition of MAO-A and –B will be carried out for selected compounds. It is important to note that reversibility of inhibition is more desirable than irreversibility.
- If the inhibition is found to be reversible, Lineweaver-Burk plots for the inhibition of MAO-A and/or –B will be constructed to determine if the mode of inhibition is of a competitive nature.
- The results of this study will be compared to that of the previously studied C3 substituted 8-(phenoxymethyl)caffeine analogues.
- A research paper describing the MAO inhibition properties of the 8-(phenoxymethyl)caffeine and 8-[(phenylsulfanyl)methyl]caffeine analogues will be prepared.

CHAPTER 2

Literature review

2.1. Parkinson's disease

Parkinson's disease (PD) is a neurodegenerative disease that is clinically characterised by bradykinesia, tremor, rigidity, flexed posture, postural instability and freezing of gait. The disease normally presents itself in the later stages of life, but can also be present in young adults (Fahn *et al*., 2004).

Dopamine replacement therapy has been found to reduce some of the symptoms of PD and improve the quality of life of the patient (Lees, 2009). A definite diagnosis of PD is defined by the presence of intracytoplasmic eosinophilic inclusions, termed Lewy bodies, in the surviving doparminergic nigral neurons of post-mortem tissue from PD patients. Confirmation of the diagnosis in patients comes from the response to L-dopa treatment (Romero-Ramos *et al*., 2004).

2.1.1. General background

In 1817 James Parkinson presented a monograph which was entitled "Shaking Palsy". The monograph described the core clinical features of the disease that we now familiarly known as Parkinson's disease.

The discovery of dopamine (DA) in the brain by Arvid Carlsson led to a better understanding of PD. There are two main neuronal groups in the midbrain which send ascending DA projections to the forebrain. These are termed the neurons of the ventral tegmental area (VTA) and the neurons of the substantia nigra pars compacta (SNpc). In PD, neurodegeneration was found to be present in both cell types, but the SNpc seemed to be more involved since cell death is more severe in this area (Dauer & Przedborski, 2003; Romero-Ramos *et al*., 2004).

Two conclusions were made after Carlsson's discovery of DA in 1958:

- Firstly, the loss of SNpc neurons leads to striatal DA deficiency, which is responsible for the major symptoms of PD.
- Secondly, replenishment of striatal DA through oral administration of the dopamine precursor, L-dopa, alleviates most of these symptoms (Dauer & Przedborski, 2003).

Although no cure has been found for this progressive, neurodegenerative disease, current research is directed toward prevention of dopaminergic neuron degeneration (Dauer & Przedborski, 2003).

2.1.1.1. Neurochemical and neuropathological features

The neuropathological hallmark of PD is the destruction of the dopaminergic neurons of the SNpc and the presence of Lewy bodies within the remaining neurons (Lees *et al.*, 2009). As described below, the SNpc is an integral part of the basal ganglia and its normal function is critical for normal movement.

The basal ganglia controls voluntary movement and is composed of a group of subcortical nuclei consisting of the:

- striatum (caudate and putamen)
- globus pallidus (externa and interna)
- substantia nigra (pars compacta and reticula)
- subthalamic nucleus (Figure 2.1)

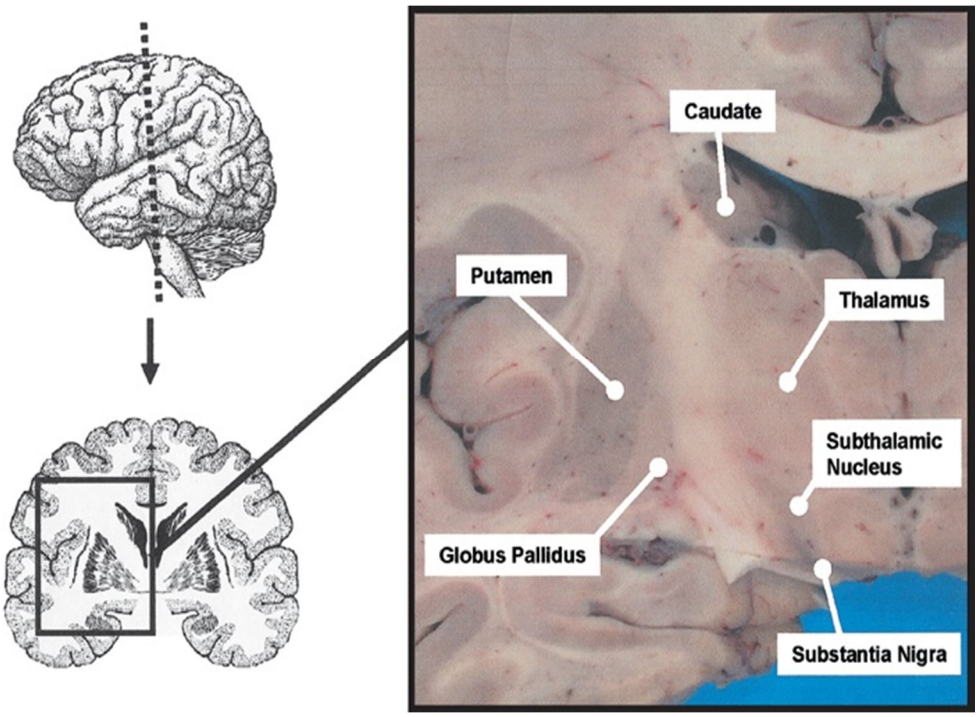

Figure 2.1: A cross-section through the brain showing the different compartments (Burton *et al*., 2003).

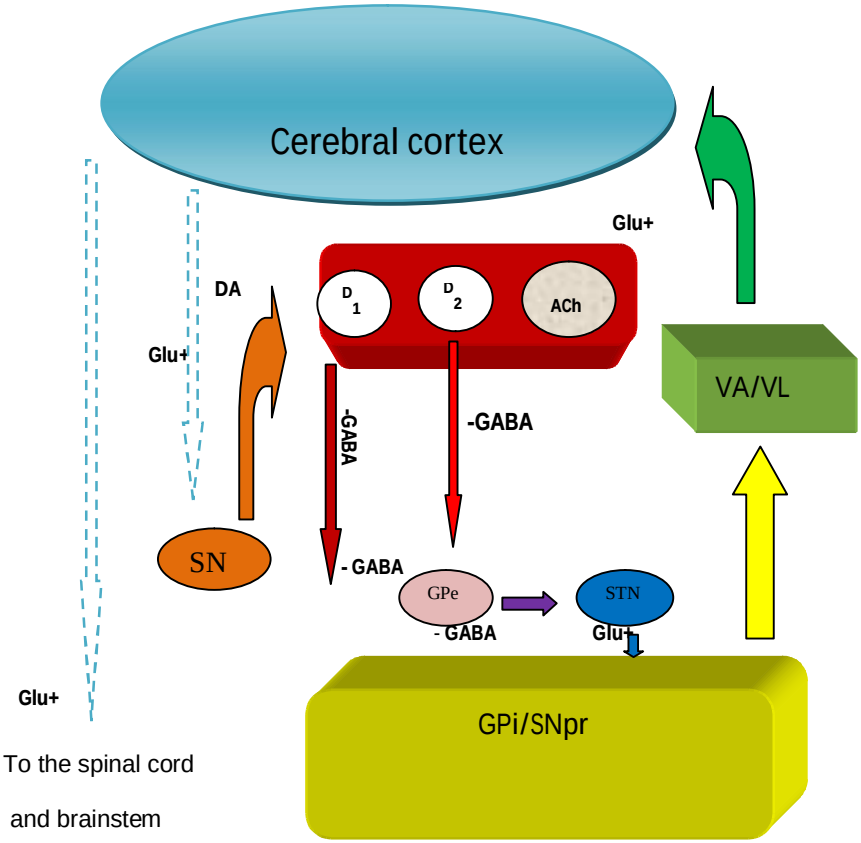

Abbreviations → ACh: Acetylcholine; GABA: γ-aminobutyric acid; GPe: Globus pallidus externa; GPi: Globus pallidus interna; SNpc: Substantia nigra pars compacta; SNpr: Substantia nigra pars reticula; STN: Subthalamic nucleus; VA/VL: Ventroanterior and ventrolateral nuclei of the thalamus

Figure 2.2: The neurocircuitary pathways of the basal ganglia (Hardman & Limbird, 2001).

The basal ganglia acts as a modulatory loop that regulates the flow of information from the motor cortex to the motor thalamus (Figure 2.2). The loop system consists of excitatory and inhibitory pathways, the balance of which is maintained by the dopaminergic pathway from the substantia nigra. The neurotransmitters that play a major role in these loops are glutamate (excitatory neurotransmitter) and γ-aminobutyric acid (inhibitory neurotransmitter). The disruption of this balance causes abnormal function of the dopaminergic nigrostriatal pathway, a situation that exists in PD. The striatal neurons giving rise to the direct pathway express primarily the excitatory D_1 dopamine receptor protein, while the striatal neurons forming the indirect pathway express primarily the inhibitory D_2 type. Therefore the dopamine released in the striatum tends to increase the activity of the direct pathway and decrease the activity of the indirect pathway. The depletion that occurs in PD has an

opposite effect. The direct pathway to the SNpr and GPi is less active, whereas the activity in the indirect pathway is increased. This reduced inhibition results in the over activity of the GPi and the increased firing of GABAergic neurons projecting from the GPi to the VA/VL thalamus. The net effect of the reduced dopaminergic input in PD increases the inhibitory outflow from the GPi and SNpr to the thalamus and subsequently reduces stimulation of the motor cortex (Hardman & Limbird, 2001).

This model of the basal ganglia has several limitations since the neuropathology of PD is not only characterised by dopaminergic neuron loss. There are other neurotransmitters besides DA, that are involved. Neurodegeneration and Lewy body formation are found in noradrenergic, serotonergic and cholinergic systems as well as in the cerebral cortex, olfactory bulb and autonomic nervous system (Dauer & Przedborski, 2003). Even with its limitations the model has proven to be useful. Firstly, it suggests that PD may be treated by restoring the balance of the system through the replacement of DA function. Secondly, it suggests that other non-dopaminergic treatment strategies may also be useful for the treatment of PD (Hardman & Limbird, 2001).

2.1.1.2. Aetiology

The cause of PD is unknown, although a number of genetic and environmental factors have been described as contributing factors (Toulouse & Sullivan, 2008). Considering the fact that only 15 to 20% of PD patients have a clear positive family history of PD, researchers have shown that PD has a very complex aetiology (Nuytemans *et al.*, 2010):

a. Environmental factors

The environmental hypothesis proposes the involvement of various toxins that, due to their dopaminergic selectivity, are able to induce PD-related neurodegeneration (Romero-Ramos *et al*., 2004). Exposure to certain environmental toxins such as pesticides may cause PD. Therefore people with a higher degree of exposure to pesticides, such as farmers, are at risk (although small) of developing PD. Another chemical toxin, called MPTP (1-methyl-4-phenyl-1,2,3,6-tetrahydropyridine), which is not chemically related to pesticides, has been shown to cause symptoms similar to PD. The pesticide paraquat is structurally similar to MPTP's active metabolite, (1-methyl-4-phenylpyridinium) MPP^+ (Figure 2.3). There is however, no convincing data about the lethal effects of paraquat (Figure 2.3) and its potential role in the development of PD. The finding that MPTP causes a syndrome nearly identical to PD is a

classic example of how an exogenous toxin can mimic the clinical and pathological features of PD (Dauer & Przedborski, 2003; Tugwell, 2008).

MPP$^+$ **Paraquat**

Figure 2.3: Structural similarity between paraquat and MPP$^+$

b. Genetic factors

The presence of Lewy bodies in post-mortem tissue has been regarded as the pathological hallmark of PD. Lewy bodies are reactive to antibodies for both α-synuclein, which is an abundant synaptic protein, and ubiquitin. It has been suggested that mutation of the gene encoding for α-synuclein may lead to the development of PD. Identification of α-synuclein mutations, which may cause familial PD and the finding of this protein in pathological deposits, emphasises the importance of genetic factors in the pathogenesis of PD (Gwinn-Hardy, 2002). According to Healy *et al.* (2008), loss of function as a result of mutation in 5 genes, α-synuclein, PARK-2 (parkin), PARK-7 (DJ-1), PINK-1 and LRRK-2, may cause PD. It was found that LRRK-2 mutations had the highest frequency in PD cases. In North African Arabs, close to a third of all patients diagnosed with PD have a LRRK-2 mutation. The latter is also true for Ashkenazi Jews and Portuguese people. Mutations in PARK-2 were found to be the second largest cause of familial PD.

2.1.1.3. Pathogenesis

There are two main hypotheses that have been formed with regard to the pathogenesis of the disease:

- Misfolding and aggregation of proteins
- Mitochondrial dysfunction and oxidative stress

Aggregated proteins may cause neurotoxicity through a number of mechanisms, either by deforming the cell or by interfering with intercellular trafficking in neurons. Protein inclusions may also alter proteins that are important for cell survival (Dauer & Przedborski, 2003). However, according to recent studies, it seems that there is no correlation between inclusion formation and cell death. It remains unclear whether misfolded proteins directly cause toxicity or whether they damage cells via formation of protein aggregates (Saudou *et al*., 1998).

The possibility that oxidative stress plays a role in the pathogenesis of PD was motivated by the discovery of the parkinsonian neurotoxin, MPTP. MPTP was found to inhibit mitochondrial respiration. Its active metabolite MPP^+, blocks the flow of electrons along the mitochondrial electron transport chain, which leads to an increased production of reactive oxygen species (ROS). The loss of electron flow is also associated with a decrease in ATP production and the reduction of available energy (Dauer & Przedborski, 2003). MPP^+ also interacts with synaptic vesicles through its binding to the vesicular monoamine transporter-2. MPP^+ thus translocates into synaptic vesicles and stimulates the extrusion of synaptic dopamine. The excess cytosolic dopamine readily undergoes auto-oxidation, and generates a burst of ROS, thus subjecting nigral neurons to oxidative stress.

After several studies on the effects of systemic administration of MPTP to mice, it was concluded that oxidative stress and an energy crisis, activate cell death-related molecular pathways, which are the real cause of neuronal injury (Przedborski, 2005).

2.1.2 Treatment

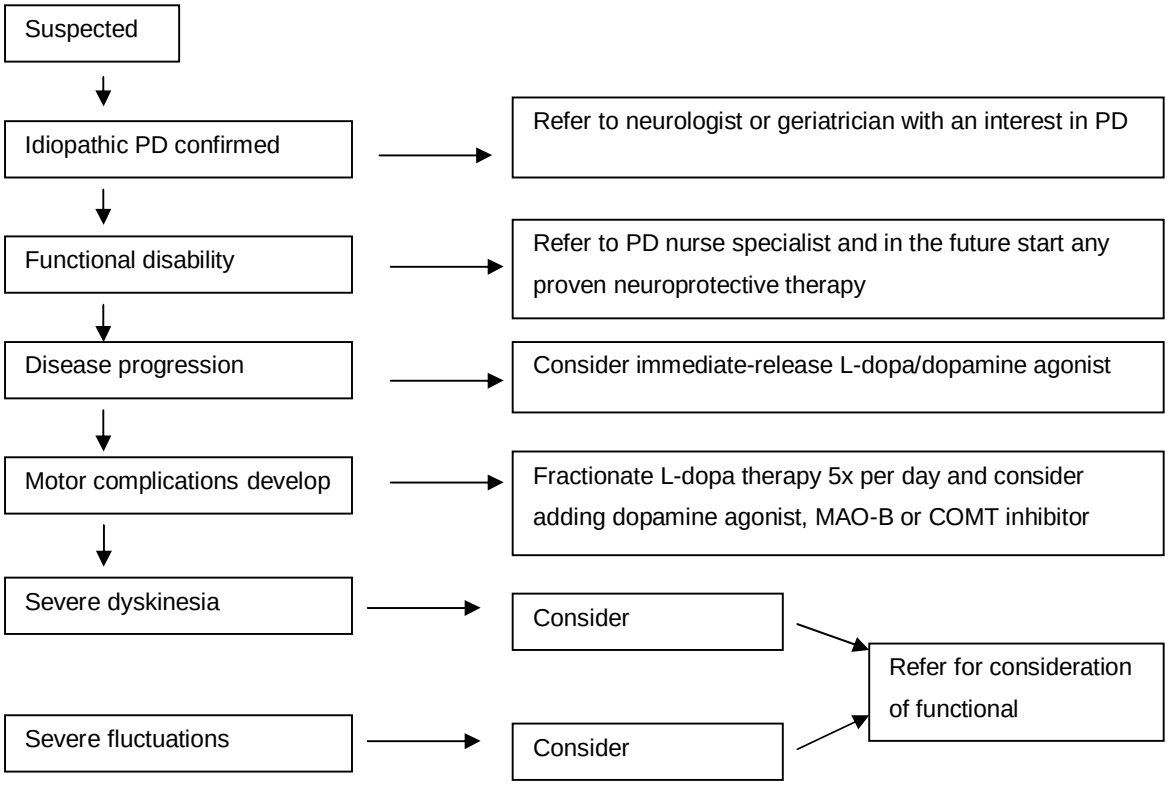

Figure 2.4: Suggested algorithm for PD therapy (Clarke, 2004).

2.1.3. Drugs for neuroprotection

Due to studies that have been carried out with animal models of PD, researchers now believe that protecting the remaining dopaminergic neurons may slow down the disease progression and in the long run improve the quality of life of a patient (Lev *et al*., 2007). Below are examples of potentially neuroprotective therapeutic options for PD.

2.1.3.1. Monoamine oxidase inhibitors

MAO inhibitors with selectivity and specificity for MAO type B prolong the activity of both endogenously and exogenously derived DA. Studies have shown that the catabolism of DA by MAO generates toxic byproducts such as hydrogen peroxide, which may lead to the formation of more damaging ROS. A drug that was found to inhibit all these effects was selegiline [(R)-deprenyl]. Selegiline is an irreversible (suicide-type) MAO-B inhibitor (LeWitt & Taylor, 2008).

In animal models of MPTP-induced parkinsonism, selegiline has shown a capacity to prevent apoptosis (cell death) by altering expression of the genes for pro- and antiapoptotic proteins. As a result mitochondrial integrity is preserved during oxidative stress. However, selegiline has neurotoxic metabolites namely, L-amphetamine and L-methamphetamine (Figure 2.5), which may oppose the neuroprotective effects of selegiline (Fernandez & Chen, 2007). In addition to its neuroprotective effects selegiline may also be used in the symptomatic treatment of PD in combination with L-dopa. Studies have shown that selegiline may retard disease progression and delay the need for L-dopa (Singh *et al*., 2007).

Another promising MAO-B inhibitor is rasagiline. Rasagiline (Figure 2.5) differs from selegiline in these aspects: its metabolite aminoindan is not neurotoxic and the neuroprotective effects of rasagiline are dose dependent and are more pronounced than those of selegiline (Fernandez & Chen, 2007). The role of rasagiline in PD seems to be multifactoral. It enhances the release of dopamine, retards its metabolism and antagonises the cellular processes that lead to apoptosis (LeWitt & Taylor, 2008).

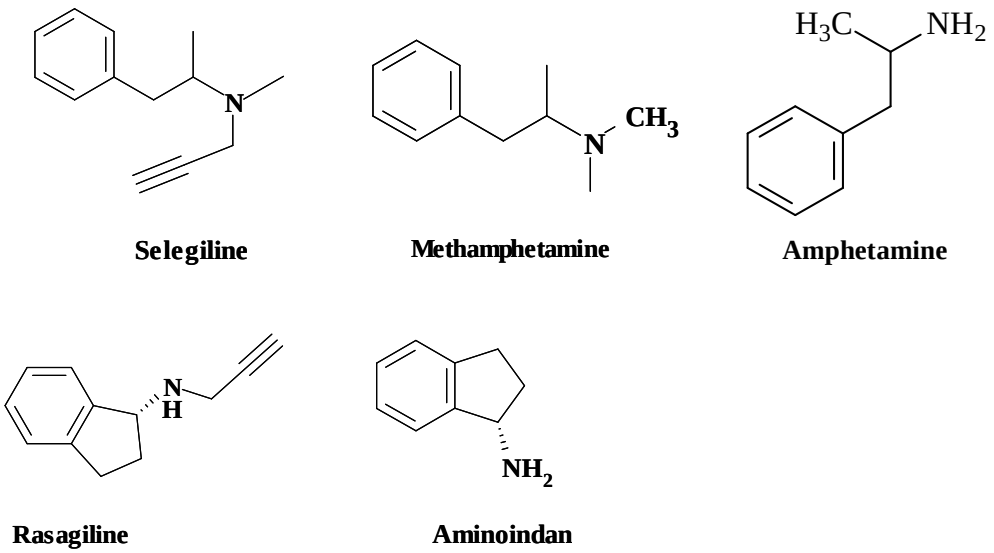

Selegiline **Methamphetamine** **Amphetamine**

Rasagiline **Aminoindan**

Figure 2.5: Structures of MAO inhibitors and their metabolites.

2.1.3.2. Dopamine agonists

Dopamine agonists are classified as ergoline and nonergoline agonists. All dopamine agonists act on D_2 receptors. Stimulation of postsynaptic D_2 receptors are linked to antiparkinsonism activity and presynaptic D_2 stimulation has been claimed to have neuroprotective effects (Lees, 2005). Dopamine agonists supposedly act on D_2 receptors which result in the suppression of dopamine release and thus reduce oxidative stress. *In vitro* animal studies have shown that dopamine receptor agonists can reduce dopaminergic cell death (Yacoubian & Standaert, 2009). The studies also suggested that pergolide, pramipexole and ropinirole may have putative neuroprotective properties (Lees, 2005).

2.1.3.3. Antioxidant therapy

Lipid peroxidation is increased in the substantia nigra of patients with PD. Vitamins A, C and E are all antioxidants that have been shown to prevent lipid peroxidation by acting as free radicals scavengers (Fahn, 1992). Levels of 4-hydroxyl-2,3-nonenal (HNE) and 8-hydroxyguanosine (HG), both markers of lipid peroxidation, are also increased in the substantia nigra of PD patients (Yoritaka *et al*., 1996; Castellani *et al*., 2002).

Below is a schematical presentation (Figure 2.6) of the role of antioxidants in the potential prevention of nigrostriatal neurodegeneration.

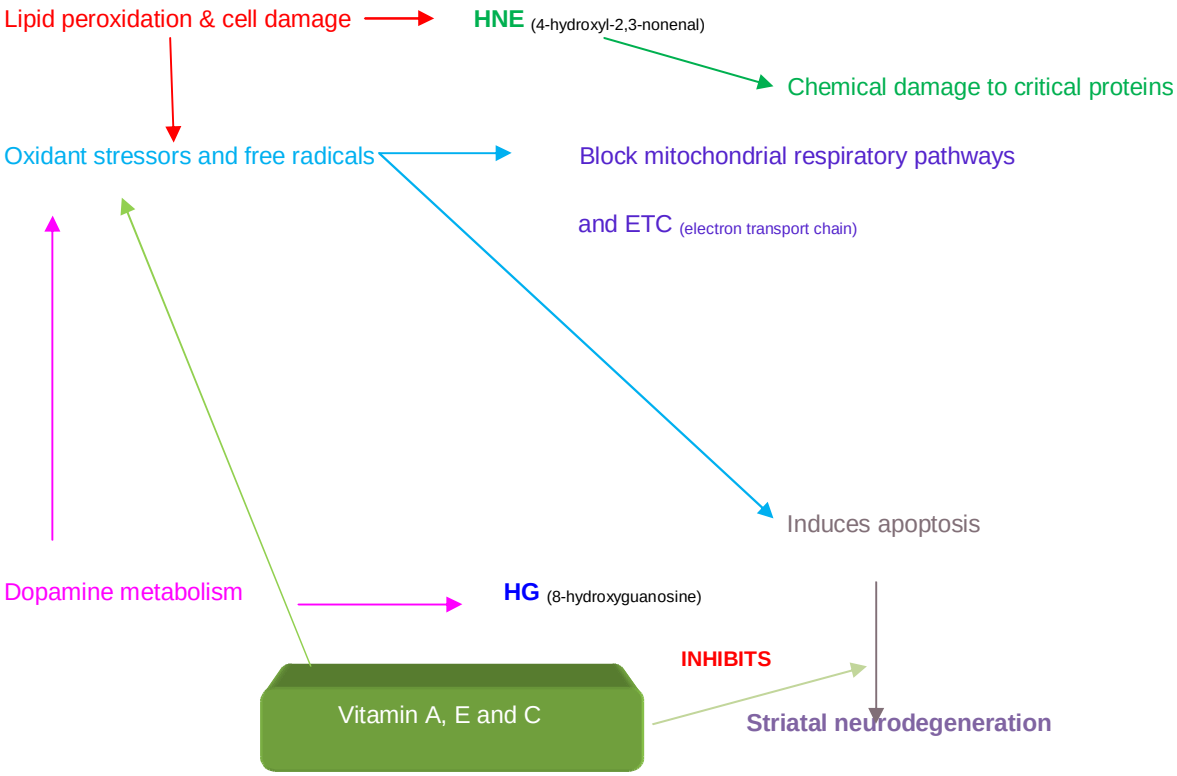

Figure 2.6: The role vitamins A, E and C in preventing nigrostriatal neurodegeneration (Singh *et al*., 2007).

2.1.3.4. Mitochondrial energy enhancement agents

Coenzyme Q10 (CoQ10) or ubiquinone is a cofactor of the electron transport chain in mitochondria and has been shown to reduce dopaminergic neurodegeneration in PD animal models (Beal *et al.,* 1998). It is also a potent antioxidant and free radical scavenger (Echtay *et al.,* 2002; Shults, 2003). Mice that were treated with both CoQ10 and MPTP showed elevated levels of striatal dopamine and 62% more tyrosine hydroxylase (TH)-immunoreactive neuronal fibres compared to the controls that were only treated with MPTP. Oral administration of CoQ10 in an aged mouse model with amyotrophic lateral sclerosis was shown to prevent neuronal damage. This finding confirmed the neuroprotective properties of CoQ10 (Beal *et al.,* 1998; Matthews *et al.,* 1998).

2.1.3.5 Anti-apoptic agents

The propargylamine, TCH346, is an anti-apoptic factor that inhibits glyceraldehyde-3-phosphate dehydrogenase (GAPDH). GADPH is a glycolytic enzyme that is involved in apoptosis. TCH346 has been shown to reduce dopamine loss in both 6-OHDA (6-hydroxydopamine) and MPTP models (Andringa *et al.,* 2003; Andringa *et al.,* 2000). But, a randomized trial involving 301 patients over 12-18 months failed to show a significant

difference in clinical outcome (Olanow, 2006). CEP147 is another anti-apoptic agent that has shown promise in preclinical studies. It is an inhibitor of mixed lineage kinases that can activate the *c*-Jun N-terminal kinase (JNK) pathway involved in cell death (Saporito *et al.,* 1999; Mathiasen *et al.,* 2004; Lotharius *et al*., 2005).

2.1.3.6 Adenosine A_{2A} receptor antagonists

A_{2A} receptors have become important in PD therapy due to their location in the human brain. The receptors are restricted to the striatum, the main target of the dopaminergic neurons that degenerate in PD (Svenningsson *et al.,* 1999). According to a study by Ikeda *et al.* (2002), oral administration of A_{2A} antagonists protect against the loss of nigral dopaminergic neuronal cells, induced by 6-OHDA in rats. It was further proven that A_{2A} antagonists prevent the MPTP-induced functional loss of dopaminergic nerve terminals in the striatum of mice. Blockade of this receptor has proven to have acute antisymptomatic and chronically neuroprotective activities (Ikeda *et al*., 2002).

2.1.3.7. Other therapies

Estrogen has been shown to have neuroprotective properties in animal models. Estrogen is a gonadal streroid hormone. A vast number of steroids have modulatory effects on neuronal physiology, morphology and degeneration (Sapolsky, 1998). Female mice which were treated with MPTP and methamphetamine exhibit a significantly slighter degree of dopaminergic toxicity than males. This effect was not due to differences in the amount of MPP^+ formed but was due to the protective effect of estrogen (Miller *et al*., 1998).

Certain studies (Baron, 1986; Morens *et al*., 1995) have suggested that cigarette smoke and nicotine may be neuroprotective in parkinsonian neurodegeneration. It binds to the nicotinic acetylcholine receptors that are present in the striatum and partially overlap with the dopaminergic system. The significance of this overlap is further supported by the fact that nicotine has been shown to modulate dopamine release (Toulouse & Sullivan, 2008). Nevertheless, cigarette smoke contains a variety of compounds that may have not been taken into consideration when these studies were conducted.

2.1.4. Caffeine

2.1.4.1. Introduction

Caffeine is the most widely used central nervous system stimulant. Almost all caffeine comes from dietary sources (coffee, tea and cocoa beverages). Caffeine was discovered in 1820 in tea (*Camellia sinensis*) and coffee (*Coffea Arabica*) (Kihlman, 1977). The reasons for caffeine use are numerous. The common belief is that caffeine has stimulant actions that elevate mood, decrease fatigue and increase capacity to work. There are however a number of reports illustrating that the use of caffeine does result in increased energy and alertness (Lorist & Tops, 2003). Higher doses of caffeine are said to produce anxiety, restlessness, insomnia, gastrointestinal disturbances and tachycardia (Nehlig, 1999). Studies done with humans have shown that caffeine may produce behavioral effects that are similar to dopaminergic drugs such as cocaine and amphetamine. Caffeine, similar to these drugs, produces feelings of well-being, alertness, delays sleep and enhances performance on psychomotor tasks. Termination of caffeine consumption produces a withdrawal syndrome, thus providing evidence of physical dependence. This link between caffeine and psychomotor stimulants has been the basis of caffeine being considered as a model drug of dependence (Garret & Griffiths, 1997; Nehlig, 1999).

2.1.4.2. Chemistry and biochemistry

Caffeine, theophylline, theobromine and the methyluric acids (Figure 2.7) belong to a group of plant alkaloids called methylxanthines. Caffeine is a purine derivative (1,3,7-trimethylxanthine) and has a very low solubility rate. The structure of caffeine shows that it contains 3 hydrogen bond acceptors, 3 methyl groups and has no proton-donor groups (Poltev *et al*., 2004). Two hypotheses have been proposed for the role of the high concentrations of caffeine that accumulates in tea and coffee:

- **The chemical defence theory** proposes that caffeine in young leaves, fruits and flower buds acts to protect soft tissues from insect larvae and beetles.
- **The allelopathetic theory** proposes that caffeine stored in the seed coats is released into the soil and inhibits the germination of foreign seeds (Hewavitharanage *et al*., 1999; Waller, 1989).

These two hypotheses suggest that caffeine might have an ecological role (Harborne, 1993).

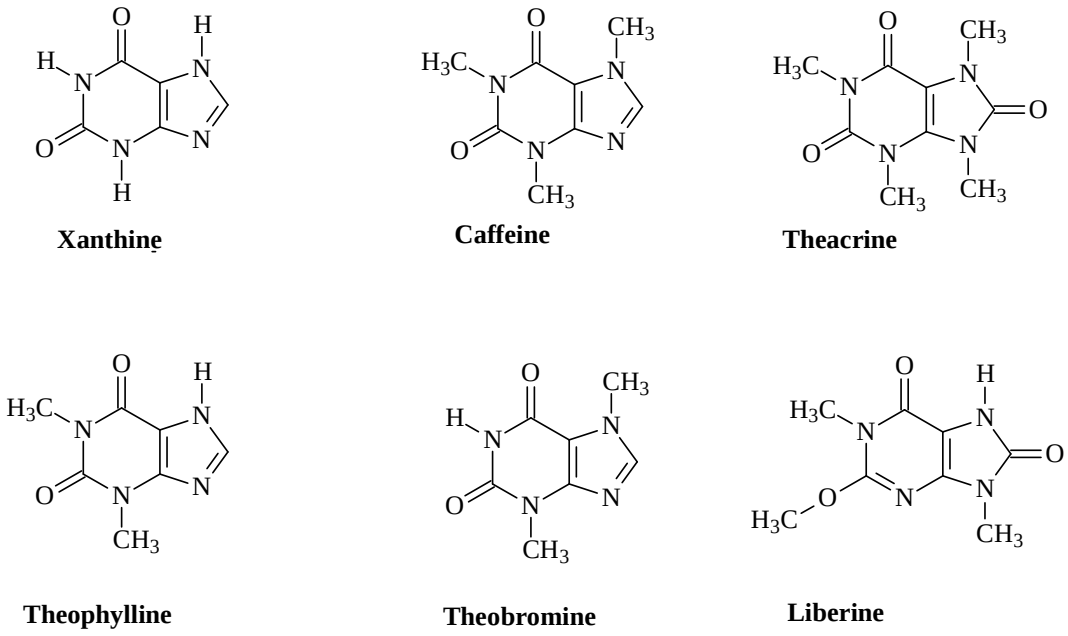

Figure 2.7: Chemical structures of the methylxanthines and the methyluric acids

Caffeine is synthesised in plants by the following route; xanthosine → 7-methylxanthosine → 7-methylxanthine → theobromine → caffeine. The xanthine skeleton of caffeine is derived from purine nucleotides that are converted to xanthose (Figure 2.8). Xanthose is synthesised from inosine 5'- monophosphate produced by *de novo* purine synthesis. The formation of caffeine by this pathway is closely associated with the activated-methyl cycle. The three methylation steps in the caffeine biosynthesis pathway use S-adenosyl-L-methionine (SAM) as the methyl donor (Figure 2.8). During the synthesis, SAM is converted to S-adenosyl-L-homocysteine (SAH), which is then hydrolysed to L-homocysteine and adenosine. The formed adenosine is used to synthesise the purine ring of caffeine and the L-homocysteine is recovered to replenish SAM levels. Methylation of the purine ring is achieved by the conversion of xanthosine to 7-methylxanthosine, which is catalysed by 7-methylxanthosine synthase (Figure 2.9). Methylxanthine nucleosidase catalyses the hydrolysis of 7-methylxanthosine to 7-methylxanthine. The latter is then methylated by N-methyltransferases to yield theobromine and then caffeine (Ashihara & Crozier, 2001).

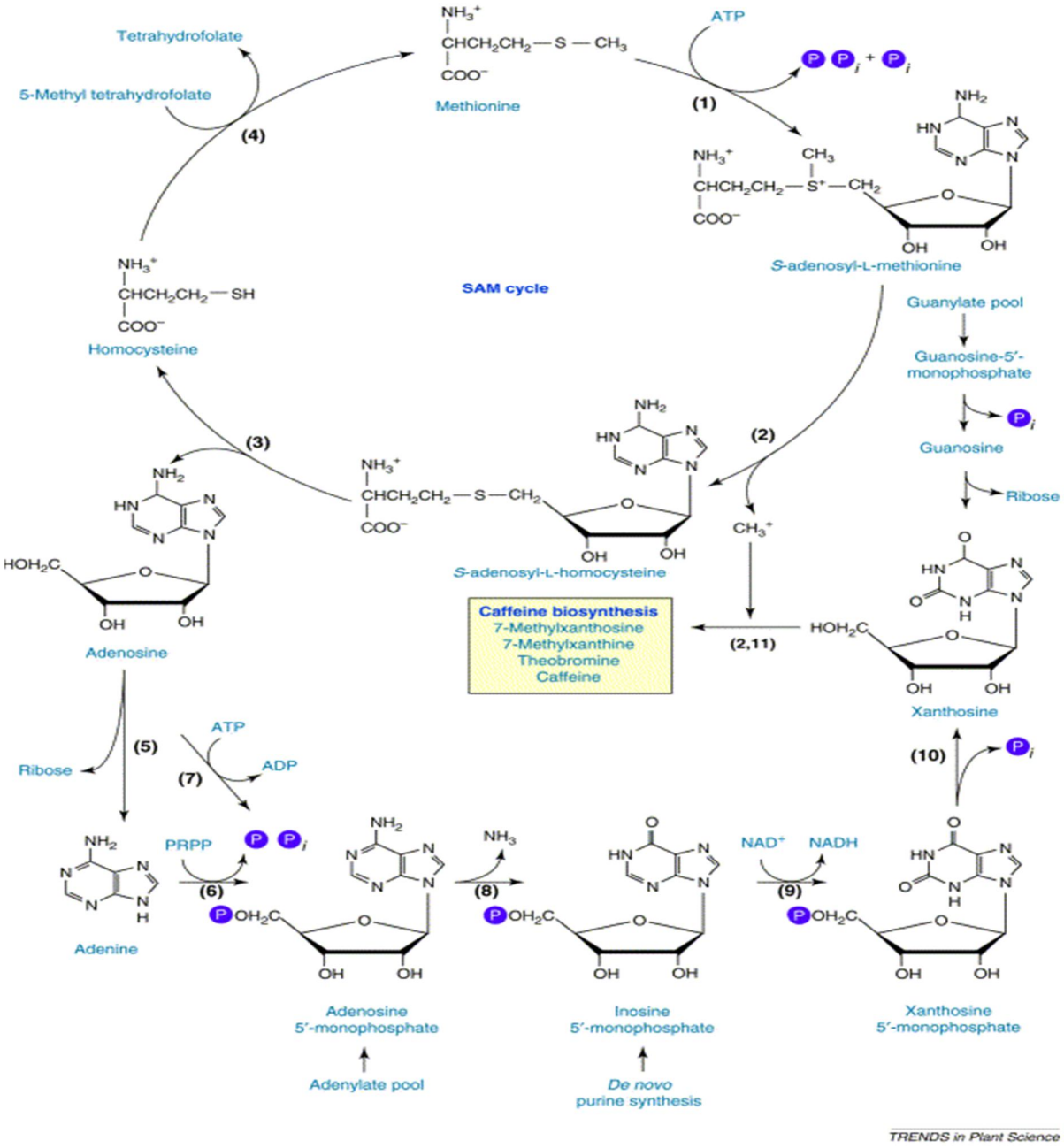

Abbreviations → ADP- adenosine 5′-diphosphate; ATP- adenosine 5′-triphosphate; NAD- nicotinamide adenine dinucleotide; NADH- reduced NAD; PRPP- 5-phosphoribosyl-1-diphosphate. Enzymes: (1) SAM synthetase; (2) SAM-dependent N-methyltransferases; (3) S-adenosyl-L-homocysteine hydrolase; (4) methionine synthase; (5) adenosine nucleosidase; (6) adenine phosphoribosyltransferase; (7) adenosine kinase; (8) adenine 5′-monophosphate deaminase; (9) inosine 5′-monophosphate dehydrogenase; (10) 5′-nucleotidase; (11) 7-methylxanthosine nucleosidase.

Figure 2.8: The biosynthesis of purine alkaloids (Ashihara & Crozier, 2001).

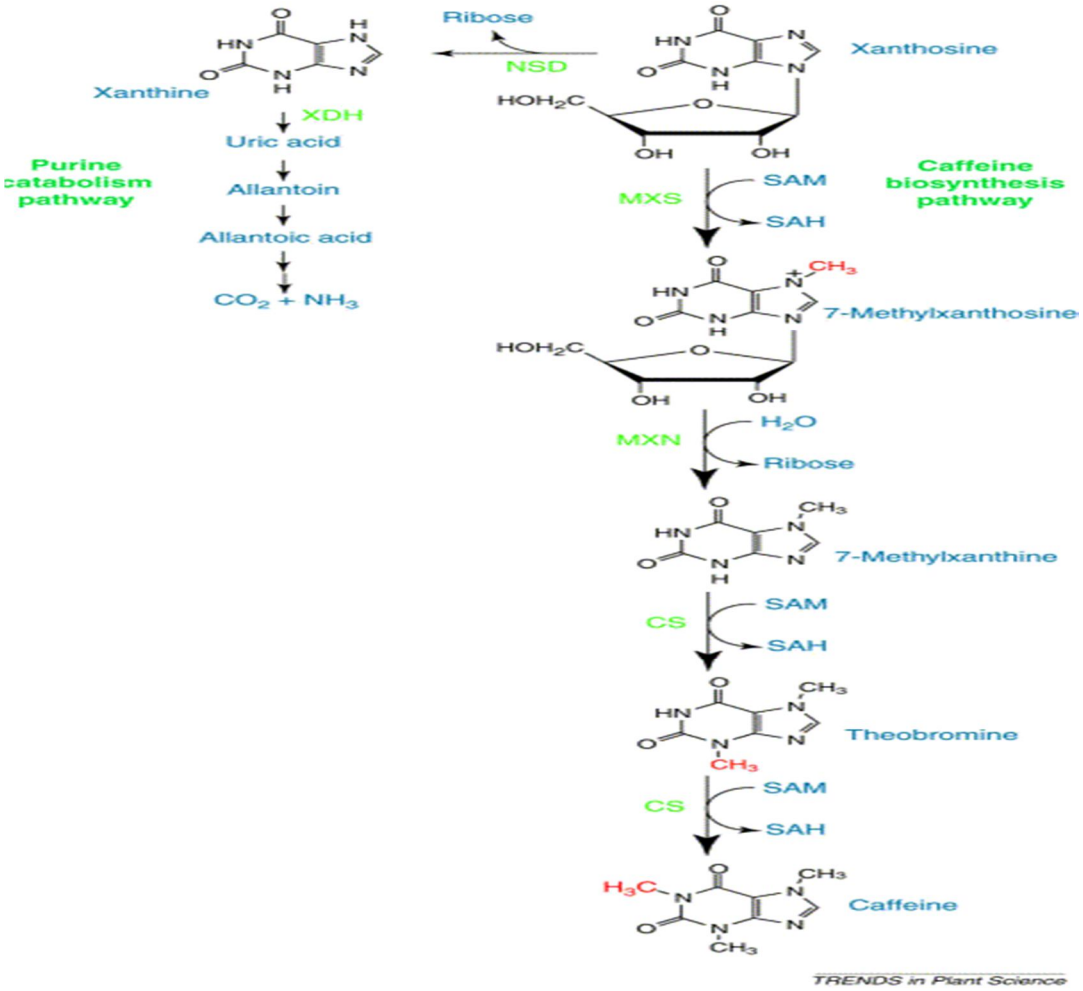

Abbreviations → CS- caffeine synthase; MXS- methylxanthosine synthase; MXN- methylxanthosine nucleotidase; NSD- inosine–guanosine nucleosidase; SAH- S-adenosyl-L-homocysteine; SAM- S-adenosyl-L-methione; XDH- xanthine dehydrogenase.

Figure 2.9: The biosynthesis of caffeine and the breakdown of xanthine (Ashihara & Crozier, 2001).

2.1.4.3. Pharmacokinetics

Caffeine is readily absorbed after oral administration. The peak plasma concentrations of caffeine are reached in about 30-60 min after consumption. The half-life is 3-5 hrs. Caffeine is distributed throughout the body and even crosses the blood-brain barrier and the placental barrier (Lorist & Tops, 2003). In adults, caffeine is completely metabolised and only about 2% is recoverable in urine unchanged. 80% of orally administered caffeine is metabolised to paraxanthine (1,7-dimethylxanthine) and 16% is converted to theobromine (3,7-dimethylxanthine) and theophylline (1,3-dimethylxanthine) (Xu *et al*., 2010).

Table 2.1: Opposing pharmacological actions of caffeine and adenosine antagonists

	Caffeine	**Adenosine**
CNS	Increases spontaneous electrical activity	Decreases spontaneous electrical activity
	Enhances neurotransmitter release	Inhibits neurotransmitter release
	Convulsant activity	Anticonvulsant activity
	Stimulates locomotor activity	Depresses locomotor activity
	Increases operant response rates	Decreases operant response rates
Heart	Positive inotropic/chronotropic effects	Negative inotropic/chronotropic effects
Renal	Diuresis; stimulates renin release	Antidiuresis; inhibits renin release
Peripheral Vasculature	Dilation	Constriction
Central Vasculature	Constriction	Dilation
Gastrointestinal	Increases gastric secretions	Inhibits gastric secretions
Respiratory	Relaxes bronchial smooth muscle	Constricts/dilates bronchial smooth muscle
Adipose	Stimulates lipolysis	Inhibits lipolysis

2.1.4.4. Mechanism of action of caffeine

Caffeine has been proposed to have three mechanisms of action, namely:

- mobilisation of intracellular calcium,
- inhibition of phosphodiesterase activity and
- antagonism of adenosine receptors.

Caffeine mobilises intracellular calcium in neurons by reducing calcium uptake in microsomal vesicles and by stimulating the release of calcium from the endoplasmic reticulum. However, the effect of caffeine to mobilise intracellular calcium is achieved at higher doses than that obtained via normal caffeine consumption. Caffeine also inhibits cyclic nucleotide activity, which results in an accumulation of cyclic adenosine monophosphate (cyclic AMP). Cyclic AMP mediates the cellular effects required to achieve the physiological and behavioural effects produced by the activation of neurotransmitter systems. It has been suggested that inhibition of phosphodiesterase activity by caffeine does not necessarily occur at higher

doses than that obtained after caffeine consumption (Garret & Griffiths, 1997). The main pharmacological effect of caffeine after one to two cups of coffee is adenosine receptor antagonism. Studies have indicated that the CNS effects of caffeine are mediated by its antagonistic actions at the A_1 and A_2 subtypes of the adenosine receptors (Lorist & Tops, 2003; Nehlig, 1999). Caffeine primarily blocks A_1, A_{2A} and A_{2B} receptors. It has lower affinity for A_3 receptors. Caffeine is a competitive antagonist of adenosine and produces effects that are opposite to those of adenosine (Table 2.1) (Garrett & Griffiths, 1997).

2.2. MONOAMINE OXIDASE

2.2.1. General background and tissue distribution

Mitochondrial MAO exists as two isoenzymes, namely MAO type A and MAO type B (Youdim & Bakhle, 2006). Although they share 70% sequence identity (Binda *et al*., 2007), these isoforms have differences that are of therapeutic significance:

- they have different pH optima and sensitivity to heat inactivation
- MAO-A is inhibited by clorgyline and metabolises noradrenaline (NA) and serotonin (5-HT)
- MAO-B is resistant to clorgyline and prefers benzylamine as substrate

Both these forms oxidize dopamine, tryptamine and tyramine. MAO is involved in the oxidative deamination of a range of monoamines, including 5-HT, histamine and catecholamines, with the generation of hydrogen peroxide (Youdim *et al.*, 2006).

According to a study done by Green & Youdim (1975), both MAO-A and −B are located throughout the brain and is attached to the membrane of mitochondria. MAO is a flavoprotein with FAD as a cofactor (Youdim & Bakhle, 2006). Although the MAOs have been identified in the brain and peripheral organs, our main focus will be on the central nervous system. The significance of MAO in central nervous system functions is demonstrated by the aggressive behaviour associated with genetic deficiencies of MAO-A activity in man (Cases *et al*., 1995; Brunner *et al*., 1993). Alterations in MAO-B activity has been implicated in PD (Sano *et al*., 1997).

MAO-A is localised in the catecholaminergic neurons, while MAO-B is the form most abundant in serotonergic and histaminergic neurons and glial cells. In the brain, MAO-A is found in the locus coeruleus and the highest concentration of MAO-B is found in the raphe nuclei (Jahng *et al*., 1997; Luque *et al*., 1995; Saura *et al*., 1994; Willoughby *et al*., 1988). In

studies done on foetal tissue, it has been shown that the liver is the organ with the highest MAO-A and MAO-B activities. MAO-A activity seems to emerge before that of MAO-B in the foetal brain, lung, aorta and digestive tract (Lewinsohn *et al*., 1980). Studies have also shown an age-related increase in MAO-B activity and little to no variation in MAO-A activity. An increase in MAO-B activity may cause oxidative stress, which may be a factor which contributes to an increase in vulnerability to neurodegeneration in the aged brain (Carlsson, 1981; Gotttries *et al*., 1975; Fahn & Cohen, 1992; Fowler *et al*., 1980; Kornhuber *et al*., 1989; Sparks *et al.,* 1991; Volchegorskii *et al*., 2001).

2.2.2. Biological function of MAO

MAO is also found in peripheral tissues such as the liver, lungs, intestine, kidneys and placenta. Three main findings indicate the importance of peripheral MAOs (Mannelli *et al*., 1990; Pizzinat *et al*., 1999):

- These enzymes are widely distributed in peripheral organs, and in some organs their expression is equivalent or even higher than that in the CNS.
- Monoamine transmitters regulate functions in a large variety of peripheral organs.
- Peripheral MAOs represent one of the major metabolic pathways of circulating catecholamines and exogenous amines.

MAO seems to protect the body by oxidizing amines in the blood or preventing their entry into circulation. MAO-B acts as a metabolic barrier in the microvessels of the blood-brain barrier. In both the peripheral tissues and CNS, intraneuronal MAO-A and MAO-B protect neurons from exogenous amines, terminate the actions of amine neurotransmitters and regulate the contents of intracellular amine stores (Youdim *et al*., 2006).

2.2.2.1. Genes

MAO-A and MAO-B are distinct proteins, with molecular weights of 59 and 58 kDA, respectively. They are located on the short arm of chromosome X, closely located between bands Xp11.23 and Xp22.1 (Chen, 2004; Shih *et al*., 1999). The MAO-A and MAO-B genes consist of 15 exons and show identical intron-exon organisation. The genes are arranged in tail-to-tail orientation (Lewis *et al*., 2007). Exon 12 codes for the covalent FAD-binding region. Binding of FAD is essential for enzyme function. This site has been identified as the most conserved exon, showing 93.9% sequence identity. This suggests that the MAO-A and MAO-B genes are derived by duplication of a single ancestral gene (Grimsby *et al*., 1991).

2.2.2.2. The cheese reaction

The cheese-reaction results from the inhibition of MAO, which is accompanied by potentiation of the effects of indirectly acting sympathomimetic amines such as tyramine. Foods that commonly cause this effect include cheese, beer and red wine. Under normal conditions, dietary amines are extensively metabolised by MAO in the gut wall and in the liver and would thus not enter the systemic circulation. During periods of MAO inhibition, this protective system is inactivated. Thus tyramine or other monoamines that are present in ingested food enter the circulation unmetabolised. From here, they induce a significant release of noradrenaline from peripheral adrenergic neurons. This results in a severe hypertensive response, which may be fatal if not treated instantly. This effect is the basis of the reaction that is known as the cheese-reaction. Selective irreversible MAO-B inhibitors do not exhibit this effect because the intestine contains a modest of amount MAO-B. These serious adverse effects prompted researchers to search for new antidepressants and limited the use of MAO-A inhibitors in depression (Finberg *et al*., 1981; Finberg & Tenne, 1982; Youdim & Bakhle, 2006).

2.2.2.3. MAO-A in depression

MAO inhibitors were first marketed as antidepressants, with iproniazid being the first MAO inhibitor to be discovered. Iproniazid was initially used for the treatment of tuberculosis but it was subsequently discovered that iproniazid produced antidepressant effects in patients. These effects were proposed to result from the selective inhibition MAO-A in the CNS, which leads to increased levels of dopamine, noradrenaline and serotonin (Youdim *et al*., 2006). As mentioned earlier, both noradrenaline and serotonin are substrates of MAO-A. The occurrence of the cheese reaction prompted researchers to develop reversible MAO-A inhibitors such as moclobemide (Youdim & Bakhle, 2006). Moclobemide was evaluated for antidepressant activity and was found to be active. The elderly respond well to moclobemide, even though it is considered to be a mild antidepressant. Moclobemide is devoid of the cheese reaction; it appears to be safe and may improve vigilance, psychomotor speed and long-term memory (Bonnet, 2003). Approximately 60% of PD patients may experience depression during disease progression. Therefore the antidepressant action of moclobemide may be useful in PD patients (Youdim & Bakhle, 2006).

2.2.2.4. Serotonin syndrome

Serotonin syndrome (ST) is best defined by the manifestation of these clinical features:

1) neuromuscular hyperactivity: tremor, clonus, myoclonus, and hyperreflexia, and in the advanced stage, pyramidal rigidity;
2) autonomic hyperactivity: diaphoresis (profuse sweat), fever, tachycardia, tachypnia and mydriasis; and
3) altered mental status: agitation and excitement, with confusion in the advanced stage only (Gillman, 2006).

According to literature any combination of MAO inhibitors and selective serotonin reuptake inhibitors (SSRI) may induce the severe symptoms of this syndrome (Whyte *et al*., 2003; Whyte & Dart, 2004). A number of drugs may precipitate ST (Table 2.2) either by inhibition of serotonin uptake, presynaptic release of serotonin or MAO inhibition. Irreversible or nonselective MAO-A inhibitors are the main precipitants of ST especially when used in combination with meperidine, dextromethorphan, an SSRI or methylenedioxymethamphetamine (ecstacy). MAO-A plays a crucial role in the synthesis and metabolism of serotonin (Figure 2.10), hence the lethal combination of MAO inhibitors and serotonin releasers (Boyer & Shannon, 2005; Gillman, 2006).

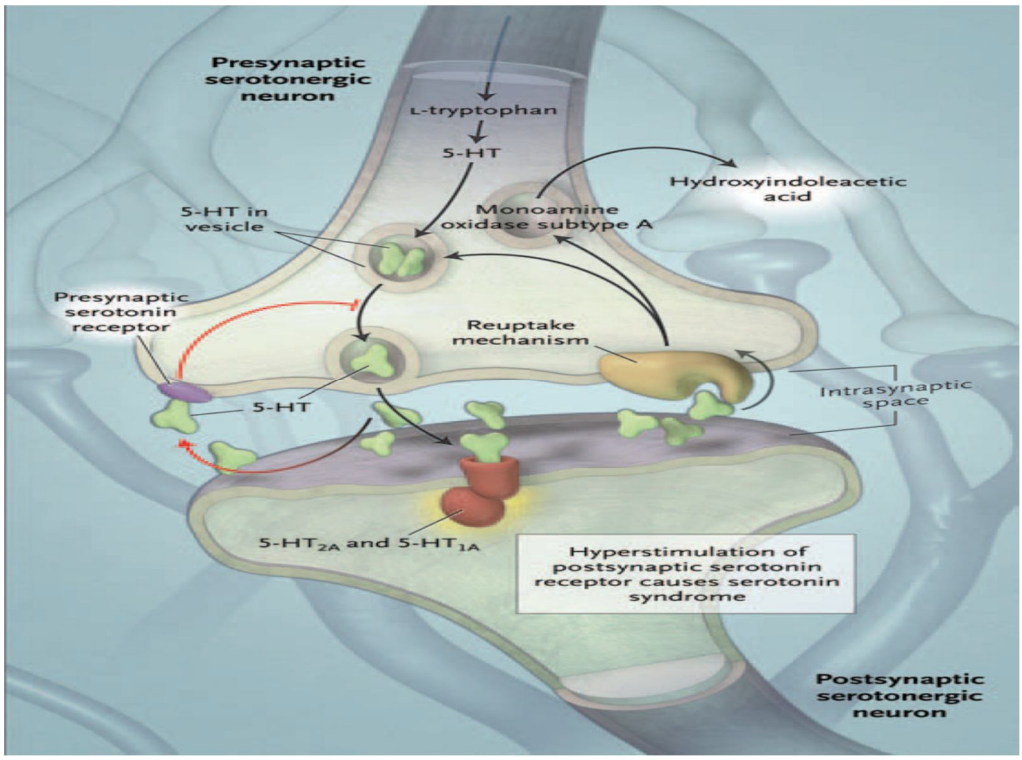

Figure 2.10: The synthesis and metabolism of serotonin (Boyer & Shannon, 2005).

According to Boyer & Shannon (2005), serotonin is generated by hydroxylation and decarboxylation of L-tryptophan. Serotonin then resides in vesicles until it is needed for neurotransmission. After axonal excitation, serotonin is released into the intrasynaptic space. Presynaptic serotonin receptors function as a feedback loop to inhibit exocytosis of vesicles. Serotonin then returns to the cytoplasm by a reuptake mechanism, where it is re-incorporated into vesicles. Serotonin is metabolised by monoamine oxidase A to hydroxyindoleacetic acid (Figure 2.10).

Table 2.2: Serotonergic Drugs

SSRIs (selective & nonselective)
Paroxetine, sertraline, fluoxitine, fluvoxamine, citalopram, chloromipramine, imipramine
Tramadol, meperidine (pethidine), fentanil, methadone, dextromethorphan, dextropropoxyphene, pentazocine
Chlorpheniramine, brompheniramine
Serotonin Precursors
5-hydroxytryptophan, L-tryptophan
5-HT1A Antagonists
LSD, dihydroergotamine, bromocriptine, buspirone
Serotonin Releasers
Amphetamine , MDMA
MAO inhibitors
Tranylcypromine, phenelzine, nialamide, isoniazid, iproniazid, isocarboxazid
Pargyline, selegiline, clorgyline, furazolidone, procarbazine, linezolid
Moclobemide

Abbreviations → 5-HT, 5-hydroxytryptamine; LSD, lysergic acid diethylamide; MDMA, 3,4-methylenedioxymethamphetamine; MAO, monoamine oxidase (Gillman, 2006).

2.2.3. The role of MAO-B in Parkinson's disease

The neuroprotective potential of MAO-B was observed when researchers discovered that MAO-B oxidises the parkinsonian neurotoxin, MPTP to its active form, MPP^+, in the brain (Markey *et al*., 1984). MPTP crosses the blood brain barrier (BBB) into the brain where it is converted in the glial cells by MAO-B to MPP^+. From there it is taken up into the nigrostriatal dopaminergic neurons where it inhibits mitochondrial respiration and induces neuronal death. Inhibitors of MAO-B were found to prevent the neurotoxic action of MPTP by blocking its metabolic activation via MAO-B. This raised the possibility that MAO-B may be involved in the activation of similar parkinsonian neurotoxins which may contribute to the development of PD. Should this be true, MAO-B inhibitors may find application as neuroprotectants in PD.

MAO-B inhibitors may also be useful as adjuvants to L-dopa in PD therapy. It was discovered that L-dopa, the dopamine precursor, may supplement dopamine deficiency in the striatum and improve the symptoms of movement disorders. L-dopa was subsequently initiated in PD therapy. Recent studies have shown that the combination of L-dopa with selegiline, a MAO-B inhibitor, may lead to a reduction of the dose of L-dopa required for PD therapy. MAO-B inhibitors may also have neurotrophic and antiapoptic activity (Carlsson, 1959; Birkmayer *et al*., 1973).

2.2.3.1. Metabolism of dopamine and the generation of toxic by-products

Intracellular dopamine may be oxidised by two mechanisms in the brain:

- MAO metabolism which leads to the production of dihydroxyphenylacetic acid (DOPAC) and hydrogen peroxide (H_2O_2), and
- auto-oxidation of dopamine which generates H_2O_2 and dopamine-quinone, which may covalently bind to proteins or be converted to neuromelanin (Figure 2.11).

The hydrogen peroxide produced during the metabolism of dopamine, may be converted to the highly active free radical, the hydroxyl radical ($HO^{\cdot}$) by Fe^{2+} ions (Fenton reaction). This radical may cause neuronal damage and possibly death. H_2O_2 may also be inactivated by glutathione peroxidase in the brain. For this reaction, glutathione (GSH) serves as a cofactor. When MAO and iron levels are increased, as seen in the case of PD, and GSH levels are low, the possibility that hydrogen peroxide may act as a substrate in the Fenton reaction is much greater, with consequent increases in oxidative damage to neurons. Thus MAO inhibition is a strategy for decreasing the formation of hydrogen peroxide and thus

decreasing the formation of the hydroxyl radical and oxidative stress (Hald & Lotharius, 2005; Youdim & Bakhle, 2006).

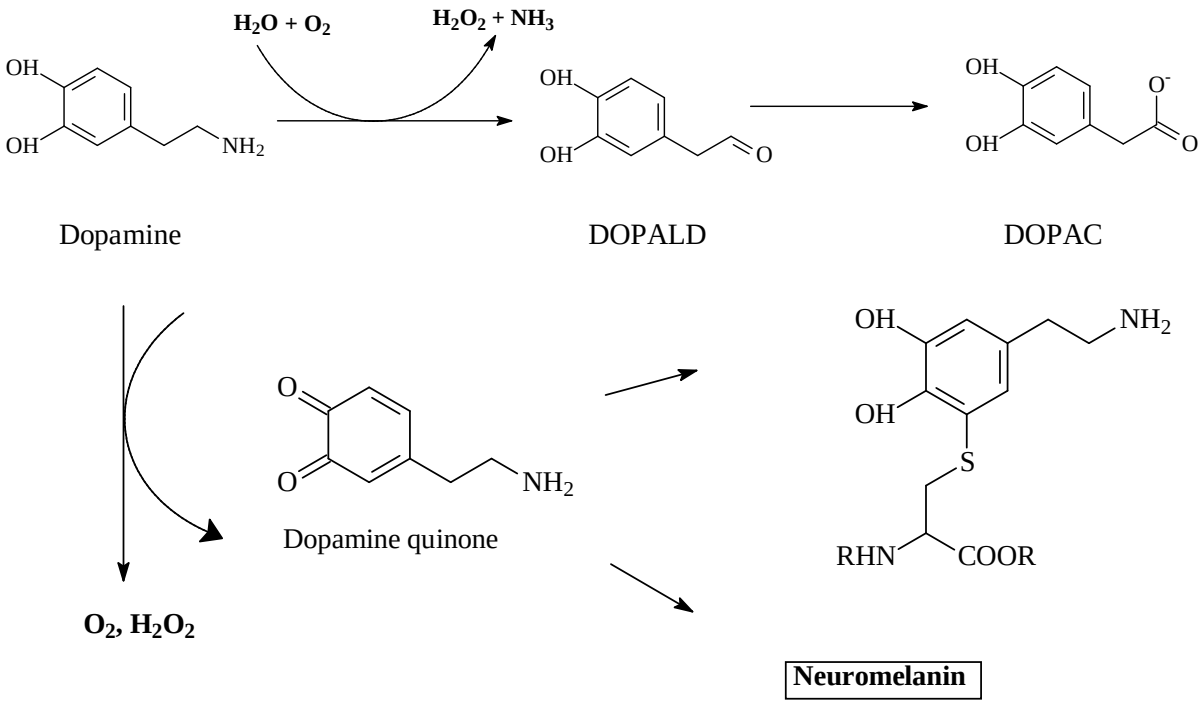

Abbreviations → DOPAC, dihydrophenylacetic acid; DOPALD, dihydroxyphenylacetaldehyde.

Figure 2.11: The oxidation of dopamine (Hald & Lotharius, 2005).

2.2.3.2. MAO levels in the brain and aging

Post-mortem brain tissues have shown that MAO-B activity increases with age, with little to no variation in MAO-A activity. This increase may be attributed to the proliferation of glial cells during aging (Fowler *et al*., 1980). Studies done by Kornhuber *et al*. (1989) have shown that MAO-A activity is high at birth and decreases rapidly during the first two years of life. The MAO-A levels remain constant thereafter. MAO-B activity follows a totally different model from that of MAO-A. MAO-B activity remains constant during early childhood and then increases with age. Increase in MAO-B activity has deleterious effects in neuronal cells and may make the brain more susceptible to neurodegenerative diseases (Nicotra *et al*., 2004).

2.2.3.3. The role of iron and glutathione in PD

GSH is a tripeptide (γ-L-Glu-L-Cys-Gly) and the most abundant nonprotein thiol compound in mammalian cells. Its crucial role is to remove the hydrogen peroxide formed during normal cellular metabolism. It thus acts as a free radical scavenger, especially of the hydroxyl radical. It has been observed though, that there are decreased levels of GSH in the brains of PD patients. It has also been proposed that GSH depletion is the first indicator of oxidative stress during PD progression. The evidence of oxidative stress in PD and the role of GSH were previously summarised by Benzi & Moretti (1995) as follows:

- Enhanced oxidation of dopamine by MAO-B and increased Mn-SOD (superoxide dismutase) activity are present, both of which stimulate the formation of H_2O_2 in mitochondria.
- There is an elevated iron content that produces free radicals via the Fenton reaction.
- The presence of neuromelanin has been observed, which is an indicator of a high level of dopamine oxidation.
- A positive correlation between cellular deficit and decreased GSH content in PD brain samples has been reported.
- Elevated levels of lipid peroxides and hydrogen peroxide are present.
- Increased oxidative damage to DNA has been detected (Bains & Shaw, 1997; Benzi & Moretti, 1995).

A reduction of GSH, as observed in the SNpc, is correlated with the severity of PD which indicates a concomitant increase in ROS. Apart from the reduction in GSH there is another component supporting the role of oxidative stress in PD, iron. Iron promotes auto-oxidation of dopamine, releasing additional H_2O_2. Iron catalyses the conversion of excess dopamine to neuromelanin. Neuromelanin is an insoluble black-brown pigment that accumulates in dopaminergic neurons with age in humans. When neuromelanin is bound to excess Fe^{3+}, it converts from being a neuroptotective agent to a pro-oxidant. Neuromelanin reduces Fe^{3+} to Fe^{2+}, which is then released from neuromelanin due to weak affinity. This increases the neuronal labile iron pool and the fraction of iron capable of reacting with H_2O_2. Under normal conditions GSH prevents the accumulation of H_2O_2 thus preventing the production of $OH^{\cdot}$ radicals. However, in conditions of depleted GSH as in the case of PD, this protection is weakened, leading to oxidative stress (Bharath *et al*., 2002; Ben-Shachar *et al*., 1991).

2.2.4. MAO-B inhibitors

Most of the previously investigated MAO-B inhibitors are irreversible, including the first identified MAO-B inhibitor, selegiline. A number of irreversible inhibitors have also been derived from selegiline, including *N*-methyl-N-2-propynyl-1-indanamine and AGN-135 (rasagiline). These drugs are known as suicide-type drugs (Foley *et al*., 2000). There are however also reversible inhibitors that have been synthesised. CSC (Figure 2.12), an adenosine A_{2A} antagonist, has been found to inhibit MAO-B with a K_i-value of 70 nM (Vlok *et al*., 2006). Safinamide (Figure 2.12), which is also a reversible inhibitor of MAO-B, may represent an alternative to currently available therapies as an adjunct to L-dopa or dopamine agonists in patients with PD (Fernandez & Chen, 2007). Another highly selective reversible inhibitor of MAO-B, lazabemide (Figure 2.12), was found to be well tolerated and may even delay the need for L-dopa in early untreated PD. Its antioxidant activity was also found to be more pronounced than that of selegiline (Riederer *et al*., 2004).

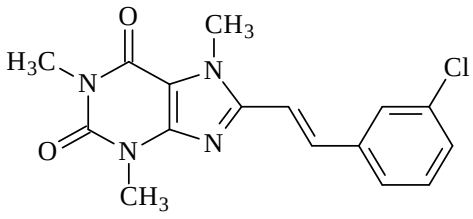

CSC

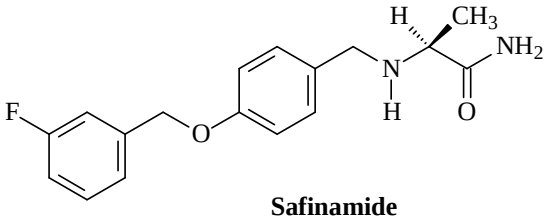

Safinamide

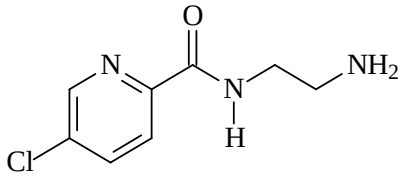

Lazabemide

Figure 2.12: Chemical structures of MAO-B inhibitors

2.2.5. Mechanism of action of MAO-B

2.2.5.1. The FAD cofactor and flavin adducts

MAO is a flavoprotein which contains FAD as a cofactor. Covalent binding to the FAD is essential for MAO activity. This cofactor was identified as the site at which irreversible inhibitors, such as pargyline and rasagiline, are covalently linked (Youdim & Bakhle, 2006). The flavin of the two isoforms (MAO-A and –B) is attached to the enzymes *via* a thioether

linkage between a cysteinyl residue and the 8α- position of the flavin ring (Figure 2.13). The cysteine linkage is to Cys_{397} in The cysteine linkage MAO-B and Cys_{406} in MAO-A. The site for covalent linkage is towards the C-terminal portion of the molecule (Bach *et al*., 1988; Kearney *et al*., 1971).

Data from Edmondson *et al.* (2004) suggests that the flavin structure facilitate the formation of adducts at either N(5) or at C(4a). Structural studies of the MAO-B-pargyline complex have suggested the nature of the covalent linkage to be an N(5) flavocyanine adduct (Figure 2.14, **A**). The binding of tranylcypromine to MAO forms a C(4a) adduct (Figure 2.14, **C**), which decays slowly on standing and more swiftly by enzyme denaturation (Paech *et al*., 1980). A 2.2 Á structure of MAO-B in complex with N-(2-aminoethyl)-p-chlorobenzamide shows an adduct formed at the N(5) position of the flavin ring (Figure 2.14, B). Thus, irreversible MAO inhibitors will form either N(5) or C(4a) flavin adducts with MAO-B (Edmondson *et al*., 2004; Silverman, 1995).

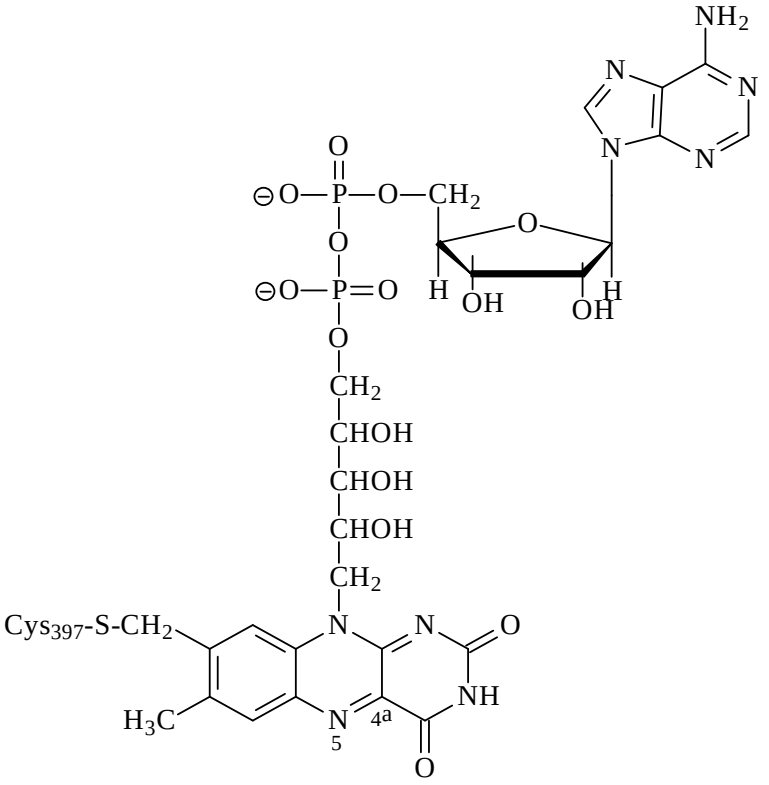

Figure 2.13: Structure of covalent FAD in MAO-B (Edmondson *et al*., 2004)

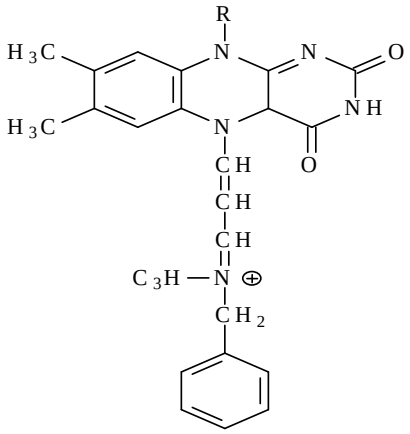

(A)

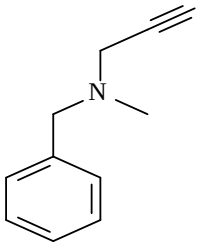

Pargyline

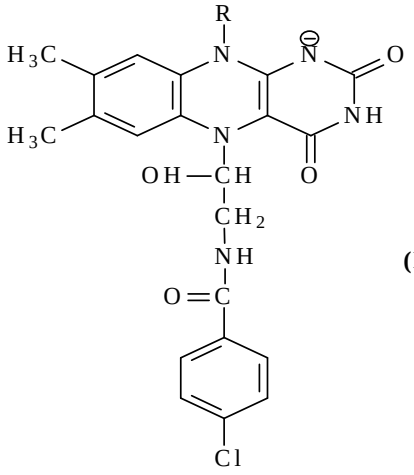

(B)

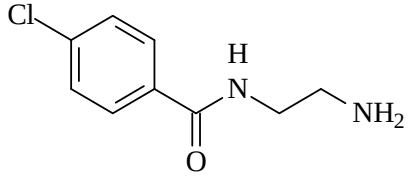

N-(2-aminoethyl)-p-chlorobenzamide

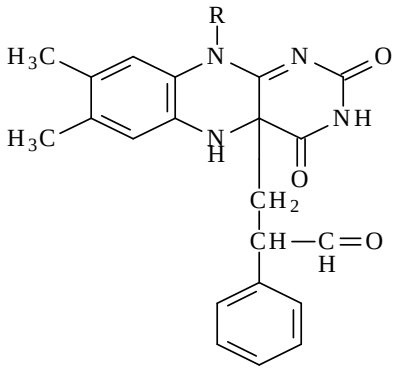

(C)

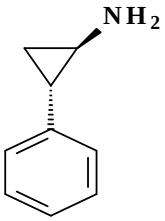

trans-2-phenylcyclopropylamine

Figure 2.14: Proposed structures of the flavin adducts with the oxidation products of (A) pargyline, (B) N-(2-aminoethyl)-*p*-chlorobenzamide and (C) trans-2-phenylcyclopropylamine

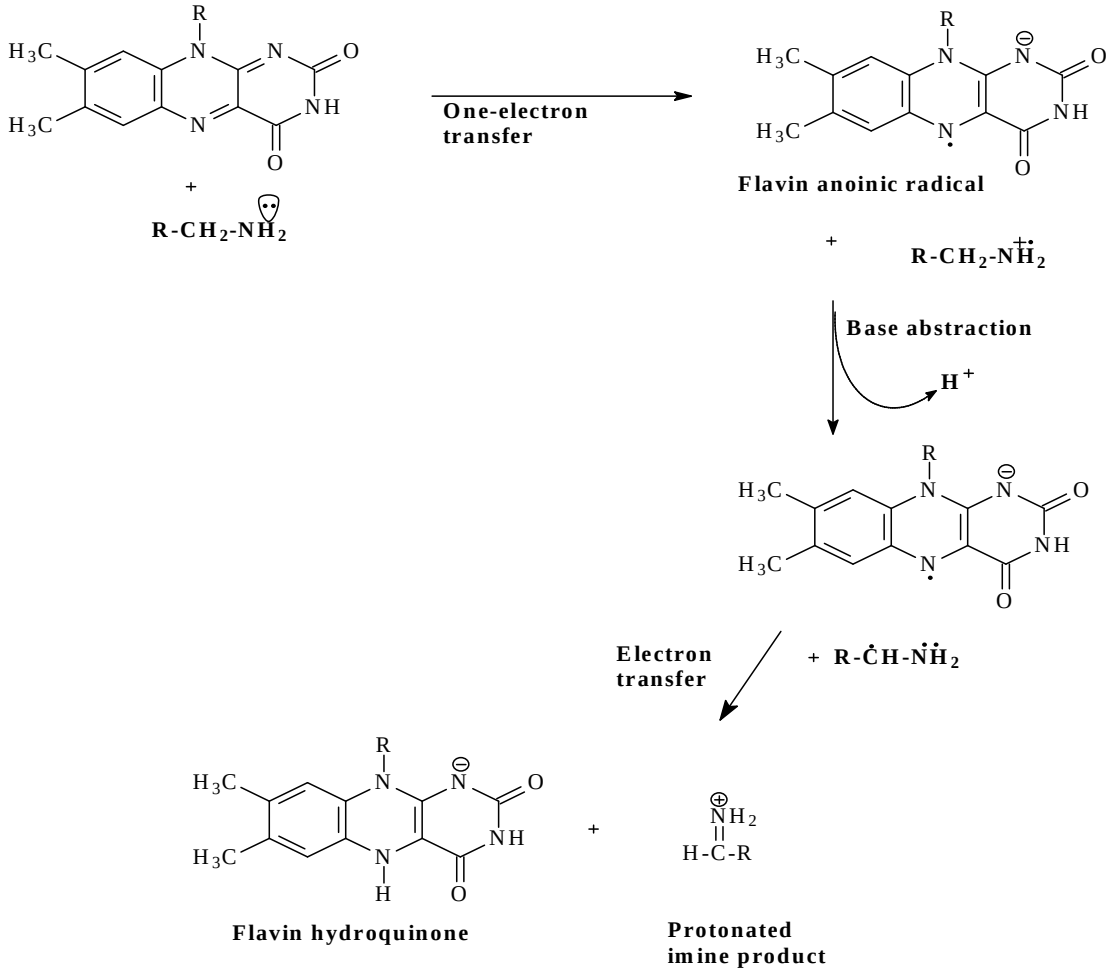

Figure 2.15: The single electron transfer mechanism proposed for MAO catalysis

2.2.5.2. The SET and polar-nucleophilic pathway

There are two mechanisms that have been proposed for the transfer of electrons from the amine to the flavin in MAO catalysis, namely:

- Single electron transfer (SET) mechanism
- Polar nucleophilic mechanism (Edmondson *et al*., 2004).

According to the SET mechanism, the first step in the reaction is a one-electron oxidation of the lone pair on the amine nitrogen to form an aminium cation radical and a flavin radical (Figure 2.15). The aminium radical lowers the pKa of the α-C-H which facilitates the withdrawal of H^+ by an active site base in the catalytic site. Current data on MAO-B shows no amino acid residues in the catalytic site that can perform this role (Edmondson *et al*., 2004, Miller *et al*., 1995).

In the polar nucleophilic mechanism (Figure 2.16), the deprotonated amine functionality nucleophilically attacks the flavin at the C(4a) position as the initial step. On formation of the C(4a) adduct, the N(5) position of the flavin becomes a strong enough base to abstract the α-pro-R-H from the substrate. However, this hypothesis still needs experimental verification. This mechanism, unlike the SET pathway is much more consistent with the current structural data on MAO-B (Edmondson *et al*., 2004).

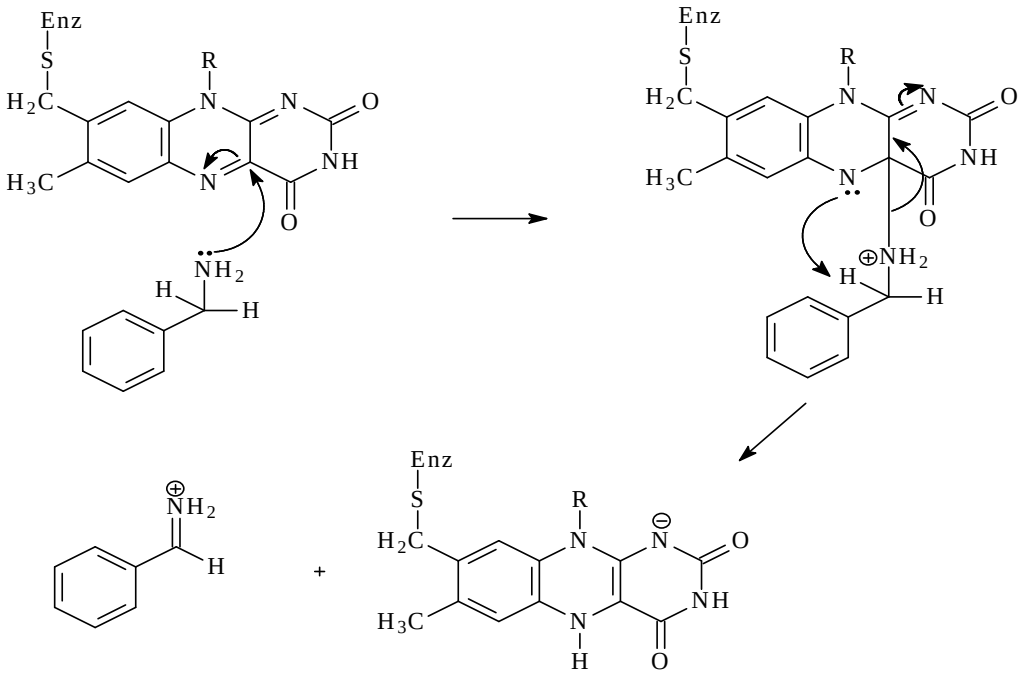

Figure 2.16: The polar nucleophilic mechanism.

2.2.6. Three dimensional structure of MAO-B

MAO-B consists of 520 amino acids. There are 3 functionally distinct domains apparent in the crystal structure of human MAO-B. The substrate domain contains two cavities. These cavities are the entrance cavity, which leads to the inner space, and a substrate binding cavity (Figure 2.17), closer to the flavin cofactor. These two cavities are separated by a gate formed by the residue Ile_{199} (Binda *et al*., 2002; Youdim & Bakhle, 2006). The C-terminal region (501-520) is believed to be a transmembrane α-helix that anchors the enzymes to the mitochondrial outer membrane, with the rest of the protein exposed to the cytoplasm. Substrate entry into the active site of human MAO-B occurs near the intersection of the enzyme with the surface of the membrane. There are four residues namely Tyr_{326}, Ile_{199}, Leu_{171} and Phe_{168} that form a boundary between the entrance cavity and the substrate cavity. The substrate cavity is believed to be of a hydrophobic nature and flat (Youdim *et al*.,

2006). The X-ray crystal structure of MAO-B, in complex with rasagiline, shows that rasagiline occupies both the entrance and substrate cavities when bound to MAO-B. Both isomers (R & S) of rasagiline bind covalently to MAO-B, although only the *R* isomer is pharmacologically active. The binding of rasagiline thus blocks access for the substrate (Youdim & Bakhle, 2006). In general, all propargyl containing MAO-B inhibitors bind covalently to the N(5) position of the flavin moiety between two tyrosine residues (Tyr_{398} and Tyr_{435}). Cys_{397}, a residue that is situated adjacent to the tyrosine residues forms a covalent thioether linkage to the 8α position of the flavin ring. The amide linkages of these two tyrosines (Tyr_{398} and Tyr_{435}) to the protein are in energetically unfavourable *cis* conformations. These conformations allow the phenolic side chains to form an 'aromatic sandwich' structure. Since inhibitors and substrates pass between the 2 tyrosine phenolic rings to reach the flavin ring, this structure is of functional significance (Youdim *et al*., 2006).

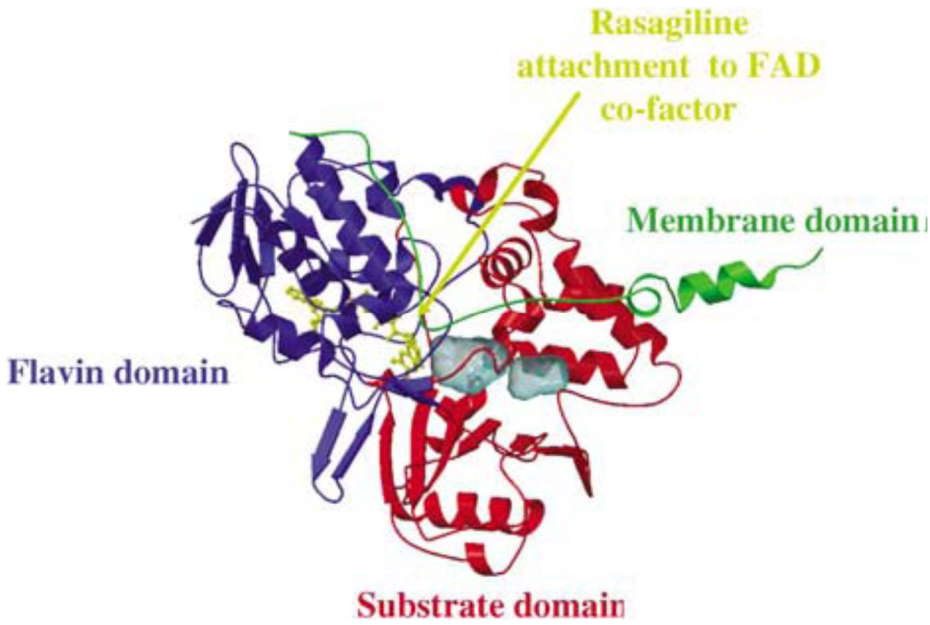

Figure 2.17: The crystal structure of MAO-B in complex with rasagiline (Youdim & Bakhle, 2006).

2.2.7. Three dimensional structure of MAO-A

The structure of MAO-A can be divided into two domains namely:

- the extra-membrane domain and
- the membrane binding domain.

The extra-membrane domain is further divided into two regions, the FAD binding region and substrate/inhibitor binding region (Son *et al*., 2008). The active site of MAO-A consists of a hydrophobic cavity of 500 $Å^3$, which is smaller than that of MAO-B (700 $Å^3$). MAO-A is unique in that it crystallises as a monomer (Figure 2.18). MAO-A consists of only one binding cavity, the active site. The cavity extends from the flavin ring to the cavity-shaping loop, consisting of residues 210-216. Similar to MAO-B, the C-terminal region forms a transmembrane α-helix that attaches the enzyme to the mitochondrial outer membrane, with the rest of the protein exposed to the cytoplasm. Substrate entry into the active site also occurs at the intersection of the enzyme and the mitochondrial membrane, and the amino acids lining the active site cavity of MAO-A are similar to that of MAO-B. The back of the cavity is formed by the flavin ring. Similar to MAO-B, an aromatic sandwich consisting of the aromatic rings of Tyr_{407} and Tyr_{444} is present in front of the flavin. This is the site where amine substrates are believed to bind upon oxidation (De Colibus *et al*., 2005).

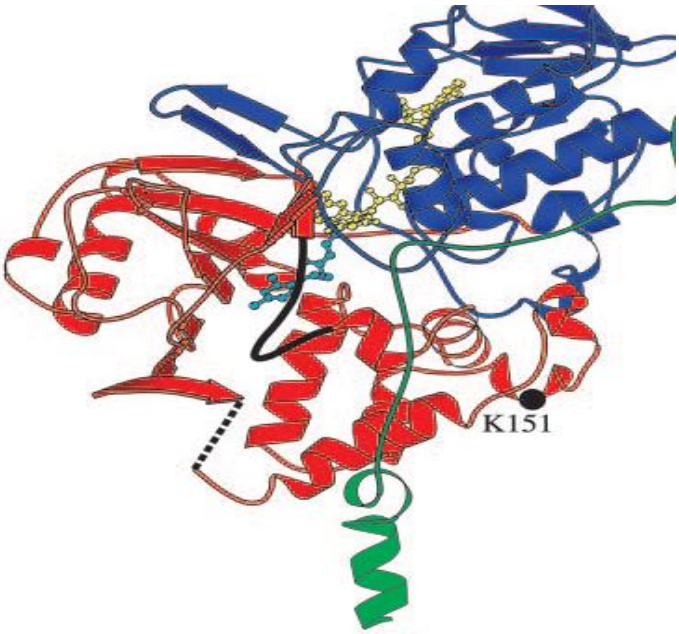

Figure 2.18: The structure of MAO-A.

2.3. Enzyme kinetics

The study of enzyme kinetics is concerned with the quantitative measurement of the rates of enzyme-catalysed reactions and the systemic study of factors affecting these rates. The study also represents the principal way to identify potential therapeutic agents that selectively improve or inhibit the rates of specific enzyme-catalysed processes. A complete

understanding of enzyme kinetics is thus important to understand how physiological stresses affect enzyme activities (Rodwell & Kennelly, 2003).

2.3.1. Michaelis-Menten kinetics

The Michaelis-Menten equation illustrates the relationship between V_i and [S].

$$V_i = \frac{V_{max} \times [S]}{K_m + [S]}$$

Equation 2.1

In the equation above K_m is the Michaelis constant, V_i is the initial velocity of the enzyme catalysed reaction and [S] is the substrate concentration. K_m is the substrate concentration at which V_i is half the maximal velocity $(V_{max}/2)$ attainable at a particular concentration of enzyme. The dependence of initial reaction velocity on [S] and K_m can be evaluated under 3 conditions.

a. When [S] is much less than K_m

$$V_i = \frac{V_{max} \times [S]}{K_m + [S]}$$

$$V_i \approx \frac{V_{max}[S]}{K_m}$$

Equation 2.2

When [S] is considerably lower than K_m, $V_i \propto k[S]$. The initial reaction velocity therefore is directly proportional to [S].

b. When [S] is much greater than K_m

$$V_i = \frac{V_{max}[S]}{K_m + [S]}$$

$$V_i \approx V_{max}$$

Equation 2.3

When [S] exceeds K_m to a great extent, the reaction velocity is maximal (V_{max}) and unaffected by further increases in substrate concentration.

c. When [S] = K_m

$$V_i = \frac{V_{max}[S]}{K_m + [S]} \approx \frac{V_{max}[S]}{2[S]} = \frac{V_{max}}{2}$$

Equation 2.4

When [S] is equal to K_m, the initial velocity is half of the maximal velocity (Cheng & Prusoff, 1973; Rodwell & Kennelly, 2003).

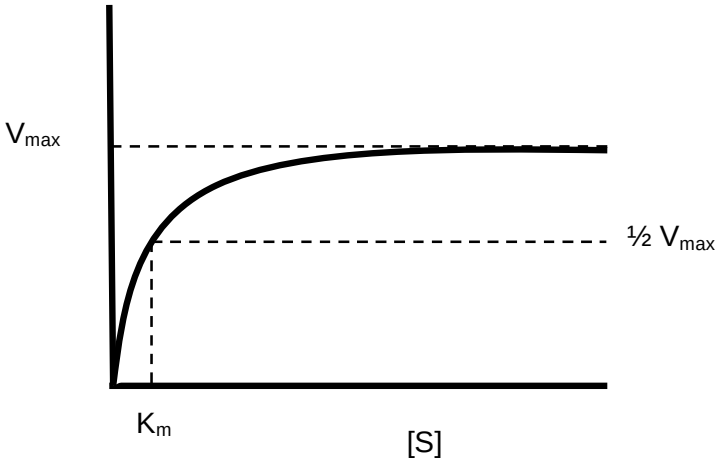

Figure 2.19: A graphical presentation of the Michaelis-Menten equation

Figure 2.19 is a graphical representation of the Michaelis-Menten equation. As can be seen, when the substrate concentration is relatively low, the rate of catalysis increases proportionally as the substrate concentration is increased. At high substrate concentrations there is no further increase of the rate since the enzyme is saturated at this point (V_{max}).

2.3.1.1. K_m and V_{max} determinations

A linear form of the Michaelis-Menten equation is used to determine K_m and V_{max}.

$$\frac{1}{v_i} = \left(\frac{K_m}{V_{max}}\right)\frac{1}{[S]} + \frac{1}{V_{max}}$$

Equation 2.5

To transform the Michaelis-Menten equation into its linear form, Equation 2.1 is inverted to yield Equation 2.5. Equation 2.5 is the equation for a straight line, $y = ax+b$, where $y = 1/v_i$

and *x* = 1/[S]. The plot of this equation is called a Lineweaver-Burk plot (Figure 2.20). From the plot, the K_m value may be obtained from the x-intercept while V_{max} may be obtained from the y-intercept.

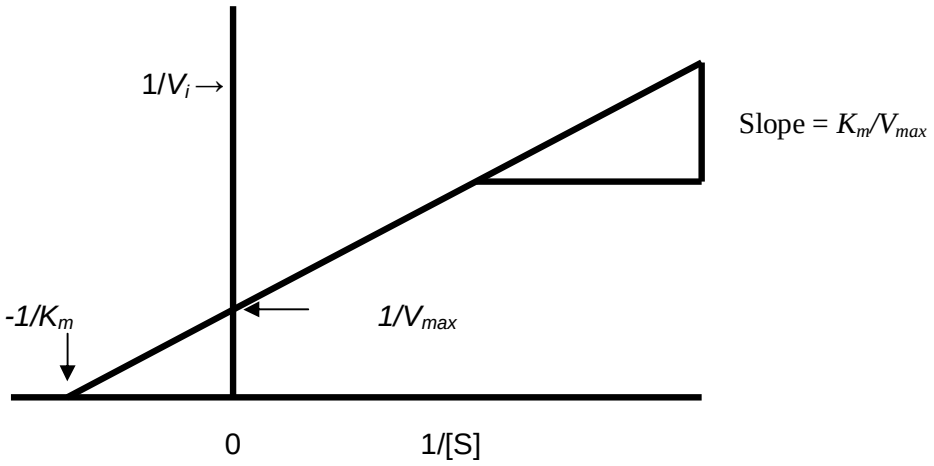

Figure 2.20: Lineweaver-Burk plot of $1/v_i$ *vs* 1/[S] (Rodwell & Kennelly, 2003).

2.3.1.2. K_i determination and competitive inhibition

K_i values are used to compare different inhibitors of the same enzyme. The K_i value is the enzyme-inhibitor dissociation constant for the reversible interaction of a competitive inhibitor with the active site of an enzyme. The lower the K_i value, the more effective the inhibitor (Rodwell & Kennelly, 2003). The K_i value may be calculated from the IC_{50} value according the following equation (Cheng, 2001):

$$K_i = \frac{IC_{50}}{1 + \frac{S}{K_m}}$$

Equation 2.6

K_i values may also be obtained by constructing a set of Lineweaver-Burk plots in the absence and presence of a competitive inhibitor. For this purpose the initial enzyme catalytic rates are measured in the absence of inhibitor and a Lineweaver-Burk plot is constructed. The initial enzyme catalytic rates are similarly measured in the presence of an inhibitor and a second Lineweaver-Burk plot is constructed. The slopes of the two plots obtained are subsequently graphed versus the inhibitor concentrations used and K_i is calculated from the x-axis intercept which is equal to $-K_i$ (Rodwell & Kennelly, 2003).

2.3.1.3. IC_{50} determination

The IC_{50} value represents the concentration of a drug that is required for 50% inhibition *in vitro.*

The relationship between the IC_{50} value and the K_i value is given by:

$$IC_{50} = K_i \left(1 + \frac{S}{K_m}\right)$$

Equation 2.7

IC_{50} values are measured by constructing a sigmoidal dose-response curve for the inhibition of an enzyme by an inhibitor. For this purpose initial enzyme catalytic rates are measured in the presence of different concentrations of the inhibitor. The initial rates are subsequently plotted versus the logarithm of the inhibitor concentration used, and the IC_{50} value may be obtained directly from the graph (Figure 2.21).

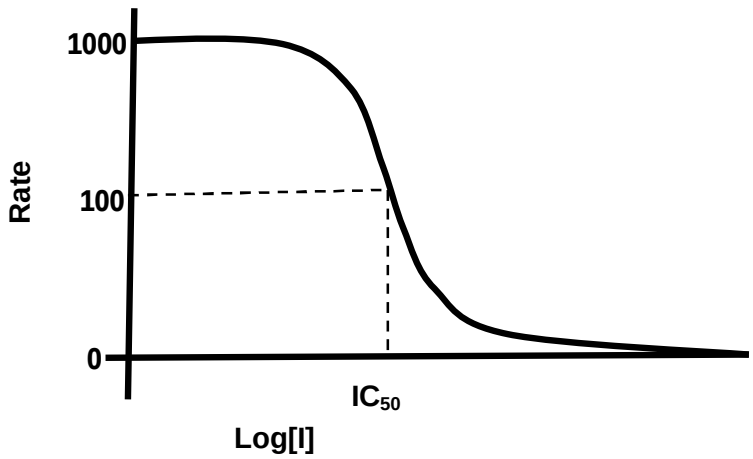

Figure 2.21: Calculation of the IC_{50} value from a sigmoidal dose-response curve (Cheng & Prusoff, 1973).

2.4. Summary

This chapter gave an overview of the pathogenesis of the PD and provided potential strategies for both the symptomatic and protective treatment of PD. It was shown that MAO-B inhibitors may be useful in the treatment of PD, both as neuroprotective agents and as adjunct to L-dopa treatment. Based on the pharmacological role of MAO-B inhibitors in PD, in this study new caffeine derivatives will be designed, synthesised and investigated as potential reversible inhibitors of this enzyme. In this regard, the known three-dimensional structures of both MAO-A and –B are of great value. This chapter gave a brief overview of the MAO structures and provided a basic background on enzyme kinetics. To evaluate test compounds as potential MAO-A and –B inhibitors, knowledge of enzyme kinetics is essential. The next chapter (Chapter 3) will detail the synthesis of new caffeine derivatives that will be evaluated as potential MAO inhibitors, as described in Chapter 4.

CHAPTER 3

Synthesis of 8-[(phenylsulfanyl)methyl]caffeine analogues

3.1. Introduction

As mentioned in the introductory chapter, substitution of caffeine at C8 produces compounds that are potent reversible inhibitors of MAO-B. In particular substitution of caffeine at C8 with a phenoxymethyl side chain yields compounds with potent MAO-B inhibition activity. In an attempt to discover new inhibitors of MAO, in this study, caffeine will be substituted with a phenylsulfanylmethyl functional group at C8 instead of a phenoxymethyl group. Therefore, one of the aims of this study is to compare the MAO-B inhibition potencies of the 8-[(phenylsulfanyl)methyl]caffeine analogues (**1a**–**g**) with the previously synthesised 8-(phenoxymethyl)caffeine analogues. Since the 8-(phenoxymethyl)caffeines also exhibited MAO-A inhibition activities, the 8-[(phenylsulfanyl)methyl]caffeine analogues will also be evaluated as human MAO-A inhibitors.

Considering that one of the aims of this study is to compare the MAO-A and MAO-B inhibition potencies of 8-(phenoxymethyl)caffeines with those of 8-[(phenylsulfanyl)methyl]caffeine analogues, similar substituents and substitution patterns as those that were previously employed for the series of 8-(phenoxymethyl)caffeines, will also be selected for the 8-[(phenylsulfanyl)methyl]caffeine analogues. The previously studied 8-(phenoxymethyl)caffeines were substituted on C3 of the phenoxy ring. Similarly, the 8-[(phenylsulfanyl)methyl]caffeine analogues examined here will also contain substituents on C3 of the phenyl ring. The selected substituents included halogens (Cl, Br and F), the methyl group, the methoxy group and the ethoxy group (Table 3.1). The halogens were incorporated in this study due to their strong electron withdrawing potential. The methoxy and ethoxy substituents were employed due to their electron donating properties. There is therefore a relatively large diversity in the properties of these substituents. Also, certain substituents are relatively large (Br, OCH_3), some are considered to be sterically bulky (Br) and some have a relatively low degree (OCH_3, OCH_2CH_3) of lipophilicity.

For comparison with the C3 substituted homologues, two C4 substituted 8-[(phenylsulfanyl)methyl]caffeine analogues (**1h**–**i**) will also be synthesised (Table 3.1). These will be substituted with chlorine and bromine, respectively. Also, five 8-[(phenylsulfanyl)ethyl]caffeine analogues (**2a**–**e**) will be synthesised (Table 3.2).

Since the phenylsulfanylethyl side chains of **2a**–**e** are longer than the phenylsulfanylmethyl side chains of **1a**–**g** by one methylene unit, the effect of chain elongation on MAO activity will be evaluated with these analogues.

Table 3.1: The structures of the 8-[(phenylsulfanyl)methyl]caffeine analogues **1a**–**i** that will be examined in this study

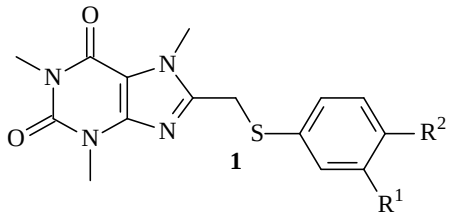

1

Compound	R^1	R^2
1a	H	H
1b	Cl	H
1c	Br	H
1d	F	H
1e	CH_3	H
1f	OCH_3	H
1g	OCH_2CH_3	H
1h	H	Cl
1i	H	Br

Table 3.2: The structures of the 8-[(phenylsulfanyl)ethyl]caffeine analogues **2a**–**e** that will be examined in this study

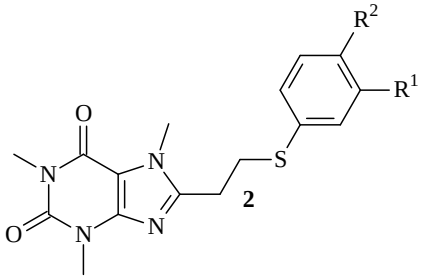

2

Compound	R^1	R^2
2a	H	H
2b	Cl	H
2c	Br	H
2d	H	Cl
2e	H	Br

3.2. General synthetic approaches

The following section is a brief discussion of the synthetic methods that were employed in this study.

3.2.1. Reaction pathway for the synthesis of 1,3-dimethyl-5,6-diaminouracil

1,3-Dimethyl-5,6-diaminouracil served as starting material for the synthesis of the caffeine analogues **1a**–**i** and **2a**–**e**. The synthesis of 1,3-dimethyl-5,6-diaminouracil was carried out according to a general method described by Traube (1900), where N,N'-dimethylurea (**A**) is condensed with cyanoacetic acid (**B**) in the presence of acetic anhydride to yield the intermediate cyanoacetylurea (**C**). The latter was treated with sodium hydroxide and ring closure took place with the formation of 1,3-dimethyl-6-aminouracil (**D**) (Papesch & Schroeder, 1951). 1,3-Dimethyl-6-aminouracil was then treated with sodium nitrite in the presence of an acid to yield the corresponding nitroso derivative (**E**). The latter was subsequently reduced to the desired 1,3-dimethyl-5,6-diaminouracil (**F**) in aqueous ammonia with sodium hydrosulfite (Speer & Raymond, 1953) (Figure 3.1).

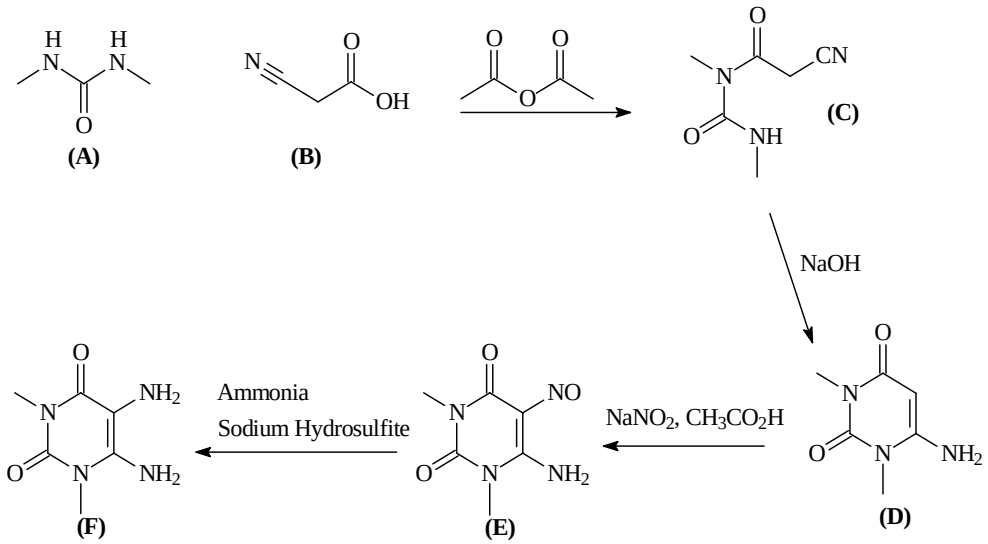

Figure 3.1: The formation of 1,3-dimethyl-5,6-diaminouracil

3.2.2. Reaction pathway for the synthesis of 8-[(phenylsulfanyl)methyl]caffeine analogues

The C8 substituted caffeine analogues were synthesised from 1,3-dimethyl-5,6-diaminouracil (**F**) (Blicke & Godt, 1954) and an appropriate 2-(phenylsulfanyl)acetic acid (**3**). The C8 substituted caffeine analogues were prepared according to the procedure previously reported for the synthesis of (E)-8-styrylcaffeinyl analogues. 1,3-Dimethyl-5,6-diaminouracil was acylated with the appropriate substituted 2-(phenylsulfanyl)acetic acid in the presence of a carbodiimide activating reagent, N-(3-dimethylaminopropyl)-N'-ethylcarbodiimide

hydrochloride (EDAC). The intermediary amide was then treated with sodium hydroxide to bring forth ring closure, yielding the corresponding 8-[(phenylsulfanyl)methyl]theophylline analogues (**G**). Without further purification the theophyline analogues were methylated with an excess of iodomethane and potassium carbonate to yield the target caffeine analogues (**1a**–**i**) (Suzuki *et al.,* 1992) (Figure 3.2).

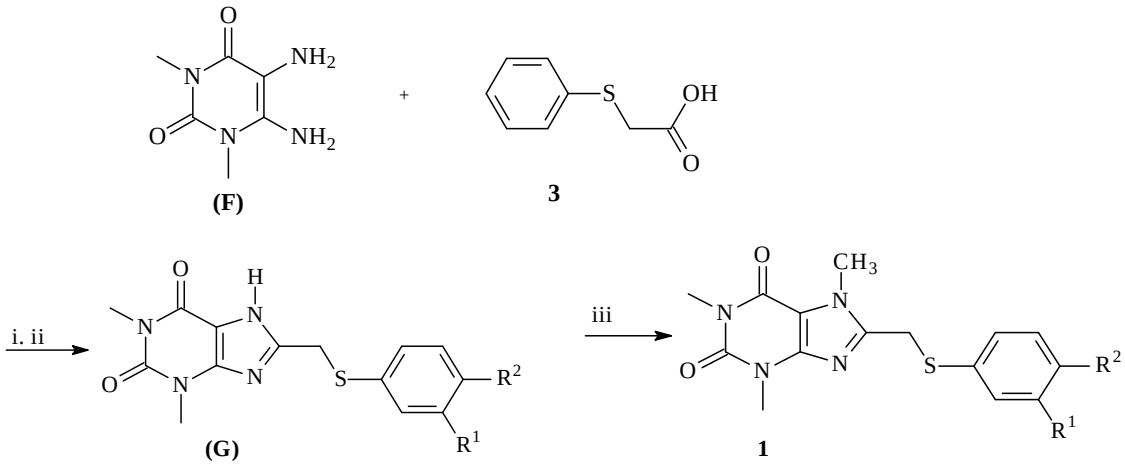

Figure 3.2: Synthetic pathway to 8-[(phenylsulfanyl)methyl]caffeine analogues. Key: (i) EDAC, dioxane/H_2O; (ii) NaOH (aq), reflux; (iii) CH_3I, K_2CO_3, DMF

3.2.3. General synthetic approaches for the synthesis of 8-[(phenylsulfanyl)ethyl]caffeine analogues

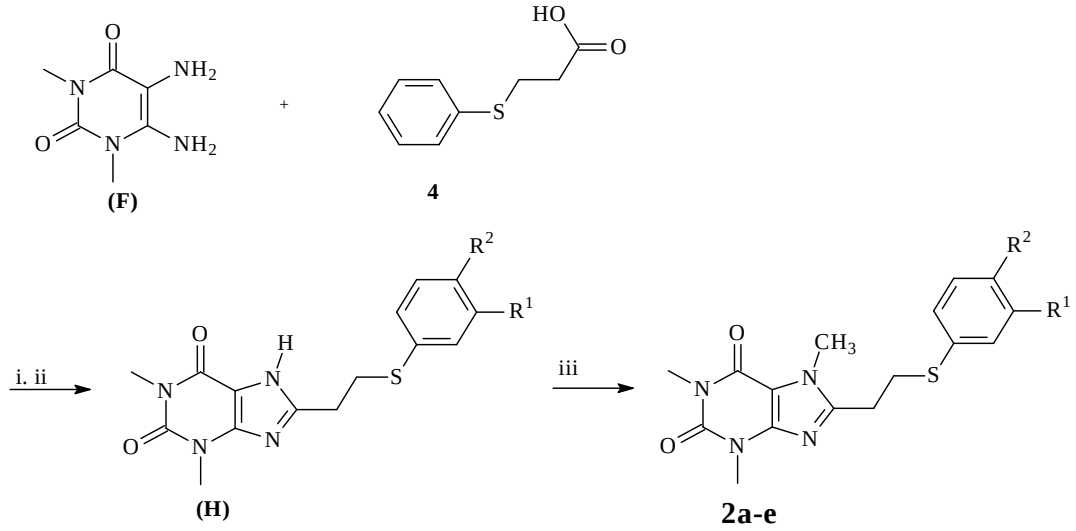

Figure 3.3: Synthetic pathway to 8-[(phenylsulfanyl)ethyl]caffeine analogues. Key: (i) EDAC, dioxane/H_2O; (ii) NaOH (aq), reflux; (iii) CH_3I, K_2CO_3, DMF

1,3-Dimethyl-5,6-diaminouracil (**F**) was acylated with the appropriately substituted 3-(phenylsulfanyl)propanoic acid (**4**) in the presence of a carbodiimide activating reagent, N-(3-dimethylaminopropyl)-N'-ethylcarbodiimide hydrochloride (EDAC). The resulting intermediary amide was then treated with sodium hydroxide to bring about ring closure, yielding the corresponding 8-[(phenylsulfanyl)ethyl]theophylline analogues (**H**). Without further purification the theophyline analogues were methylated with an excess of iodomethane and potassium carbonate to yield the target caffeine analogues (**2a**–**e**) (Suzuki *et al.,* 1992) (Figure 3.3).

*3.2.4. Reaction pathway for the synthesis of 2-(phenylsulfanyl)acetic acids (**3**)*

The 2-(phenylsulfanyl)acetic acids (**3**) were required for the synthesis of the 8-[(phenylsulfanyl)methyl]caffeine analogues (**1a**–**i**). An appropriately substituted thiophenol (**I**) was reacted in a solution of sodium hydroxide in water with chloroacetic acid. The reaction was subsequently heated and the mixture was acidified with concentrated hydrochloric acid. The product (**3**) was then extracted to diethylether (Wang *et al*., 2009) (Figure 3.4).

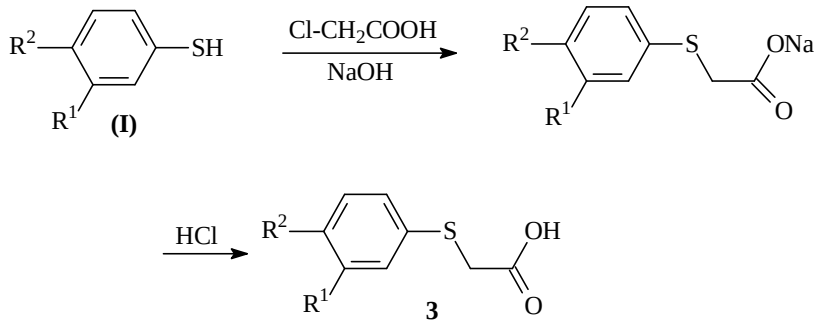

Figure 3.4: The formation of 2-(phenylsulfanyl)acetic acids (**3**)

3.2.5. Reaction pathway for the synthesis of 3-(phenylsulfanyl)propanoic acids (**4**)

The 3-(phenylsulfanyl)propanoic acids (**4**) were required for the synthesis of the 8-[(phenylsulfanyl)ethyl]caffeine analogues (**2a**–**e**). An appropriately substituted thiophenol (**I**) was reacted with chloropropanionic acid in the presence of sodium hydroxide. The reaction was then acidified with concentrated hydrochloric acid. The product (**4**) was extracted to an organic solvent such as diethylether (Figure 3.5).

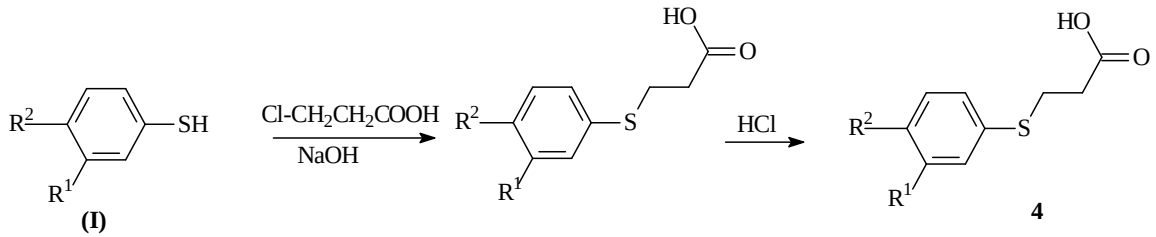

Figure 3.5: The formation of 3-(phenylsulfanyl)propanoic acids (**4**)

3.3. Experimental methods

3.3.1. Materials and methods

Chemicals: Unless otherwise noted, all starting materials were obtained from Sigma-Aldrich and were used without further purification.

NMR spectroscopy: Proton (^{1}H) and carbon (^{13}C) NMR spectra were recorded on a Bruker Avance III 600 spectrometer at frequencies of 600 MHz and 150 MHz, respectively. All NMR measurements were conducted in $CDCl_3$ and the chemical shifts are reported in parts per million (δ) downfield from the signal of tetramethylsilane. Spin multiplicities are given as s (singlet), brs (broad singlet), d (doublet), dd (doublet of doublets), t (triplet), q (quartet), qn (quintet) or m (multiplet).

Mass spectroscopy (MS): High resolution mass spectra (HRMS) were obtained on a DFS high resolution magnetic sector mass spectrometer (Thermo Electron Corporation) in electron ionisation (EI) mode.

Melting point determination: Melting points (mp) were determined on a Buchi M-545 melting point apparatus and are uncorrected.

Thin layer chromatography (TLC): TLC was carried out using neutral alumina sheets (Merck) and ethyl acetate/dichloromethane (8:3) as mobile phase. The sheets were visualised under UV light at a wavelength of 254 nm.

HPLC analyses: The purity of the synthesised compounds were estimated via HPLC analyses, which were conducted with an Agilent 1100 HPLC system equipped with a quaternary pump and an Agilent 1100 series diode array detector (see Supplementary Material). HPLC grade acetonitrile (Merck) and Milli-Q water (Millipore) were used for the chromatography.

3.3.2. Detailed synthetic methods

3.3.2.1. 1,3-Dimethyl-5-nitroso-6-aminouracil **(E)**

The formation of 1,3-dimethyl-5-nitroso-6-aminouracil (Figure 3.6) was effected by the following method: N,N'-Dimethylurea (100 mmol), cyanoacetic acid (100 mmol) and 12.5 ml of acetic anhydride were heated with the exclusion of moisture ($CaCl_2$ trap) at 60 °C for 3 h. The excess anhydride and the acetic acid were removed under reduced pressure. A solution of 5% sodium hydroxide (150 ml) was slowly added to the cooled, stirred residue whereupon the 1,3-dimethyl-6-aminouracil precipitated. An amount of sodium nitrite (120 mmol) in 50 ml of water was added to the cooled stirred mixture and it was acidified by the dropwise addition of 12 ml glacial acetic acid over a period of 1 h. Stirring was continued for an additional 2 h at room temperature. After cooling of the reaction on ice, a red-violet precipitate was collected by filtration and washed with 30 ml diethylether (Blicke & Godt, 1954). The precipitate was dried at 60 °C and used in subsequent reactions without purification.

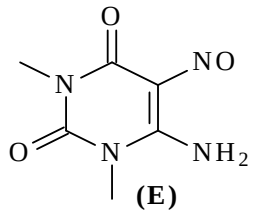

(E)

Figure 3.6: Chemical structure of 1,3-dimethyl-5-nitroso-6-aminouracil

3.3.2.2. 1,3-Dimethyl-5,6-diaminouracil **(F)**

The formation of 1,3-dimethyl-5,6-diaminouracil (Figure 3.7) was achieved according to the following method: To 1,3-dimethyl-5-nitroso-6-aminouracil (**E**, 87.11 mmol), 82 ml of ammonia water (35%) was added. The resulting yellow-orange ammonium salt was heated at 100 °C and, while stirring, a solution of 48 g of sodium hydrosulfite in 218 ml of water was added during a 20 min period. The salt dissolved and the reaction turned to a red solution and eventually light green to yellow. The solution was stirred and heated for an additional 15 min. The solution was filtered while hot and the filtrate was cooled on ice for 2 h. Light yellow crystals formed which were collected by filtration. The crystals were dried overnight at room temperature and were suitable for use without further purification (Blicke & Godt, 1954).

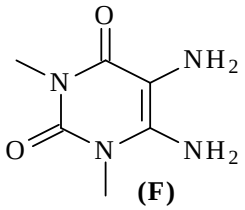

(F)

Figure 3.7: Chemical structure of 1,3-dimethyl-5,6-diaminouracil

3.3.2.3. 8-[(Phenylsulfanyl)methyl]caffeine analogues **(1a–i)**

To a solution of 1,3-dimethyl-5,6-diaminouracil (**F**, 5 mmol) and 1-ethyl-2-[3-(dimethylamino) propyl]carbodiimide hydrochloride (EDAC, 6.70 mmol) in 100 ml dioxane-H_2O (1:1), the appropriately substituted 2-(phenylsulfanyl)acetic acid (**3**) (5 mmol) was added. The pH of the suspension was adjusted to 5 with 2 M aqueous hydrochloric acid and stirring was continued for 2 h. After neutralisation (pH 7) with 1 M aqueous sodium hydroxide, the reaction was cooled to 0 °C and the precipitate was collected by filtration. The crude product was heated in 60 ml aqueous sodium hydroxide (1 M)-dioxane (1:1) under reflux for 60 min. After cooling to 0 °C, the solution was acidified to a pH of 4 with aqueous hydrochloric acid (4 M) and the precipitate was collected by filtration. The resulting 8-[(phenylsulfanyl)methyl]theophylline analogues (**G**) were used in the subsequent reaction without further purification (Figure 3.8).

Iodomethane (5.31 mmol) was added to a stirred suspension of the theophylline analogue **G** (2.66 mmol) and potassium carbonate (6.84 mmol) in 13 ml DMF. After stirring at 50 °C for 60 min, the progression of the reaction was followed with TLC, utilising neutral alumina sheets and ethyl acetate/dichloromethane (8:3) as mobile phase. After completion of the reaction, the insoluble materials were removed by filtration, and sufficient water (150 ml) was added to the filtrate to precipitate the product (**1a-i**) which was collected by filtration (Vlok *et al*., 2006).

Recrystallisation: The product was suspended in 25 ml boiling methanol. While still boiling, 7 ml ethyl acetate was added to obtain a clear solution. Crystallisation was allowed overnight at room temperature and the light yellow crystals were collected and washed with 20 ml methanol. The crystals were air dried at room temperature overnight.

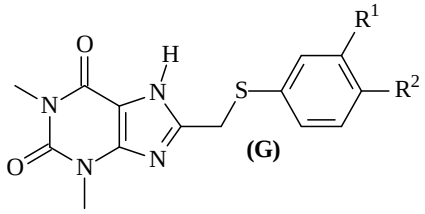

(G)

Figure 3.8: Chemical structure of the 8-[(phenylsulfanyl)methyl]theophylline analogues

3.3.2.3. 8-[(Phenylsulfanyl)ethyl]caffeine analogues **(2a–e)**

The appropriately substituted 3-(phenylsulfanyl)propanoic acids (**4**, 5 mmol) was added to a mixture of 1,3-dimethyl-5,6-diaminouracil (**F**, 5 mmol) and EDAC (6.70 mmol) in 60 ml dioxane-H_2O (1:1). The pH of the suspension was adjusted to 5 with 2 M aqueous hydrochloric acid and stirring was continued for 2 h. After neutralisation with 1 M aqueous sodium hydroxide, the reaction was cooled to 0 °C and the precipitate was collected by filtration. The crude product was heated in 40 ml aqueous sodium hydroxide (1 M)-dioxane (1:1) under reflux for 60 min. After cooling to 0 °C, the solution was acidified to a pH of 4 with aqueous hydrochloric acid (4 M) and the precipitate was collected by filtration. The resulting 8-[(phenylsulfanyl)ethyl]theophylline analogues were used in the subsequent reaction without further purification (Figure 3.9).

Iodomethane (5.31 mmol) was added to a stirred suspension of the theophylline analogue (**H**) (2.66 mmol) and potassium carbonate (6.84 mmol) in 13 ml DMF. After stirring at 50 °C for 60 min, TLC indicated that the reaction was complete and the insoluble materials were removed by filtration and water (150 ml) was added to the filtrate. An emulsion was obtained which was extracted to chloroform (2 x 50 ml). Anhydrous magnesium sulphate (5 g) was added to the chloroform phase and the organic phase was dried for 15 min. The magnesium sulphate was then removed by filtration and the reaction was placed on a rotary evaporator to remove the chloroform solvent. A light yellow precipitate was obtained.

Recrystallisation: The product was suspended in 30 ml boiling methanol. While still boiling, 10 ml ethyl acetate was added to obtain a clear solution. Crystallisation was allowed to occur overnight at room temperature and the light yellow crystals were collected and washed with 50 ml methanol. The crystals were air dried at room temperature overnight.

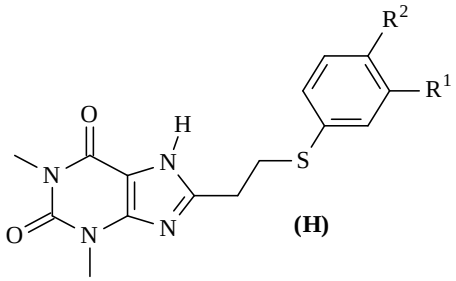

Figure 3.9: Chemical structure of the 8-[(phenylsulfanyl)ethyl]theophylline analogues

3.3.2.4. The synthesis of the required 2-(phenylsulfanyl)acetic acids (**3**)

An appropriate thiophenol (10 mmol) was dissolved in ethanol (5 ml) and a solution of NaOH (10 mmol) in H_2O (3 ml) was added. In a separate flask, chloroacetic acid (11 mmol) was dissolved in H_2O (3 ml) and Na_2CO_3 (5.5 mmol) was added. The resulting solution was added to the thiophenol containing reaction and the reaction was allowed to stir at room temperature for 3 h. The reaction was subsequently heated under reflux for 1 h, cooled to room temperature and acidified with 2 N HCl to pH 2. Water (25 ml) was added and the brown oil fraction was extracted to diethylether (50 ml). The ether fraction was extracted with an aqueous solution of 5% Na_2CO_3 (25 ml). The aqueous Na_2CO_3 fraction was acidified to pH 2 with concentrated HCl and the resulting precipitate was collected by filtration and oven dried to obtain the required acids (Wang *et al*., 2009) (Figure 3.10).

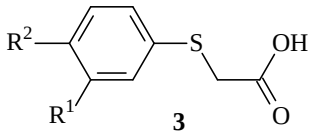

3

Compound	R^1	R^2
3a	H	H
3b	Cl	H
3c	Br	H
3d	F	H
3e	CH_3	H
3f	OCH_3	H
3g	OCH_2CH_3	H
3h	H	Cl
3i	H	Br

Figure 3.10: The structures of the phenylsulfanylacetic acids (**3**)

3.3.2.5. The synthesis of the required 3-(phenylsulfanyl)propanoic acids (**4**)

An appropriate thiophenol (10 mmol) was dissolved in ethanol (5 ml) and a solution of NaOH (10 mmol) in H_2O (3 ml) was added. In a separate flask, 3-chloropropionic acid (11.0 mmol) was dissolved in H_2O (3 ml) and Na_2CO_3 (5.5 mmol) was added. The resulting solution was added to the thiophenol containing reaction and the reaction was allowed to stir at room temperature for 3 h. The reaction was subsequently heated under reflux for 1 h, cooled to room temperature and acidified with 2 N HCl to pH 2. The resulting crystals were collected by filtration and dried overnight to obtain the required acids (Wang *et al*., 2009) (Figure 3.11).

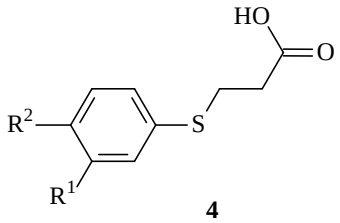

4

Compound	R^1	R^2
4a	H	H
4b	Cl	H
4c	Br	H
4d	H	Cl
4e	H	Br

Figure 3.11: The structures of the 3-(phenylsulfanyl)propanoic acids (**4**)

3.4. Physical characterisation

The structures of 8-[(phenylsulfanyl)methyl]caffeine (**1a**–**i**) and 8-[(phenylsulfanyl)ethyl]caffeine (**2a**–**e**) analogues were confirmed by ^{1}H-NMR and ^{13}C-NMR, as well as by high resolution mass spectrometry. The purities of the target compounds were estimated by HPLC analysis. Strong elution conditions were employed for the HPLC analysis by using up to 85% acetonitrile and the eluent was monitored at 210 nm, a wavelength where most organic compounds absorb UV light. Therefore, if there are any impurities present, they are expected to elute and be detected under these conditions. The HPLC conditions and chromatograms that were obtained are given in the Appendix.

3.5. Results

3.5.1. 2-(Phenylsulfanyl)acetic acids (3) and the 3-(phenylsulfanyl)propanoic acids (4)

Thirteen of the required phenylsulfanyl acetic acids (**3**) and 3-(phenylsulfanyl)propanoic acids (**4**) were not commercially available and were thus synthesised in the laboratory. These acids were required for the synthesis of the 8-[(phenylsulfanyl)methyl]caffeine (**1a–i**) and 8-[(phenylsulfanyl) ethyl]caffeine (**2a–e**) analogues. The chemical structures and melting points of the acids which were synthesised are shown in Table 3.3.

Table 3.3: Chemical structures of the 2-(phenylsulfanyl)acetic acids (**3**) and 3-(phenylsulfanyl)propanoic acids (**4**) which were required as starting materials for this study

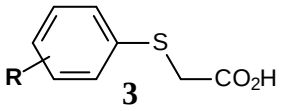

3

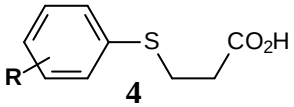

4

	R	mp (°C)	Literature mp (°C)
3a	H	Commercially available	
3b	3-Cl	86	81.5–82.2 (Pasto *et al*., 1965)
3c	3-Br	90	86.8–87.6 (Pasto *et al*., 1965)
3d	3-F	74	73.5–74.2 (Pasto *et al*., 1965)
3e	3-CH_3	70	66.8–67.4 (Pasto *et al*., 1965)
3f	3-OCH_3	72	62.3–63.5 (Pasto *et al*., 1965)
3g	3-OCH_2CH_3	106	New compound
3h	4-Cl	107	107–108 (Pasto *et al*., 1965)
3i	4-Br	117	118–118.5 (Pasto *et al*., 1965)
4a	H	63	58.5–59.5 (Ahn & Cohen, 1994)
4b	3-Cl	83	77–78 (Degani *et al*., 1966)
4c	3-Br	91	90–91 (Degani *et al*., 1966)
4d	4-Cl	88	90–91 (Degani *et al*., 1966)
4e	4-Br	116	114–115 (Degani *et al*., 1966)

3.5.2. The NMR spectral data for the 8-[(phenylsulfanyl)methyl]caffeine analogues (1a–i)

8-[(Phenylsulfanyl)methyl]caffeine (1a)

The title compound was prepared from 2-(phenylsulfanyl)acetic acid in a yield of 74.3%: mp 154–156 °C (methanol/ethyl acetate 7:2). ^{1}H NMR (Bruker Avance III 600, $CDCl_3$) δ; 3.34 (s, 3H), 3.47 (s, 3H), 3.78 (s, 3H), 4.13 (s, 2H), 7.24 (m, 3H), 7.35 (m, 2H); ^{13}C NMR (Bruker Avance III 600, $CDCl_3$) δ 27.8, 29.6, 30.8, 32.0, 107.9, 127.0, 129.1, 131.9, 133.3, 147.5, 149.4, 151.5, 155.2; EI-HRMS m/z: calcd for $C_{15}H_{16}N_4O_2S$, 316.0994, found 316.0988; Purity (HPLC): 99%.

8-{[(3-Chlorophenyl)sulfanyl]methyl}caffeine (1b)

The title compound was prepared from 2-[(3-chlorophenyl)sulfanyl]acetic acid in a yield of 56.0%: mp 174–177 °C (methanol/ethyl acetate 7:2). ^{1}H NMR (Bruker Avance III 600, $CDCl_3$) δ; 3.35 (s, 3H), 3.49 (s, 3H), 3.90 (s, 3H), 4.17 (s, 2H), 7.19 (m, 2H), 7.23 (m, 1H), 7.41 (m, 1H); ^{13}C NMR (Bruker Avance III 600, $CDCl_3$) δ 27.9, 29.6, 30.1, 32.1, 108.1, 127.7, 128.9, 130.1, 130.6, 134.7, 135.5, 147.4, 148.8, 151.5, 155.2; EI-HRMS m/z: calcd for $C_{15}H_{15}ClN_4O_2S$, 350.0604, found 350.0615; Purity (HPLC): 89.2%.

8-{[(3-Bromophenyl)sulfanyl]methyl}caffeine (1c)

The title compound was prepared from 2-[(3-bromophenyl)sulfanyl]acetic acid in a yield of 75.2%: mp 151–152 °C (methanol/ethyl acetate 7:2). ^{1}H NMR (Bruker Avance III 600, $CDCl_3$) δ; 3.35 (s, 3H), 3.49 (s, 3H), 3.89 (s, 3H), 4.16 (s, 2H), 7.12 (t, 1H, J= 7.9Hz), 7.26 (m, 1H), 7.34 (m, 1H), 7.56 (m, 1H); ^{13}C NMR (Bruker Avance III 600, $CDCl_3$) δ 27.9, 29.6, 30.1, 32.1, 108.1, 122.8, 129.4, 130.3, 130.6, 133.4, 135.8, 147.4, 148.8, 151.5, 155.2; EI-HRMS m/z: calcd for $C_{15}H_{15}BrN_4O_2S$, 394.0099, found 394.0100; Purity (HPLC): 98.5%.

8-{[(3-Fluorophenyl)sulfanyl]methyl}caffeine (1d)

The title compound was prepared from 2-[(3-fluorophenyl)sulfanyl]acetic acid in a yield of 29.9%: mp 155–156 °C (methanol/ethyl acetate 7:2). ^{1}H NMR (Bruker Avance III 600, $CDCl_3$) δ; 3.45 (s, 3H), 3.48 (s, 3H), 3.89 (s, 3H), 4.18 (s, 2H), 6.92 (m, 1H), 7.13 (m, 2H), 7.22 (m, 1H); ^{13}C NMR (Bruker Avance III 600, $CDCl_3$) δ; 27.9, 29.6, 30.1, 32.1, 108.1, 114.5. 114.6, 117.5, 117.6, 126.3, 130.3, 130.4, 135.8, 135.9, 147.4, 148.8, 151.5, 155.2, 161.8, 163.4; EI-HRMS m/z: calcd for $C_{15}H_{15}FN_4O_2S$, 334.0900, found 334.0893; Purity (HPLC): 99%.

8-{[(3-Methylphenyl)sulfanyl]methyl}caffeine (1e)

The title compound was prepared from 2-[(3-methylphenyl)sulfanyl]acetic acid in a yield of 36.8%: mp 124–126 °C (methanol/ethyl acetate 7:2). ^{1}H NMR (Bruker Avance III 600, $CDCl_3$) δ; 2.32 (s, 3H), 3.39 (s, 3H), 3.53 (s, 3H) 3.85 (s, 3H), 4.18 (s, 2H), 7.09 (brs, 1H), 7.19 (s, 2H), 7.24 (s, 1H); ^{13}C NMR (Bruker Avance III 600, $CDCl_3$) δ; 21.2, 27.8, 29.6, 30.7, 32.0, 107.9, 128.6, 128.7, 128.9, 132.3, 133.1, 139.0, 147.5, 149.5, 151.5, 155.2; EI-HRMS m/z: calcd for $C_{16}H_{18}N_4O_2S$, 330.1150, found 330.1157; Purity (HPLC): 99%.

8-{[(3-Methoxyphenyl)sulfanyl]methyl}caffeine (1f)

The title compound was prepared from 2-[(3-methoxyphenyl)sulfanyl]acetic acid in a yield of 41.0%: mp 161–165 °C (methanol/ethyl acetate 7:2). ^{1}H NMR (Bruker Avance III 600, $CDCl_3$) δ; 3.36 (s, 3H), 3.50 (s, 3H), 3.75 (s, 3H), 3.84 (s, 3H), 4.16 (s, 2H), 6.78 (dd, 1H, J = 1.9, 7.9 Hz), 6.93 (m, 2H), 7.17 (t, 1H, J = 7.9 Hz); ^{13}C NMR (Bruker Avance III 600, $CDCl_3$) δ; 27.9, 29.7, 30.5, 32.1, 55.3, 108.0, 113.6, 116.5, 123.3, 130.0, 134.8, 147.5, 149.4, 151.5, 155.2, 159.9; EI-HRMS m/z: calcd for $C_{16}H_{18}N_4O_3S$, 346.1100, found 346.1091; Purity (HPLC): 99%.

8-{[(3-Ethoxyphenyl)sulfanyl]methyl}caffeine (1g)

The title compound was prepared from 2-[(3-ethoxyphenyl)sulfanyl]acetic acid in a yield of 54.6%: mp 147–149 °C (methanol/ethyl acetate 7:2). ^{1}H NMR (Bruker Avance III 600, $CDCl_3$) δ; 1.35 (t, 3H, J = 6. 8 Hz), 3.34 (s, 3H), 3.48 (s, 3H), 3.82 (s, 3H), 3.95 (q, 2H, J = 6.8 Hz), 4.15 (s, 2H), 6.75 (d, 1H, J = 8.28 Hz), 6.91 (m, 2H), 7.14 (t, 1H, J = 7.5 Hz); ^{13}C NMR (Bruker Avance III 600, $CDCl_3$) δ 27.9, 29.7, 30.5, 32.1, 55.3, 108.0, 113.6, 116.5, 123.3, 130.0, 134.8, 147.5, 149.4, 151.5, 155.2, 159.9; EI-HRMS m/z: calcd for $C_{17}H_{20}N_4O_3S$, 360.1256, found 360.1261; Purity (HPLC): 99%.

8-{[(4-Chlorophenyl)sulfanyl]methyl}caffeine (1h)

The title compound was prepared from 2-[(4-chlorophenyl)sulfanyl]acetic acid in a yield of 59.2%: mp 149–150 °C (methanol/ethyl acetate 7:2). ^{1}H NMR (Bruker Avance III 600, $CDCl_3$) δ; 3.34 (s, 3H), 3.46 (s, 3H), 3.86 (s, 3H), 4.12 (s, 2H), 7.23 (d, 2H, J = 7.5 Hz), 7.29 (d, 2H, J = 7.5 Hz); ^{13}C NMR (Bruker Avance III 600, $CDCl_3$) δ; 27.9, 29.6, 30.8, 32.1, 108.0, 129.3, 133.0, 131.8, 134.1, 147.4, 149.0, 151.4, 155.2; EI-HRMS m/z: calcd for $C_{15}H_{15}ClN_4O_2S$, 350.0604, found 350.0597; Purity (HPLC): 99%.

8-{[(4-Bromophenyl)sulfanyl]methyl}caffeine (1i)

The title compound was prepared from 2-[(4-bromophenyl)sulfanyl]acetic acid in a yield of 73.1%: mp 160–164 °C (methanol/ethyl acetate 7:2). ^{1}H NMR (Bruker Avance III 600, $CDCl_3$) δ; 3.39 (s, 3H), 3.51 (s, 3H), 3.92 (s, 3H), 4.17 (s, 2H), 7.27 (d, 2H, J = 7.5 Hz), 7.42 (d, 2H, J = 7.5 Hz); ^{13}C NMR (Bruker Avance III 600, $CDCl_3$) δ; 27.9, 29.6, 30.6, 32.1, 108.0, 122.1, 132.2, 132.5, 133.0, 147.4, 149.0, 151.4, 155.2; EI-HRMS m/z: calcd for $C_{15}H_{15}BrN_4O_2S$, 394.0099, found 394,0092; Purity (HPLC): 99%.

3.4.2. The physical data for the 8-[(phenylsulfanyl)ethyl]caffeine analogues (2a–e)

8-{[(Phenylsulfanyl)ethyl]}caffeine (2a)

The title compound was prepared from 3-(phenylsulfanyl)propanoic acid in a yield of 45%: mp 143–145 °C (methanol/ethyl acetate 7:2). ^{1}H NMR ($CDCl_3$) *δ*; 3.00 (t, 2H, J = 7.2 Hz), 3.35 (s, 3H), 3.35 (t, 2H, J = 7.2 Hz), 3.50 (s, 3H), 3.79 (s, 3H), 7.15 (m, 1H), 7.24 (m, 2H), 7.31 (m, 2H); ^{13}C NMR ($CDCl_3$) *δ*; 26.9, 27.8, 29.6, 31.7, 31.8, 107.3, 126.6, 129.0, 129.7, 134.7, 147.9, 151.6, 151.9, 155.2; EI-HRMS *m*/*z*: calcd for $C_{16}H_{18}N_4O_2S$, 330.1150, found 330.1148.

8-{[(3-Chlorophenyl)sulfanyl]ethyl}caffeine (2b)

The title compound was prepared from 3-[(3-chlorophenyl)sulfanyl]propanoic acid in a yield of 3%: mp 181–183 °C (methanol/ethyl acetate 7:2). ^{1}H NMR ($CDCl_3$) *δ*; 3.04 (t, 2H, J = 6.8 Hz), 3.37 (s, 3H), 3.39 (t, 2H, J = 6.8 Hz); 3.52 (s, 3H), 3.84 (s, 3H), 7.12 (m, 1H), 7.18 (m, 2H); 7.24 (m, 1H); ^{13}C NMR ($CDCl_3$) *δ*; 26.9, 27.8, 29.7, 31.6, 31.8, 107.3, 126.5, 127.4, 128.7, 130.0, 134.7, 137.0, 147.8, 151.5, 155.2; EI-HRMS *m*/*z*: calcd for $C_{16}H_{17}ClN_4O_2S$, 364.0761, found 364.0743.

8-{[(3-Bromophenyl)sulfanyl]ethyl}caffeine (2c)

The title compound was prepared from 3-[(3-bromophenyl)sulfanyl]propanoic acid 2-{[(3-bromophenyl)methyl]sulfanyl}acetic acid in a yield of 61%: mp 175–177 °C (methanol/ethyl acetate 7:2). ^{1}H NMR ($CDCl_3$) *δ*; 2.90 (t, 2H, J = 6.4 Hz); 3.23 (s, 3H); 3.25 (t, 2H, J = 6.4 Hz); 3.38 (s, 3H), 3.70 (s, 3H), 6.97 (t, 1H, J = 7.5 Hz); 7.09 (d, 1H, J = 7.5 Hz); 7.13 (d, 1H, J = 6.8 Hz), 7.24 (s, 1H); ^{13}C NMR ($CDCl_3$) *δ*; 27.0, 27.8, 29.7, 31.7, 31.7, 107.3, 122.8, 127.9, 129.4, 130.2, 131.6, 137.3, 147.8, 151.5, 151.5, 155.1; EI-HRMS *m*/*z*: calcd for $C_{16}H_{17}BrN_4O_2S$, 408.0256, found 408.0255.

8-{[(4-Chlorophenyl)sulfanyl]ethyl}caffeine (2d)

The title compound was prepared from 3-[(4-chlorophenyl)sulfanyl]propanoic acid in a yield of 23%: mp 148–150 °C (methanol/ethyl acetate 7:2). ^{1}H NMR ($CDCl_3$) δ; 2.99 (t, 2H, J = 6.8 Hz); 3.34 (t, 2H, J = 6.8 Hz), 3.36 (s, 3H), 3.50 (s, 3H), 3.82 (s, 3H), 7.20 (d, 2H, J = 8.3 Hz); 7.23 (d, 2H, J = 8.3 Hz); ^{13}C NMR ($CDCl_3$) δ 26.9, 27.9, 29.6, 31.8, 32.1, 107.3, 129.1, 131.1, 132.7, 133.3, 147.9, 151.6, 151.6, 155.2; EI-HRMS *m*/*z*: calcd for $C_{16}H_{17}ClN_4O_2S$, 364.0761, found 364.0755.

8-{[(4-Bromophenyl)sulfanyl]ethyl}caffeine (2e)

The title compound was prepared from 3-[(4-bromophenyl)sulfanyl]propanoic acid in a yield of 26%: mp 159–161 °C (methanol/ethyl acetate 7:2). ^{1}H NMR ($CDCl_3$) δ; 3.00 (t, 2H, J = 6.8 Hz), 3.34 (t, 2H, J = 6.8 Hz), 3.35 (s, 3H), 3.49 (s, 3H), 3.81 (s, 3H), 7.15 (d, 2H, J = 8.3 Hz), 7.34 (d, 2H, J = 8.3 Hz); ^{13}C NMR ($CDCl_3$) δ 26.9, 27.8, 29.6, 31.7, 31.9, 107.2, 120.4, 131.2, 131.9, 133.9, 147.8, 151.5, 151.5, 155.2; EI-HRMS *m*/*z*: calcd for $C_{16}H_{17}BrN_4O_2S$, 408.0256, found 408.0255.

Table 3.4: Correlation of the ^{1}H NMR data with the structures of the 8-[(phenylsufanyl)methyl]caffeine **(1a–i)** and 8-[(phenylsulfanyl)ethyl]caffeine analogues **(2a–e)**

Structure	**^{1}H NMR signal assignment**
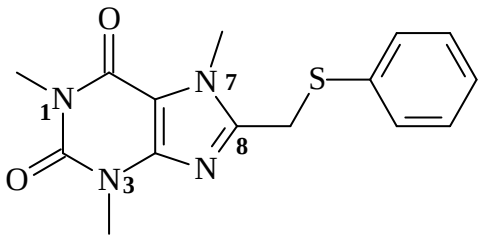	**a.** Methyl groups at N-1, N-3 and N-7– singlets at 3.34 (3H), 3.47 (3H), 3.78 (3H) ppm. **b.** CH_2– singlet at 4.13 (2H) ppm. **c.** Aromatic protons– signals at 7.24 (3H), 7.35 (2H) ppm.
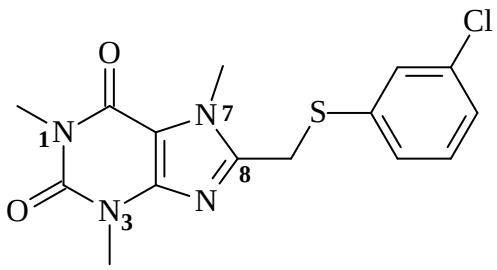	**a.** Methyl groups at N-1, N-3 and N-7– singlets at 3.35 (3H), 3.49 (3H), 3.90 (3H) ppm. **b.** CH_2– singlet at 4.17 (2H) ppm. **c.** Aromatic protons– signals at 7.19 (2H), 7.23 (1H), 7.41 (1H) ppm.

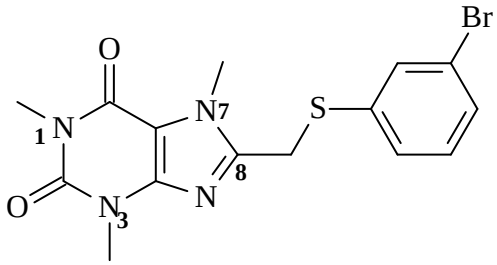	**a.** Methyl groups at N-1, N-3 and N-7– singlets at 3.35 (3H), 3.49 (3H), 3.89 (3H) ppm. **b.** CH_2– singlet at 4.16 (2H) ppm. **c.** Aromatic protons– signals at 7.12 (1H), 7.27 (1H), 7.34 (1H), 7.56 (1H) ppm.
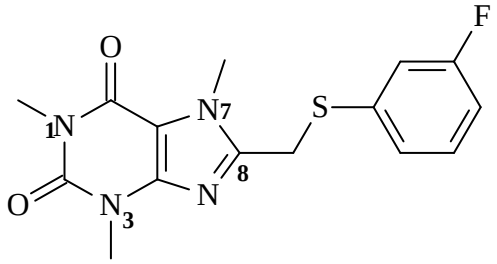	**a.** Methyl groups at N-1, N-3 and N-7– singlets at 3.45 (3H), 3.48 (3H), 3.89 (3H) ppm. **b.** CH_2– singlet at 4.18 (2H) ppm. **c.** Aromatic protons– signals at 6.92 (1H), 7.13 (2H), 7.22 (1H) ppm.
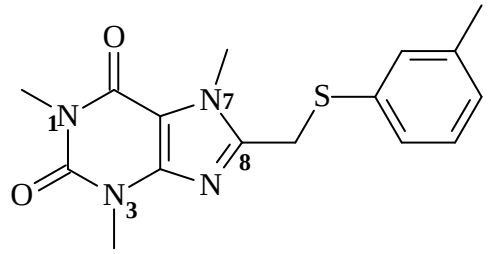	**a.** Methyl group on the phenyl ring– singlet at 2.32 (3H) ppm. **b.** Methyl groups at N-1, N-3 and N-7– singlets at 3.39 (3H), 3.53 (3H) 3.85 (3H) ppm. **c.** CH_2– singlet at 4.18 (2H) ppm. **d.** Aromatic protons– signals at 7.09 (1H), 7.19 (2H), 7.24 (1H) ppm.
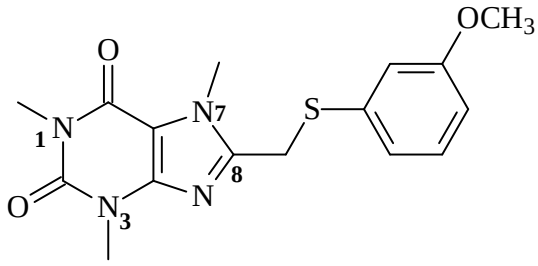	**a.** Methoxy methyl group on the phenyl ring– singlet at 3.75 (3H) ppm. **b.** Methyl groups at N-1, N-3 and N-7 – singlets at 3.36 (3H), 3.50 (s, 3H) 3.84 (3H) ppm. **c.** CH_2– singlet at 4.16 (2H) ppm. **d.** Aromatic protons– signals at 6.78 (1H), 6.93 (2H), 7.17 (1H) ppm.
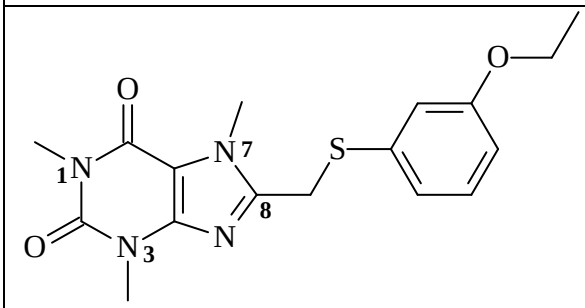	**a.** Ethoxy group on the phenyl ring– triplet at 1.35 (3H) ppm and quartet at 3.95 (2H) ppm. **b.** Methyl groups at N-1, N-3 and N-7 – singlets at 3.34 (3H), 3.48 (3H), 3.82 (3H) ppm.

	c. CH_2– singlet at 4.15 (2H) ppm. **d.** Aromatic protons– signals at 6.75 (1H), 6.91 (2H), 7.14 (1H) ppm.
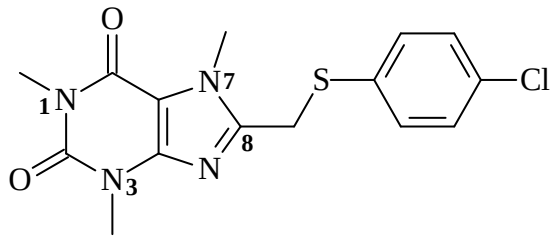	**a.** Methyl groups at N-1, N-3 and N-7– singlets at 3.34 (3H), 3.46 (3H), 3.86 (3H) ppm. **b.** CH_2– singlet at 4.12 (2H) ppm. **c.** Aromatic protons– signals at 7.23 (2H), 7,29 (2H) ppm.
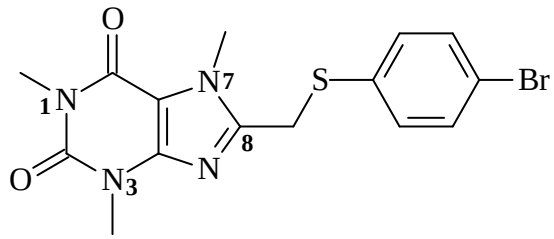	**a.** Methyl groups at N-1, N-3 and N-7– singlets at 3.39 (3H), 3.51 (3H), 3.92 (3H) ppm. **b.** CH_2– singlet at 4.17 (2H) ppm. **c.** Aromatic protons– signals at 7.27 (2H), 7.42 (2H) ppm.
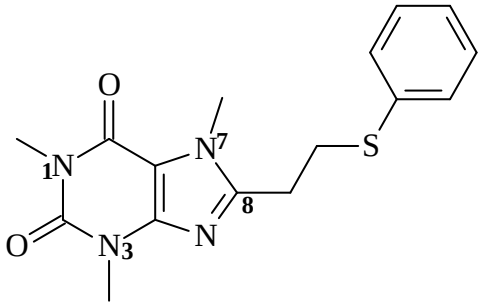	**a.** Methyl groups at N-1, N-3 and N-7 – singlets at 3.35 (3H), 3.50 (3H) and 3,79 (3H) ppm. **b.** CH_2CH_2– triplets at 3.00 (2H) and 3.35 (2H) ppm. **c.** Aromatic protons– signals at 7.15 (1H), 7.24 (2H), 7.31 (2H) ppm.
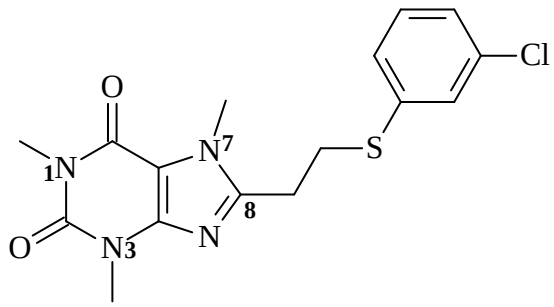	**a.** Methyl groups at N-1, N-3 and N-7 – singlets at 3.37 (3H), 3.52 (3H) and 3,84 (3H) ppm. **b.** CH_2CH_2– triplets at 3.04 (2H) and 3.39 (2H) ppm. **c.** Aromatic protons– signals at 7.12 (1H), 7.18 (2H), 7.24 (1H) ppm.

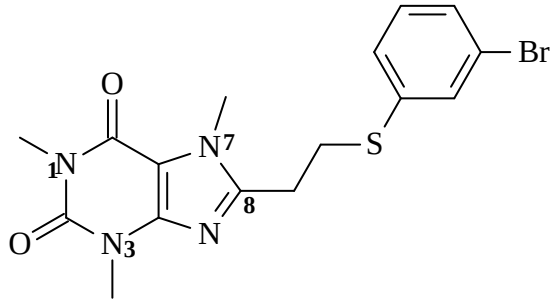	**a.** Methyl groups at N-1, N-3 and N-7 – singlets at 3.23 (3H), 3.38 (3H) and 3.70 (3H) ppm. **b.** CH_2CH_2– triplets at 2.90 (2H) and 3.25 (2H) ppm. **c.** Aromatic protons– signals at 6.97 (1H), 7.09 (1H), 7.13 (1H) and 7.24 (1H) ppm.
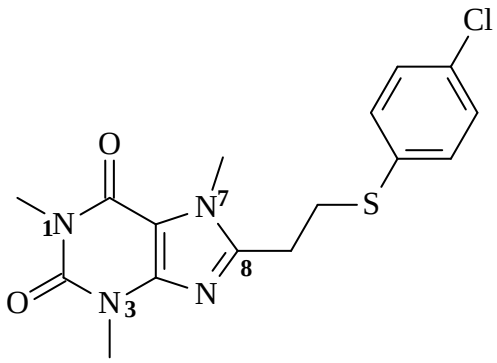	**a.** Methyl groups at N-1, N-3 and N-7 – singlets at 3.36 (3H), 3.50 (3H) and 3.82 (3H) ppm. **b.** CH_2CH_2– triplets at 2.99 (2H) and 3.34 (2H) ppm. **c.** Aromatic protons– signals at 7.20 (2H), 7.23 (2H) ppm.
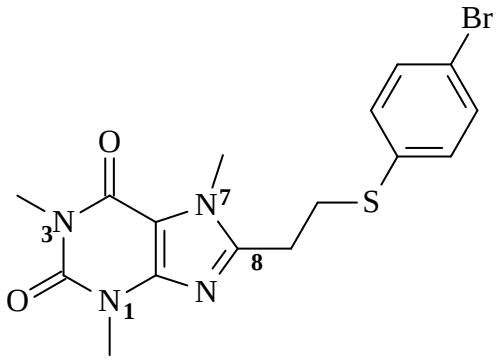	**a.** Methyl groups at N-1, N-3 and N-7 – singlets at 3.35 (3H), 3.49 (3H) and 3.81 (3H) ppm. **b.** CH_2CH_2– triplets at 3.00 (2H) and 3.34 (2H) ppm. **c.** Aromatic protons– signals at 7.15 (2H), 7.34 (2H) ppm.

3.5.3. The mass spectral data for the 8-[(phenylsufanyl)methyl]caffeine (1a-i) and 8-[(phenylsulfanyl) ethyl]caffeine (2a–e) analogues

The high resolution masses were recorded for each of the synthesised caffeine analogues. As shown in Table 3.5, the exact masses that were measured for each of the caffeine analogues very closely corresponded to the calculated values. In each instance the measured values deviated by less than 5 ppm from the theoretical value. This is further confirmation of the structures of these compounds.

Table 3.5: Correlation of the calculated exact masses with the experimentally obtained masses of both the 8-[(phenylsufanyl)methyl]caffeine and 8-[(phenylsulfanyl)ethyl]caffeine analogues

Compound	R^1	R^2	Formula	Calculated	Found	ppm
1a	H	H	$C_{15}H_{16}N_4O_2S$	316.0994	316.0988	-1.89
1b	Cl	H	$C_{15}H_{15}ClN_4O_2S$	350.0604	350.0615	3.14
1c	Br	H	$C_{15}H_{15}BrN_4O_2S$	394.0099	394.0100	0.25
1d	F	H	$C_{15}H_{15}FN_4O_2S$	334.0900	334.0893	-2.10
1e	CH_3	H	$C_{16}H_{18}N_4O_2S$	330.1150	330.1157	2.12
1f	OCH_3	H	$C_{16}H_{18}N_4O_3S$	346.1100	346.1091	-2.60
1g	OCH_2CH_3	H	$C_{17}H_{20}N_4O_3S$	360.1256	360.1261	1.39
1h	H	Cl	$C_{15}H_{15}ClN_4O_2S$	350.0604	350.0597	-2.00
1i	H	Br	$C_{15}H_{15}ClN_4O_2S$	394.0099	394.0092	-1.78
2a	H	H	$C_{16}H_{18}N_4O_2S$	330.1150	330.1148	-0.61
2b	Cl	H	$C_{16}H_{17}ClN_4O_2S$	364.0761	364.0743	-4.94
2c	Br	H	$C_{16}H_{17}BrN_4O_2S$	408.0256	408.0255	-0.25
2d	H	Cl	$C_{16}H_{17}ClN_4O_2S$	364.0761	364.0755	-1.65
2e	H	Br	$C_{16}H_{17}BrN_4O_2S$	408.0256	408.0255	-0.25

ppm→[(found – calcd.)/calcd]. x 1000000. In general a ppm difference of less than 5 is considered to be good agreement.

3.6. HPLC analysis

The purities of the 8-[(phenylsulfanyl)methyl]caffeine (**1a–i**) and 8-[(phenylsulfanyl)ethyl]caffeine (**2a–e**) analogues, all of which are previously unreported, were estimated by HPLC analysis. For the purpose of HPLC analysis, strong eluting conditions (85% acetonitrile) were employed and the eluent was monitored at 210 nm. Most organic compounds absorb UV light at 210 nm. Therefore if any impurities were to be present they would elute under these conditions and be detected at this wavelength. The chromatograms of these analyses are given in the Appendix. The purities of the caffeine analogues were found to be 89.2–99.0%. This may be considered as satisfactory.

3.7. Summary

This chapter describes the successful synthesis of nine 8-[(phenylsufanyl)methyl]caffeine (**1a–i**) and five 8-[(phenylsulfanyl)ethyl]caffeine (**2a–e**) analogues. The structures of the analogues were confirmed by NMR and MS, and the purities were estimated by HPLC. HPLC analysis revealed single peaks for the analysed compounds. The ^{1}H NMR and ^{13}C NMR spectra corresponded well with the proposed structures, and the appropriate integration values and chemical shifts were observed for all signals. The calculated exact masses also corresponded with the experimentally obtained masses. This is further confirmation of these structures.

CHAPTER 4

Enzymology

4.1. Measurement of *in vitro* catalytic activity of MAO

Several methods have been employed for determining MAO activity. Both direct and indirect measurements have been used for assaying MAO-A and MAO-B activities. The direct measurements include (a) detection of O_2 consumption, (b) detection of the formation of the co-product H_2O_2 and (c) detection of the absorbance or fluorescence of the oxidised monoamine product. Indirect measurements are based on the horseradish peroxidase (HRP)-coupled reaction system. Here, the H_2O_2 that is generated in the MAO catalytic cycle is detected by a HRP-catalysed oxidation of H_2O_2-sensitive probes, such as scopoletin and Amplex Red (Zhou & Panchuk-Voloshina, 1997). MAO activity may also be measured by monitoring the disappearance of the amine substrate or by the formation of ammonia, when the substrate is a primary amine (Nicrota & Parvez, 1999). Below are a few examples of assay techniques that may be used to determine MAO activity.

- Radiometric. A method originally developed by Wurtman & Axelrod (1963), relies on the formation of radio-labeled aldehydes. It is a discontinuous method that is highly sensitive and specific (Nicrota & Parvez, 1999).
- Ammonia detection. This fluorometric procedure uses a coupled reaction to determine ammonia continuously. The method is rapid and efficient. However, not all amines form ammonia during their oxidation by MAO (Holt *et al*., 1997; Nicrota & Parvez, 1999).
- Polarographic. Oxygen consumption is measured as an indicator of the extent to which oxidation takes place. This method is very accurate and reproducible but it lacks sensitivity and specificity (Holt *et al*., 1997).
- Luminometric. This is a highly sensitive method (Nicrota & Parvez, 1999). In this method, H_2O_2 catalyses a reaction that transforms luminal into a substance that emits light. MAO activity is proportional to the amount of light emitted (O' Brien *et al*., 1993).

For the purpose of this study, a simple and robust fluorometric assay will be employed using kynuramine as substrate. This method may be used to measure both MAO-A and –B activities since kynuramine is a mixed MAO-A/B substrate.

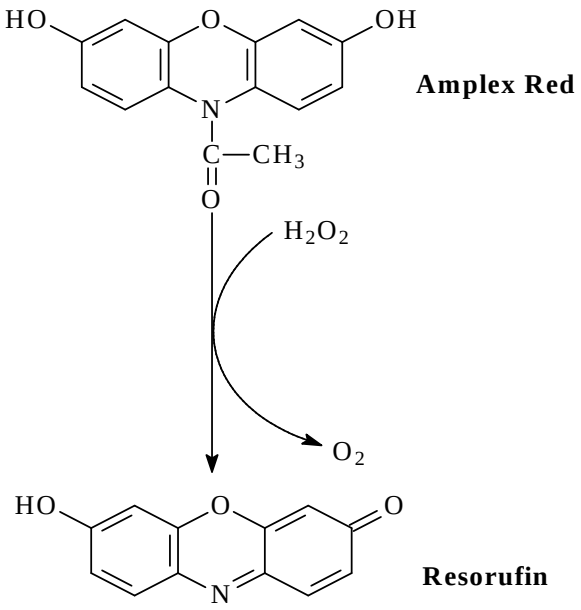

Figure 4.1: Reaction scheme for the formation of resorufin

For the purpose of determining IC_{50} values of compounds **2a-e**, the amount of H_2O_2 produced, as a result of the oxidation kynuramine by MAO, is used to measure the activity of both MAO-A and -B. H_2O_2 is reacted in a horseradish peroxidase-coupled reaction with the Amplex Red (N-acetyl-3,7,-dihydroxyphenoxazine) reagent. Amplex Red is a highly sensitive and stable H_2O_2 probe. When Amplex Red and H_2O_2 react, resorufin is produced (Figure 4.1.). The amount of resorufin formed can be measured by fluorescence spectrophotometry since the fluorescence of the generated resorufin is directly proportional to the amount of H_2O_2 produced by MAO. Resorufin has excitation and emission wavelengths of 560 and 590 nm, respectively (Zhou & Panchuk-Voloshina, 1997). Compounds **2a-e** were found to be highly fluorescent at the excitation (310 nm) and emission wavelengths (400 nm) used to directly measure 4-hydroxyquinoline concentrations. Because **2a-e** interfered with the direct measurement of 4-hydroxyquinoline (see below) their MAO inhibitory properties were measured with the HRP-coupled reaction system. At excitation and emission wavelength of 560 and 590 nm, respectively, the inhibitors did not interfere with the detection of resorufin.

To determine the IC_{50} values for MAO inhibition by compounds **1a-i**, to carry out time-dependent studies and to determine the mode of inhibition, this study also used kynuramine as substrate to measure the catalytic rates of MAO-A and –B. In this case, however, kynuramine concentrations were measured directly via spectrofluorometry. Kynuramine is oxidised to yield 4-hydroxyquinoline (Figure 4.2.), a fluorescent compound which is readily

measurable in the presence of the non-fluorescent substrate. The excitation and emission wavelengths of 4-hydroxyquinoline are 310 and 400 nm, respectively. Under these assay conditions **1a-i** do not fluoresce and do not interfere with the detection of 4-hydroxyquinoline.

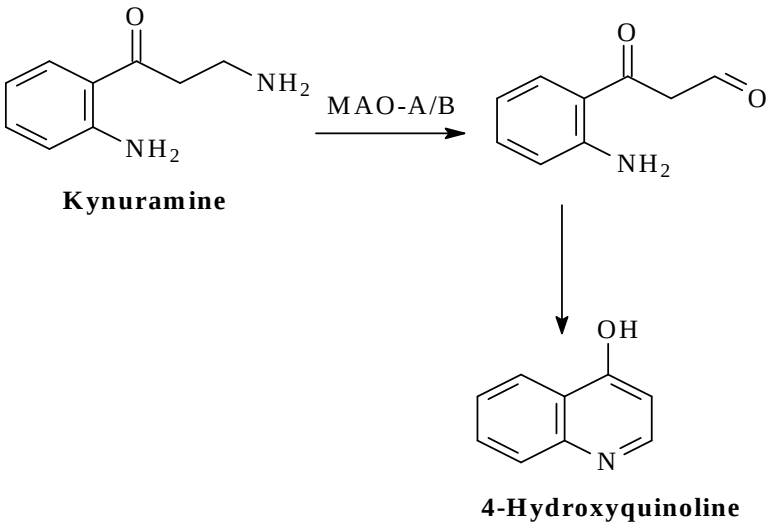

Kynuramine **4-Hydroxyquinoline**

Figure 4.2: The oxidation of kynuramine

4.1.1. Chemicals and instrumentation

For fluorescence spectrophotometry, a Varian Cary Eclipse fluorescence spectrophotometer was employed. Microsomes from insect cells containing recombinant human MAO-A and -B (5 mg/ml) and kynuramine.2HBr were obtained from Sigma-Aldrich. The Amplex Red (10-acetyl-3,7-dihydroxyphenoxazine) reagent, HRP and H_2O_2 (3%) were also from Sigma-Aldrich.

4.2. Measurement of IC_{50} values

The IC_{50} value of an inhibitor represents the concentration of the drug that is needed for 50% inhibition *in vitro*. For the determination of IC_{50} values, the rate of the MAO catalysed oxidation of the kynuramine is plotted graphically against the logarithm of the different concentrations of the inhibitor. A sigmoidal dose-response curve is obtained and the concentration of the inhibitor which reduces the rate to half of the maximal value is equal to the IC_{50}.

4.2.1. Detailed protocol for the HRP-coupled reaction system

- Recombinant human MAO-A and −B (5 mg/ml) was obtained from Sigma–Aldrich, pre-aliquoted and stored at -70 °C.

- Potassium phosphate buffer (100 mM, pH 7.4, made isotonic with KCl) was used for all the enzymatic reactions.
- The enzyme reactions contained:
    - MAO-A or MAO-B (0.0075 mg/ml),
    - various concentrations of the test inhibitor (0–100 µM),
    - kynuramine, at a final concentration of 45 µM and 30 µM for MAO-A and MAO-B, respectively, served as substrate.
    - HRP and Amplex Red. The HRP/Amplex Red working solution contained HRP (5 units/ml) and Amplex Red (1 mM) in potassium phosphate buffer.
- The final volumes of the reactions were 500 µl and contained the following:
    - 50 µl kynuramine (substrate),
    - 20 µl test inhibitor. Stock solutions of the test inhibitors were prepared in DMSO and added to the reactions to yield final concentrations of 4% (v/v) DMSO.
    - 280 µl potassium phosphate buffer,
    - 100 µl HRP/Amplex Red working solution and
    - 50 µl enzyme.
- The reactions were incubated for 20 min at 37 °C and terminated with the addition of 10 µl pargyline (5 mM) for MAO-A and 10 µl (R)-deprenyl (5 mM) for MAO-B.
- Distilled water (1400 µl) was added to each reaction before it was centrifuged for 10 min at 16,000 g (Scheme 4.1).
- The concentrations of the MAO generated resorufin in the reactions were determined by measuring the fluorescence of the supernatant at an excitation wavelength of 560 nm and an emission wavelength of 590 nm (Zhou & Panchuk-Voloshina, 1997).
- Quantitative estimations of resorufin were made by means of a linear calibration curve consisting of H_2O_2 at concentrations ranging from 0.05 to 0.65 µM. Each calibration standard was prepared to a final volume of 500 µL in potassium phosphate buffer (100 mM, pH 7.4) and contained 4% DMSO. To each standard was added 10 µl pargyline (5 mM) for MAO-A 10 µl (R)-deprenyl (5 mM) for MAO-B and 1400 µl distilled water.
- The IC_{50} values were determined by plotting the initial rate of oxidation versus the logarithm of the inhibitor concentration to obtain a sigmoidal dose-response curve. For this purpose the GraphPad Prism 5 software package was used. All measurements were carried out in triplicate and are expressed as mean ± standard error of the mean (SEM).

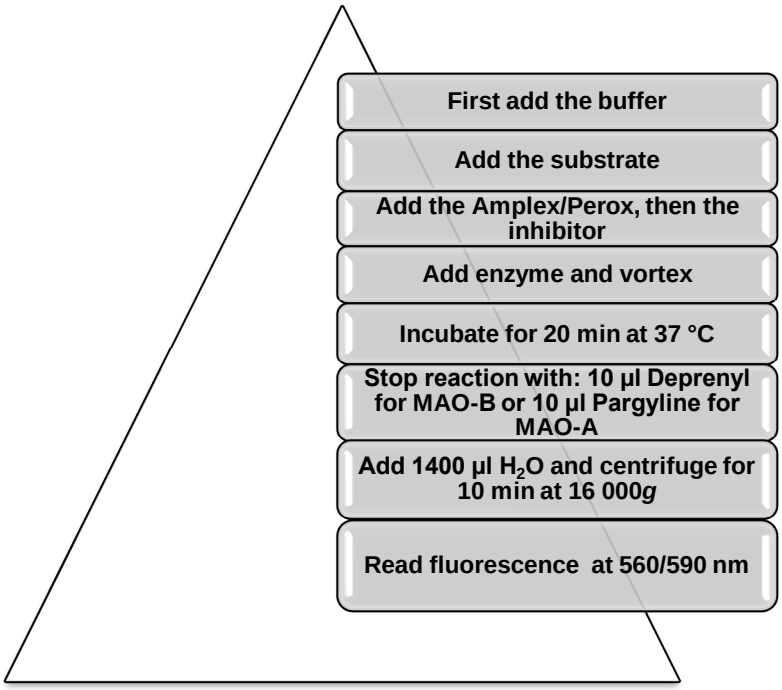

Scheme 4.1: IC_{50} determination with the HRP-coupled reaction system

4.2.2. Detailed protocol for the direct measurement of 4-hydroxyquinoline

- Recombinant human MAO-A or −B (5 mg/ml) was obtained from Sigma-Aldrich, pre-aliquoted and stored at -70 °C.
- Potassium phosphate buffer (100 mM, pH 7.4, made isotonic with KCl) was used for all the enzymatic reactions.
- The enzyme reactions contained:
    - MAO-A and MAO-B (0.0075 mg/ml),
    - various concentrations of the test inhibitor (0–100 µM),
    - kynuramine at final concentrations of 45 µM and 30 µM for MAO-A and MAO-B, respectively.
- The final volumes of the reactions were 500 µl and contained the following:
    - 50 µl kynuramine (substrate),
    - 20 µl test inhibitor. Stock solutions of the test inhibitors were prepared in DMSO and added to the reactions to yield final concentrations of 4% (v/v) DMSO.
    - 380 µl potassium phosphate buffer and
    - 50 µl enzyme.

- The reactions were incubated for 20 min at 37 °C and terminated with the addition of 400 µl NaOH [2 N]
- Distilled water (1000 µl) was added to each reaction before it was centrifuged for 10 min at 16,000 g (Scheme 4.2).
- The concentrations of the MAO generated 4-hydroxyquinoline in the reactions were determined by measuring the fluorescence of the supernatant at an excitation wavelength of 310 nm and an emission wavelength of 400 nm
- Quantitative estimations of 4-hydroxyquinoline were made by means of a linear calibration curve consisting of 4-hydroxyquinoline at concentrations ranging from 0.188-6.25 µM. Each calibration standard was prepared to a final volume of 500µl in potassium phosphate buffer and contained 4% DMSO. To each standard was added 400 µl NaOH (2 N) and 1000 µl distilled water.
- The IC_{50} values were determined by plotting the initial rate of oxidation versus the logarithm of the inhibitor concentration to obtain a sigmoidal dose-response curve. For this purpose the GraphPad Prism 5 software package was used. All measurements were carried out in triplicate and are expressed as mean ± SEM.

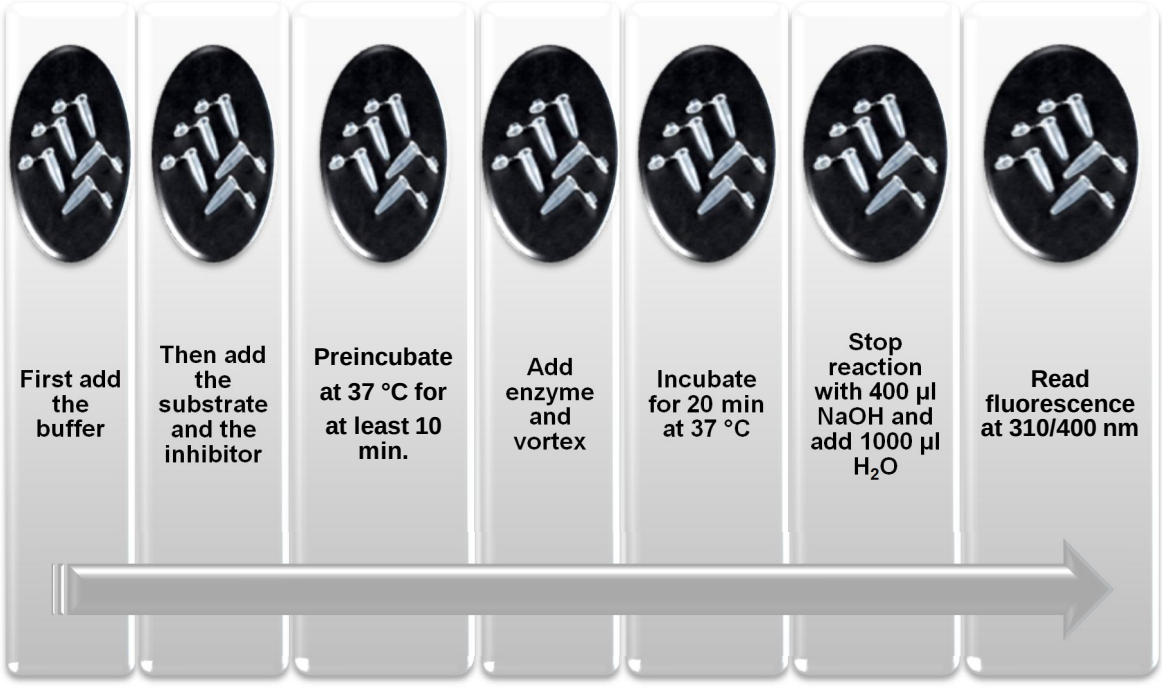

Scheme 4.2: IC_{50} determination by direct measurement of 4-hydroxyquinoline

4.3. Time-dependent inhibition studies

4.3.1. Introduction

Also known as reversibility studies, time-dependent studies evaluate whether an inhibitor binds covalently (irreversible) or non-covalently (reversible) to an enzyme. In this study the inhibitor was pre-incubated with the enzyme for various periods of time (0, 15, 30, 60 min) and the rate of the substrate oxidation was subsequently measured. The rate of substrate oxidation versus the range of pre-incubation times was subsequently plotted on a bar graph. If the oxidation rate remains unchanged for all of the incubation times, the inhibitor acts reversibly (Strydom *et al*., 2010).

4.3.2. Method

Recombinant MAO-B was prepared as described in Section 4.2. Kynuramine was used as substrate.

- Human recombinant MAO-B preparations were pre-incubated for periods of 0, 15, 30, 60 min at 37 °C with compound **1i** at a concentration of 8.1 µM. The volumes of these reactions were 120 µl.
- For the purpose of this study, a concentration of 0.03 mg/ml human MAO- B was used. The incubations were carried out in potassium phosphate buffer (100 mM, pH 7.4, made isotonic with KCl).
- A final concentration of 30 µM kynuramine was subsequently added to the preincubated enzyme preparations and the resulting reactions were incubated at 37 °C for a further 15 min. The final volume of the incubation was 500 µl and the final concentration of **1i** was 4.05 µM. The final concentration of the enzyme preparation was 0.015 mg/ml human MAO-B.
- The reactions with the recombinant human enzyme wereas terminated with 400 µl NaOH (2 M). A volume of 1000 µl distilled water was added to the incubations.
- The rates of formation of 4-hydroxyquinoline were measured fluorometrically at excitation and emission wavelengths of 310 and 400 nm, respectively.
- Quantitative estimations of 4-hydroxyquinoline were made by means of a linear calibration curve ranging from 0.188–6.25 µM. Each calibration standard was prepared to a final volume of 500 µl in potassium phosphate buffer and also contained 400 µl NaOH (2 N) and 1000 µl distilled water. All measurements were carried out in triplicate and are expressed as mean ± SEM.

4.4. Determining the mode of inhibition

4.4.1. Introduction

To determine whether an enzyme inhibitor acts competitively, a set of Lineweaver–Burk plots is constructed. For this purpose, the assay principles that were used for the time-dependent studies were also employed. Recombinant human MAO-B served as enzyme source. Linear regression analysis was performed using the GraphPad Prism 5 software package.

4.4.2. Method

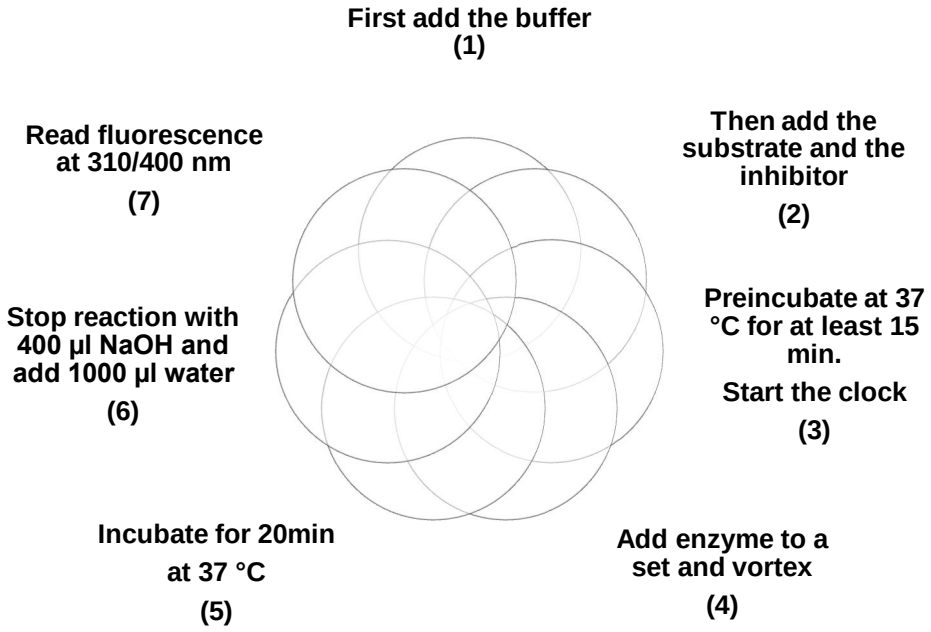

Scheme 4.3: Determining the mode of inhibition

To evaluate the mode of MAO-B inhibition, a set of Lineweaver–Burk plots for the inhibition of this enzyme by a selected test compound is constructed. By employing four different concentrations of the substrate, kynuramine (15, 30, 60 and 90 µM), the initial catalytic rates of the recombinant human enzyme was measured in the absence and presence of three different concentrations of the inhibitors. The 16 different incubations containing different substrate and inhibitor concentrations were pre-warmed for 15 min and human MAO-B (0.015 mg/ml) was added (Scheme 4.3). After 20 min of incubation, the reactions were terminated with the addition of 400 µl NaOH (2 N) and 1000 µl water was added. The amount of fluorescence, which represents the amount of 4-hydroxyquinoline formed, was

measured fluorometrically at excitation and emission wavelengths of 310 and 400 nm, respectively. Quantitative estimations of 4-hydroxyquinoline were made by means of a linear calibration curve with concentrations ranging from 0.0469 µM to 1.5 µM. Each calibration standard was prepared to a final volume of 500 µl in potassium phosphate buffer and also contained 400 µl NaOH (2 N) and 1000 µl distilled water.

4.5. Results: Sigmoidal curves

The IC_{50} value of an inhibitor represents the concentration of the drug that is needed for 50% inhibition *in vitro*. For the determination of IC_{50} values, the rate of the MAO catalysed oxidation of the kynuramine is plotted graphically against the logarithm of the inhibitor concentration and the concentration of the inhibitor which reduces the rate to half of the maximal value is equal to the IC_{50}. The sigmoidal curve for the determination of the IC_{50} value towards MAO-B of the most potent compound (**1i**) is given in Figure 4.3 as an example.

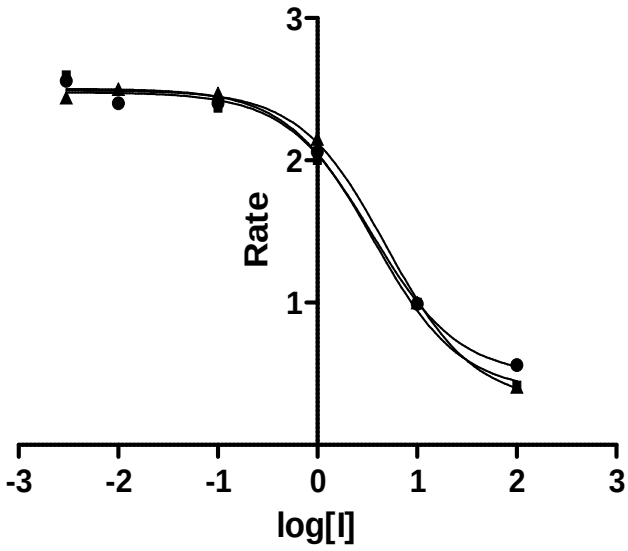

Figure 4.3: The sigmoidal dose-response curve of the initial rates of oxidation of kynuramine by recombinant human recombinant human MAO-B vs. the logarithm of concentration of inhibitor **1i** (expressed in µM). The determinations were carried out in triplicate. The concentration of kynuramine used was 30 µM and the rate data are expressed as nmoles 4-hydroxyquinoline formed/min/mg protein.

4.6. Results: Tables with IC_{50} values

Tables 4.1 and 4.2 give the IC_{50} values that were determined for the inhibition of both recombinant human MAO-A and MAO-B by the 8-[(phenylsulfanyl)methyl]caffeine (**1a–i**) and 8-[(phenylsulfanyl)ethyl]caffeine (**2a–e**) analogues. Lower IC_{50} values indicate that an inhibitor has a higher binding affinity for the enzyme and is therefore a more potent inhibitor. Also given is the selectivity index (SI) of every compound. A high selectivity index indicates that an inhibitor is selective for MAO-B.

Table 4.1: The IC_{50} values for the inhibition of recombinant human MAO-A and –B by compounds **1a–i**

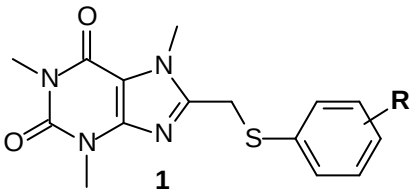

1

		IC_{50} (μM)[a,b]		
	R	**MAO-A**	**MAO-B**	**SI[c]**
1a	H	66.2± 5.32	23.4 ± 9.83	2.8
1b	3-Cl	19.4 ± 0.35	6.12 ± 0.45	3.2
1c	3-Br	23.8 ± 0.95	4.90 ± 1.04	4.9
1d	3-F	50.1 ± 1.84	22.30 ± 3.82	2.2
1e	3-CH_3	51.8 ± 4.20	17.90 ± 0.99	2.9
1f	3-OCH_3	41.3 ± 2.56	8.42 ± 0.10	4.9
1g	3-OCH_2CH_3	44.7 ± 2.29	18.40 ± 0.70	2.4
1h	4-Cl	31.6 ± 0.54	6.91 ± 0.65	4.6
1i	4-Br	20.8 ± 1.62	4.05 ± 0.77	5.1

[a] All values are expressed as the mean ± SEM of triplicate determinations.

[b] MAO activities were determined by directly measuring 4-hydroxyquinoline formation via fluorescence spectrophotometry.

[c] The selectivity index is the selectivity for the MAO-B isoform and is given as the ratio of IC_{50}(MAO-A)/IC_{50}(MAO-B).

From the data given above it is clear that the 8-[(phenylsulfanyl)methyl]caffeine analogues evaluated in this study were inhibitors of both MAO-A and MAO-B. The following general observations were made with regard to the IC_{50} values given in Table 4.1:

- Compound **1b** is the most potent inhibitor of MAO-A with an IC_{50} value of 19.4 µM. This compound also shows a relatively low degree of isoform selectivity, with an SI value of 3.2. Interestingly, those homologues containing chlorine and bromine on the phenyl ring were the most potent MAO-A and –B inhibitors in this series. For example, the chlorine substituted analogues (**1b** and **1h**) exhibited IC_{50} values for MAO-B of 6.12 µM and 6.91 µM, and the bromine substituted analogues (**1c** and **1i**) exhibited IC_{50} values for MAO-B of 4.90 µM and 4.05 µM. Similarly, for the inhibition of MAO-A, the chlorine substituted analogues (**1b** and **1h**) exhibited IC_{50} values of 19.4 µM and 31.6 µM, and the bromine substituted analogues (**1c** and **1i**) exhibited IC_{50} values of 23.8 µM and 20.8 µM.
- Compounds **1c** and **1i** are the most potent inhibitors of MAO-B with IC_{50} values of 4.90 and 4.05 µM, respectively. Interestingly, both these inhibitors are substituted with bromine on the phenyl ring. This suggests that bromine substitution is most favourable for MAO-B inhibition. This trend was also observed in the previously synthesised 8-(phenoxymethyl)caffeine analogues (Swanepoel, 2010).
- Compound **1a** was found to be the weakest MAO-B inhibitor of the series. Since **1a** does not contain substituents on the phenyl ring, it may be concluded that substitution on the phenyl ring enhances the MAO-B inhibition potencies.
- Based on the SI values, compounds **1a**–**i** are all selective for the MAO-B isoform. It may therefore be concluded that 8-[(phenylsulfanyl)methyl]caffeine are in general MAO-B selective inhibitors.

Table 4.2: The IC_{50} values for the inhibition of recombinant human MAO-A and –B by compounds **2a–e**

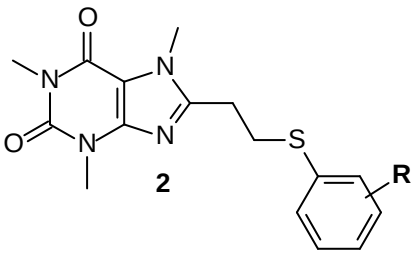

2

	R	IC_{50} (μM)[a,b] MAO-A	MAO-B	SI[c]
2a	H	139 ± 8.82	107.80 ± 32.70	1.30
2b	3-Cl	No inhibition	5.64 ± 3.55	–
2c	3-Br	372 ± 121.00	64.10 ± 9.73	5.80
2d	4-Cl	142 ± 40.60	7.79 ± 0.66	18.20
2e	4-Br	117 ± 13.70	124.10 ± 14.20	0.94

[a] All values are expressed as the mean ± SEM of triplicate determinations.

[b] The HRP-coupled reaction with Amplex Red was used to measure MAO activities.

[c] The selectivity index is the selectivity for the MAO-B isoform and is given as the ratio of IC_{50}(MAO-A)/IC_{50}(MAO-B)

The following general observations were made with regard to the IC_{50} values given in Table 4.2:

- Compound **2b**, the homologue containing chlorine at C3 of the phenyl ring, is the most potent inhibitor of MAO-B with an IC_{50} value of 5.67 μM. Interestingly, this compound did not display any inhibition towards MAO-A, even at a tested concentration of 100 μM.
- Compared to the other members of this series, compound **2d**, the homologue containing chlorine at C4 of the phenyl ring was also found to be a relatively good inhibitor of MAO-B with an IC_{50} value of 7.79 μM. Compound **2d** also displayed selectivity for MAO-B with a SI value of 18.
- Interestingly, **2e** was found to be the weakest inhibitor of MAO-B. Among **1a–i**, it was observed that inhibitors bearing a bromine substituent on the phenyl ring were the most potent inhibitors of MAO-B. However, the finding that **2e** is a weak MAO-B inhibitor is in contrast to this finding.

Table 4.3: A comparison of the IC_{50} values for the inhibition of MAO-B of the 8-[(phenylsulphanyl)methyl]caffeine analogues bearing Cl, Br and F substituents on C3 of the phenyl ring with the analogue bearing CH_3

C3 substituent	IC_{50} value (μM)	Ratio CH_3/X[a]
CH_3	17.90	–
Cl	6.12	2.9
Br	4.90	3.6
F	22.30	0.8

[a] The ratio of $IC_{50}(CH_3)/IC_{50}$(Cl, Br or F)

The comparison given in Table 4.3 shows that both the chlorine (**1b**) and bromine (**1c**) substituted homologues are better inhibitors than the methyl (**1e**) substituted compound. The fluorine (**1d**) substituted compound, however, was approximately as potent as the methyl substituted compound. This result indicates that substituents such as chlorine and bromine, which are larger electron withdrawing substituents, are more suitable for enhancing the MAO-B inhibition potency of 8-[(phenylsulphanyl)methyl]caffeine analogues when placed on C3 of the phenyl ring. The methyl group, which is electron releasing, is less suitable for enhancing the MAO-B inhibition potency of 8-[(phenylsulphanyl)methyl]caffeine analogues. Although the fluorine also is electron withdrawing, its small size compared to chlorine and bromine makes it less effective for enhancing the MAO-B inhibition potency of 8-[(phenylsulphanyl)methyl]caffeine analogues.

Table 4.4: A comparison of the IC_{50} values for the inhibition of MAO-B of the 8-[(phenylsulphanyl)methyl]caffeine analogues bearing Cl, Br and F substituents on C3 of the phenyl ring with the analogue bearing OCH_3

C3 substituent	IC_{50} value (μM)	Ratio OCH_3/X[a]
OCH_3	8.42	–
Cl	6.12	1.4
Br	4.90	1.7
F	22.30	0.4

[a] The ratio of $IC_{50}(OCH_3)/IC_{50}$(Cl, Br or F)

The comparison given in Table 4.4 shows that both the chlorine (**1b**) and bromine (**1c**) substituted homologues also are better inhibitors than the methoxy (**1f)** substituted homologue. This results support the analysis above, which suggests that larger electron withdrawing substituents, are more suitable for enhancing the MAO-B inhibition potency of 8-[(phenylsulphanyl)methyl]caffeine analogues when placed on C3 of the phenyl ring. The

methoxy group, which is an electron donating group, is therefore less suitable for enhancing the MAO-B inhibition potency of 8-[(phenylsulphanyl)methyl]caffeine analogues.

Table 4.5: A comparison of the IC_{50} values for the inhibition of MAO-B of the 8-[(phenylsulphanyl)methyl]caffeine analogues bearing Cl, Br and F substituents on C3 of the phenyl ring with the analogue bearing OCH_2CH_3

C3 substituent	IC_{50} value (μM)	Ratio OCH_2CH_3/X[a]
OCH_2CH_3	18.4	–
Cl	6.12	3.0
Br	4.90	3.8
F	22.3	0.8

[a] The ratio of $IC_{50}(OCH_2CH_3)/IC_{50}$(Cl, Br or F)

The comparison given in Table 4.5 also supports the finding that electron withdrawing substituents, are more suitable for enhancing the MAO-B inhibition potency of 8-[(phenylsulphanyl)methyl]caffeine analogues when substituted on C3 of the phenyl ring. The ethoxy group (**1g**), which is electron donating, leads to less potent MAO-B inhibitors than the chlorine (**1b**) and bromine (**1c**) substituents. Although also electron withdrawing, the fluorine (**1d**) substituted compound, is a particularly weak MAO-B inhibitor among compounds **1a**–**i**.

Table 4.6: A comparison of the IC_{50} values for the inhibition of MAO-B of the 8-[(phenylsulphanyl)methyl]caffeine analogues bearing substituents on C3 of the phenyl ring with the unsubstituted analogue

C3 substituent	IC_{50} value (μM)	Ratio H/X[a]
H	23.4	–
Cl	6.12	3.8
Br	4.90	4.8
F	22.30	1.0
CH_3	17.90	1.2
OCH_3	18.40	1.0
OCH_2CH_3	8.42	2.2

[a] The ratio of $IC_{50}(H)/IC_{50}$(Cl, Br, F, CH_3, OCH_3 or OCH_2CH_3)

The comparison given in Table 4.6 shows that substitution on the C3 position of the phenyl ring of 8-[(phenylsulphanyl)methyl]caffeine leads to enhanced MAO-B inhibition. With the exception of the fluorine (**1d**) substituted homologue, all other compounds in this series were better MAO-B inhibitors than the unsubstituted compound **1a**. Since fluorine is a small atom, this indicates that the addition of steric bulk to the phenyl ring of 8-[(phenylsulphanyl)methyl]caffeine yields enhanced MAO-B inhibition. Interestingly, the substituent may also be in the C4 position since the C4 substituted homologues, **1h** and **1i**, also are better MAO-B inhibitors that **1a**.

Table 4.7: A comparison of the IC_{50} values for the inhibition of MAO-B of the 8-[(phenylsulphanyl)methyl]caffeine analogues bearing Cl and Br substituents on C4 of the phenyl ring with the analogue bearing H

C4 substituent	IC_{50} value (μM)	Ratio H/X[a]
H	23.40	–
Cl	6.91	3.4
Br	4.05	5.8

[a] The ratio of IC_{50}(H)/IC_{50}(Cl or Br)

As shown in Table 4.7 substitution on the C4 position of the phenyl ring of 8-[(phenylsulphanyl)methyl]caffeine also leads to enhanced MAO-B inhibition. This is based on the observation that the C4 substituted homologues, **1h** and **1i**, also are better MAO-B inhibitors that **1a**.

Table 4.8: A comparison of the IC_{50} values for the inhibition of MAO-B of the 8-[(phenylsulphanyl)methyl]caffeine analogues bearing Cl and Br substituents on C3 of the phenyl ring with those bearing Cl and Br substituents on C4 of the phenyl ring

Substituent	IC_{50} (C3 position)	IC_{50} (C4 position)	Ratio (C3/C4)
Cl	6.12	6.91	0.9
Br	4.90	4.05	1.2

Compounds substituted with bromine on the *meta* and *para* positions of the phenyl ring led to potent MAO-B inhibition with IC_{50} values of 4.90 and 4.05 μM, respectively. Similarly, substitution with chlorine on the *meta* and *para* positions of the phenyl ring led to relatively good MAO-B inhibition with IC_{50} values of 6.12 and 6.91 μM, respectively. As shown in Table 4.8, the placement of the substituent on C3 or C4 yields similar MAO-B inhibition

potencies. It may therefore be concluded that substitution on both C3 and C4 is suitable for enhancing the MAO-B inhibition potency of 8-[(phenylsulphanyl)methyl]caffeine analogues.

Table 4.9: A comparison of the IC_{50} values for the inhibition of MAO-A of the 8-[(phenylsulphanyl)methyl]caffeine analogues bearing substituents on C3 of the phenyl ring with the unsubstituted analogue

C3 substituent	IC_{50} value (μM)	Ratio H/X[a]
H	66.2	–
Cl	19.4	3.4
Br	23.8	0.8
F	50.1	0.5
CH_3	44.7	1.1
OCH_3	41.3	1.1
OCH_2CH_3	51.8	0.8

[a]The ratio of IC_{50}(H)/IC_{50}(Cl, Br, F, CH_3, OCH_3 or OCH_2CH_3)

Table 4.9 shows that, in contrast to MAO-B, substitution on the C3 position of the phenyl ring of 8-[(phenylsulphanyl)methyl]caffeine does not necessarily lead to enhanced MAO-A inhibition. The MAO-A inhibition potency may be best enhanced with the addition of a chlorine at C3.

Table 4.10 A comparison of the IC_{50} values for the inhibition of MAO-B of the 8-[(phenylsulphanyl)ethyl]caffeine analogues bearing Cl and Br substituents on C3 of the phenyl ring with those bearing Cl and Br substituents on C4 of the phenyl ring

Substituent	IC_{50} (C3 position)	IC_{50} (C4 position)
Cl	5.67	7.79
Br	64.10	124.10

Compounds substituted with bromine on the *meta* and *para* positions of the phenyl ring yielded relatively poor MAO-B inhibitors with IC_{50} values of 64.1 μM and 124.1 μM, respectively. This result is surprising since substitution with bromine on the 8-[(phenylsulphanyl)methyl]caffeine analogues yielded structures **1c** and **1i** with comparatively good inhibition potencies (IC_{50} value of 4.90 and 4.05 μM, respectively). In contrast, substitution with chlorine on the *meta* and *para* positions of the phenyl ring yielded better MAO-B inhibitors with IC_{50} values of 5.67 μM and 7.79 μM for **2b** and **2d**, respectively. This result is in agreement with the results obtained with the 8-[(phenylsulphanyl)methyl]caffeine

analogues, in which case chlorine substitution on the *meta* and *para* positions of the phenyl ring led to relatively good MAO-B inhibition with IC_{50} values of 6.12 and 6.91 μM for **1b** and **1h**, respectively. The results in Table 4.10 show that for both chlorine and bromine substituents, substitution on the C3 position is more favourable than substitution on the C4 position for MAO-B inhibition.

In conclusion: The results indicate that a high degree of steric bulk plays an important role, especially towards enhancing MAO-B inhibition. Importantly, those homologues containing chlorine and bromine on the phenyl ring, in both the C3 and C4 positions of the phenyl ring of 8-[(phenylsulphanyl)methyl]caffeine, were the most potent MAO-A and –B inhibitors in this series. In each instance, the bromine substituted analogues are the most potent inhibitors followed by chlorine substituted analogues. The size and higher degree of steric hindrance of bromine compared to that of chlorine may explain this trend. Although the methyl, methoxy and ethoxy groups are also relatively large, they were weaker MAO-A and –B inhibitors than the chlorine and bromine substituted homologues. This results shows that the degree of electronegativity of the C3 substituent also plays a role. Substituents with a higher degree of electronegativity lead to better MAO-A and –B inhibition. In spite of this, when comparing the 8-[(phenylsulfanyl)methyl]caffeine analogues bearing a methyl, methoxy and an ethoxy group on the phenyl ring with the unsubstituted analogue, the importance of steric bulkiness is also apparent. Since the methyl, methoxy and ethoxy substituted analogues are more potent than the unsubstituted analogue, it can be concluded that substitution on the phenyl ring with a substituent that adds steric bulk to the 8-[(phenylsulfanyl)methyl]caffeine structure may be favorable for MAO-B inhibition.

4.7. Comparison of the 8-[(phenylsulfanyl)methyl)]caffeine MAO potencies with those of the 8-(phenoxymethyl)caffeines

Since the 8-(phenoxymethyl)caffeine analogues were used as a lead compounds for this study, the MAO inhibitions potencies of the previously reported 8-(phenoxymethyl)caffeine analogues (Swanepoel, 2010) were compared with those of the 8-[(phenylsulfanyl)methyl)]caffeine analogues examined here. Given below are the IC_{50} values for the 8-(phenoxymethyl)caffeine analogues for the inhibition of recombinant human MAO-A and –B.

Table 4.11: The IC_{50} values for the inhibition of recombinant human MAO-A and –B by 8-(phenoxymethyl)caffeine analogues (Swanepoel, 2010).

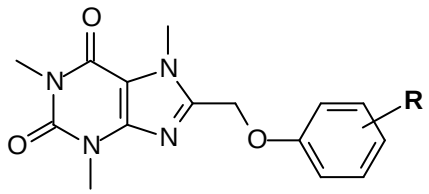

Compound	R	MAO-A IC_{50} (µM)	MAO-B IC_{50} (µM)	SI[a]
3a	H	21.10	5.780	3.7
3b	3-Cl	No inhibition	0.334	–
3c	3-Br	34.00	0.148	229.7
3d	3-F	13.20	1.610	8.2
3e	3-CF_3	4.59	0.641	7.1
3f	3-CH_3	18.80	1.230	15.3
3g	3-OCH_3	No inhibition	1.960	–
3h	4-Cl	20.40	0.250	81.6
3i	4-Br	10.70	0.189	56.6

[a] The selectivity index is the selectivity for the MAO-B isoform and is given as the ratio of IC_{50}(MAO-A)/IC_{50}(MAO-B)

The following observations may be made when comparing the inhibition potencies of the 8-(phenoxymethyl)caffeine analogues (Table 4.11) with the inhibition potencies of the 8-[(phenylsulfanyl)methyl)]caffeine analogues (Table 4.1):

- Compared to the 8-[(phenylsulfanyl)methyl]caffeine analogues, the 8-(phenoxymethyl)caffeine analogues are more potent MAO-A and –B inhibitors. However, both the 8-[(phenylsulfanyl)methyl]caffeine and 8-(phenoxymethyl)caffeine analogues are selective for MAO-B.
- The 8-(phenoxymethyl)caffeine analogues have an isoform selectivity ranging from 4.0–230.0, while the SI values of the 8-[(phenylsulfanyl)methyl]caffeine analogues range from 2.2–5.1.
- Similar to the results of the 8-(phenoxymethyl)caffeine analogues, compounds substituted on the *meta* and *para* position of the phenylsulfanyl ring with bromine yielded the most potent compounds. For example, sulfanyl analogues **1c** and **1i** have IC_{50} values of 4.05 µM and 4.90 µM, respectively, while the phenoxy analogues, compounds **3c** and **3i**, exhibited IC_{50} values of 0.148 µM and 0.189 µM, respectively. According to these results the 8-[(phenylsulfanyl)methyl]caffeine analogues,

compounds **1c** and **1i**, are 21–33 fold weaker as MAO-B inhibitors than the corresponding 8-(phenoxymethyl)caffeine, compounds **3c** and **3i**.

- The most potent MAO-A inhibitor among the 8-(phenoxymethyl)caffeine analogues is compound **3e** with an IC_{50} value of 4.59 µM, while the most potent MAO-A inhibitor among the 8-[(phenylsulfanyl)methyl]caffeine analogues is **1b** with an IC_{50} of 19.4 µM.
- This leads to the conclusion that the 8-(phenoxymethyl)caffeine analogues are in general better MAO-B inhibitors than the 8-[(phenylsulfanyl)methyl]caffeine analogues and the phenoxy side-chain is therefore better suited for the design of MAO-B inhibitors than the phenylsulfanyl side-chain.

4.8. Results: Time-dependent studies

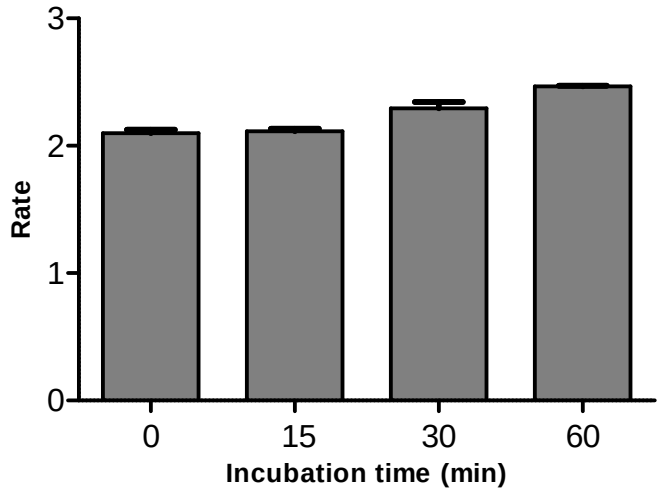

Figure 4.4: Time-dependent inhibition of recombinant human MAO-B by compound **1i**. The enzyme was preincubated for various periods of time (0-60 min) with **1i** (MAO-B) at a concentration of 8.1 µM. The concentration of kynuramine, the enzyme substrate, was 30 µM. The catalytic rates are expressed as nmoles 4-hydroxyquinoline formed/min/mg protein.

Time-dependent studies are used to evaluate whether an inhibitor binds irreversibley or reversibly to an enzyme. In this study inhibitor **1i** was selected to evaluate whether the 8-[(phenylsulfanyl)methyl]caffeine analogues are reversible or irreversible inhibitors of MAO-B. The reversibility of MAO-A inhibition was not examined since the 8-[(phenylsulfanyl)methyl]caffeine analogues were found to be weak MAO-A inhibitors. For the purpose of the time-dependent studies, the inhibitor was pre-incubated with the enzyme for

various periods of time (0, 15, 30, 60 min) at a concentration of 8.1µM. This concentration is equal to 2-fold the IC_{50} value for the inhibition of MAO-B by **1i**. The rates of the substrate oxidation were subsequently measured. The rates of substrate oxidation *versus* the pre-incubation times were then subsequently plotted on a bar graph. As already discussed, if the oxidation rate remains unchanged for all of the incubation times, the inhibitor acts reversibility.

As shown in Figure 4.4 there is no time-dependent reduction in the rate of MAO-B catalysed oxidation of kynuramine when compound **1i** is pre-incubated with MAO-B for the various periods of time. Since the oxidation rate remains unchanged for all of the incubation times, it can be concluded that the inhibitor possesses a reversibile mode of action, at least for the 60 min and at a concentration of 2-fold the IC_{50} value.

4.9. Results: Construction of Lineweaver-Burk plots

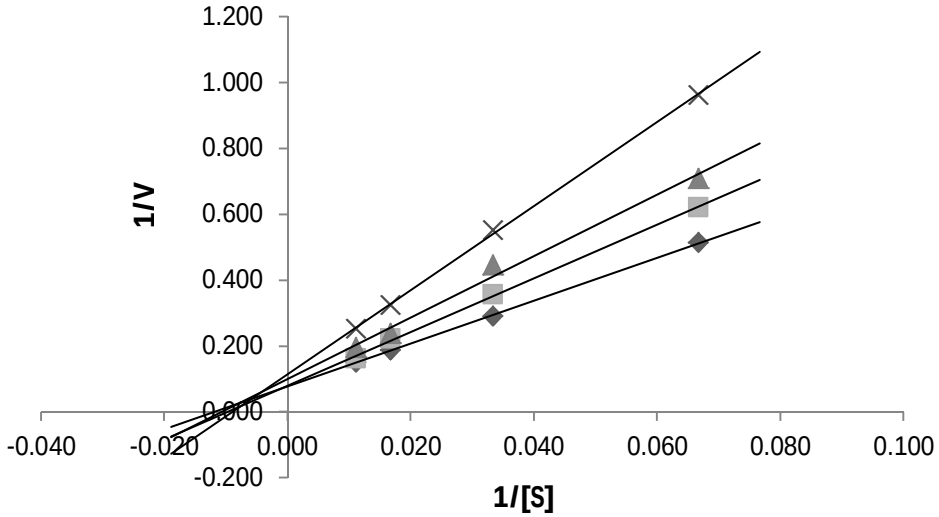

Figure 4.5: Lineweaver-Burk plots constructed for recombinant human MAO-B in the absence (diamonds) and presence of various concentrations of **1i** (squares, 1.0125 µM; triangle, 2.0250 µM and cross, 4.0500 µM). The rate (V) is expressed as nmol product formed/min/mg protein.

The purpose of constructing Lineweaver–Burke plots for an inhibitor is to determine whether an enzyme inhibitor acts competitively. In this study inhibitor **1i** was selected to evaluate whether the 8-[(phenylsulfanyl)methyl]caffeine analogues are competitive inhibitors of MAO-B. The results are given in Figure 4.5. As can be seen competitive inhibition was observed for compound **1i** since the Lineweaver-Burk plots are linear and intersected on the y-axis. It

can thus be concluded that the 8-[(phenylsulfanyl)methyl]caffeine analogues are reversible competitive inhibitors of MAO-B.

4.10. Summary

This chapter demonstrates that both 8-[(phenylsulfanyl)methyl]caffeine and 8-[(phenylsulfanyl)ethyl]caffeine analogues are inhibitors of MAO-A and –B. Compound **1i** was found to be a competitive and reversible inhibitor of MAO-B. The compounds did not exhibit high binding affinities towards MAO-A. It can be thus concluded that the compounds analysed in this study are selective for MAO-B. The MAO-A and –B inhibition potencies of 8-[(phenylsulfanyl)methyl]caffeine analogues were compared to those of the 8-(phenoxymethyl)caffeine analogues and the 8-[(phenylsulfanyl)methyl]caffeine analogues proved to be relatively weaker inhibitors with IC_{50} values for the inhibition of MAO-B ranging from 4.05–23.40 µM. The 8-[(phenylsulfanyl)ethyl]caffeine were found to be weaker inhibitors of MAO than the 8-[(phenylsulfanyl)methyl]caffeine analogues. This study shows that, compared to the (phenylsulfanyl)methyl side-chain, the phenoxymethyl moiety is more suitable for enhancing the MAO-B inhibition potency of caffeine when substituted on C8 of the caffeine ring.

CHAPTER 5

Summary

As mentioned in the introductory chapter, based on the observation that the 8-(phenoxymethyl)caffeine analogues are potent inhibitors of MAO-B (Swanepoel, 2010), a series of nine 8-[(phenylsulfanyl)methyl]caffeine analogues (**1a-i**) were synthesised and evaluated as inhibitors of MAO-A and –B. An additional series of five 8-[(phenylsulfanyl)ethyl]caffeine analogues (**2a-e**) was synthesised to determine the effect that carbon chain elongation at position C8 has on the MAO inhibition potency. The compounds evaluated in this study did not exhibit high binding affinities towards MAO-A, but did demonstrate better affinities toward MAO-B and can therefore be regarded as MAO-B selective inhibitors. These compounds were found to bind reversibly and competitively to MAO-B with K_i values ranging from 4.05–23.40 μM for the first series, the 8-[(phenylsulfanyl)methyl]caffeine analogues (**1a-i**), and 5.67–124.10 μM for the second series, the 8-[(phenylsulfanyl)ethyl]caffeine analogues (**2a-e**). As mentioned in Chapter 1, a reversible mode of inhibition is more desirable than an irreversibile mode of inhibition since irreversibility often presents with adverse effects, such as the life-threatening hypertensive crises, which may arise when MAO-A is inhibited (Youdim & Bakhle, 2006; Foley *et al*., 2000).

Monoamine oxidase is an essential protein of the outer mitochondrial membrane and it plays a role in the inactivation of biogenic and diet derived amines, in both the CNS and the peripheral neurons. MAO-A is responsible for the deamination of serotonin and noradrenaline. In the intestine it also catalyses the oxidation of tyramine. MAO-B in the human brain is primarily responsible for the catabolism of dopamine and β-phenylethylamine (Foley *et al*., 2000). Hydrogen peroxide produced during the metabolism of dopamine may lead to the formation of potentially toxic compounds, such as hydrogen peroxide, which in turn, may be converted to the hydroxyl radical. This radical may cause neuronal damage and even neuronal death. Thus, MAO inhibition is a strategy for decreasing the formation of hydrogen peroxide and thus decreasing the formation of the hydroxyl radical and the levels of oxidative stress in the brains of PD patients. For this reason, MAO-B inhibitors may be considered to be neuroprotective in PD. MAO-B inhibitors may also be useful as adjuvants to L-dopa in PD therapy and thereby conserve the amount of dopamine in the brain.

Caffeine was considered as the lead compound for the design of new MAO-B inhibitors for the current study. Although caffeine is a weak inhibitor of MAO, it has been previously reported that substitution at the C8 position of the caffeine may enhance the inhibition potency of caffeine to a large extent. A previously studied compound, CSC, is an example of

a potent inhibitor of MAO-B which is substituted at the C8 position of caffeine (Pretorius *et al*., 2008). It was recently also shown that a series of 8-(phenoxymethyl)caffeine analogues are exceptionally potent inhibitors of MAO (Swanepoel, 2010). These compounds were however, found to be less potent towards MAO-A, and were therefore classified as MAO-B selective. The inhibition potencies of these compounds ranged from 0.148–5.780 μM, with the homologues containing halogens on the phenyl ring being the most potent. For the purpose of this study these results were expanded upon by synthesising a homologous series of 8-[(phenylsulfanyl)methyl]caffeines of which the C8 phenyl ring contained a variety of halogen and alkyl substituents. In addition, a second series, consisting of five 8-[(phenylsulfanyl)ethyl]caffeines were synthesised to determine the effect of carbon chain elongation on the MAO inhibition potency. Subsequently, it was determined if these derivatives also act as inhibitors of MAO-A and –B. The MAO-A and –B inhibition potencies of the 8-[(phenylsulfanyl)methyl]caffeines were then compared to that of the previously studied 8-(phenoxymethyl)caffeine analogues.

Chemistry: Compounds **1a–i** and **2a–e** were synthesised from 1,3-dimethyl-5,6-diaminouracil by reaction with an appropriate 2-(phenylsulfanyl)acetic acid or 3-(phenylsulfanyl)propanoic acid in the presence of the carbidiimide dehydrating agent, EDAC. Thirteen of the acids were not commercially available and were synthesised successfully in the laboratory from the corresponding phenols. The structures of 8-[(phenylsulfanyl)methyl]caffeine (**1a–i**) and 8-[(phenylsulfanyl)ethyl]caffeine (**2a–e**) analogues were confirmed by ^{1}H-NMR and ^{13}C-NMR, as well as MS analysis. The purities of the target compounds were estimated by HPLC analysis. The ^{1}H NMR and ^{13}C NMR spectra corresponded well with the proposed structures and the HPLC analysis revealed mostly single peaks for the analysed compounds.

MAO inhibition studies: The inhibitory potencies of the caffeine derivatives were measured by using commercially available recombinant MAO-A and –B as enzyme sources. Two fluorometric methods were utilised in measuring the inhibitory potencies of the caffeine derivatives. These methods are characterised by (a) measuring the amount of 4-hydroxyquinoline released from the MAO catalysed oxidation of kynuramine and (b) measuring the amount of MAO generated H_2O_2. 4-Hydroxyquinoline is a fluorescent compound which is readily measured in the presence of the non-fluorescent kynuramine. 4-Hydroxyquinoline fluoresces at an excitation wavelength of 310 nm and an emission wavelength of 400 nm and, since compounds **1a-i** do not fluoresce at these wavelengths, their MAO inhibitory potencies were measured by directly measuring 4-hyroxyquinoline formation. The inhibitory potencies of compounds **2a-e** could not be measured by this

method as they fluoresce at these wavelengths. Their inhibitory potencies were therefore measured by quantifying the amount of hydrogen peroxide that is produced in the MAO oxidation cycle. H_2O_2 reacts with Amplex Red to yield resorufin which was subsequently measured fluorometrically. Resorufin fluoresces at excitation and emission wavelengths of 560 and 590 nm, respectively (Zhou & Panchuk-Voloshina, 1997).

The studies revealed that 8-[(4-bromophenyl)sulfanyl]methyl]caffeine (**1b)** was the most potent inhibitor of MAO-A with an IC_{50} value of 19.4 µM. This compound also showed a relatively low degree of isoform selectivity (SI = 3.2). Although most of these compounds showed some inhibition towards MAO-A, they were classified as MAO-B selective. The bromo substituted compounds, **1c** and **1i,** were found to be the most potent inhibitors of MAO-B, with IC_{50} values of 4.90 and 4.05 µM, respectively. This trend was also observed for the previously synthesised 8-(phenoxymethyl)caffeine derivatives (Swanepoel, 2010). The unsubstituted 8-[(phenylsulfanyl)methyl]caffeine (**1a**) was found to be the weakest MAO-B inhibitor of the series. Since **1a** did not contain any substituent on the phenyl ring, it can be concluded that substitution on the phenyl ring enhances the MAO-B inhibition potencies. The results for the second series (**2a-e**) revealed that the homologue containing chlorine at C3 of the phenyl ring (**2b**) was the most potent inhibitor of MAO-B with an IC_{50} value of 5.67 µM. Interestingly, this compound did not show any inhibition towards MAO-A, even when tested at a high concentration of 100 µM. Compound **2e** was found to be the weakest inhibitor of MAO-B. Among the first series (**1a-i**), it was observed that inhibitors bearing bromine on the phenyl ring were the most potent inhibitors of MAO-B. However, the finding that **2e** is a weak inhibitor of MAO-B, is in contrast to this finding. In general, the 8-[(phenylsulfanyl)ethyl]caffeines were found to be weaker inhibitors of MAO than the 8-[(phenylsulfanyl)methyl]caffeine analogues.

As mentioned above, one of the aims of this study was to compare the MAO inhibition potencies of the 8-[(phenylsulfanyl)methyl]caffeine analogues to those of the previously studied 8-(phenoxymethyl)caffeine analogues. The 8-(phenoxymethyl)caffeine analogues were found to be more potent inhibitors of MAO-A than the 8-[(phenylsulfanyl)methyl]caffeine analogues. The most potent inhibitor of MAO-A among the 8-(phenoxymethyl)caffeine analogues was [8-(bromophenoxy)methyl] with an IC_{50} value of 4.59 µM, while the most potent MAO-A inhibitor among the 8-[(phenylsulfanyl)methyl]caffeine analogues was compound **1b** with an IC_{50} of 19.4 µM. Similar to the 8-(phenoxymethyl)caffeine analogues, compounds substituted on the *meta* and *para* position of the phenylsulfanyl ring of the 8-[(phenylsulfanyl)methyl]caffeines with a bromine substituent yielded the most potent compounds. It can thus be concluded that

bromine substitution on the *meta* and *para* position of the phenylsulfanyl ring may be favourable for MAO-B inhibition. However, 8-[(phenylsulfanyl)methyl]caffeine analogues had less isoform selectivity (SI = 2.2–5.1) than the 8-(phenoxymethyl)caffeine analogues (SI = 4–230). This demonstrates that, although the 8-[(phenylsulfanyl)methyl]caffeine analogues are structurally similar to the 8-(phenoxymethyl)caffeine analogues, the 8-(phenoxymethyl)caffeine analogues are in general better as MAO-B inhibitors than the 8-[(phenylsulfanyl)methyl]caffeine analogues. It may thus be concluded that the phenoxy side-chain is better suited for the design of MAO-B inhibitors than the phenylsulfanyl side-chain.

Time dependency and mode of inhibition: For the purpose of determining the reversibility of MAO-B inhibition of the test compounds, the time-dependency of inhibition of MAO-B by the best inhibitor was evaluated. Compound **1i** was preincubated for various periods of time with MAO-B and did not cause a significant time-dependent reduction in the rate of MAO-B catalysed oxidation of kynuramine. From this result, it may be concluded that the inhibition of MAO-B by compound **1i** is reversible. To determine the mode of inhibition a set of Lineweaver-Burk plots was constructed. Here again the best inhibitor of MAO-B (compound **1i**) was used. The results showed that the Lineweaver-Burk plots were linear and intersected on the y-axis. It can be thus concluded that **1i** is a competitive inhibitor of MAO-B.

Conclusion

From this discussion above it can be concluded that, compared to the 8-[(phenylsulfanyl)methyl]caffeine analogues, the 8-(phenoxymethyl)caffeine analogues may be considered as better lead compounds for the design of potent caffeine derived inhibitors of MAO-B. In many instances, the 8-(phenoxymethyl)caffeine analogues were several orders of magnitude more potent MAO-B inhibitors than the 8-[(phenylsulfanyl)methyl]caffeine analogues. Although they may have similar structural features, 8-(phenoxymethyl)caffeines are significantly more potent MAO-B inhibitors than the corresponding 8-[(phenylsulfanyl)methyl]caffeine and 8-[(phenylsulfanyl)ethyl]caffeine analogues.

REFERENCES

Ahn, Y. & Cohen, T. 1994, "A general diastereoselective synthesis of spiroacetals related to those in ionophores via the reaction of lactones with cerium(III)-γ-cerioalkoxide. MAD reverses the diastereoselectivity of the addition of methylmetallics to *α-beta-keto* ether", The Journal of Organic Chemistry, vol. 59, no. 11, pp. 3142-3150.

Alexi, T., Borlongan, C.V., Faull, R.L.M., Williams, C.E., Clark, R.G., Gluckman, P.D. & Hughes, P.E. 2000, "Neuroprotective strategies for basal ganglia degeneration: Parkinson's and Huntington's diseases", Progress in Neurobiology, vol. 60, no. 5, pp. 409-470.

Andringa, G., Van Oosten, R.V., Unger, W., Hafmans, T.G.M., Veening, J., Stoof, J.C. & Cools, A.R. 2000, "Systemic administration of the propargylamine CGP 3466B prevents behavioural and morphological deficits in rats with 6-hydroxydopamine-induced lesions in the substantia nigra", European Journal of Neuroscience, vol. 12, no. 8, pp. 3033-3043.

Andringa, G., Eshuis, S., Perentes, E., Maguire, R.P., Roth, D., Ibrahim, M., Leenders, K.L. & Cools, A.R. 2003, "TCH346 prevents motor symptoms and loss of striatal FDOPA uptake in bilaterally MPTP-treated primates", Neurobiology of Disease, vol. 14, no. 2, pp. 205-217.

Ashihara, H. & Crozier, A. 2001, "Caffeine: a well known but little mentioned compound in plant science", Trends in Plant Science, vol. 6, no. 9, pp. 407-413.

Bach, A.W., Lan, N.C., Johnson, D.L., Abell, C.W., Bembenek, M.E., Kwan, S.W., Seeburg, P.H. & Shih, J.C. 1988, "cDNA cloning of human liver monoamine oxidase A and B: molecular basis of differences in enzymatic properties", Proceedings of the National Academy of Sciences of the United States of America, vol. 85, no. 13, pp. 4934-4938.

Bains, J.S. & Shaw, C.A. 1997, "Neurodegenerative disorders in humans: the role of glutathione in oxidative stress-mediated neuronal death", Brain Research Reviews, vol. 25, no. 3, pp. 335-358.

Baron, J.A. 1986, "Cigarette smoking and Parkinson's disease", Neurology, vol. 36, no. 11, pp. 1490-1490.

Beal, M.F., Matthews, R.T., Tieleman, A. & Shults, C.W. 1998, "Coenzyme Q10 attenuates the 1-methyl-4-phenyl-1,2,3,6-tetrahydropyridine (MPTP) induced loss of striatal dopamine and dopaminergic axons in aged mice", Brain Research, vol. 783, no. 1, pp. 109-114.

Ben-Shachar, D., Riederer, P. & Youdim, M.B.H. 1991, "Iron-melanin interaction and lipid peroxidation: Implications for Parkinson's disease", Journal of Neurochemistry, vol. 57, no. 5, pp. 1609-1614.

Benzi, G. & Moretti, A. 1995, "Age- and peroxidative stress-related modifications of the cerebral enzymatic activities linked to mitochondria and the glutathione system", Free Radical Biology and Medicine, vol. 19, no. 1, pp. 77-101.

Bharath, S., Hsu, M., Kaur, D., Rajagopalan, S. & Andersen, J.K. 2002, "Glutathione, iron and Parkinson's disease", Biochemical Pharmacology, vol. 64, no. 5-6, pp. 1037-1048.

Binda, C., Wang, J., Pisani, L., Caccia, C., Carotti, A., Salvati, P., Edmondson, D.E. & Mattevi, A. 2007, "Structures of human monoamine oxidase B complexes with selective noncovalent inhibitors: Safinamide and coumarin analogs", Journal of Medicinal Chemistry, vol. 50, no. 23, pp. 5848-5852.

Birkmayer, W., Riederer, P., Youdim, M.B.H. & Linauer, W. 1973, "The potentiation of the anti akinetic effect after L-dopa treatment by an inhibitor of MAO-B, deprenil", Journal of Neural Transmission, vol. 36, no. 3-4, pp. 303-326.

Blicke, F.F. & Godt Jr., H.C. 1954, "Reactions of 1,3-dimethyl-5,6-diaminouracil", Journal of the American Chemical Society, vol. 76, no. 10, pp. 2798-2800.

Bonnet, U. 2003, "Moclobemide: Therapeutic use and clinical studies", CNS Drug Reviews, vol. 9, no. 1, pp. 97-140.

Boyer, E.W. & Shannon, M. 2005, "The serotonin syndrome", New England Journal of Medicine, vol. 352, no. 11, pp. 1112-1120.

Brunner, H., Nelen, M., Breakefield, X., Ropers, H. & van Oost, B. 1993, "Abnormal behavior associated with a point mutation in the structural gene for monoamine oxidase A", Science, vol. 262, no. 5133, pp. 578-580.

Burton, E.A., Glorioso, J.C. & Fink, D.J. 2003, "Gene therapy progress and prospects: Parkinson's disease", Gene Therapy, vol. 10, no. 20, pp. 1721-1727.

Carlsson A. 1981, "Aging and brain neurotransmitter". (*In*: Platt D., *ed*. Funktionsstorungen des Gehirns im Alter. Schattauer: Stuttgar, pp. 67-81).

Carlsson, A. 1959, "The occurrence, distribution and physiological role of catecholamines in the nervous system ", Pharmacological Reviews, vol. 11, no. 2, pp. 490-493.

Cases, O., Seif, I., Grimsby, J., Gaspar, P., Chen, K., Pournin, S., Müller, U., Aguet, M., Babinet, C., Shih, J.C. & Maeyer, E.D. 1995, "Aggressive behavior and altered amounts of brain serotonin and norepinephrine in mice lacking MAO-A", Science, vol. 268, no. 5218, pp. 1763-1766.

Cases, O., Vitalis, T., Seif, I., De Maeyer, E., Sotelo, C. & Gaspar, P. 1996, "Lack of barrels in the somatosensory cortex of monoamine oxidase A–deficient mice: Role of a serotonin excess during the critical period", Neuron, vol. 16, no. 2, pp. 297-307.

Castellani, R., Hirai, K., Aliev, G., Drew, K.L., Nunomura, A., Takeda, A., Cash, A.D., Obrenovich, M.E., Perry, G. & Smith, M.A. 2002, "Role of mitochondrial dysfunction in Alzheimer's disease", Journal of Neuroscience Research, vol. 70, no. 3, pp. 357-360.

Chen, K. 2004, "Organization of MAO-A and MAO-B promoters and regulation of gene expression", Neurotoxicology, vol. 25, no. 1-2, pp. 31-36.

Cheng, Y. & Prusoff, W.H. 1973, "Relationship between the inhibition constant (K_i) and the concentration of inhibitor which causes 50 per cent inhibition (IC_{50}) of an enzymatic reaction", Biochemical pharmacology, vol. 22, no. 23, pp. 3099-3108.

Cheng, H.C. 2001, "The power issue: determination of K_B or K_i from IC_{50}: A closer look at the Cheng–Prusoff equation, the Schild plot and related power equations", Journal of Pharmacological and Toxicological Methods, vol. 46, no. 2, pp. 61-71.

Clarke, C.E. 2004, "Neuroprotection and pharmacotherapy for motor symptoms in Parkinson's disease", The Lancet Neurology, vol. 3, no. 8, pp. 466-474.

Dauer, W. & Przedborski, S. 2003, "Parkinson's disease: Mechanisms and models", Neuron, vol. 39, no. 6, pp. 889-909.

De Colibus, L.D., Li, M., Binda, C., Lustig, A., Edmondson, D.E., Mattevi, A. & Klinman, J.P. 2005, "Three-dimensional structure of human monoamine oxidase A (MAO-A): Relation to the structures of rat MAO-A and Human MAO-B", Proceedings of the National Academy of Sciences of the United States of America, vol. 102, no. 36, pp. 12684-12689.

Degani, I., Fochi, R. & Spunta, G. 1966, Bollettino Scientifico della Facolta di Chimica Industriale di Bologna, vol. 24, pp. 75.

Echtay, K.S., Roussel, D., St.-Pierre, J., Jekabsons, M.B., Cadenas, S., Stuart, J.A., Harper, J.A., Roebuck, S.J., Morrison, A., Pickering, S., Clapham, J.C., Brand, M.D. 2002, "Superoxide activates mitochondrial uncoupling proteins", Nature, vol. 415, no. 6867, pp. 96-99.

Edmondson, D.E., Mattevi, A., Binda, C., Li, M. & Hubáleka, F. 2004, "Structure and Mechanism of Monoamine Oxidase", Current Medicinal Chemistry, vol. 11, no. 15, pp. 1983-1993.

Fahn, S., Oakes, D., Shoulson, I., Kieburtz, K., Rudolph, A., Lang, A., Olanow, CW., Tanner, C., Marek, K., Parkinson Study Group. 2004, "Levodopa and the progression of Parkinson's disease", New England Journal of Medicine, vol. 351, no. 24, pp. 2498-2508.

Fahn, S. & Cohen, G. 1992, "The oxidant stress hypothesis in Parkinson's disease: Evidence supporting it", Annals of Neurology, vol. 32, no. 6, pp. 804-812.

Fernandez, H.H. & Chen, J.J. 2007, "Monoamine oxidase-B inhibition in the treatment of Parkinson's disease", Pharmacotherapy: The Journal of Human Pharmacology and Drug Therapy, vol. 27, no. 12P2, pp. 174S-185S.

Finberg, J.P. & Tenne, M. 1982, "Relationship between tyramine potentiation and selective inhibition of monoamine oxidase types A and B in the rat vas deferens", British Journal of Pharmacology, vol. 77, no. 1, pp. 13-21.

Finberg, J.P., Tenne, M. & Youdim, M.B. 1981, "Tyramine antagonistic properties of AGN 1135, an irreversible inhibitor of monoamine oxidase type B", British Journal of Pharmacology, vol. 73, no. 1, pp. 65-74.

Foley, P., Gerlach, M., Youdim, M.B.H. & Riederer, P. 2000, "MAO-B inhibitors: multiple roles in the therapy of neurodegenerative disorders?", Parkinsonism & Related Disorders, vol. 6, no. 1, pp. 25-47.

Fowler CJ, Wiberg A, Oreland L, Marcusson J, Winblad B. 1980 "The effect of age on the activity and molecular properties of human brain monoamine oxidase", Journal of Neural Transmission, vol. 49, no. 1, pp.1-20.

Garrett, B.E. & Griffiths, R.R. 1997, "The role of dopamine in the behavioral effects of caffeine in animals and humans", Pharmacology, Biochemistry and Behavior, vol. 57, no. 3, pp. 533-541.

Gillman, P.K. 2006, "A review of serotonin toxicity data: Implications for the mechanisms of antidepressant drug action", Biological Psychiatry, vol. 59, no. 11, pp. 1046-1051.

Gotttries, C.G., Oreland, L., Wiberg, Å. & Winblad, B. 1975, "Lowered monoamine oxidase activity in brains from alcoholic suicides", Journal of Neurochemistry, vol. 25, no. 5, pp. 667-673.

Green A.R & Youdim M.B.H. 1975, "Effects of monoamine oxidase inhibition by clorgyline, deprenil or tranylcypromine on 5-hydroxytryptamine concentrations in rat brain and hyperactivity following subsequent tryptophan administration", British Journal of Pharmacology, vol. 55, no. 3, pp. 415-422.

Grimsby, J., Chen, K., Wang, L.J., Lan, N.C. & Shih, J.C. 1991, "Human monoamine oxidase A and B genes exhibit identical exon-intron organization", Proceedings of the National Academy of Sciences of the United States of America, vol. 88, no. 9, pp. 3637-3641.

Gwin-Hardy, K. 2002, "Genetics of Parkinsonism ", Movement Disorders, vol. 17, no. 4, pp. 645-656.

Hald, A. & Lotharius, J. 2005, "Oxidative stress and inflammation in Parkinson's disease: is there a causal link?", Experimental Neurology, vol. 193, no. 2, pp. 279-290.

Harborne, J.B. 1993. Introduction to ecological biochemistry. 4th ed., Harcourt Brace and Company, London: Elsevier, UK, pp. 256-257

Hardman, J.G. & and Limbird, L.E. 2001, "Treatment of central nervous system degenerative disorders." (*In* Goodman, L.S., Gilam, A.G., *ed*. Goodman & Gilman's: The pharmacological basis of therapeutics., 20th edn. New York, McGraw-Hill, pp. 1-27.

Healy, D.G., Falchi, M., O'Sullivan, S.S., Bonifati, V., Durr, A., Bressman, S., Brice, A., Aasly, J., Zabetian, C.P., Goldwurm, S., Ferreira, J.J., Tolosa, E., Kay, D.M., Klein, C., Williams, D.R., Marras, C., Lang, A.E., Wszolek, Z.K., Berciano, J., Schapira, A.H., Lynch, T., Bhatia, K.P., Gasser, T., Lees, A.J. & Wood, N.W. 2008, "Phenotype, genotype, and

worldwide genetic penetrance of LRRK2-associated Parkinson's disease: a case-control study", The Lancet Neurology, vol. 7, no. 7, pp. 583-590.

Hewavitharanage, P., Karunaratne, S. & Kumar, N.S. 1999, "Effect of caffeine on shot-hole borer beetle (Xyleborusfornicatus) of tea (Camellia sinensis)", Phytochemistry, vol. 51, no. 1, pp. 35-41.

Holt, A., Sharman, D.F., Baker, G.B. & Palcic, M.M. 1997, "A continuous spectrophotometric assay for monoamine oxidase and related enzymes in tissue homogenates", Analytical Biochemistry, vol. 244, no. 2, pp. 384-392.

Ikeda, K., Kurokawa, M., Aoyama, S. & Kuwana, Y. 2002, "Neuroprotection by adenosine A_{2A} receptor blockade in experimental models of Parkinson's disease", Journal of Neurochemistry, vol. 80, no. 2, pp. 262-270.

Jahng, J.W., Houpt, T.A., Wessel, T.C., Chen, K., Shih, J.C. & Joh, T.H. 1997, " Localization of monoamine oxidase A and B mRNA in the rat brain by *in situ* hybridization", Synapse, vol. 25, no. 1, pp. 30-36.

Johnston, J.P. 1968, "Some observations upon a new inhibitor of monoamine oxidase in brain tissue", Biochemical Pharmacology, vol. 17, no. 7, pp. 1285-1297.

Kearney, E.B., Salach, J.I., Walker, W.H., Seng, R.L., Kenney, W., Zeszotek, E. & Singer, T.P. 1971, "The covalently-bound flavin of hepatic monoamine oxidase", European Journal of Biochemistry, vol. 24, no. 2, pp. 321-327.

Kihlman, B.A. 1977, Caffeine and chromosomes, Elsevier Scientific Publishing, Amsterdam.

Kornhuber, J., Konradi, C., Mack-Burkhardt, F., Riederer, P., Heinsen, H. & Beckmann, H. 1989, "Ontogenesis of monoamine oxidase-A and -B in the human brain frontal cortex", Brain Research, vol. 499, no. 1, pp. 81-86.

Lees, A.J., Hardy, J. & Revesz, T. 2009, "Parkinson’s disease", Lancet, vol. 373, pp.2055–2066.

Lees, A. 2005, "Alternatives to levodopa in the initial treatment of early Parkinson's disease", Drugs & Aging, vol. 22, no. 9, pp. 731-740.

Lev, N., Djaldetti, R. & Melamed, E. 2007, "Initiation of symptomatic therapy in Parkinson's disease: Dopamine agonists versus levodopa", Journal of Neurology, vol. 254, no. 5, pp. 19-26.

Lewinsohn, R., Glover, V. & Sandler, M. 1980, "Development of benzylamine oxidase and monoamine oxidase A and B in man", Biochemical Pharmacology, vol. 29, no. 9, pp. 1221-1230.

Lewis, A., Miller, J.H. & Lea, R.A. 2007, "Monoamine oxidase and tobacco dependence", Neurotoxicology, vol. 28, no. 1, pp. 182-195.

LeWitt, P.A. & Taylor, D.C. 2008, "Protection against Parkinson's disease progression: Clinical experience", Neurotherapeutics, vol. 5, no. 2, pp. 210-225.

Lorist, M.M. & Tops, M. 2003, "Caffeine, fatigue, and cognition", Brain and Cognition, vol. 53, no. 1, pp. 82-94.

Lotharius, J., Falsig, J., van Beek, J., Payne, S., Dringen, R., Brundin, P. & Leist, M. 2005, "Progressive degeneration of human mesencephalic neuron-derived cells triggered by dopamine-dependent oxidative stress is dependent on the mixed-lineage kinase pathway", The Journal of Neuroscience, vol. 25, no. 27, pp. 6329-6342.

Luque, J.M., Kwan, S., Abell, C.W., Prada, M.D. & Richards, J.G. 1995, "Cellular expression of mRNAs encoding monoamine oxidases A and B in the rat central nervous system", The Journal of Comparative Neurology, vol. 363, no. 4, pp. 665-680.

Mannelli, M., Pupilli, C., Lanzillotti, R., Ianni, L. & Serio, M. 1990, "Catecholamines and blood pressure regulation", Hormone Research, vol. 34, no. 3-4, pp. 156-160.

Markey, S.P., Johannessen, J.N., Chiueh, C.C., Burns, R.S. & Herkenham, M.A. 1984, "Intraneuronal generation of a pyridinium metabolite may cause drug-induced parkinsonism", Nature, vol. 311, pp. 464 - 467.

Mathiasen, J.R., McKenna, B.A.W., Saporito, M.S., Ghadge, G.D., Roos, R.P., Holskin, B.P., Wu, Z., Trusko, S.P., Connors, T.C., Maroney, A.C., Thomas, B.A., Thomas, J.C. & Bozyczko-Coyne, D. 2004, "Inhibition of mixed lineage kinase 3 attenuates MPP^+-induced neurotoxicity in SH-SY5Y cells", Brain Research, vol. 1003, no. 1–2, pp. 86-97.

Matthews, R.T., Yang, L., Browne, S., Baik, M. & Beal, M.F. 1998, "Coenzyme Q10 administration increases brain mitochondrial concentrations and exerts neuroprotective effects", Proceedings of the National Academy of Sciences of the United States of America, vol. 95, no. 15, pp. 8892-8897.

Miller, D.B., Ali, S.F., O'Callaghan, J.P. & Laws, S.C. 1998, "The impact of gender and estrogen on striatal dopaminergic neurotoxicity", Annals of the New York Academy of Sciences, vol. 844, pp. 153–165.

Miller, J.R., Edmondson, D.E. & Grissom, C.B. 1995, "Mechanistic probes of monoamine oxidase B catalysis: Rapid-scan stopped flow and magnetic field independence of the reductive half-reaction", Journal of the American Chemical Society, vol. 117, no. 29, pp. 7830-7831.

Morens, D.M., Grandinetti, A., Reed, D., White, L.R. & Ross, G.W. 1995, "Cigarette smoking and protection from Parkinson's disease", Neurology, vol. 45, no. 6, pp. 1041-1051.

Nagatsu, T. 2004, "Progress in monoamine oxidase (MAO) research in relation to genetic engineering", Neurotoxicology, vol. 25, no. 1-2, pp. 11-20.

Nehlig, A. 1999, "Are we dependent upon coffee and caffeine? A review on human and animal data", Neuroscience & Biobehavioral Reviews, vol. 23, no. 4, pp. 563-576.

Nicotra, A. & Parvez, S.H. 1999, "Methods for assaying monoamine oxidase A and B activities: Recent developments", Biogenic Amines, vol. 15, no. 3, pp. 307-320.

Nicotra, A., Pierucci, F., Parvez, H. & Senatori, O. 2004, "Monoamine oxidase expression during development and aging", Neurotoxicology, vol. 25, no. 1-2, pp. 155-165.

Nuytemans, K., Theuns, J., Cruts, M. & Van Broeckhoven, C. 2010, "Genetic etiology of Parkinson’s disease associated with mutations in the SNCA, PARK2, PINK1, PARK7, and LRRK2 genes: A mutation update", Human Mutation, vol. 31, no. 7, pp. 763-780.

O'Brien, E.M., Kiely, K.A. & Tipton, K.F. 1993, "A discontinuous luminometric assay for monoamine oxidase", Biochemical Pharmacology, vol. 46, no. 7, pp. 1301-1306.

Olanow, C.W., Schapira, A.H., LeWitt, P.A., Kieburtz, K., Sauer, D., Olivieri, G., Pohlmann, H. & Hubble, J. 2006, "TCH346 as a neuroprotective drug in Parkinson's disease: A double-blind, randomised, controlled trial", The Lancet Neurology, vol. 5, no. 12, pp. 1013-1020.

Paech, C., Salach, J.I. & Singer, T.P. 1980, "Suicide inactivation of monoamine oxidase by trans-phenylcyclopropylamine", Journal of Biological Chemistry, vol. 255, no. 7, pp. 2700-2704.

Papesch, V. & Schroeder Elmer, F. 1951, "Synthesis of 1-Mono- and 1,3-di-substituted 6-aminouracils. Diuretic activity", The Journal of Organic Chemistry, vol. 16, no. (12), pp. 1879-1890.

Parkinson, J. 1817, An essay on the Shaky Palsy, Garwell Street, London: Printed by Whittingham and Rowland.

Pasto, D.J., McMillan, D. & Murphy, T.J. 1965, "Determination of Hammett p Values for Substituted

Phenylmercapto-, Phenylsulfinyl-, and Phenylsulfonylacetic Acids" The Journal of Organic Chemistry, vol. 30, pp. 2688–2691.

Pizzinat, N., Marti, L., Remaury, A., Leger, F., Langin, D., Lafontan, M., Carpéné, C. & Parini, A. 1999, "High expression of monoamine oxidases in human white adipose tissue: Evidence for their involvement in noradrenaline clearance", Biochemical Pharmacology, vol. 58, no. 11, pp. 1735-1742.

Poltev, V.I., Grokhlina, T.I., González, E., Deriabina, A., Cruz, A., Gorb, L., Leszczynski, J., Djimant, L.N. & Veselkov, A.N. 2004, "The study of three-dimensional structure of caffeine associates using computational and experimental methods", Journal of Molecular Structure: THEOCHEM, vol. 709, no. 1-3, pp. 123-128.

Pretorius, J., Malan, S.F., Castagnoli Jr., N., Bergh, J.J. & Petzer, J.P. 2008, "Dual inhibition of monoamine oxidase B and antagonism of the adenosine A_{2A} receptor by (E,E)-8-(4-phenylbutadien-1-yl)caffeine analogues", Bioorganic & Medicinal Chemistry, vol. 16, no. 18, pp. 8676-8684.

Przedborski, S. 2005, "Pathogenesis of nigral cell death in Parkinson's disease", Parkinsonism & Related Disorders, vol. 11, no. 1, pp. S3-S7.

Riederer, P., Lachenmayer, L. & Laux, G. 2004, "Clinical applications of MAO-inhibitors", Current Medicinal Chemistry, vol. 11, no. 15, pp. 2033-2043.

Rodwell, V.W. & Kennelly, P., J. 2003, "Enzymes: Kinetics. Chapter 8" (*In* Murray, R.K. Granner D.K., Mayes P.A. & Rodwell V.W., *eds*. Harper's Illustrated Biochemistry, 26th edn., McGraw-Hill, pp. 60-67).

Romero-Ramos, M., Maingay, M. & Kirik, D. 2004, (*In* Bahr, M., *ed*. Neuroprotection. Models, Mechanisms and Therapies. Die Deutche Bibliothek, pp. 31-34).

Sano, M., Ernesto, C., Thomas, R.G., Klauber, M.R., Schafer, K., Grundman, M., Woodbury, P., Growdon, J., Cotman, C.W., Pfeiffer, E., Schneider, L.S. & Thal, L.J. 1997, "A controlled trial of selegiline, alpha-tocopherol, or both as treatment for Alzheimer's disease", New England Journal of Medicine, vol. 336, no. 17, pp. 1216-1222.

Sapolsky, R.M. 1998, "Deleterious and salutary effects of steroid hormones in the nervous system: possible mediating cellular mechanisms" (*In* Mattson, M.P., *ed*. Neuroprotective Signal Transduction. Humana Press, Totowa, NJ: USA, pp. 259-283).

Saporito, M.S., Brown, E.M., Miller, M.S. & Carswell, S. 1999, "CEP-1347/KT-7515, an inhibitor of c-jun N-terminal kinase activation, attenuates the 1-methyl-4-phenyl tetrahydropyridine-mediated loss of nigrostriatal dopaminergic neurons *in vivo*", Journal of Pharmacolology and Experimental Therapuetics, vol. 288, no. 2, pp. 421-427.

Saudou, F., Finkbeiner, S., Devys, D. & Greenberg, M.E. 1998, "Huntingtin acts in the nucleus to induce apoptosis but death does not correlate with the formation of intranuclear inclusions", Cell, vol. 95, no. 1, pp. 55-66.

Saura, J., Richards, J.G. & Mahy, N. 1994, "Differential age-related changes of MAO-A and MAO-B in mouse brain and pe peripheral organs", Neurobiology of Aging, vol. 15, no. 4, pp. 399-408.

Shih, J.C., Chen, K. & Ridd, M.J. 1999, "Monoamine oxidase: From genes to behavior", Annual Review of Neuroscience, vol. 22, no. 1, pp. 197.

Shults, C.W. 2003, "Coenzyme Q10 in neurodegenerative diseases", Current Medicinal Chemistry, vol. 10, no. 19, pp. 1917-1921.

Silverman, R.B. 1995, "Mechanism-based enzyme inactivators" (*In* Purich, D.L., *ed*. Methods in Enzymology, Academic Press, vol 249: pp. 240-283).

Singh, N., Pillay, V. & Choonara, Y.E. 2007, "Advances in the treatment of Parkinson's disease", Progress in Neurobiology, vol. 81, no. 1, pp. 29-44.

Son, S., Ma, J., Kondou, Y., Yoshimura, M., Yamashita, E. & Tsukihara, T. 2008, "Structure of human monoamine oxidase A at 2.2-Å resolution: The control of opening the entry for substrates/inhibitors", Proceedings of the National Academy of Sciences of the United States of America, vol. 105, no. 15, pp. 5739-5744.

Sparks, D.L., Woeltz, V.M & Markesbery, W.R. 1991, "Alterations in brain monoamine oxidase activity in aging, Alzheimer's disease, and Pick's disease", Archives of Neurology, vol. 48, no. 7, pp. 718-721.

Speer J.H. & Raymond, A.L. 1953, "Some alkyl homologs of theophylline", Journal of the American Chemical Society, vol. 75, no. 1, pp. 114-115.

Strydom, B., Malan, S.F., Castagnoli Jr., N., Bergh, J.J. & Petzer, J.P. 2010, "Inhibition of monoamine oxidase by 8-benzyloxycaffeine analogues", Bioorganic & Medicinal Chemistry, vol. 18, no. 3, pp. 1018-1028.

Suzuki, F., Shimada, J., Mizumoto, H., Karasawa, A., Kubo, K., Nonaka, H., Ishii, A. & Kawakita, T. 1992, "Adenosine A_1 antagonists. 2. Structure-activity relationships on diuretic activities and protective effects against acute renal failure", Journal of Medicinal Chemistry, vol. 35, no. 16, pp. 3066-3075.

Svenningsson, P., Le Moine, C., Fisone, G. & Fredholm, B.B. 1999, "Distribution, biochemistry and function of striatal adenosine A_{2A} receptors", Progress in Neurobiology, vol. 59, no. 4, pp. 355-396.

Swanepoel, B. 2010. The synthesis and evaluation of phenoxymethylcaffeine analogues as inhibitors of monoamine oxidase, Potchefstroom: NWU. (Dissertation – Msc).

Toulouse, A. & Sullivan, A.M. 2008, "Progress in Parkinson's disease—Where do we stand?", Progress in Neurobiology, vol. 85, no. 4, pp. 376-392.

Traube, W. 1900, "Der synthetische aufbau der harnsäure, des xanthins, theobromins, theophyllins und caffeïns aus der cyanessigsäure", Berichte der Deutschen Chemischen Gesellschaft, vol. 33, no. 3, pp. 3035-3056.

Tugwell, C. 2008, Parkinson's disease in focus. London: Pharmaceutical Press.

Vlok, N., Malan, S.F., Castagnoli Jr., N., Bergh, J.J. & Petzer, J.P. 2006, "Inhibition of monoamine oxidase B by analogues of the adenosine A_{2A} receptor antagonist (E)-8-(3-chlorostyryl)caffeine (CSC)", Bioorganic & Medicinal Chemistry, vol. 14, no. 10, pp. 3512-3521.

Volchegorskii, I.A., Shemyakov, S.E., Turygin, V.V. & Malinovskaya, N.V. 2001, "Comparative analysis of age-related changes in activities of monoamine oxidase-B and antioxidant defense enzymes in various structures of human brain", Bulletin of Experimental Biology and Medicine, vol. 132, no. 2, pp. 760-762.

Waller, G.R. 1989, "Biochemical frontiers of allelopathy", Biologia Plantarum, vol. 31, no. 6, pp. 418-447.

Wang, T., Zhang, Y., Kong, X., Lai, Y., Ji, H., Chen, Y. & Peng, S. 2009, "Synthesis and biological evaluation of nitric oxide-donating thalidomide analogues as anticancer agents", Chemistry & Biodiversity, vol. 6, no. 4, pp. 466-474.

Whyte, I.M. & Dart, R. 2004. Serotonin toxicity/syndrome. (*In* Dart, R., *ed*. Medical Toxicology, 3rd edn., Philadelphia, USA: Lippincott Williams & Wilkins.

Whyte, I.M., Dawson, A.H. & Buckley, N.A. 2003, "Relative toxicity of venlafaxine and selective serotonin reuptake inhibitors in overdose compared to tricyclic antidepressants", International Journal of Medicine, vol. 96, no. 5, pp. 369-374.

Willoughby, J., Glover, V. & Sandler, M. 1988, "Histochemical localisation of monoamine oxidase A and B in rat brain", Journal of Neural Transmission, vol. 74, no. 1, pp. 29-42.

Wurtman, R.J. & Axelrod, J. 1963, "A sensitive and specific assay for the estimation of monoamine oxidase", Biochemical Pharmacology, vol. 12, pp. 1439-1441.

Xu, K., Xu, Y., Chen, J. & Schwarzschild, M.A. 2010, "Neuroprotection by caffeine: time course and role of its metabolites in the MPTP model of Parkinson's disease", Neuroscience, vol. 167, no. 2, pp. 475-481.

Xu, K., Bastia, E. & Schwarzschild, M. 2005, "Therapeutic potential of adenosine A_{2A} receptor antagonists in Parkinson's disease", Pharmacology & Therapeutics, vol. 105, no. 3, pp. 267-310.

Yacoubian, T.A. & Standaert, D.G. 2009, "Targets for neuroprotection in Parkinson's disease", Biochimica et Biophysica Acta, vol. 1792, no. 7, pp. 676-687.

Yoritaka, A., Hattori, N., Uchida, K., Tanaka, M., Stadtman, E.R. & Mizuno, Y. 1996, "Immunohistochemical detection of 4-hydroxynonenal protein adducts in Parkinson disease", Proceedings of the National Academy of Sciences of the United States of America, vol. 93, no. 7, pp. 2696-2701.

Youdim, M.B.H. & Bakhle, Y.S. 2006, "Monoamine oxidase: isoforms and inhibitors in Parkinson's disease and depressive illness", British Journal of Pharmacology, vol. 147, no. 1, pp. S287-S296.

Youdim, M.B.H., Edmondson, D. & Tipton, K.F. 2006, "The therapeutic potential of monoamine oxidase inhibitors", Nature Reviews Neuroscience, vol. 7, no. 4, pp. 295-309.

Zhou, M. & Panchuk-Voloshina, N. 1997, "A one-step fluorometric method for the continuous measurement of monoamine oxidase activity", Analytical Biochemistry, vol. 253, no. 2, pp. 169-174.

APPENDIX A

List of ^{1}H and ^{13}C NMR spectra

- 8-[(Phenylsulfanyl)methyl]caffeine (**1a**)
- 8-{[(3-Chlorophenyl)sulfanyl]methyl}caffeine (**1b**)
- 8-{[(3-Bromophenyl)sulfanyl]methyl}caffeine (**1c**)
- 8-{[(3-Flourophenyl)sulfanyl]methyl}caffeine (**1d**)
- 8-{[(3-Methylphenyl)sulfanyl]methyl}caffeine (**1e**)
- 8-{[(3-Methoxyphenyl)sulfanyl]methyl}caffeine (**1f**)
- 8-{[(3-Ethoxyphenyl)sulfanyl]methyl}caffeine (**1g**)
- 8-{[(4-Chlorophenyl)sulfanyl]methyl}caffeine (**1h**)
- 8-{[(4-Bromophenyl)sulfanyl]methyl}caffeine (**1i**)
- 8-{[(Phenylsulfanyl)ethyl]}caffeine (**2a**)
- 8-{[(3-Chlorophenyl)sulfanyl]ethyl}caffeine (**2b**)
- 8-{[(3-Bromophenyl)sulfanyl]ethyl}caffeine (**2c**)
- 8-{[(4-Chlorophenyl)sulfanyl]ethyl}caffeine (**2d**)
- 8-{[(4-Bromophenyl)sulfanyl]ethyl}caffeine (**2e**)

Proton (^{1}H) and carbon (^{13}C) NMR spectra were recorded on a Bruker Avance III 600 spectrometer at frequencies of 600 MHz and 150 MHz, respectively. All NMR measurements were conducted in $CDCl_3$ and the chemical shifts are expressed in parts per million.

^{1}H and ^{13}C NMR

8-[(Phenylsulfanyl)methyl]caffeine (1a)

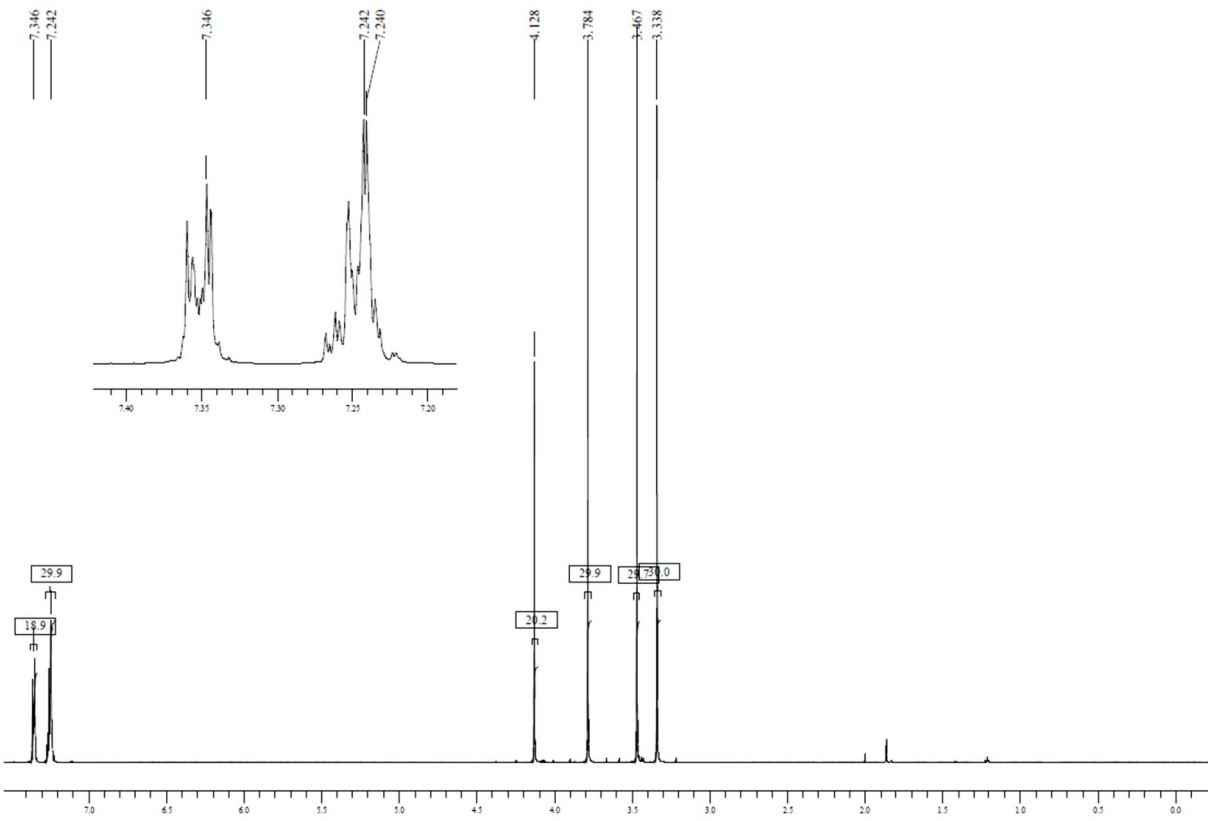

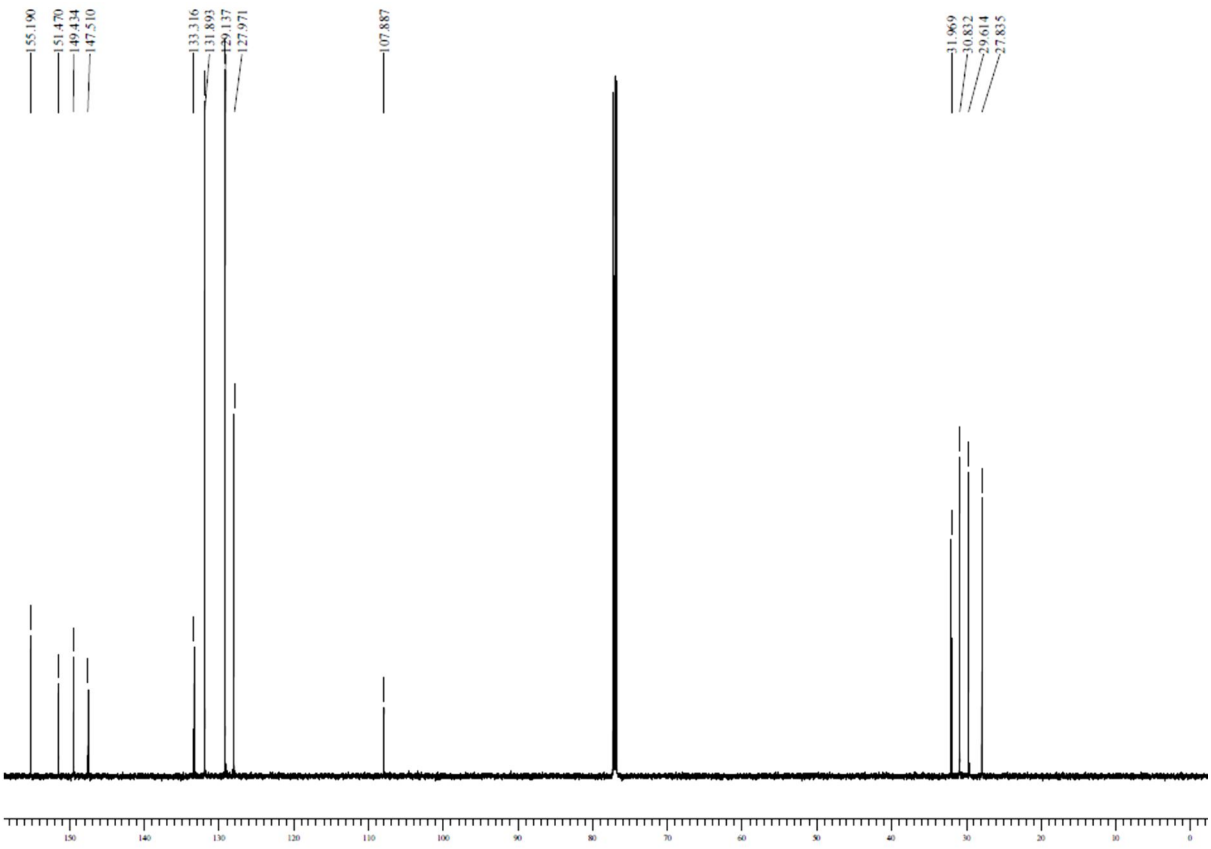

^{1}H and ^{13}C NMR

8-{[(3-Chlorophenyl)sulfanyl]methyl}caffeine (1b)

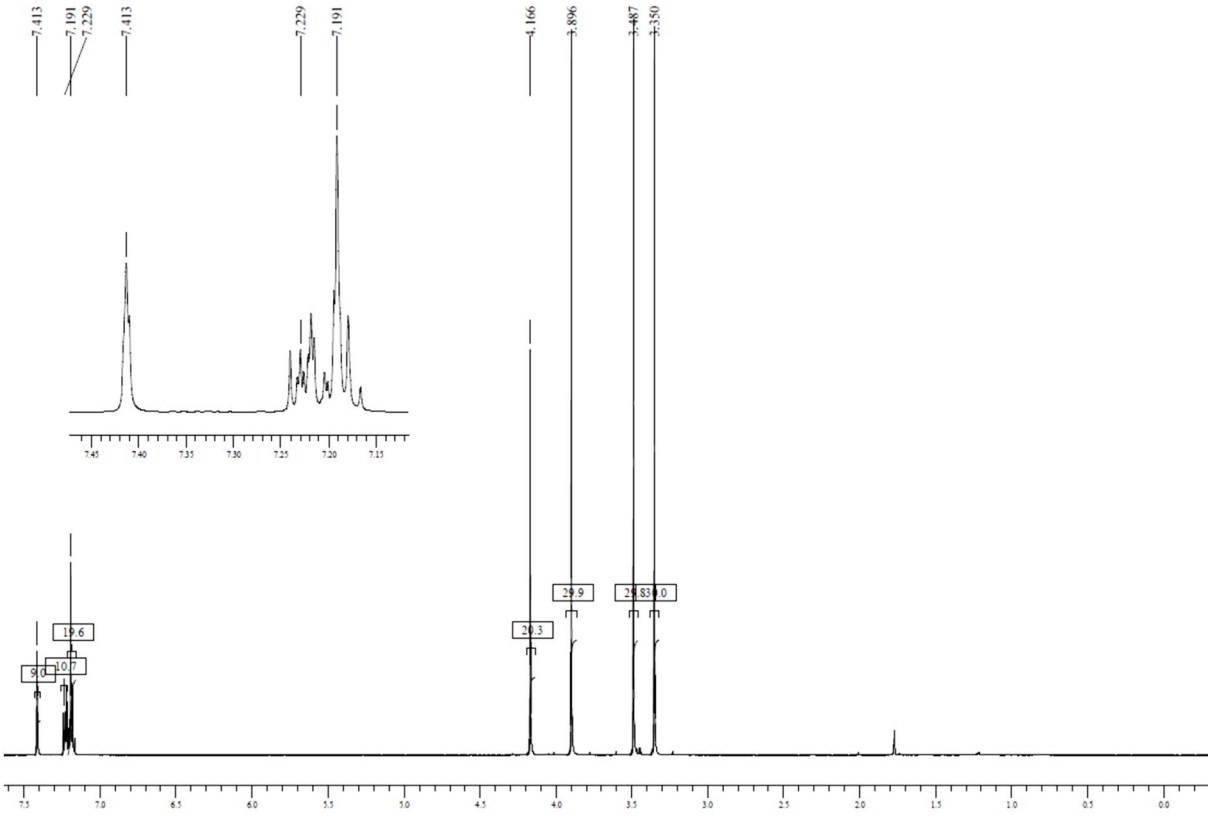

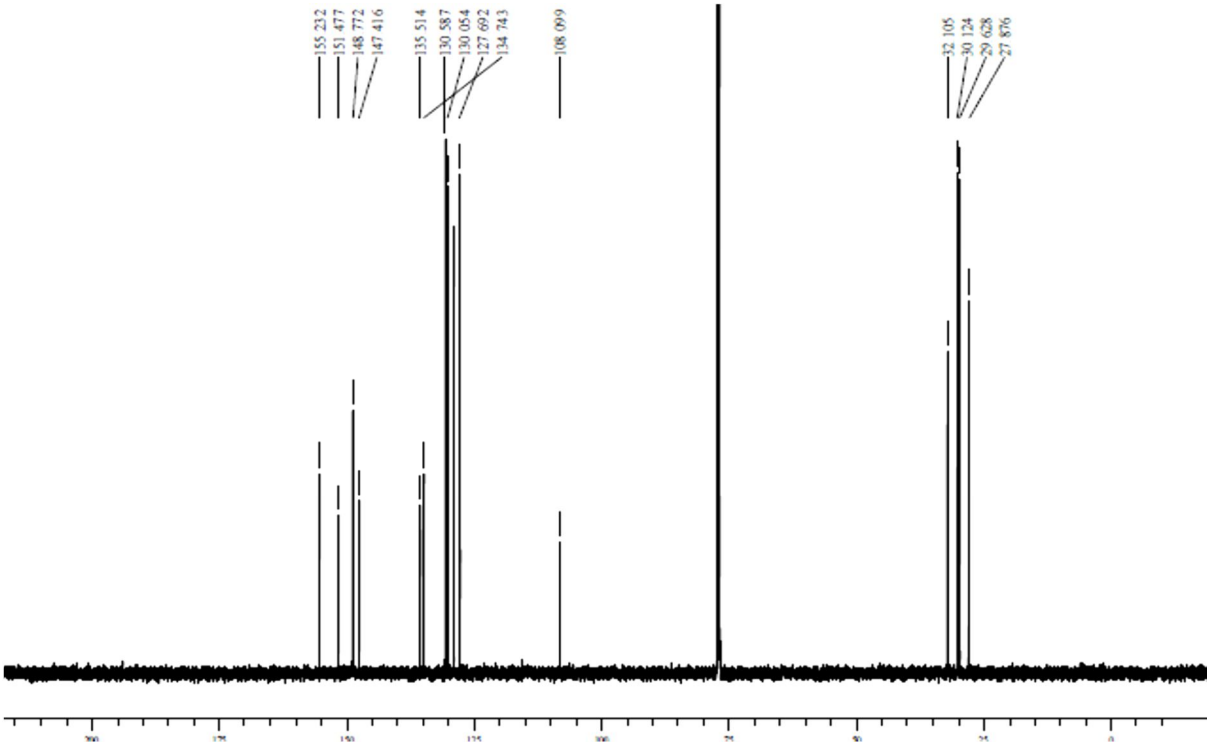

^{1}H and ^{13}C NMR

8-{[(3-Bromophenyl)sulfanyl]methyl}caffeine (1c)

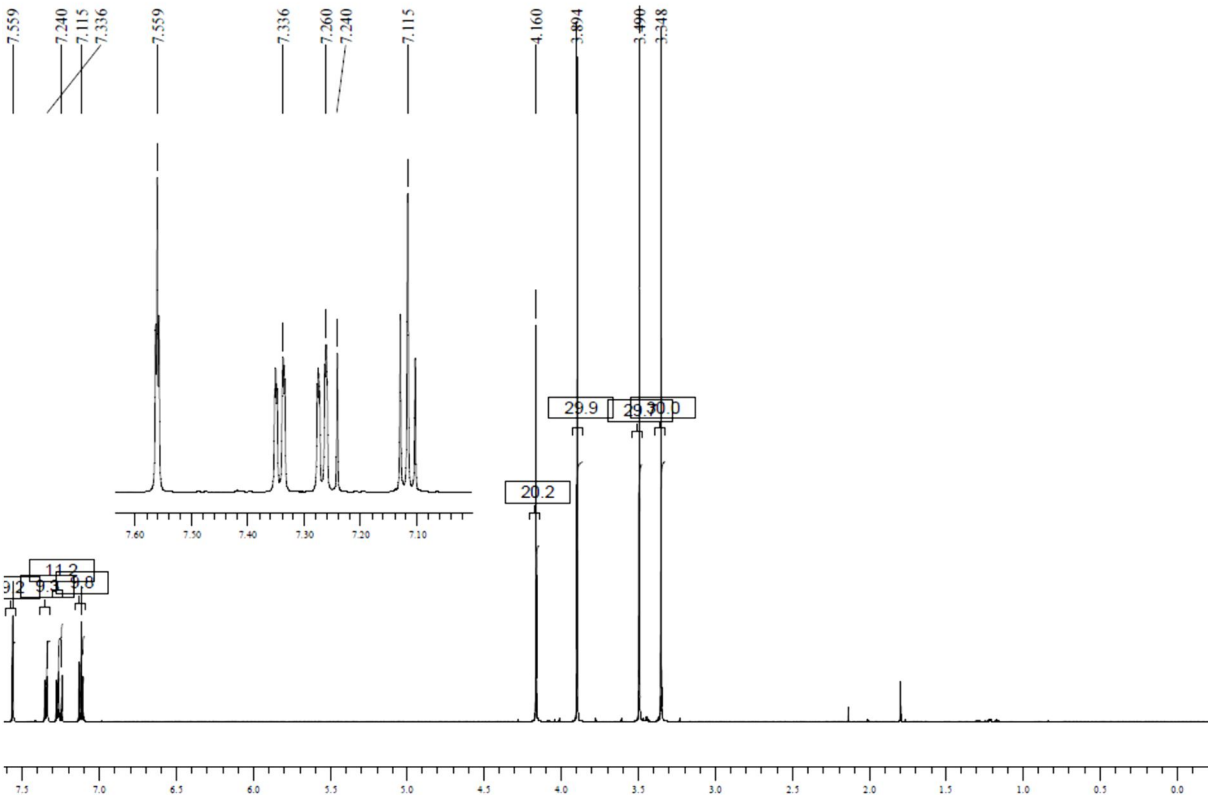

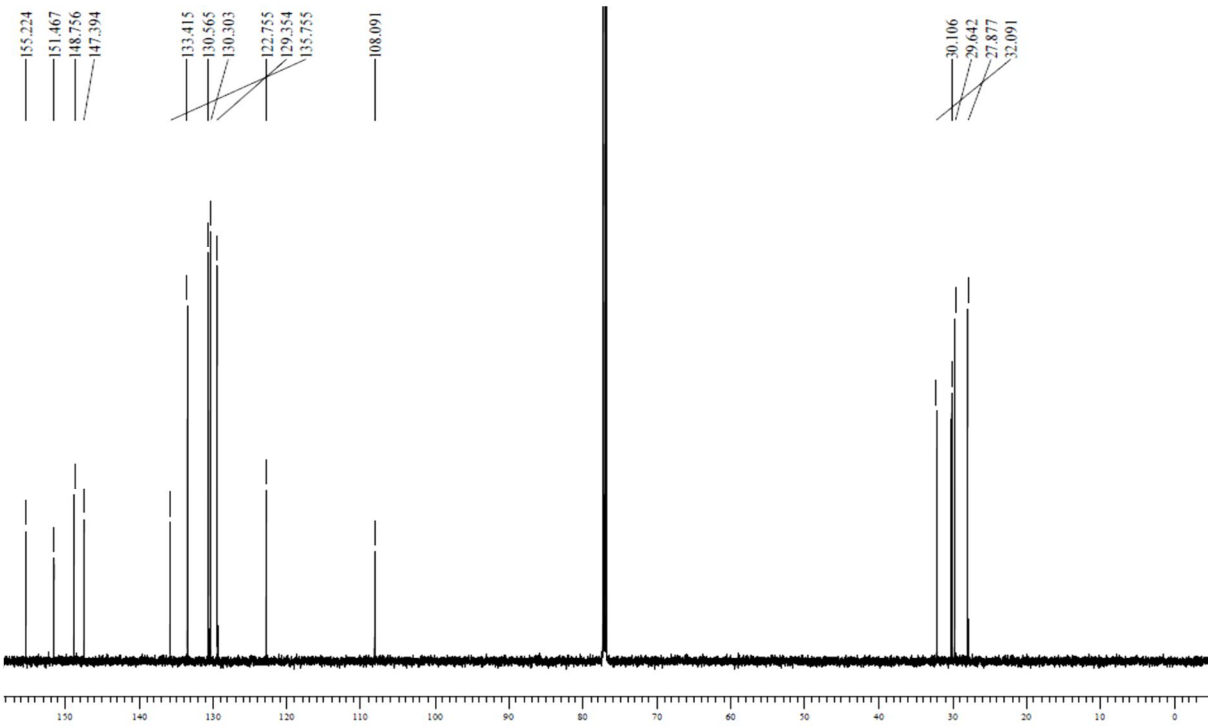

^{1}H and ^{13}C NMR

8-{[(3-Flourophenyl)sulfanyl]methyl}caffeine (1d)

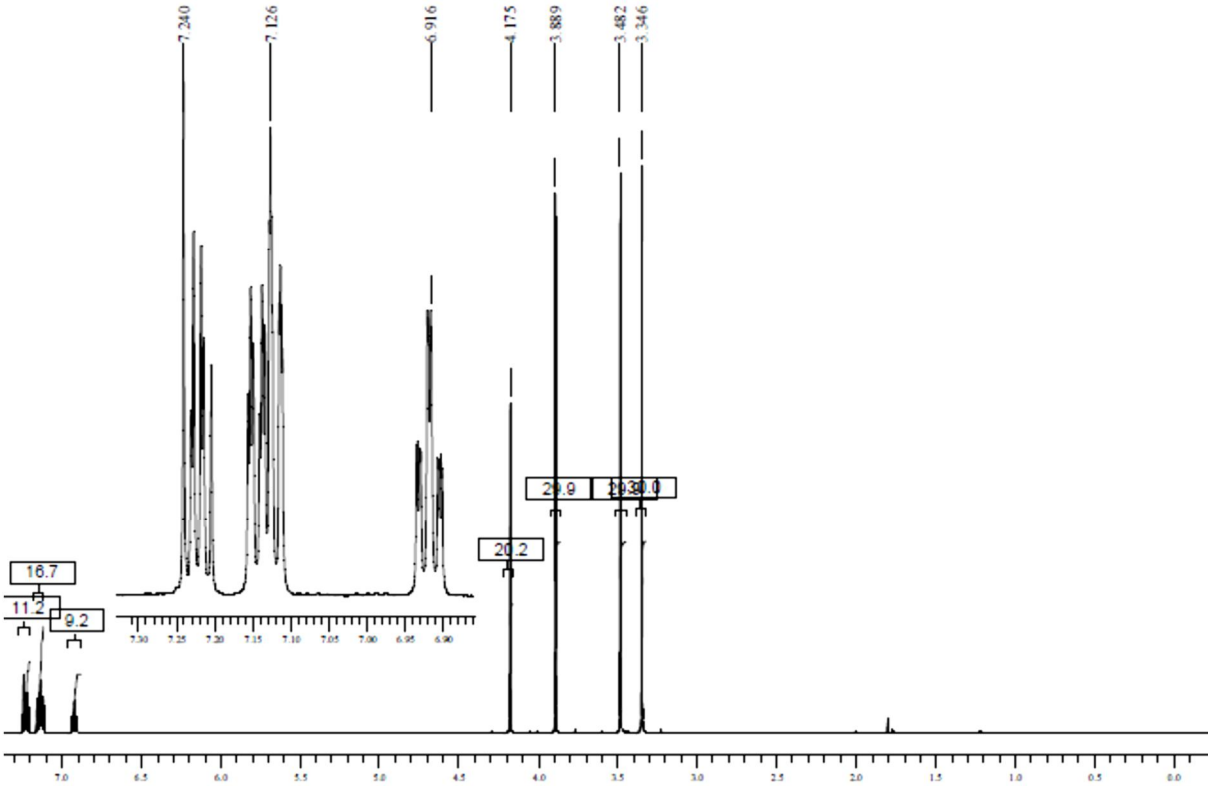

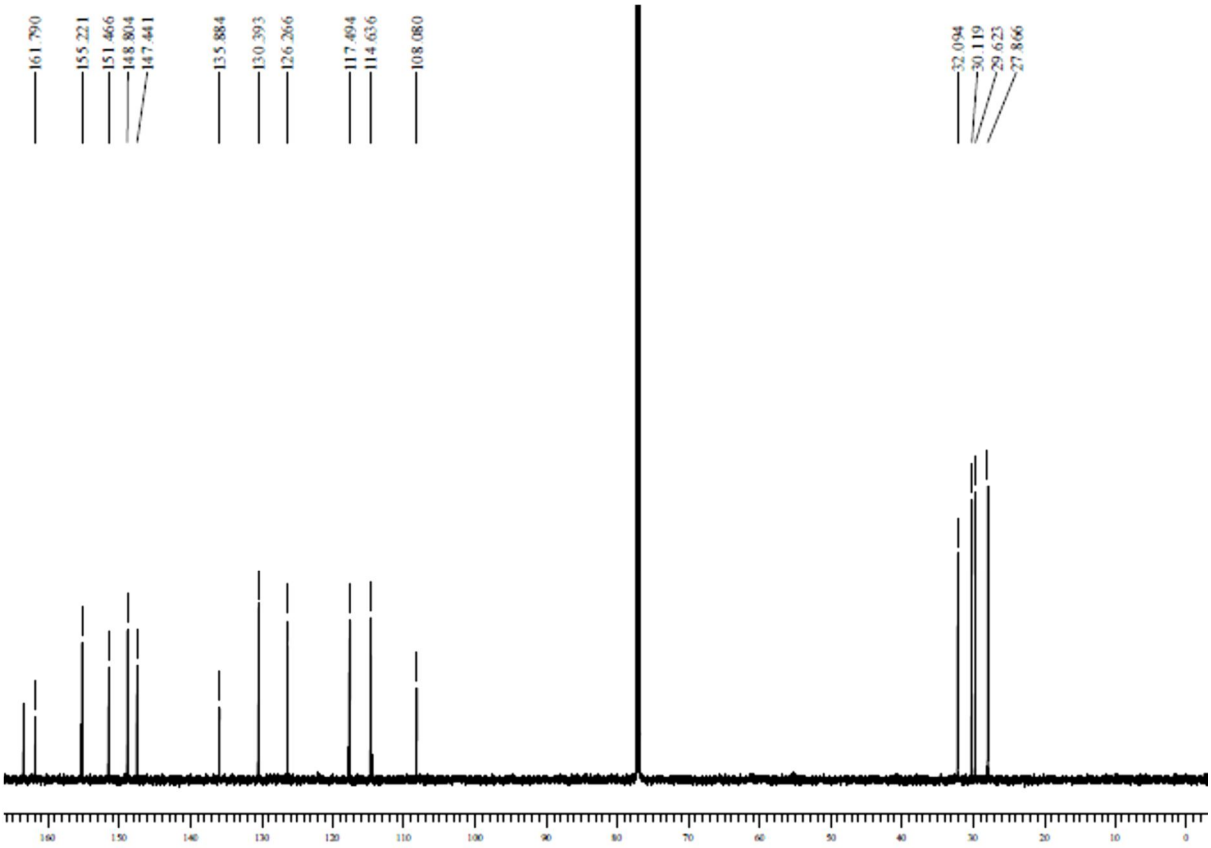

^{1}H and ^{13}C NMR

8-{[(3-Methylphenyl)sulfanyl]methyl}caffeine (1e)

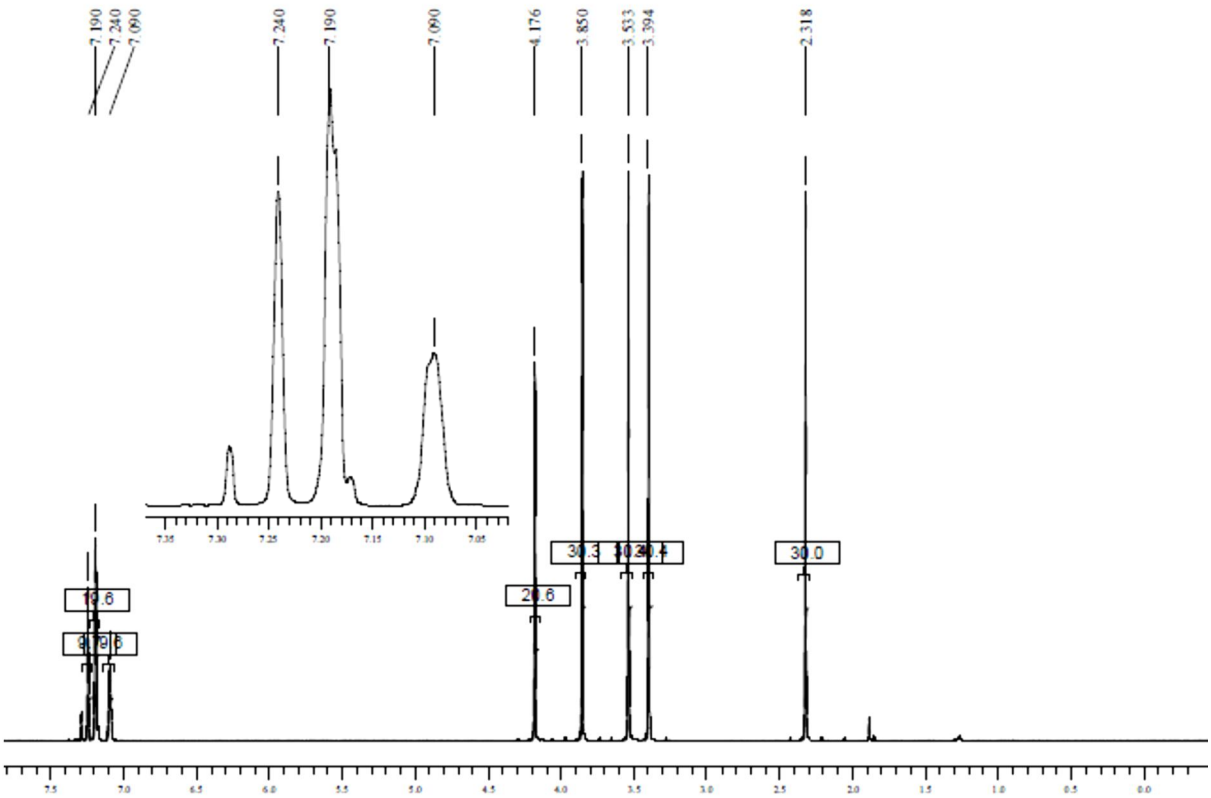

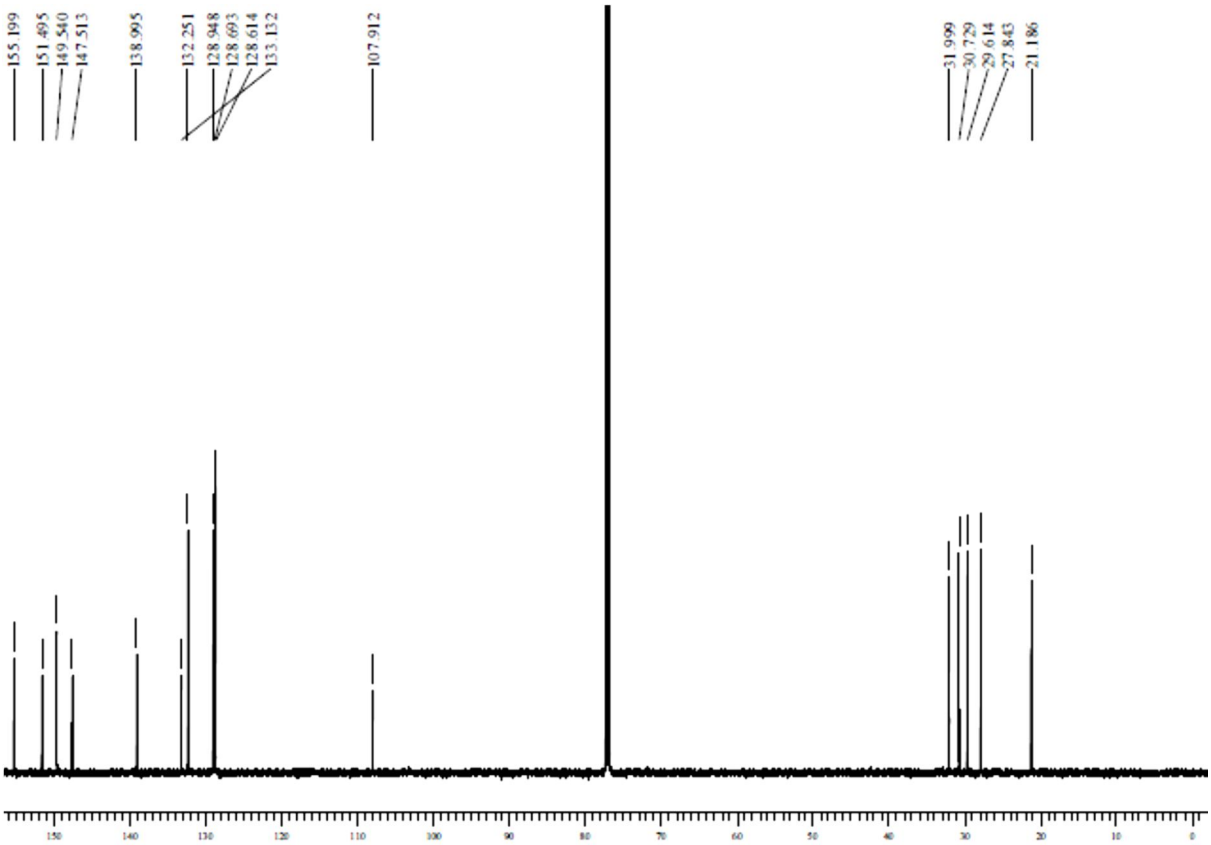

^{1}H and ^{13}C NMR

8-{[(3-Methoxyphenyl)sulfanyl]methyl}caffeine (1f)

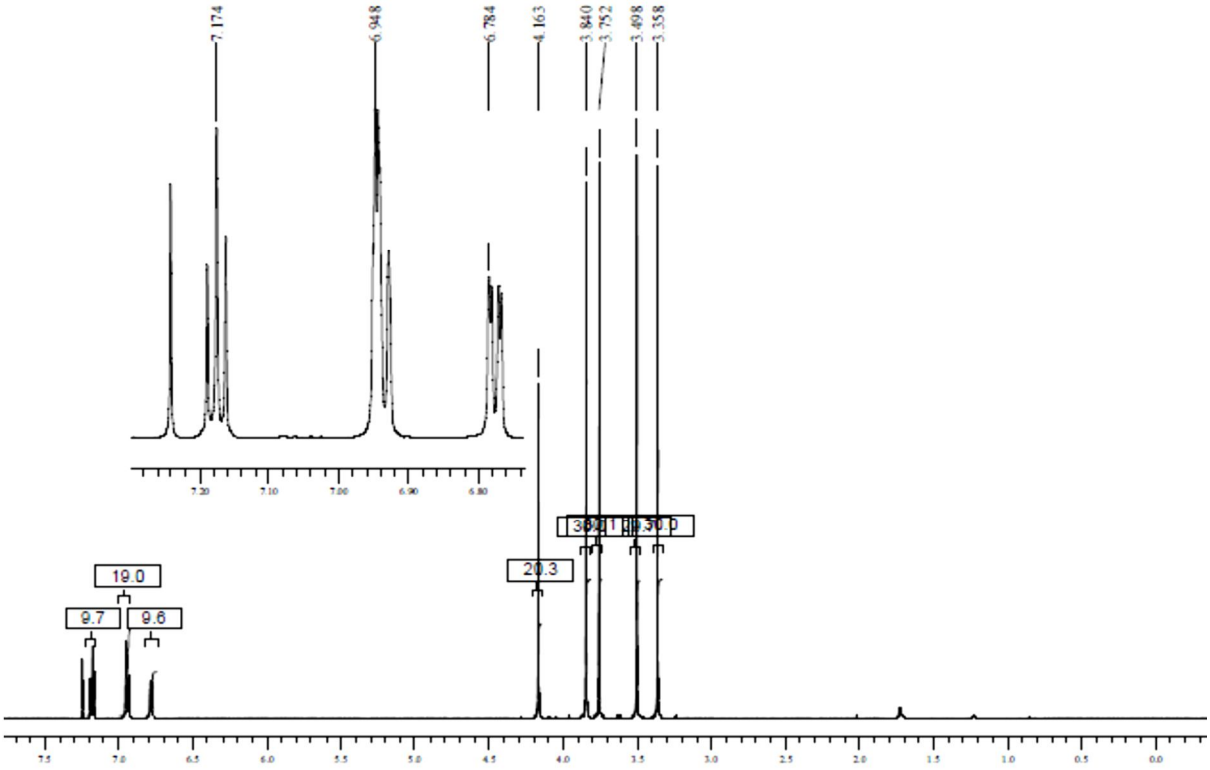

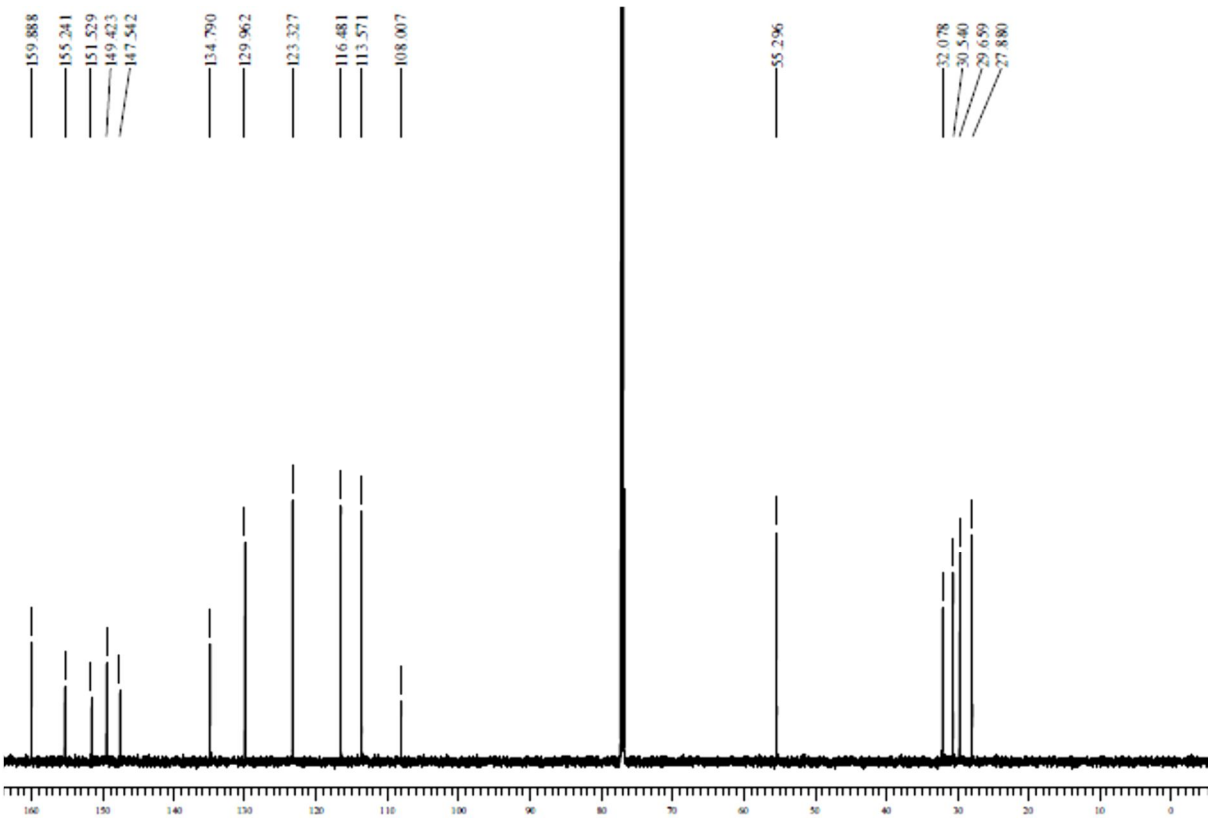

^{1}H and ^{13}C NMR

8-{[(3-Ethoxyphenyl)sulfanyl]methyl}caffeine (1g)

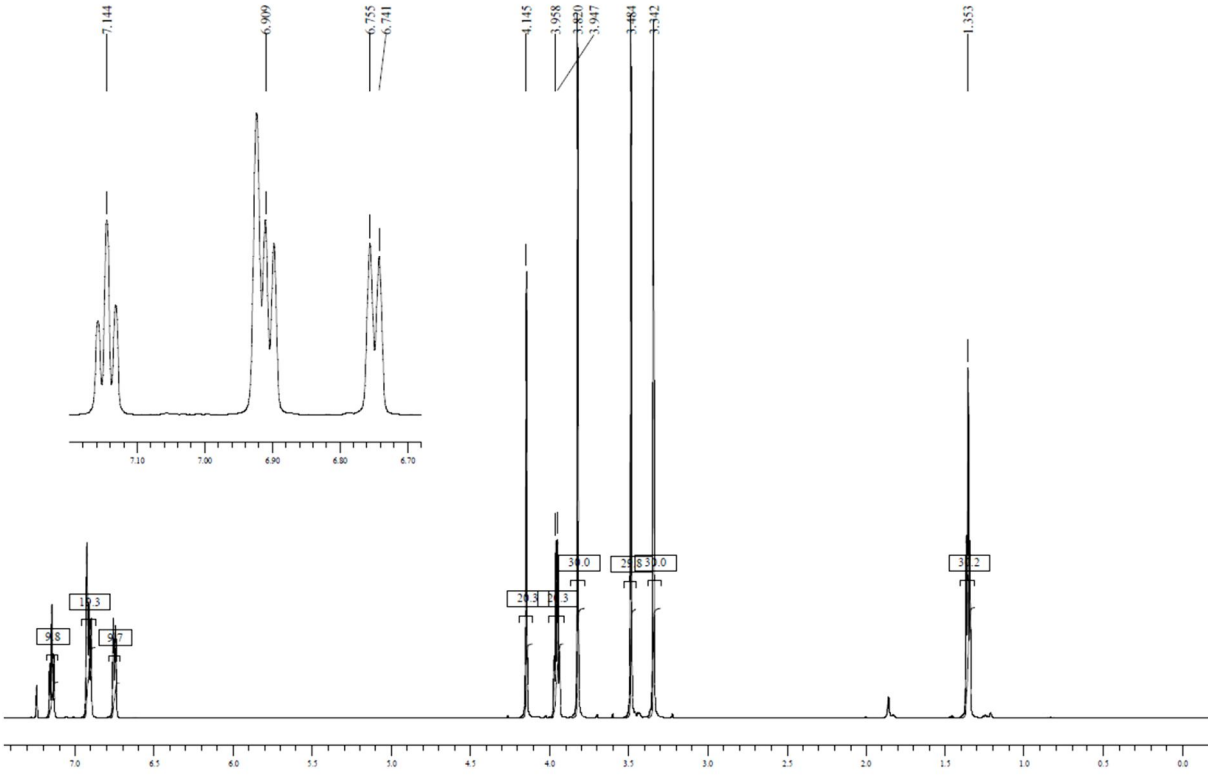

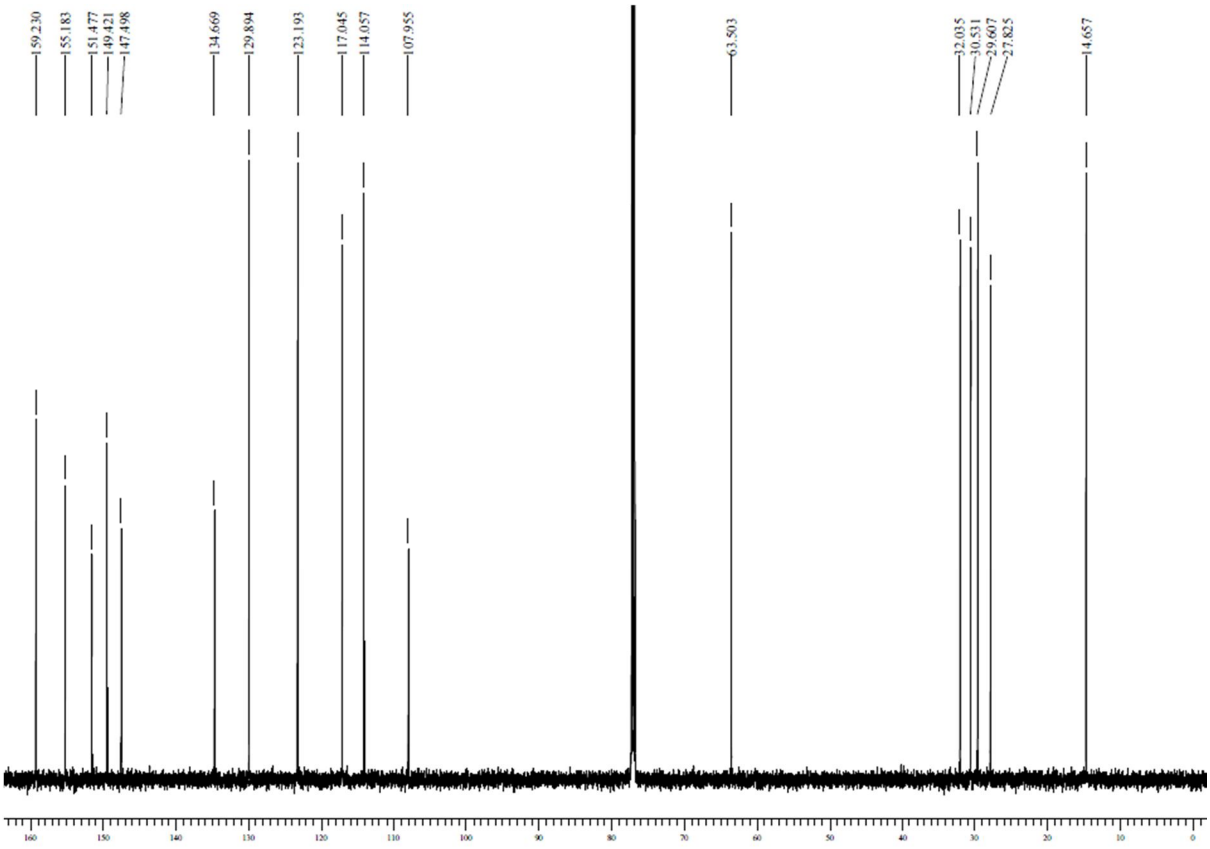

^{1}H and ^{13}C NMR

8-{[(4-Chlorophenyl)sulfanyl]methyl}caffeine (1h)

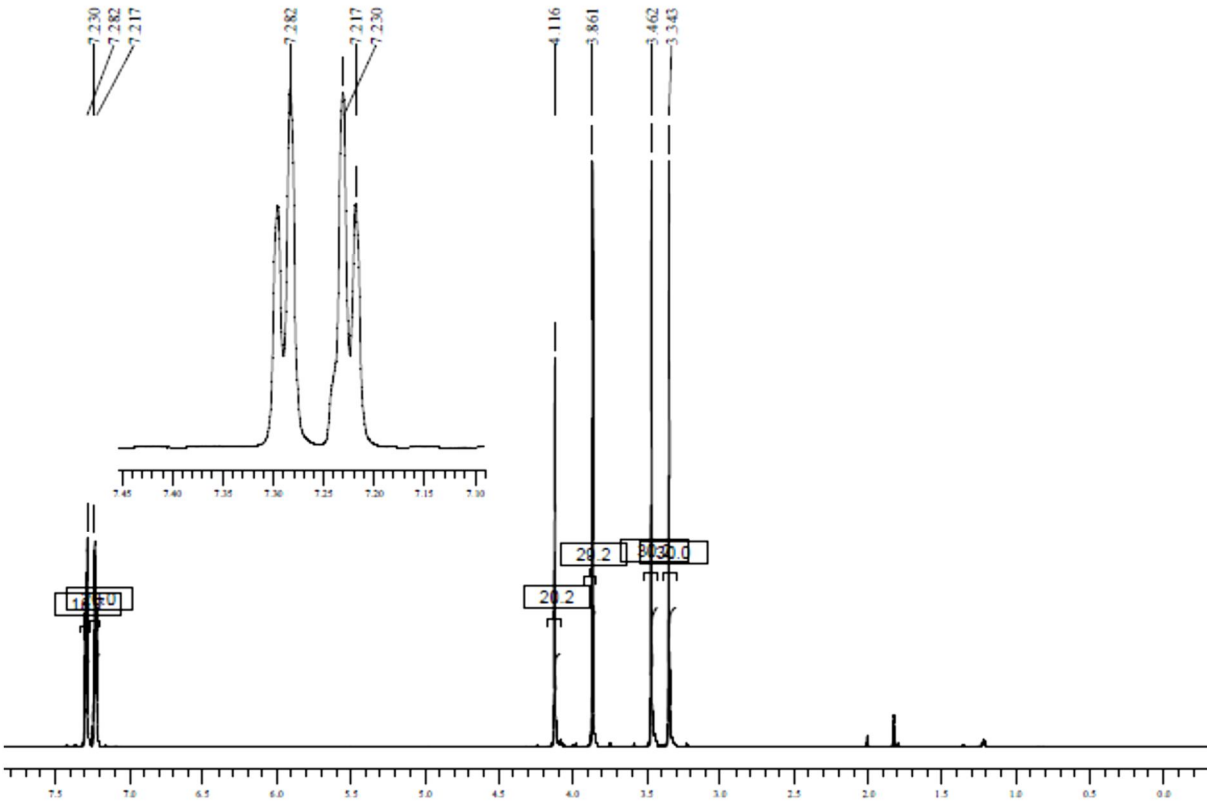

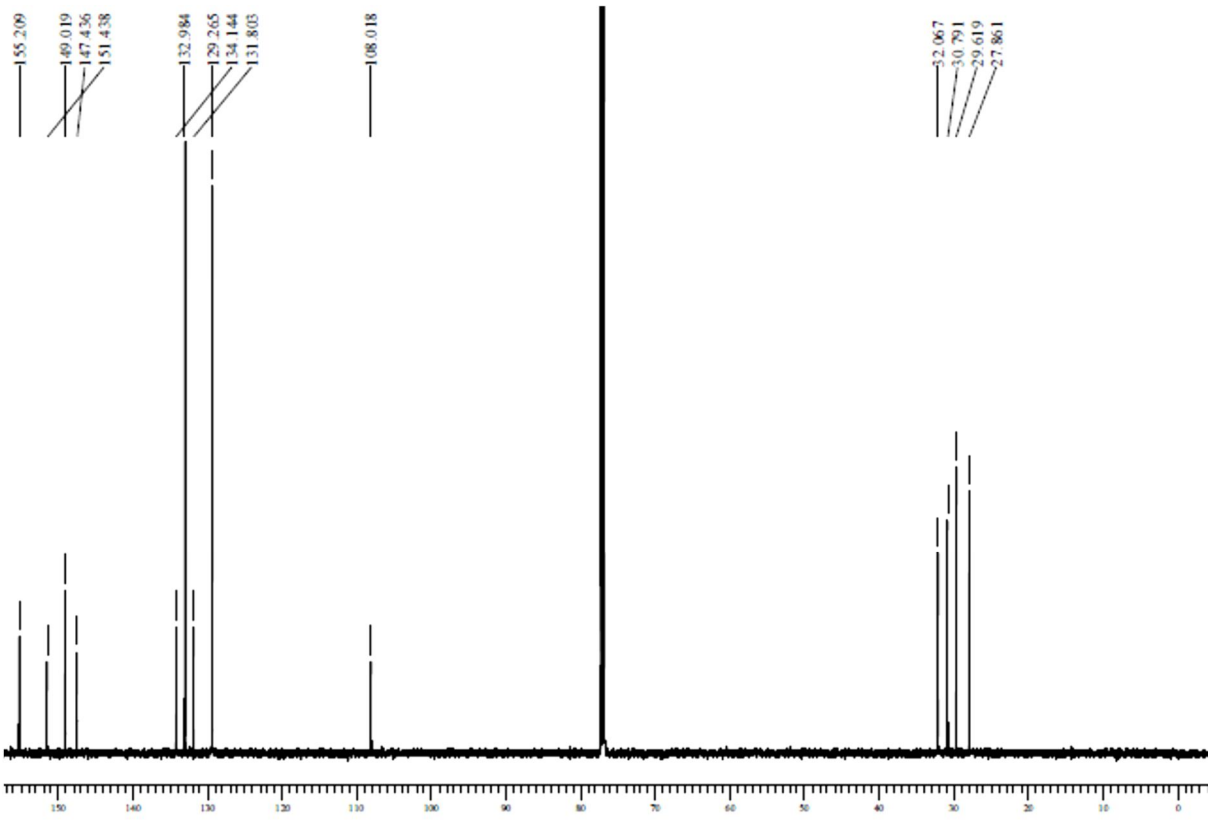

^{1}H and ^{13}C NMR

8-{[(4-Bromophenyl)sulfanyl]methyl}caffeine (1i)

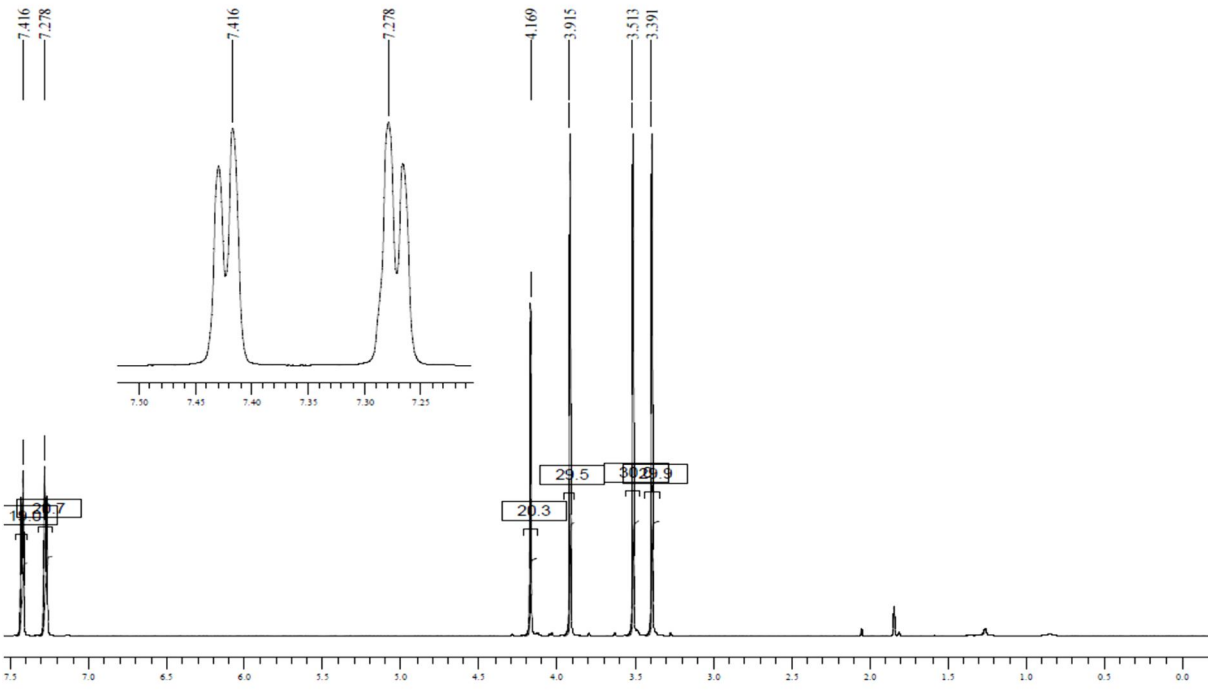

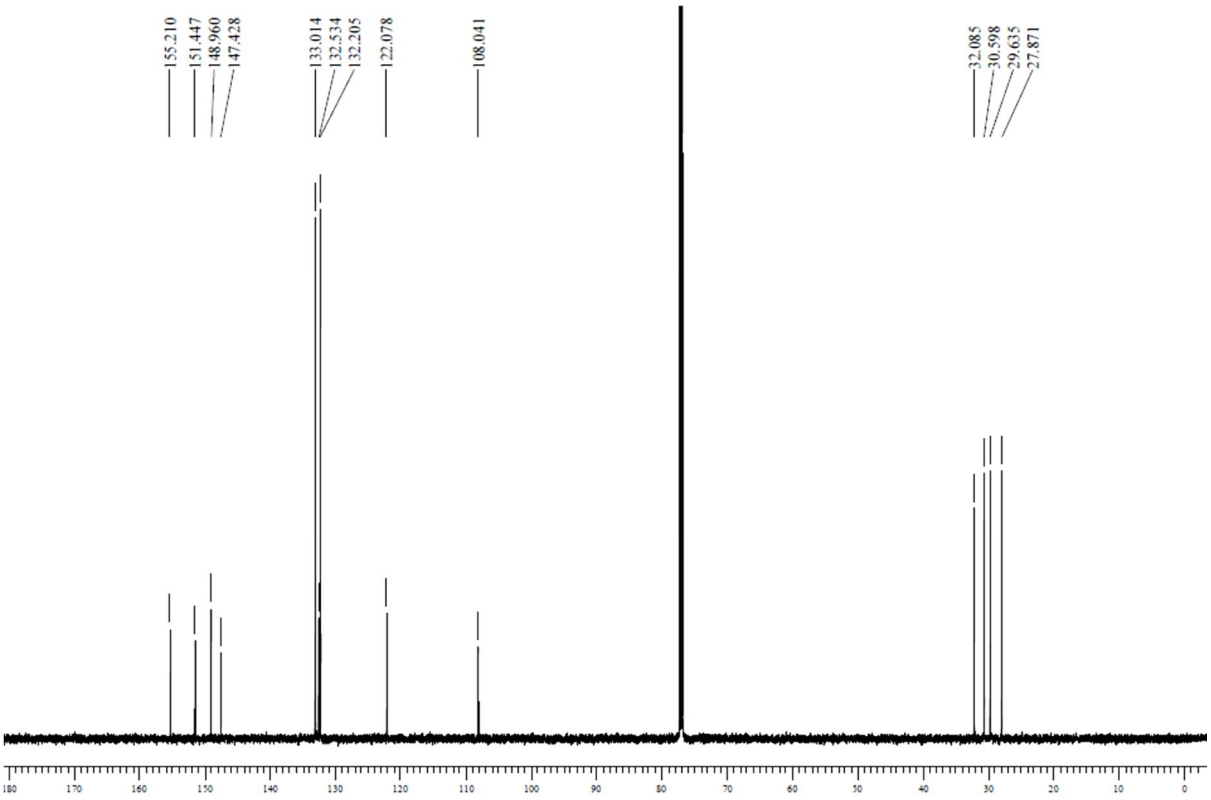

^{1}H and ^{13}C NMR

8-{[(Phenylsulfanyl)ethyl]}caffeine (2a)

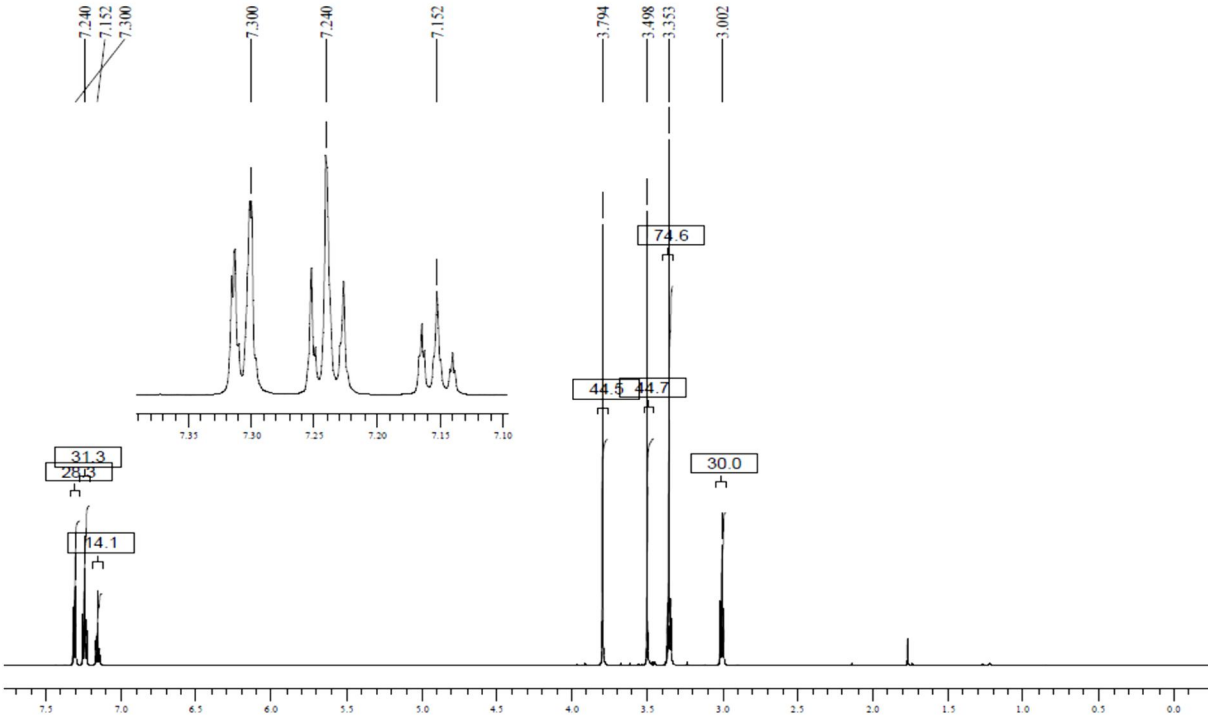

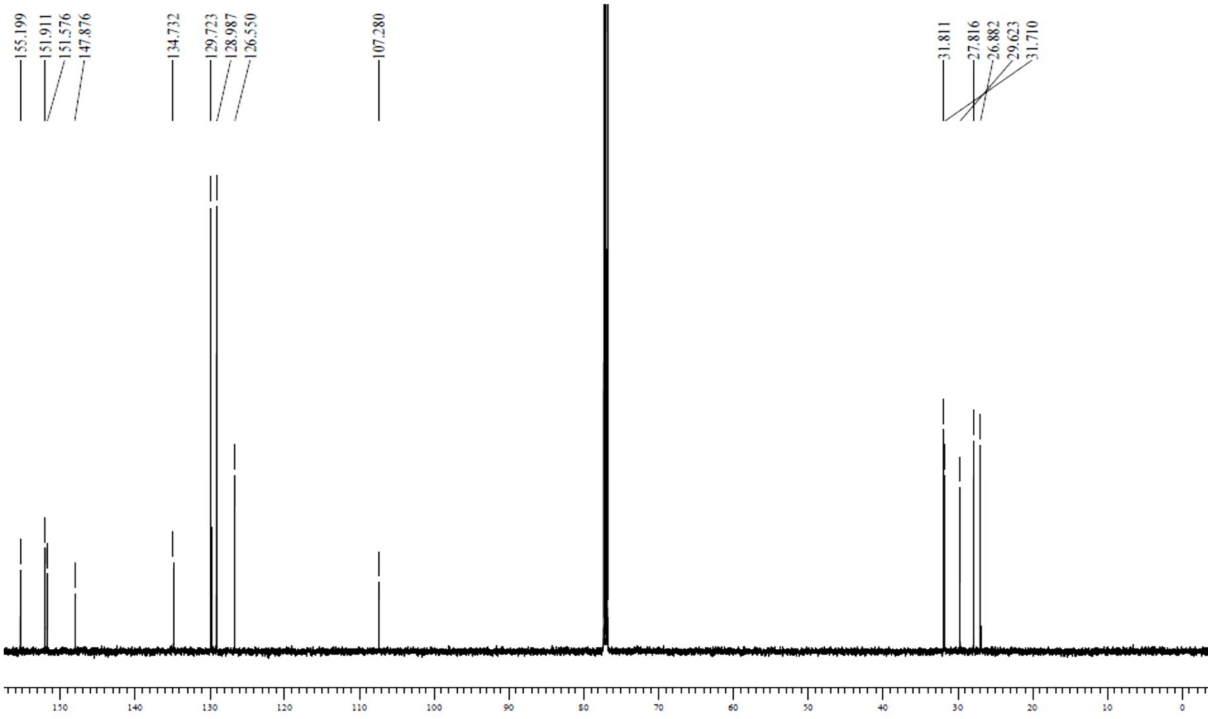

^{1}H and ^{13}C NMR

8-{[(3-Chlorophenyl)sulfanyl]ethyl}caffeine (2b)

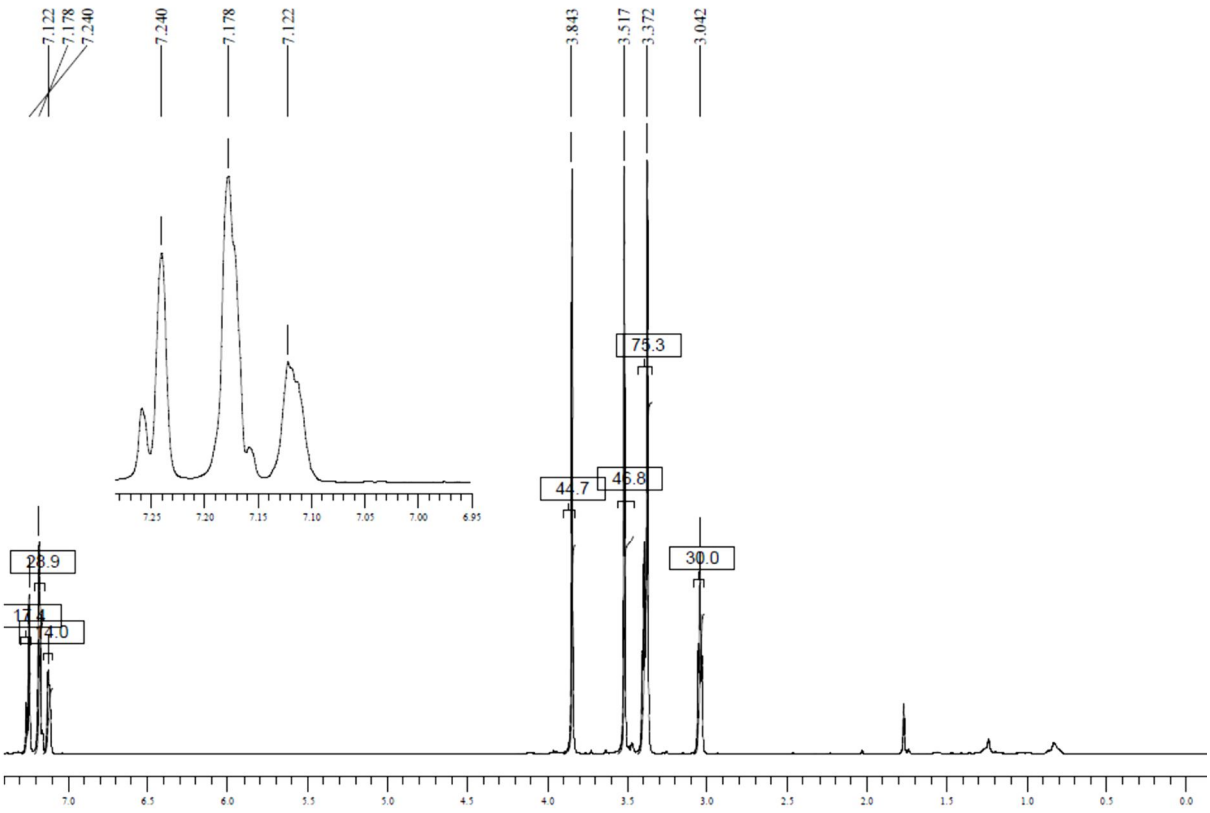

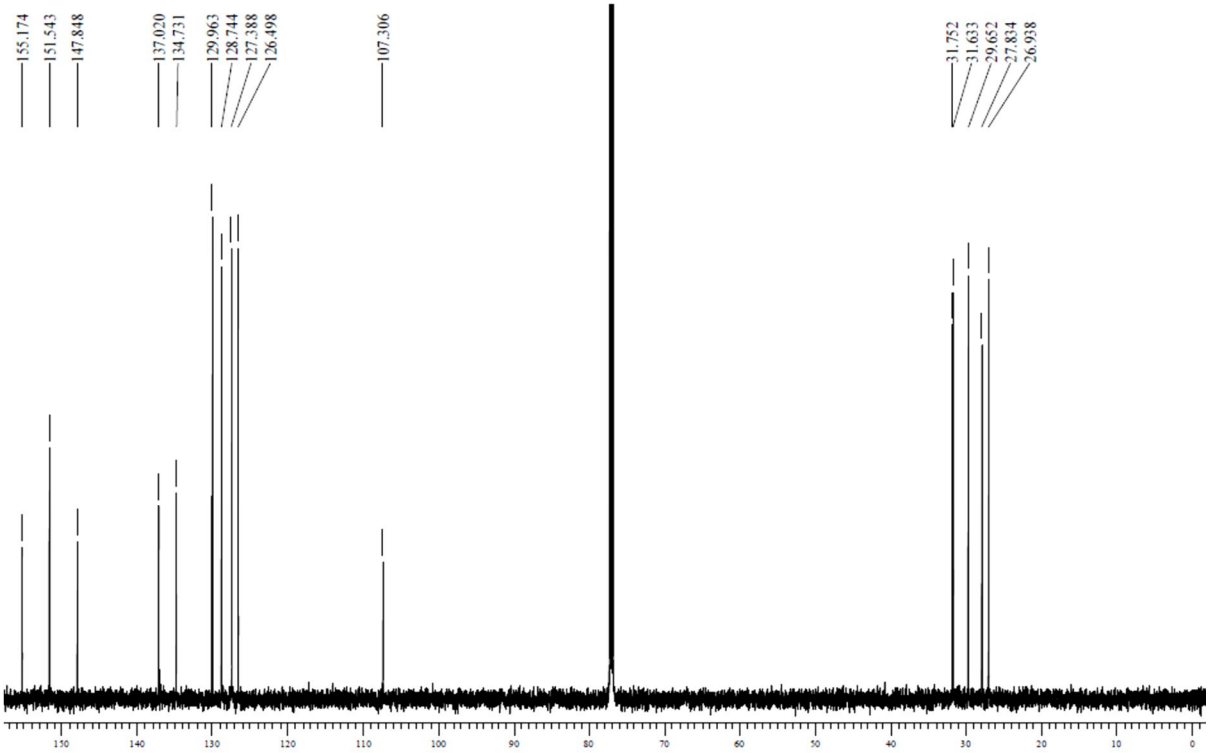

^{1}H and ^{13}C NMR

8-{[(3-Bromophenyl)sulfanyl]ethyl}caffeine (2c)

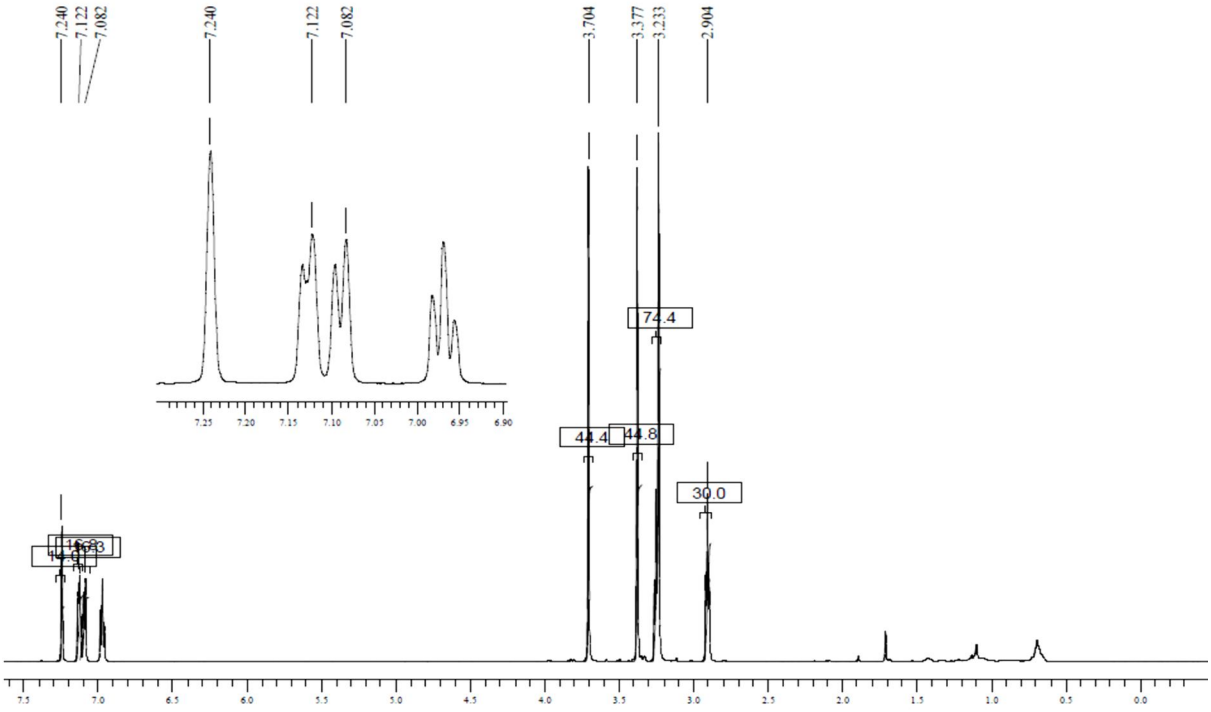

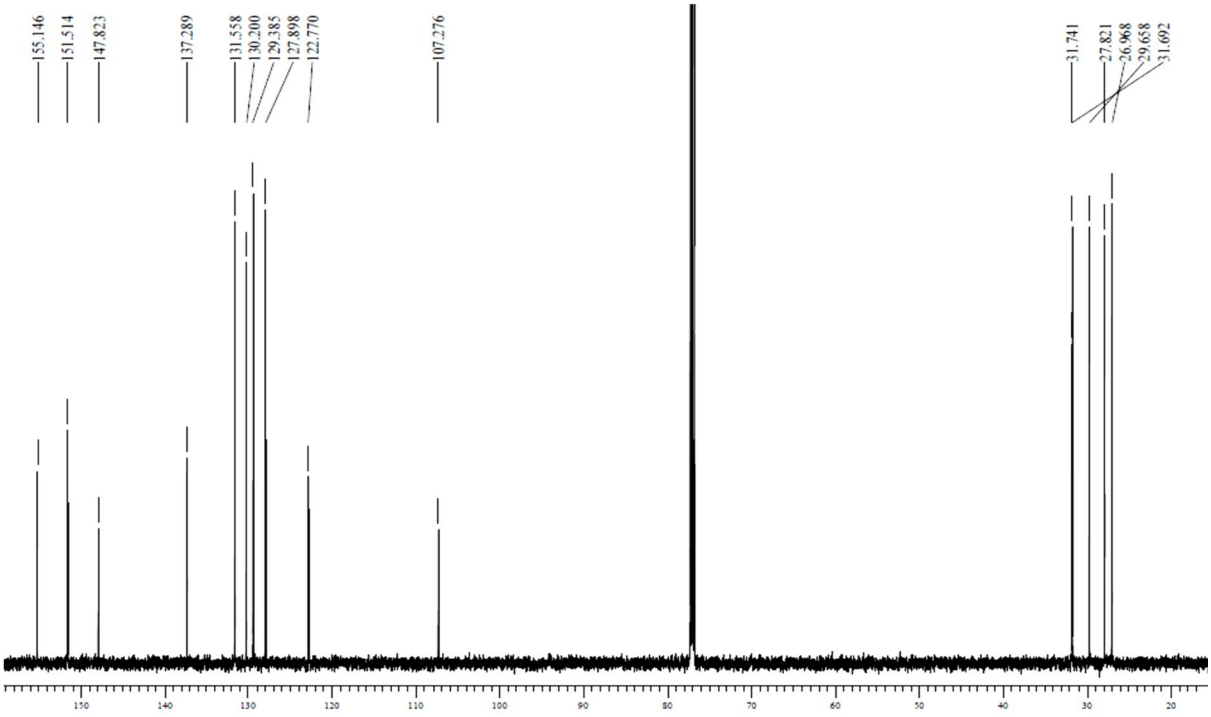

^{1}H and ^{13}C NMR

8-{[(4-Chlorophenyl)sulfanyl]ethyl}caffeine (2d)

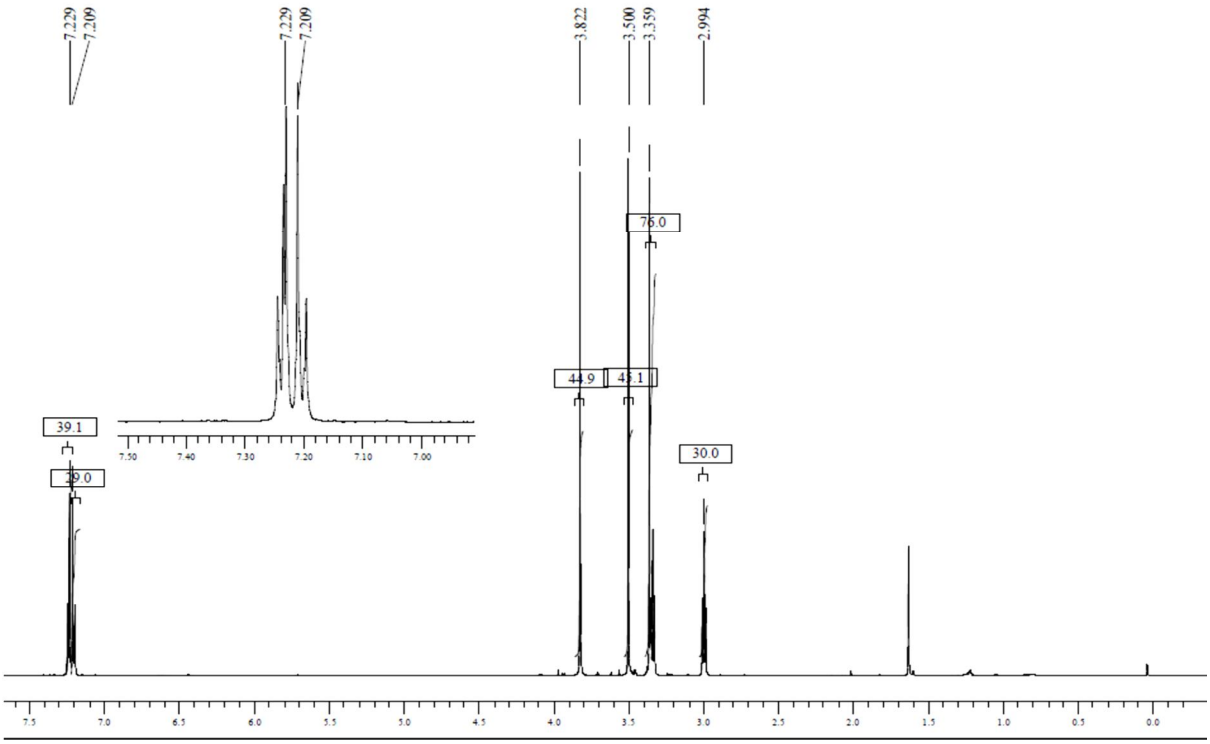

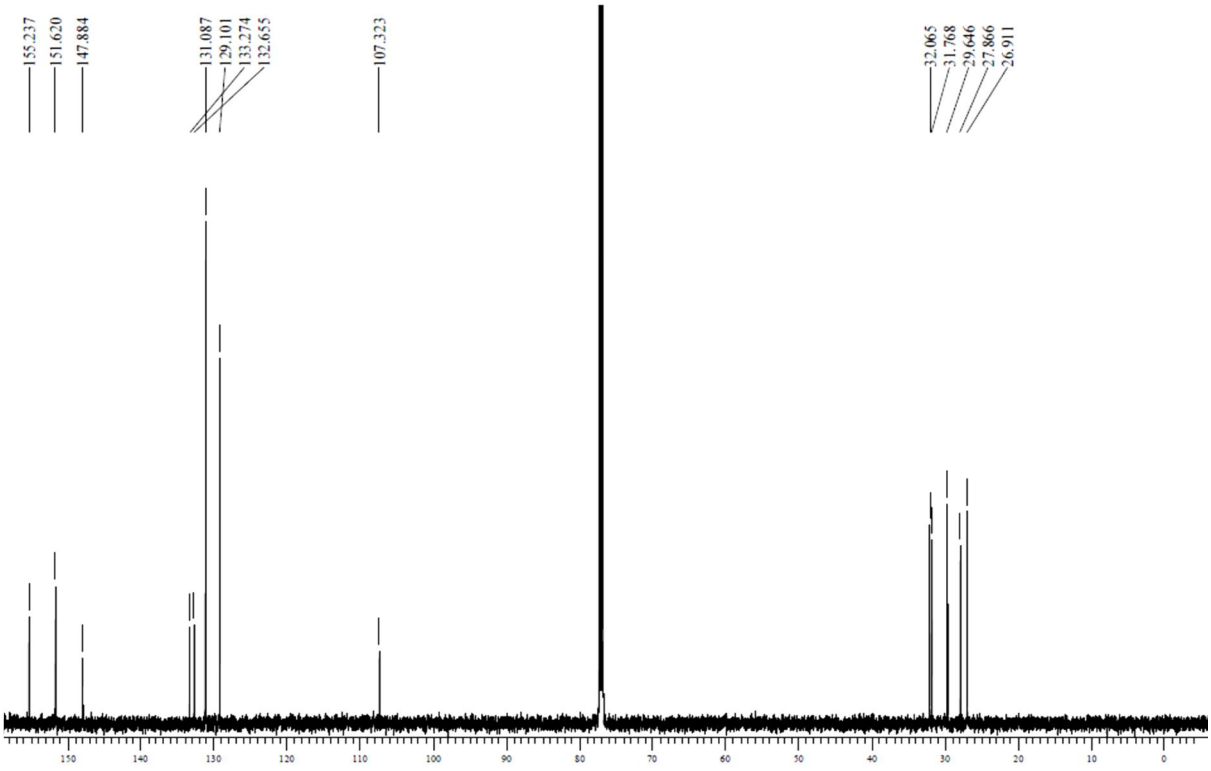

^{1}H and ^{13}C NMR

8-{[(4-Bromophenyl)sulfanyl]ethyl}caffeine (2e)

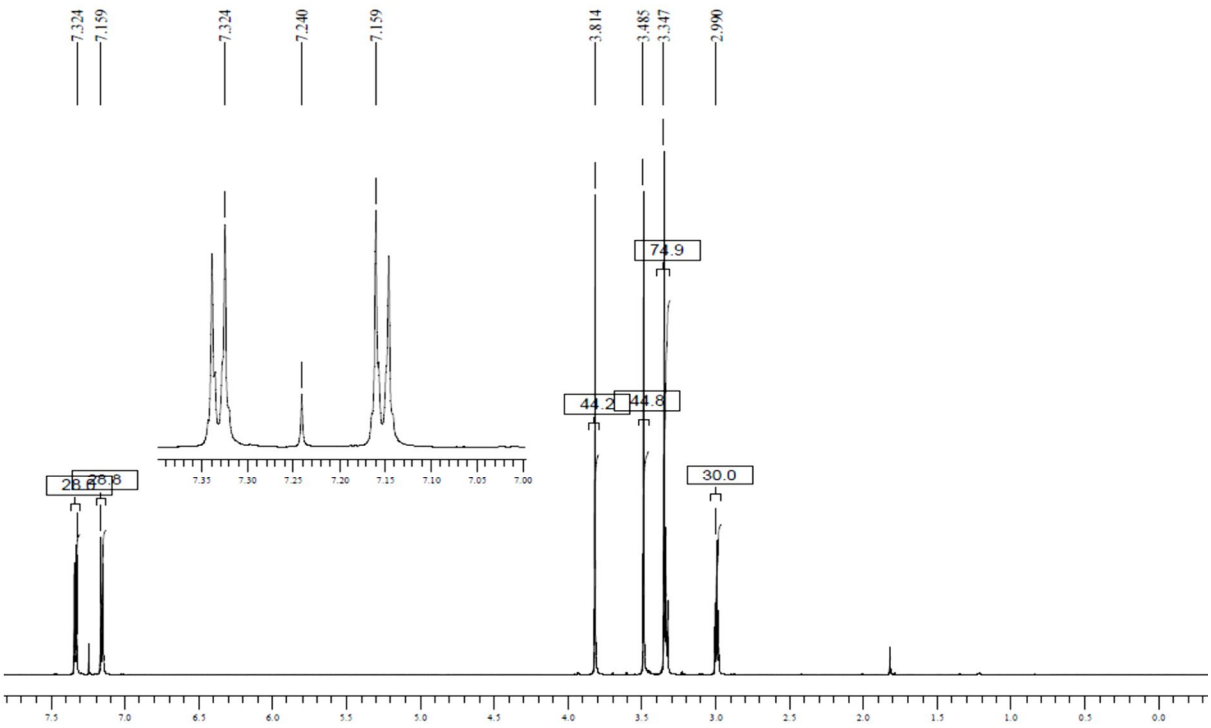

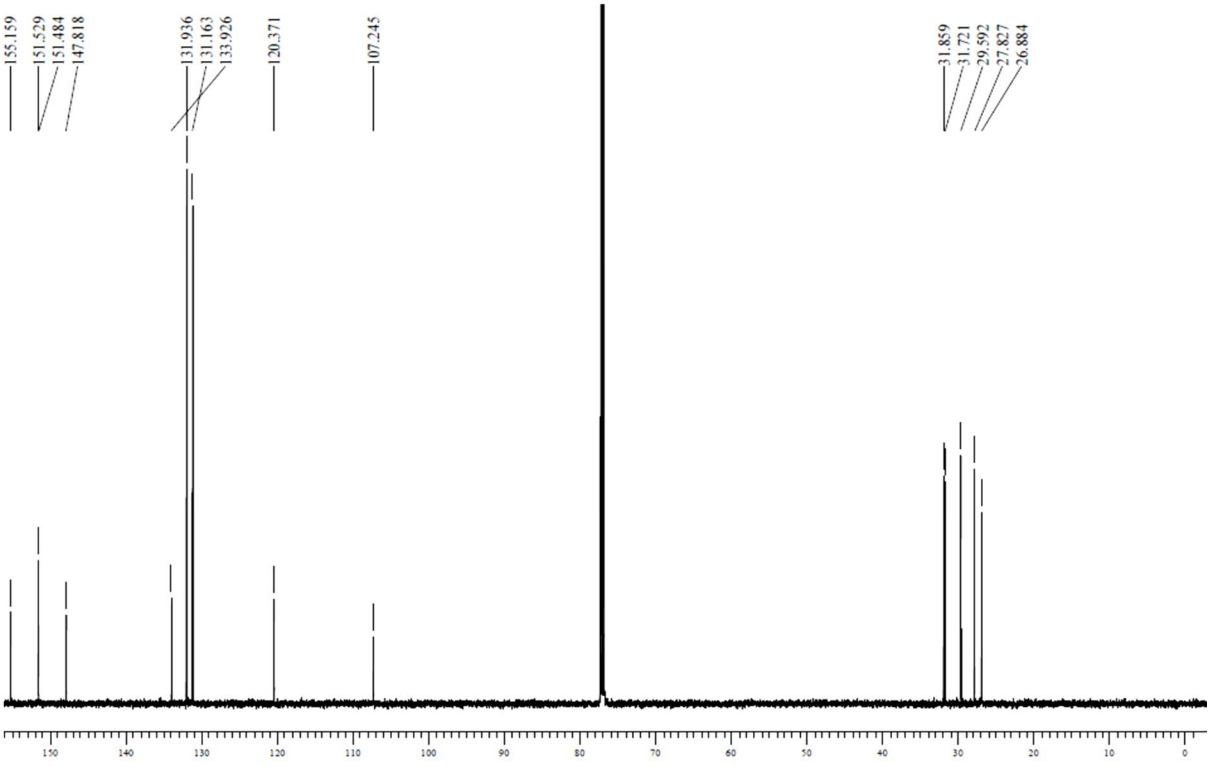

HPLC traces of the following compounds

- 8-[(Phenylsulfanyl)methyl]caffeine (**1a**)
- 8-{[(3-Chlorophenyl)sulfanyl]methyl}caffeine (**1b**)
- 8-{[(3-Bromophenyl)sulfanyl]methyl}caffeine (**1c**)
- 8-{[(3-Flourophenyl)sulfanyl]methyl}caffeine (**1d**)
- 8-{[(3-Methylphenyl)sulfanyl]methyl}caffeine (**1e**)
- 8-{[(3-Methoxyphenyl)sulfanyl]methyl}caffeine (**1f**)
- 8-{[(3-Ethoxyphenyl)sulfanyl]methyl}caffeine (**1g**)
- 8-{[(4-Chlorophenyl)sulfanyl]methyl}caffeine (**1h**)
- 8-{[(4-Bromophenyl)sulfanyl]methyl}caffeine (**1i**)
- 8-{[(Phenylsulfanyl)ethyl]}caffeine (**2a**)
- 8-{[(3-Chlorophenyl)sulfanyl]ethyl}caffeine (**2b**)
- 8-{[(3-Bromophenyl)sulfanyl]ethyl}caffeine (**2c**)
- 8-{[(4-Chlorophenyl)sulfanyl]ethyl}caffeine (**2d**)
- 8-{[(4-Bromophenyl)sulfanyl]ethyl}caffeine (**2e**)

HPLC method

HPLC analyses were carried out to determine the purity of the above mentioned compounds. HPLC analyses were conducted with an Agilent 1100 HPLC system equipped with a quaternary pump and an Agilent 1100 series diode array detector. HPLC grade acetonitrile (Merck) and Milli-Q water (Millipore) were used for the chromatography.

8-[(Phenylsulfanyl)methyl]caffeine (1a)

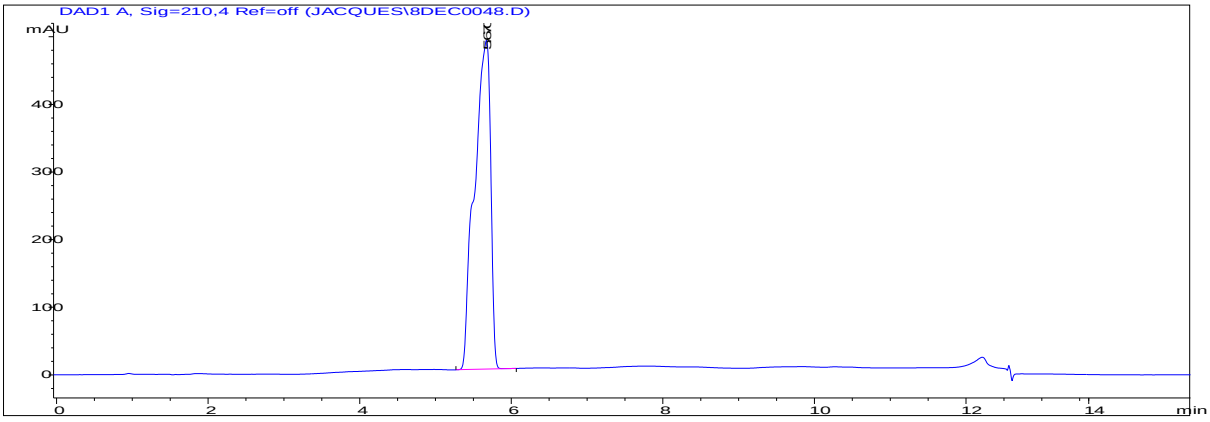

8-{[(3-Chlorophenyl)sulfanyl]methyl}caffeine (1b)

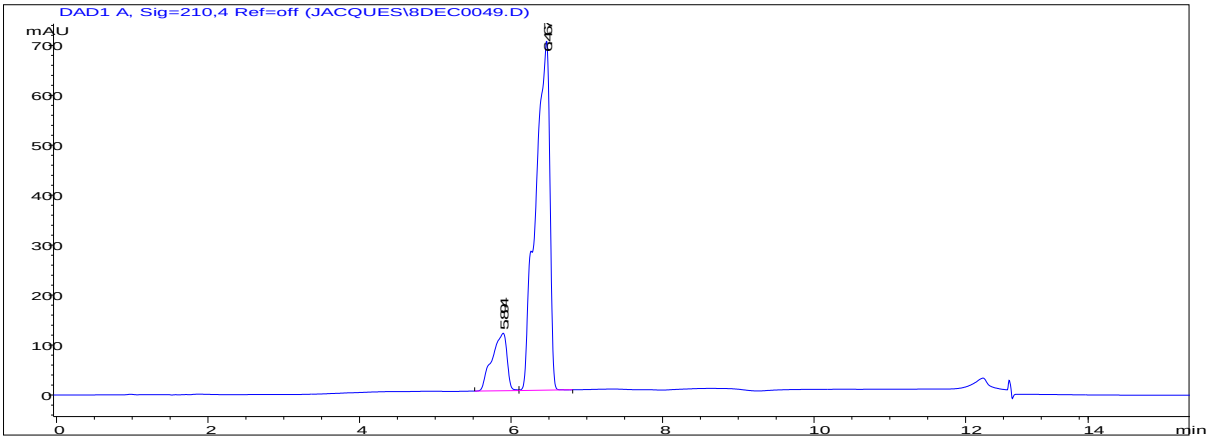

8-{[(3-Bromophenyl)sulfanyl]methyl}caffeine (1c)

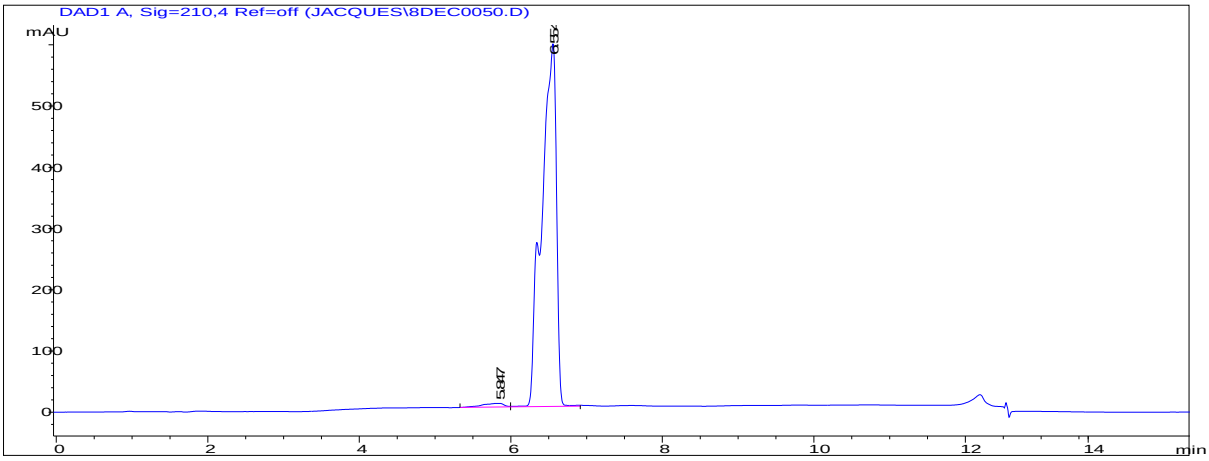

8-{[(3-Flourophenyl)sulfanyl]methyl}caffeine (1d)

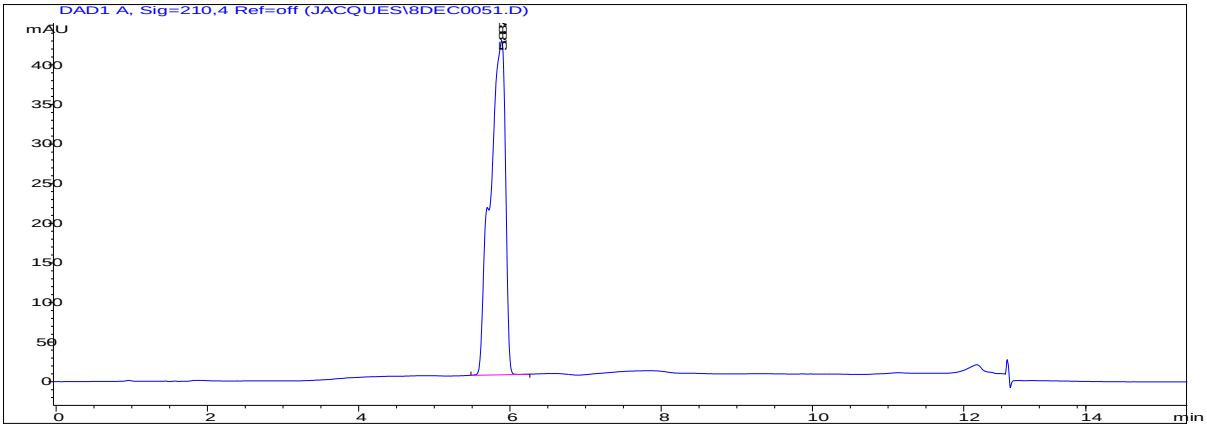

8-{[(3-Methylphenyl)sulfanyl]methyl}caffeine (1e)

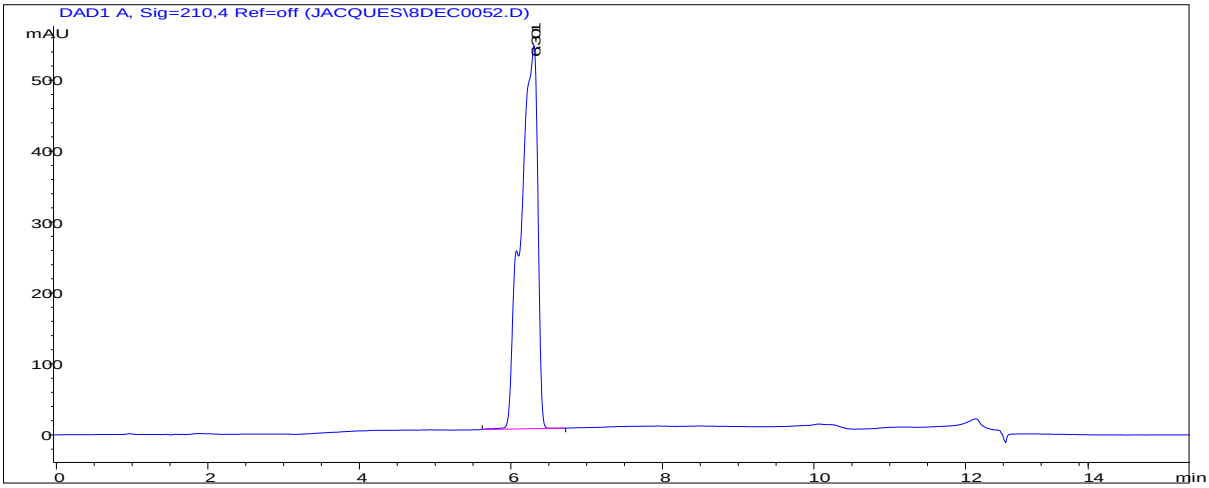

8-{[(3-Methoxyphenyl)sulfanyl]methyl}caffeine (1f)

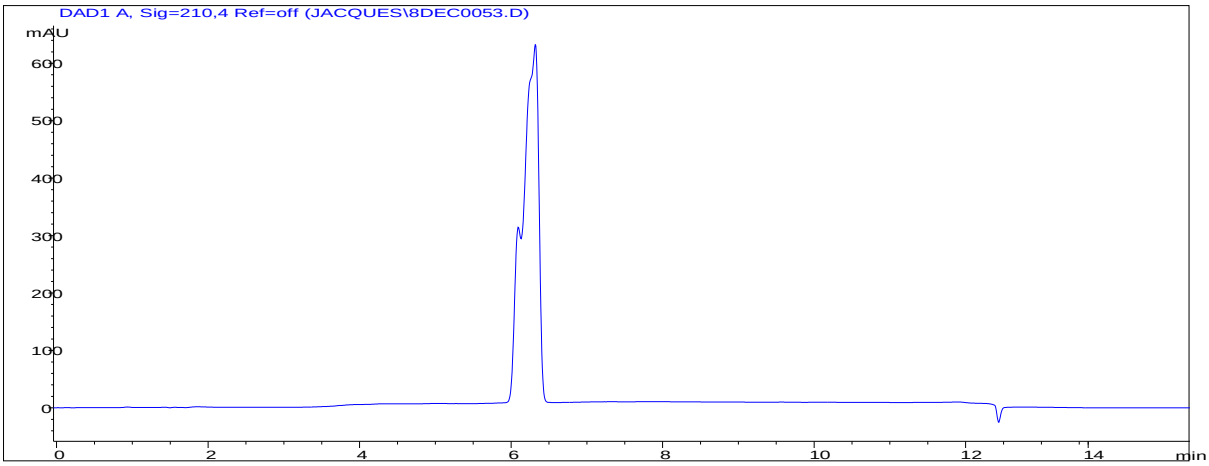

8-{[(3-Ethoxyphenyl)sulfanyl]methyl}caffeine (1g)

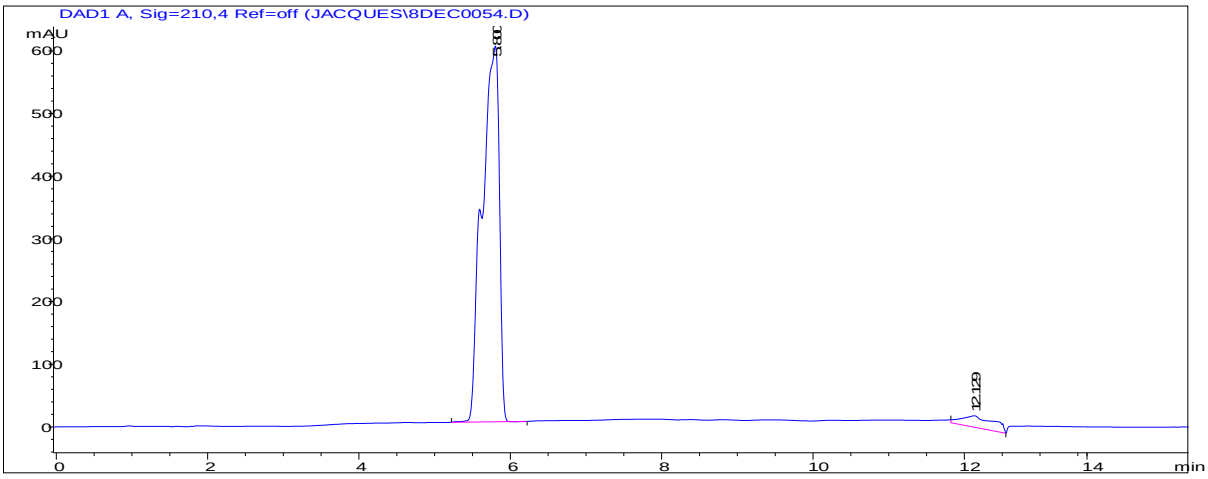

8-{[(4-Chlorophenyl)sulfanyl]methyl}caffeine (1h)

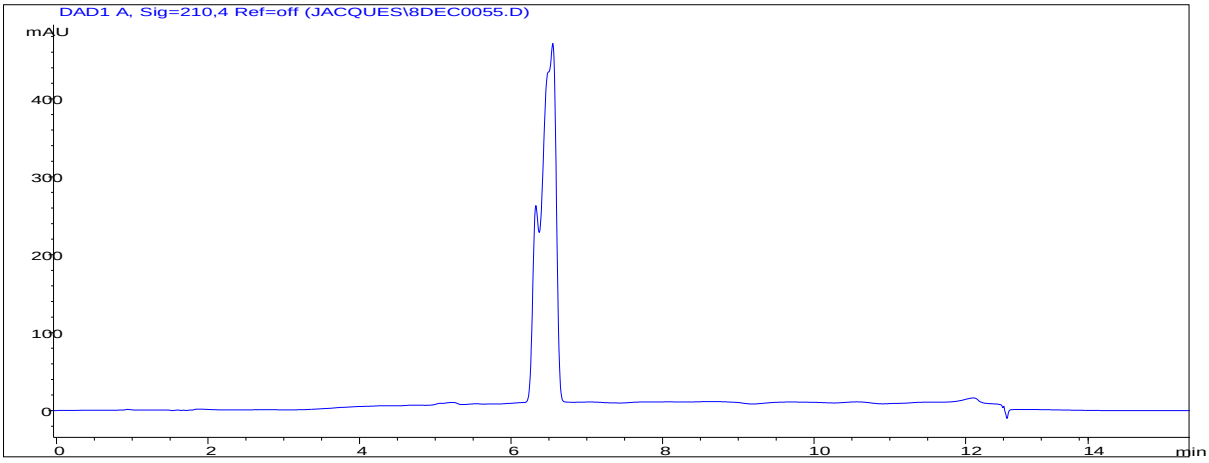

8-{[(4-Bromophenyl)sulfanyl]methyl}caffeine (1i)

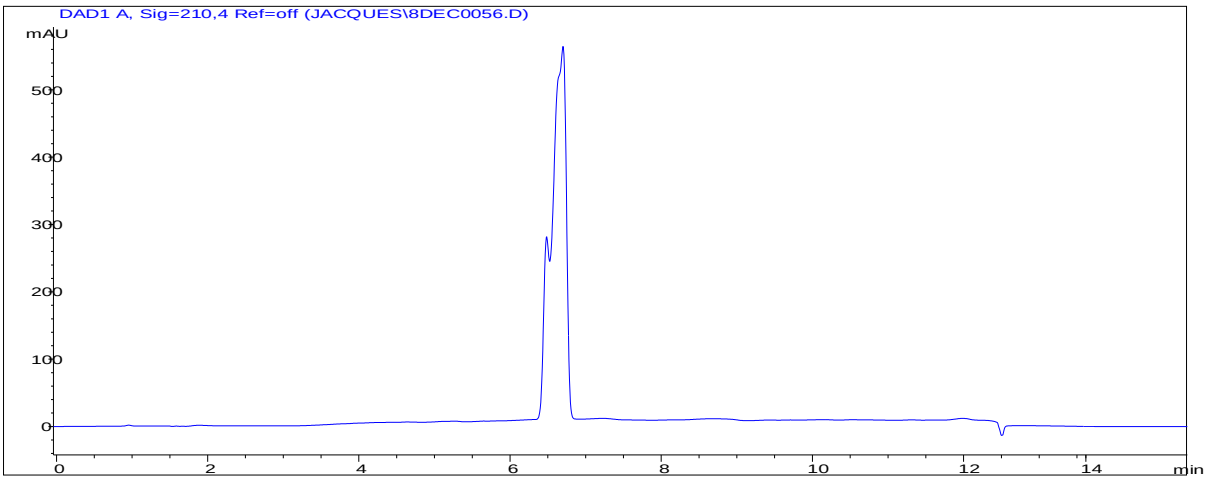

8-{[(Phenylsulfanyl)ethyl]}caffeine (2a)

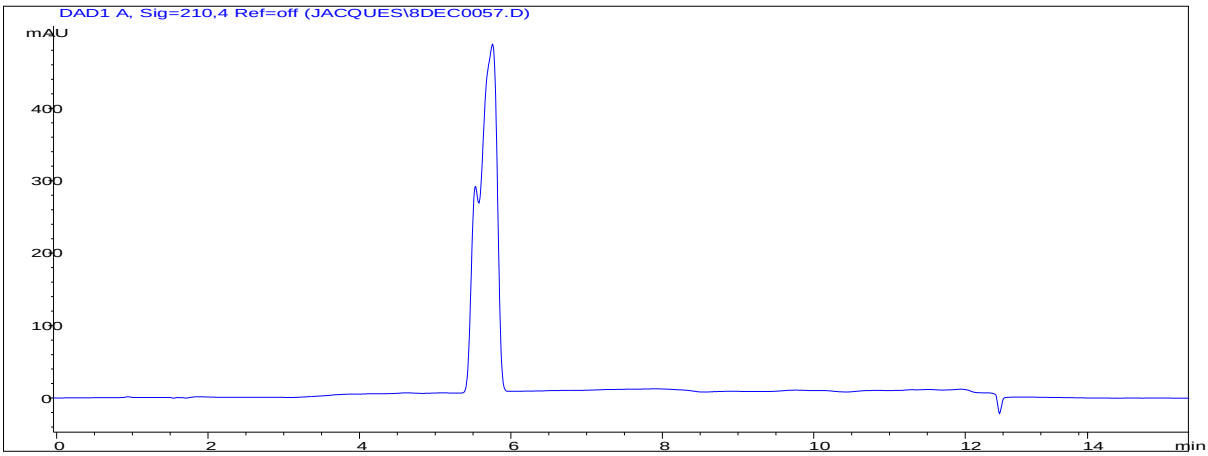

8-{[(3-Chlorophenyl)sulfanyl]ethyl}caffeine (2b)

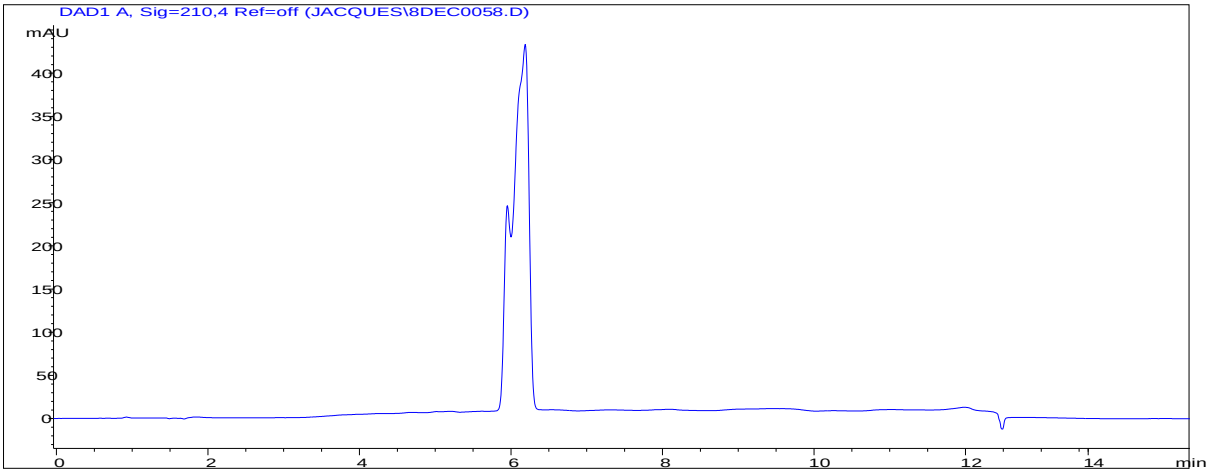

8-{[(3-Bromophenyl)sulfanyl]ethyl}caffeine (2c)

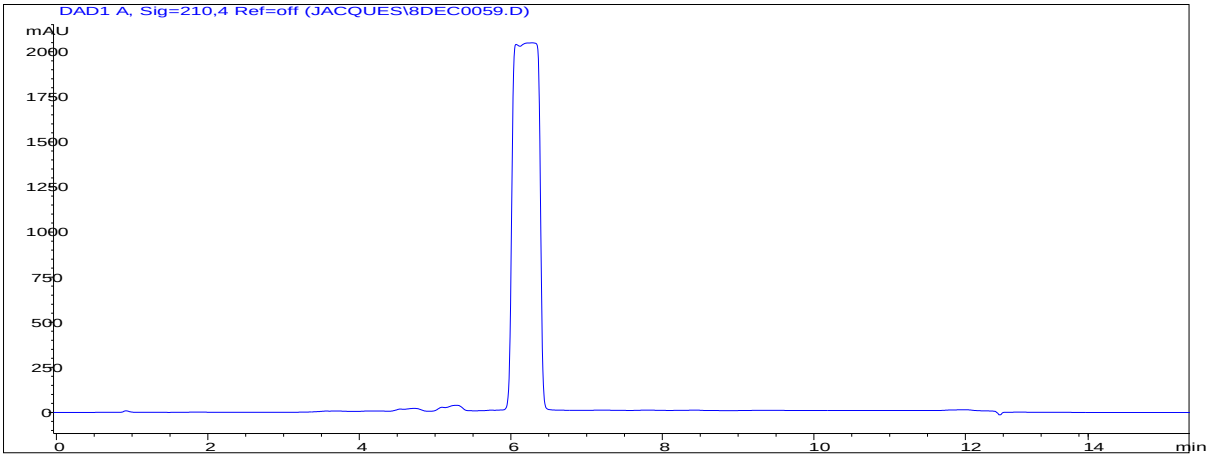

8-{[(4-Chlorophenyl)sulfanyl]ethyl}caffeine (2d)

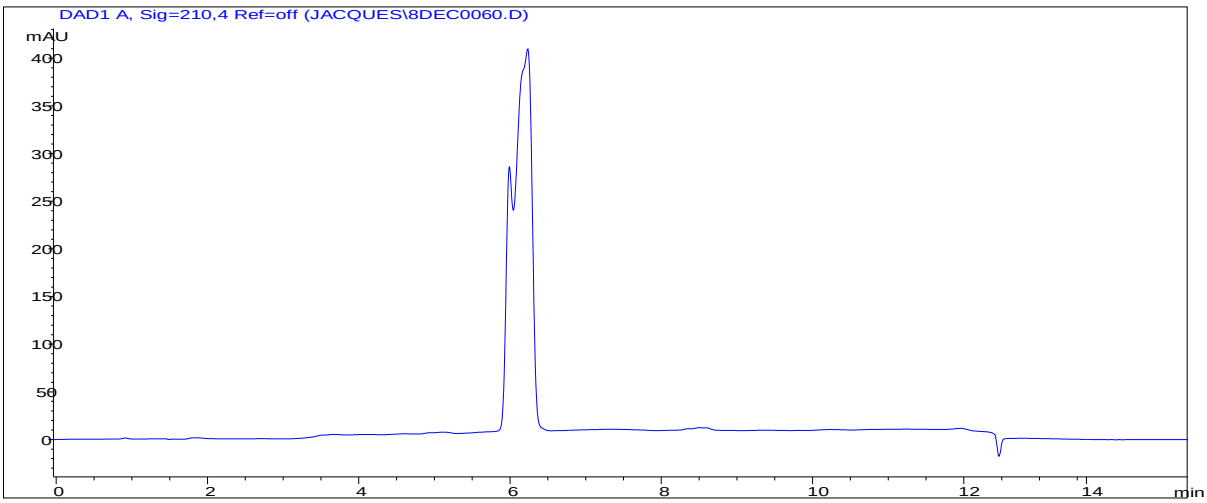

8-{[(4-Bromophenyl)sulfanyl]ethyl}caffeine (2e)

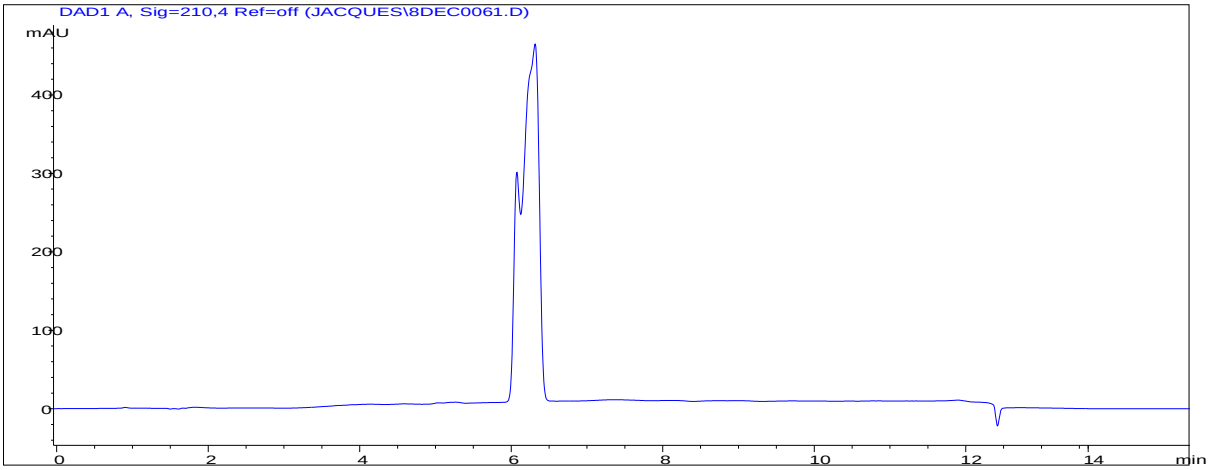

Acetonitrile solvent

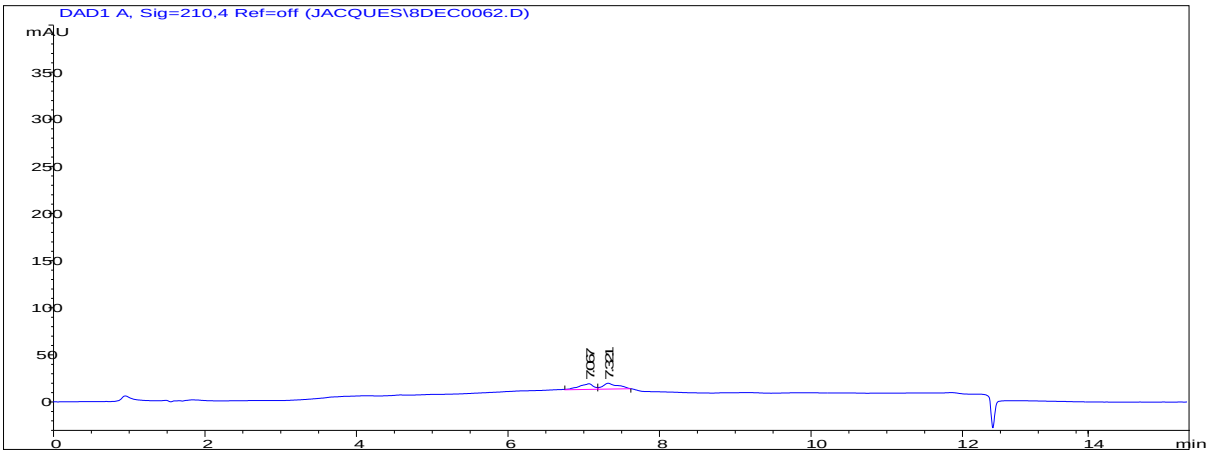

Mass spectra of the following compounds

- 8-[(Phenylsulfanyl)methyl]caffeine (**1a**)
- 8-{[(3-Chlorophenyl)sulfanyl]methyl}caffeine (**1b**)
- 8-{[(3-Bromophenyl)sulfanyl]methyl}caffeine (**1c**)
- 8-{[(3-Flourophenyl)sulfanyl]methyl}caffeine (**1d**)
- 8-{[(3-Methylphenyl)sulfanyl]methyl}caffeine (**1e**)
- 8-{[(3-Methoxyphenyl)sulfanyl]methyl}caffeine (**1f**)
- 8-{[(3-Ethoxyphenyl)sulfanyl]methyl}caffeine (**1g**)
- 8-{[(4-Chlorophenyl)sulfanyl]methyl}caffeine (**1h**)
- 8-{[(4-Bromophenyl)sulfanyl]methyl}caffeine (**1i**)
- 8-{[(Phenylsulfanyl)ethyl]}caffeine (**2a**)
- 8-{[(3-Chlorophenyl)sulfanyl]ethyl}caffeine (**2b**)
- 8-{[(3-Bromophenyl)sulfanyl]ethyl}caffeine (**2c**)
- 8-{[(4-Chlorophenyl)sulfanyl]ethyl}caffeine (**2d**)
- 8-{[(4-Bromophenyl)sulfanyl]ethyl}caffeine (**2e**)

8-[(Phenylsulfanyl)methyl]caffeine (1a)

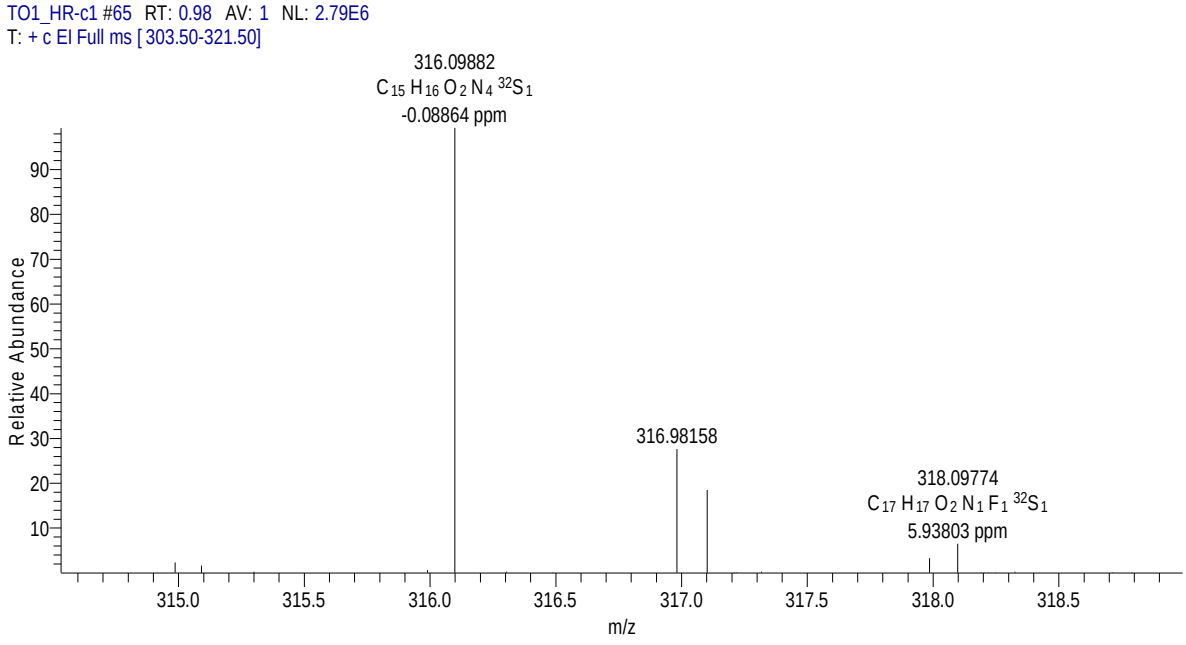

8-{[(3-Chlorophenyl)sulfanyl]methyl}caffeine (1b)

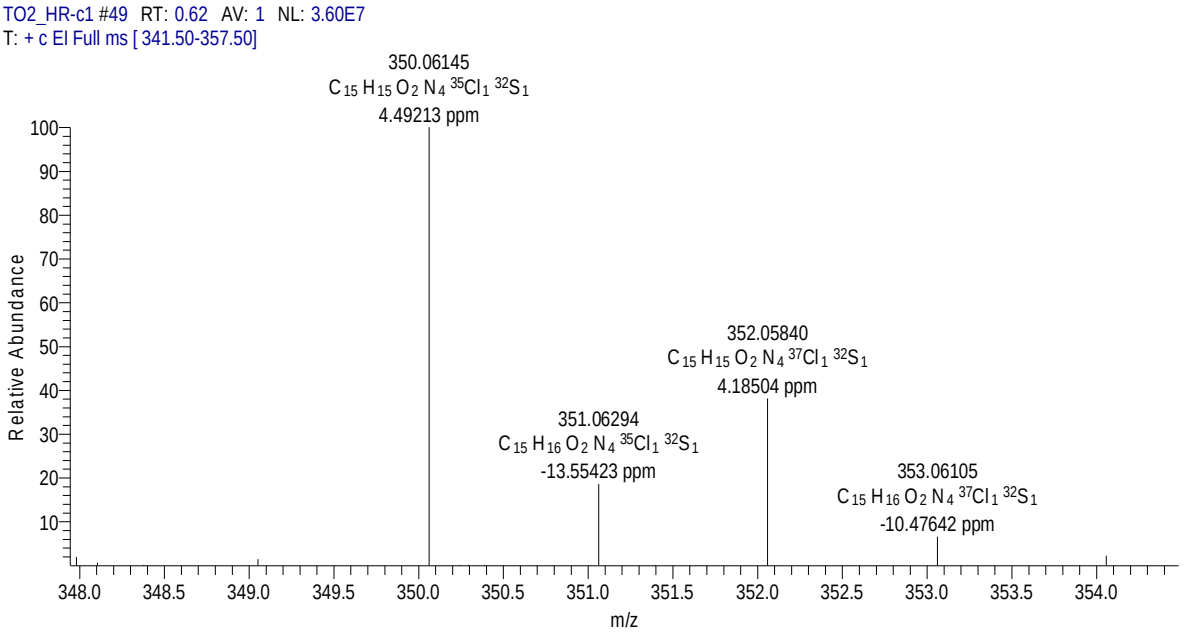

8-{[(3-Bromophenyl)sulfanyl]methyl}caffeine (1c)

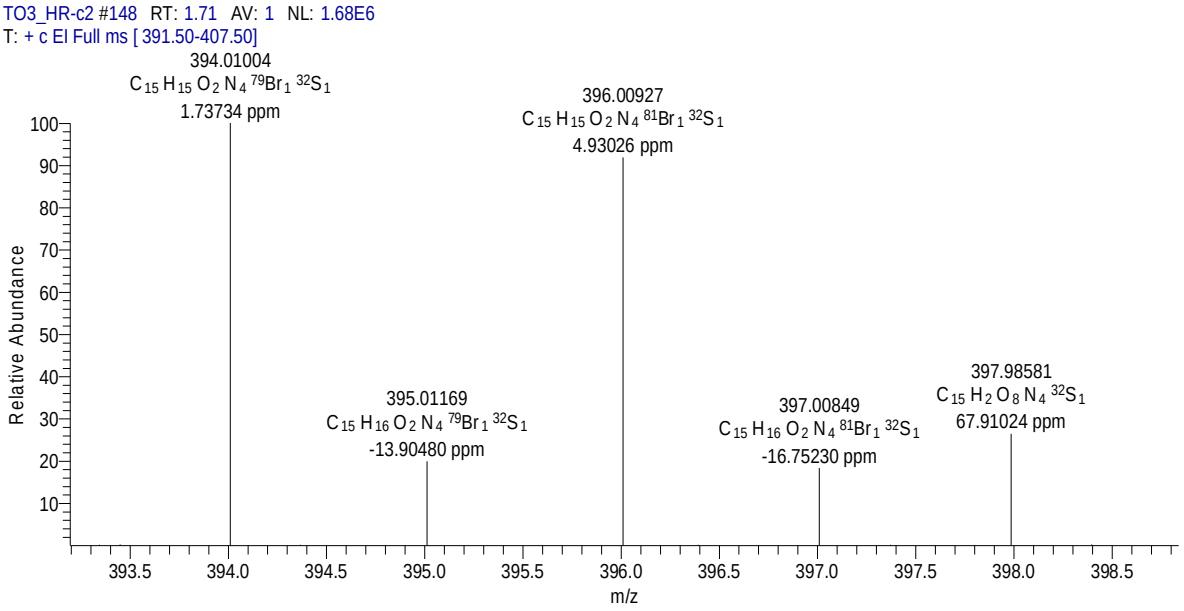

8-{[(3-Flourophenyl)sulfanyl]methyl}caffeine (1d)

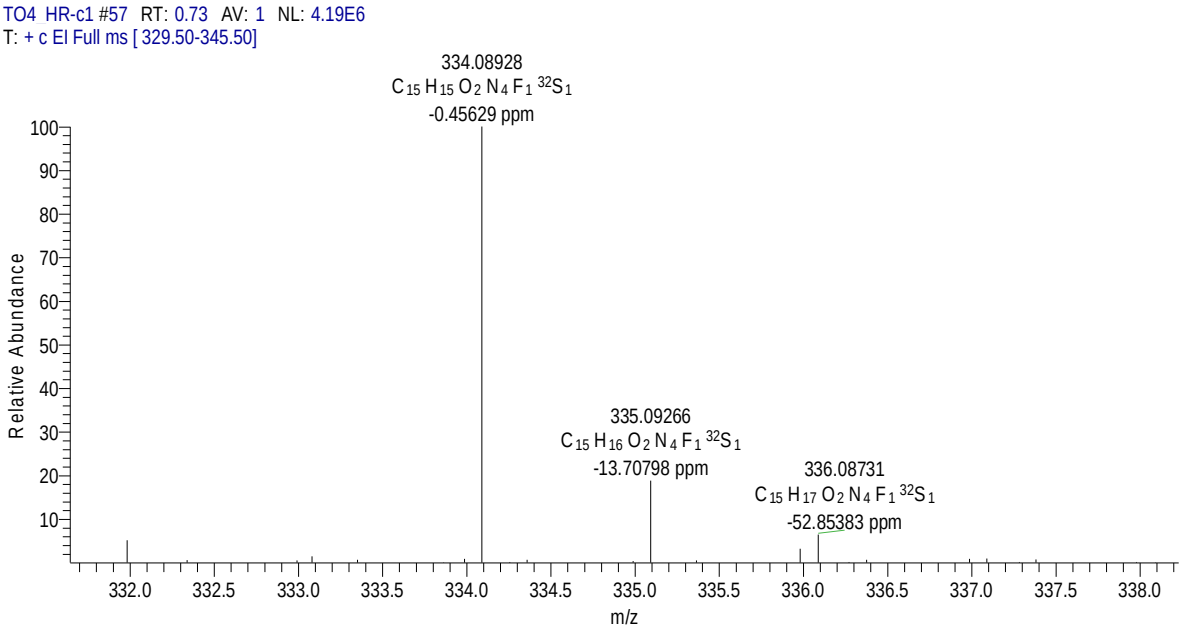

8-{[(3-Methylphenyl)sulfanyl]methyl}caffeine (1e)

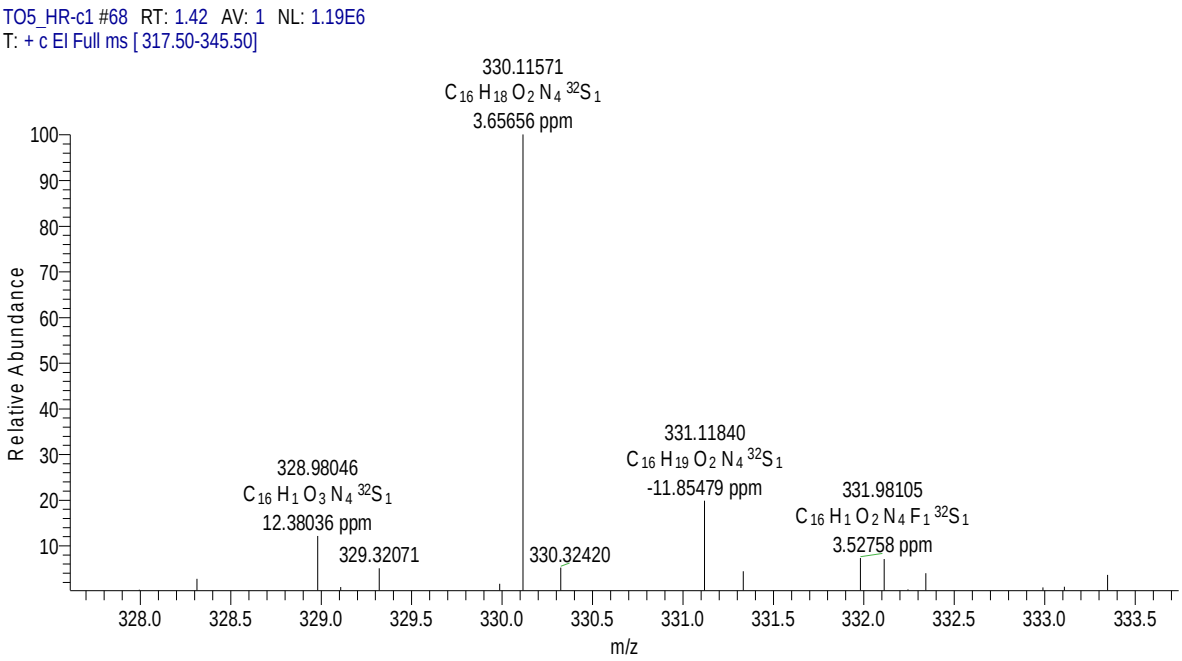

8-{[(3-Methoxyphenyl)sulfanyl]methyl}caffeine (1f)

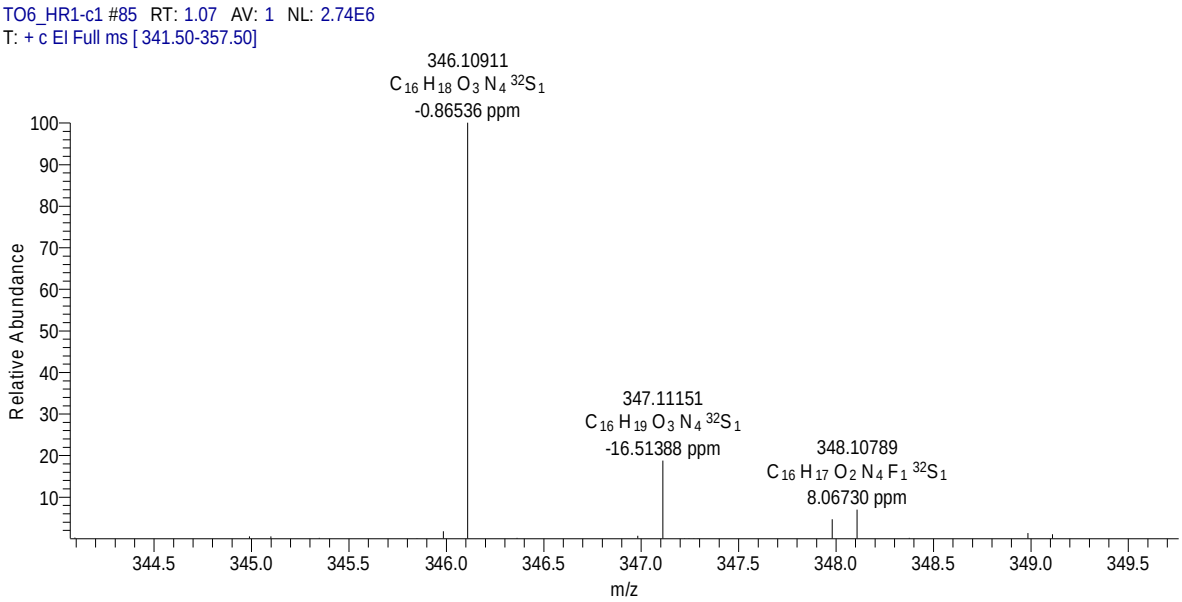

8-{[(3-Ethoxyphenyl)sulfanyl]methyl}caffeine (1g)

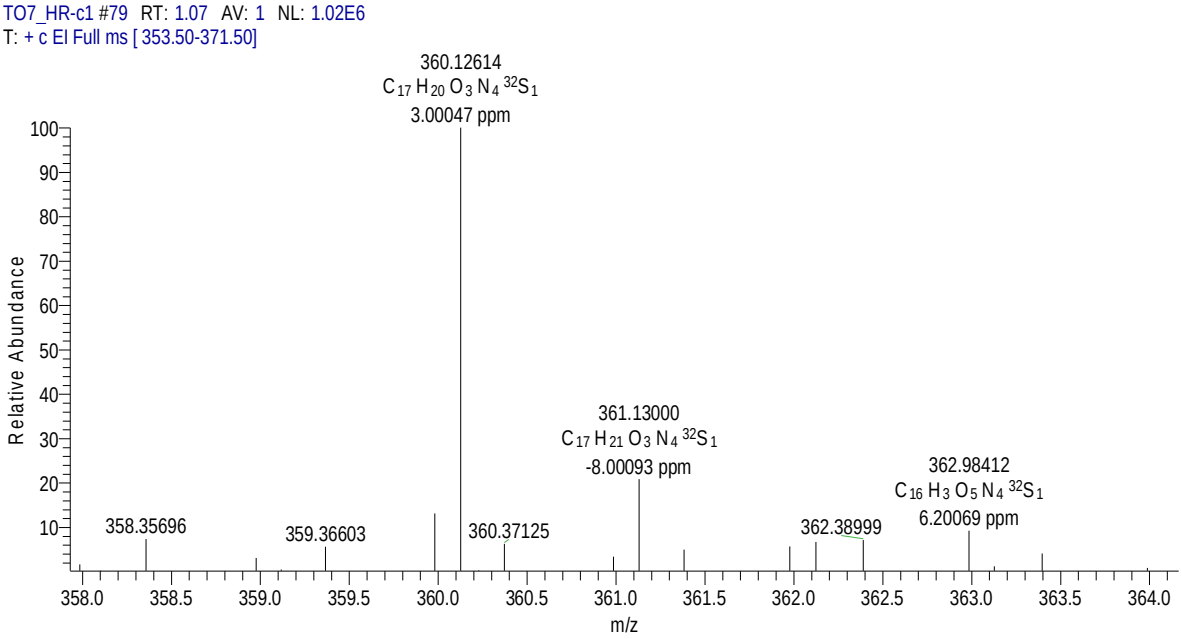

8-{[(4-Chlorophenyl)sulfanyl]methyl}caffeine (1h)

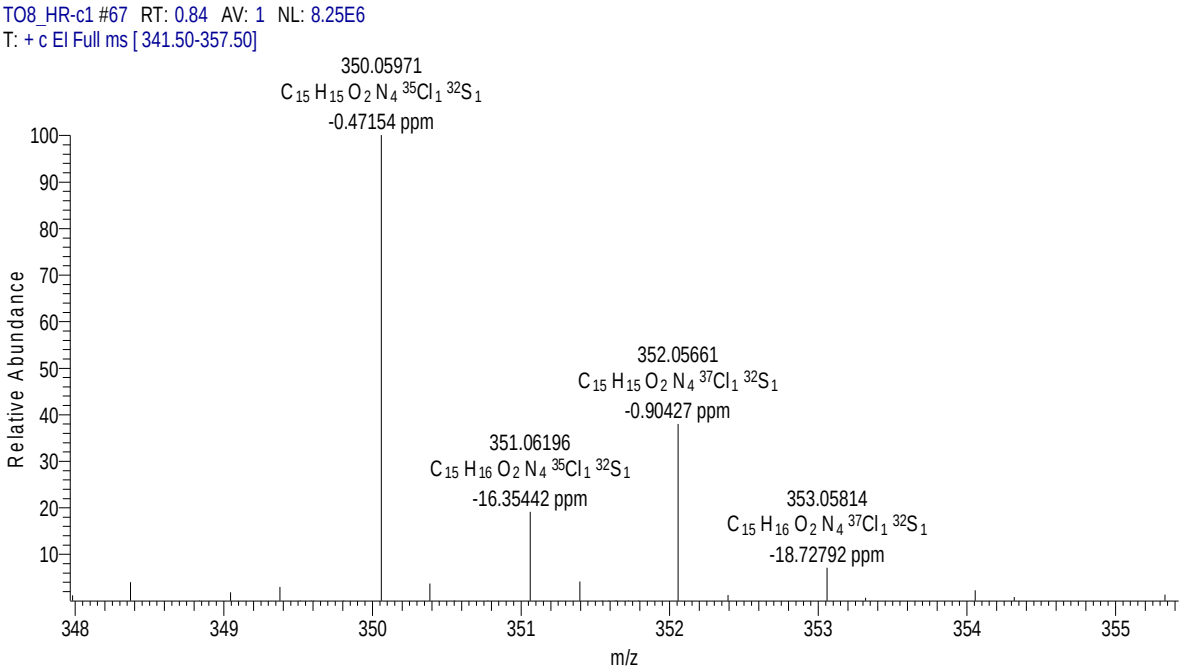

8-{[(4-Bromophenyl)sulfanyl]methyl}caffeine (1i)

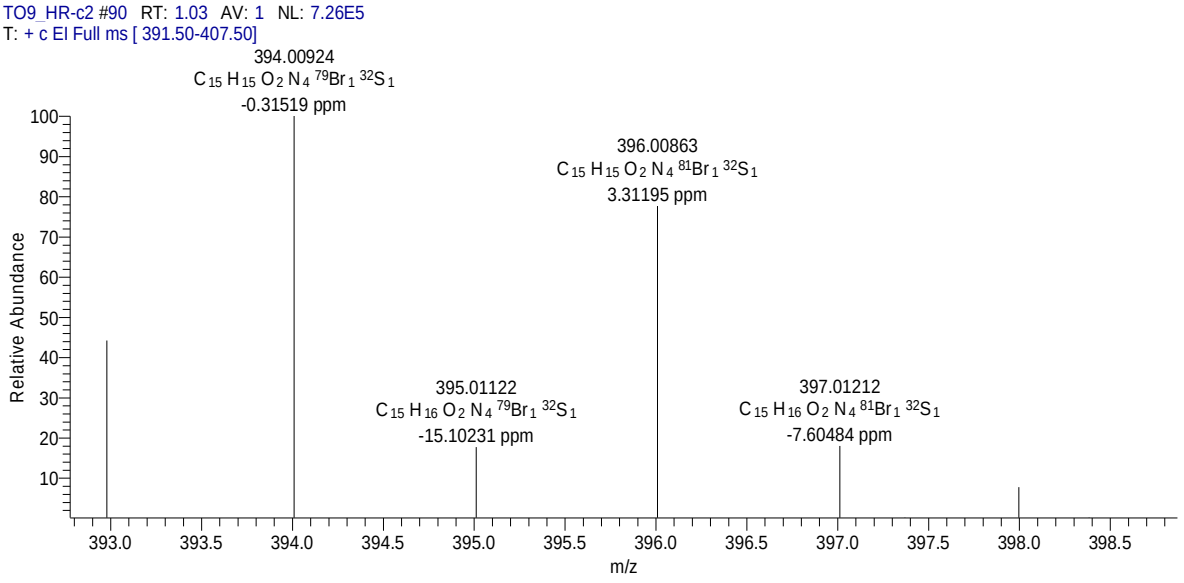

8-{[(Phenylsulfanyl)ethyl]}caffeine (2a)

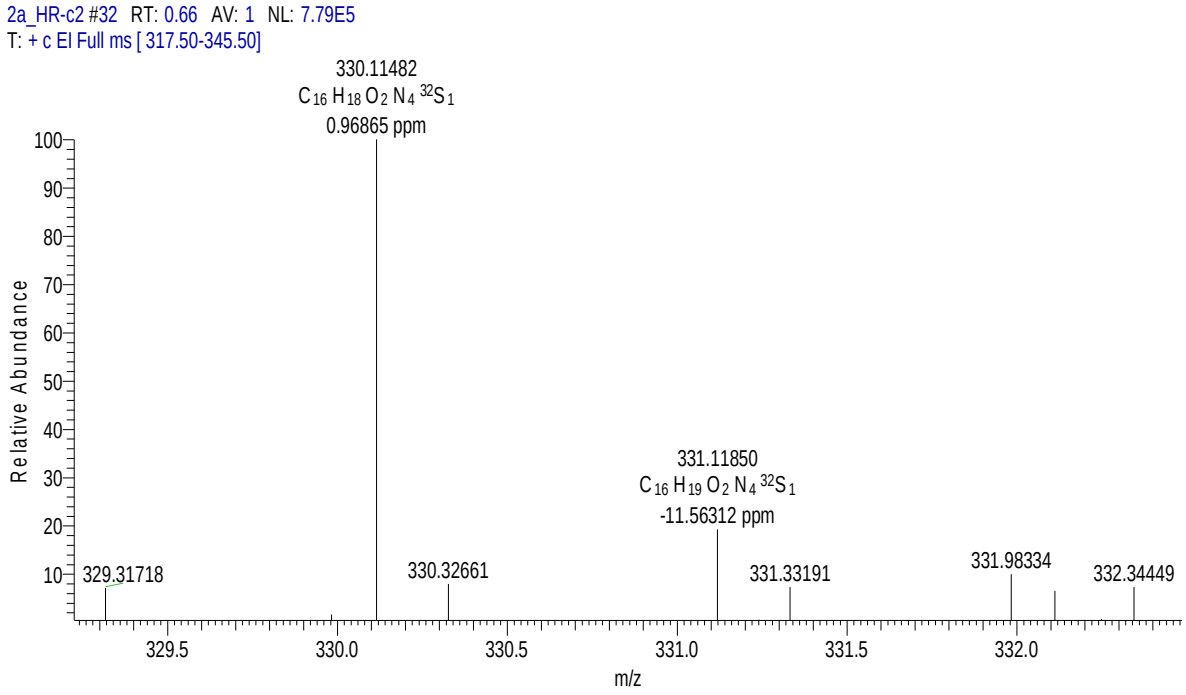

8-{[(3-Chlorophenyl)sulfanyl]ethyl}caffeine (2b)

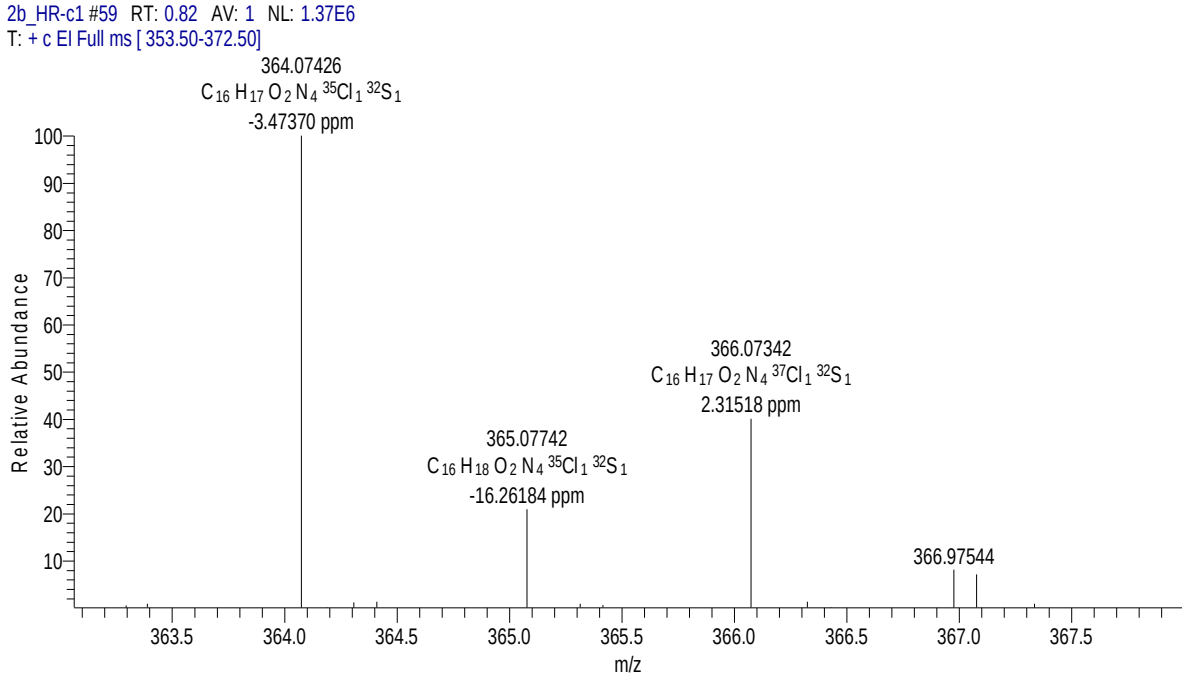

8-{[(3-Bromophenyl)sulfanyl]ethyl}caffeine (2c)

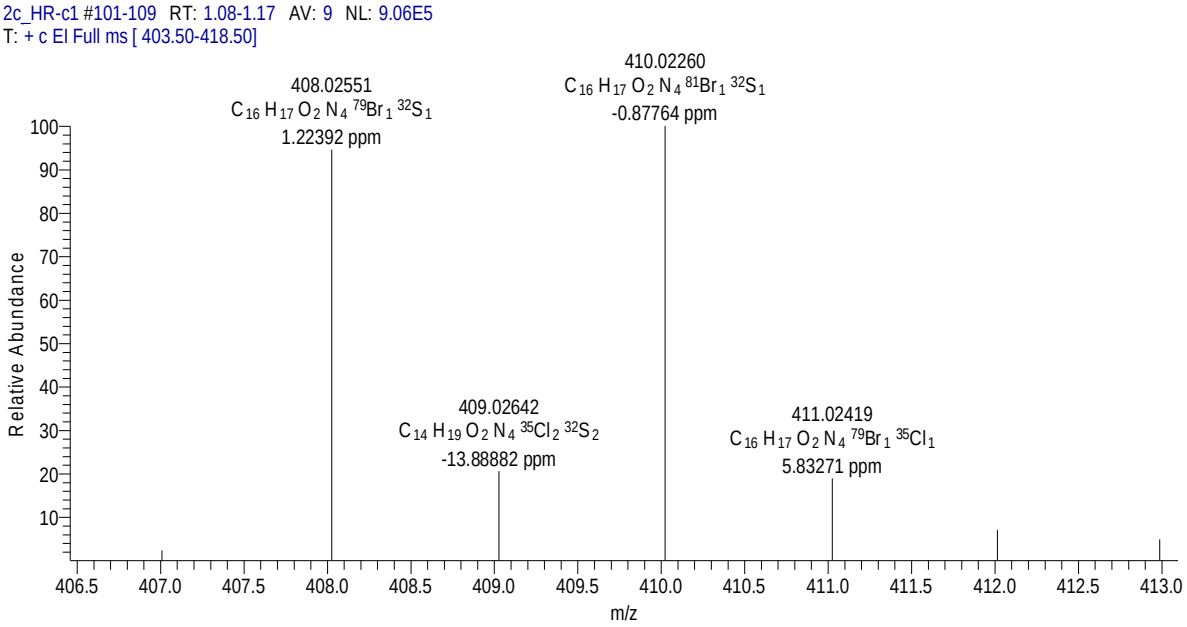

8-{[(4-Chlorophenyl)sulfanyl]ethyl}caffeine (2d)

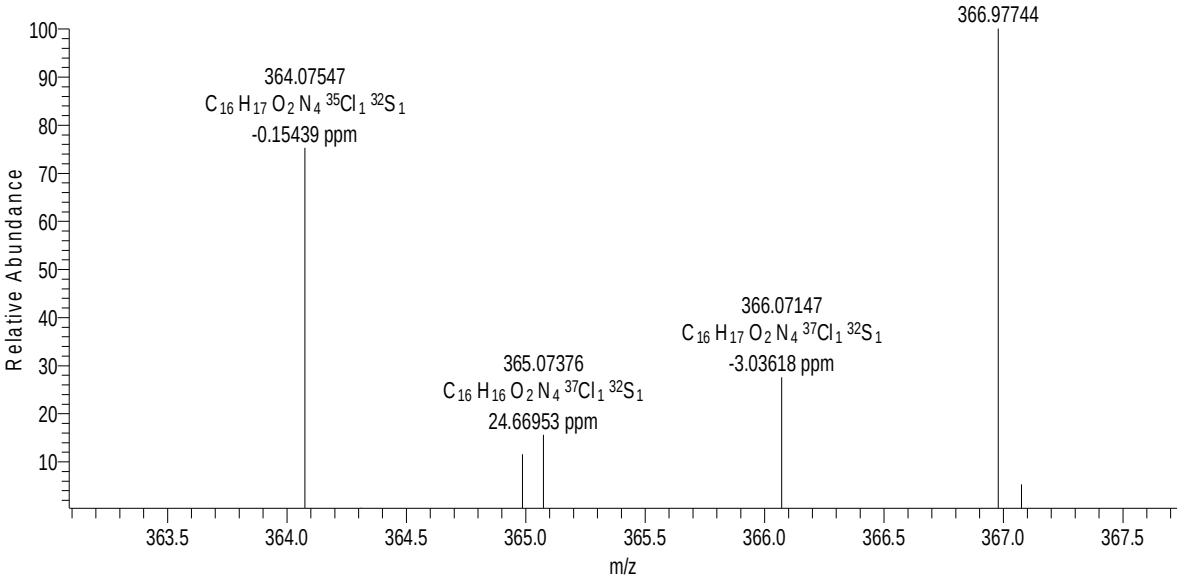

8-{[(4-Bromophenyl)sulfanyl]ethyl}caffeine (2e)

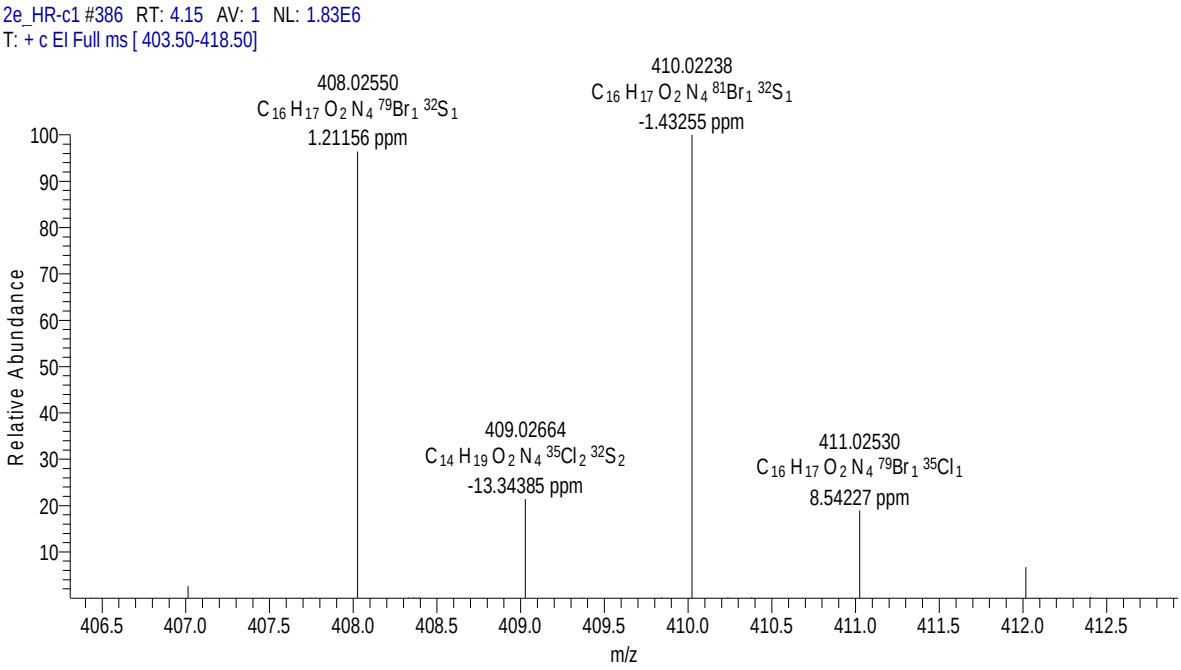

APPENDIX B

Published article

[*Bioorganic & Medicinal Chemistry 20 (2012) 4336–4347***]**

Inhibition of monoamine oxidase by 8-phenoxymethylcaffeine derivatives

Thokozile Okaecwe,[a] Abraham J. Swanepoel,[a] Anél Petzer,[b] Jacobus J. Bergh,[a] and Jacobus P. Petzer[a],*

[a] *Pharmaceutical Chemistry, School of Pharmacy, North-West University, Private Bag X6001, Potchefstroom, 2520, South Africa*

[b] *Unit for Drug Research and Development, School of Pharmacy, North-West University, Private Bag X6001, Potchefstroom, 2520, South Africa*

Abstract—A recent study has reported that a series of 8-benzyloxycaffeines are potent and reversible inhibitors of both human monoamine oxidase (MAO) isoforms, MAO-A and –B. In an attempt to discover additional caffeine derivatives with potent MAO inhibitory activities, and to contribute to the known structure-activity relationships of MAO inhibition by caffeine derived compounds, the present study investigates the MAO inhibitory potencies of series of 8-phenoxymethylcaffeine and 8-[(phenylsulfanyl)methyl]caffeine derivatives. The results document that the 8-phenoxymethylcaffeine derivatives act as potent reversible inhibitors of MAO-B, with IC_{50} values ranging from 0.148–5.78 μM. In contrast, the 8-[(phenylsulfanyl)methyl]caffeine derivatives were found to be weak inhibitors of MAO-B, with IC_{50} values ranging from 4.05–124 μM. Neither the 8-phenoxymethylcaffeine nor the 8-[(phenylsulfanyl)methyl]caffeine derivatives exhibited high binding affinities for MAO-A. While less potent than the 8-benzyloxycaffeines as MAO-B inhibitors, this study concludes that 8-phenoxymethylcaffeines may act as useful leads for the design of MAO-B selective inhibitors. Such compounds may find application in the therapy of neurodegenerative disorders such as Parkinson's disease. Using molecular docking experiments, this study also proposes possible binding orientations of selected caffeine derivatives in the active sites of MAO-A and –B.

Keywords: monoamine oxidase; reversible inhibition; competitive; selectivity; caffeine; phenoxymethylcaffeine; 8-[(phenylsulfanyl)methyl]caffeine; molecular docking.

*Corresponding author. Tel.: +27 18 2992206; fax: +27 18 2994243

e-mail: jacques.petzer@nwu.ac.za

1. Introduction

The monoamine oxidases (MAO) A and B are apoenzymes, which require flavin adenine dinucleotide (FAD) as cofactor.[1] The MAO enzymes are bound to the outer surface of mitochondria and are expressed in most human tissues, including the brain.[2,3] An important function of the MAOs is to catalyze the oxidative catabolism of neurotransmitters, including serotonin, dopamine and epinephrine, thereby terminating their actions.[4] The MAOs also function as metabolic barriers by restricting the access of extraneous amines to the systemic circulation and the central nervous system. By metabolizing false neurotransmitters such as benzylamine and β-phenylethylamine,[4,5] brain microvessel MAO-B limits their passage into the brain tissue and thus protects neurons from their stimulatory effects.[6] In the gut wall, intestinal MAO-A metabolizes tyramine, an indirectly-acting sympathomimetic amine which is present in certain foods. MAO-A thereby restricts the amount of tyramine that enters the systemic circulation and prevents the tyramine-induced release of catecholamines from peripheral neurons.[7]

Although the amino acid sequences of MAO-A and –B are approximately 73% identical, they exhibit different substrate and inhibitor specificities.[8] Most notably, the MAO-A isoform selectively oxidizes serotonin while MAO-B selectively catalyzes the oxidation of the arylalkylamines, benzylamine and β-phenylethylamine. Both isoforms utilize dopamine, epinephrine and norepinephrine as substrates.[4] The interest in the MAOs as drug targets stems from their roles in the catabolism of these neurotransmitters. MAO-A inhibitors have been employed as antidepressant agents while MAO-B inhibitors have been developed as therapy for Parkinson's disease.[4,9] These clinical applications of MAO-A and –B inhibitors are thought to be, for the most part, dependent on the blocking of the central catabolism of serotonin and dopamine, respectively. In Parkinson's disease therapy, MAO-B inhibitors are frequently combined with levodopa, the metabolic precursor of dopamine.[10] The inhibition of the MAO-B catalyzed oxidation of dopamine in the brain may elevate the levels of dopamine derived from levodopa and may allow for a reduction of the levodopa dose required for a therapeutic effect.[11] MAO-B inhibitors are of particular relevance in Parkinson's disease since MAO-B is the major isoform in the basal ganglia, the affected brain region in Parkinson's disease.[12,13] Furthermore, MAO-B activity and density increases in most brain regions with age while MAO-A activity remains constant.[14,15] This presents a further rationale for targeting MAO-B in age-related neurodegenerative disorders such as Parkinson's disease.[16] Another point of interest is that the MAOs may be major sources of hydrogen peroxide in cells. Following the oxidation of a substrate molecule, the reoxidation of the flavin requires the reduction of molecular oxygen to yield hydrogen peroxide. Hydrogen peroxide may lead to pathological oxidative stress and promote the neurodegenerative processes

associated with Parkinson's disease.[17,18] Also, the aldehydic products, formed as a result of the MAO catalyzed oxidative deamination of amines, may act as neurotoxic metabolites by reacting with exocyclic amino groups of nucleosides, and N-terminal and lysine ε-amino groups of proteins. MAO-B inhibitors may therefore also exert a neuroprotective effect by reducing the formation of these potentially toxic by-products.[1]

Considering the pharmacological importance of MAO inhibitors, the present study aims to discover new inhibitors of the MAOs with particular emphasis on the MAO-B isoform. For this purpose, caffeine derived structures will serve as lead compounds (Fig. 1). Recent studies have reported that 8-benzyloxycaffeines (**1**) act as potent reversible inhibitors of both MAO-A and –B.[19] A homologous series of and 8-sulfanylcaffeines (**2**) has similarly been shown to inhibit MAO-B, and to a lesser degree MAO-A.[20] The 8-benzyloxycaffeines are of particular interest since, unlike most caffeine derived MAO inhibitors, they also possess high binding affinities for MAO-A. The ability of these compounds to also bind to MAO-A may be attributed to the relatively large degree of rotational freedom of the C8 side chain at the carbon-oxygen ether bond. It has been suggested that structures with a relatively larger degree of conformational freedom may be better suited for binding to MAO-A than relatively rigid structures.[19] MAO-A inhibition may also have a role in Parkinson's disease therapy since, in the primate brain, MAO-A also contributes to the catabolism of dopamine.[21] Nonselective MAO-A/B inhibitors may therefore be more efficacious in blocking the oxidation of dopamine and thereby prolonging its effect in the basal ganglia.[1] Based on the promising activities of the 8-benzyloxycaffeines and 8-sulfanylcaffeines, the present study investigates the human MAO inhibitory potencies of series of 8-phenoxymethylcaffeine (**3**) and 8-[(phenylsulfanyl)methyl]caffeine (**4** and **5**) derivatives (Fig. 2). The 8-phenoxymethylcaffeines (**3**) are isomers of **1** while the 8-[(phenylsulfanyl)methyl]caffeines (**4** and **5**) are close structural analogues of **2**. The major difference between the structures of compounds **3**–**5** and that of 8-benzyloxycaffeine is in the placement of the hetero atom in the C8 side chain. In compounds **3**–**5** the position of the hetero atom is distal from the caffeine ring and these compounds are expected to exhibit a differing degree of flexibility than 8-benzyloxycaffeine. Since the degree of flexibility of the 8-benzyloxycaffeine C8 side chain plays an important role in its binding to particularly MAO-A, compounds **3**–**5** may differ in their MAO inhibitory properties compared to the 8-benzyloxycaffeines. The possibility therefore exists that compounds **3**–**5** may display limited inhibition of MAO-A, making them MAO-B selective inhibitors. This study aims to explore this possibility. This study may also contribute to the known structure-activity relationships of MAO inhibition by caffeine derived compounds.

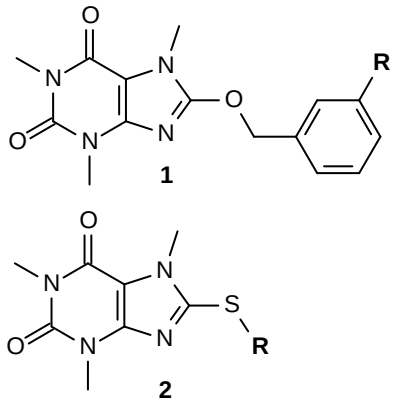

Figure 1. The structures of 8-benzyloxycaffeines (**1**) and 8-sulfanylcaffeines (**2**).

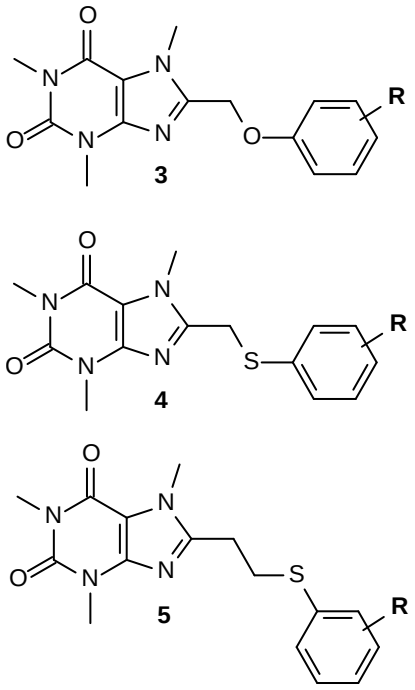

Figure 2. The structures of the 8-phenoxymethylcaffeine (**3**), 8-[(phenylsulfanyl)methyl]caffeine (**4**) and 8-[(phenylsulfanyl)ethyl]caffeine (**5**) derivatives that were investigated in this study.

2. Results

2.1. Chemistry

The syntheses of the 8-phenoxymethylcaffeine derivatives **3a**–**j** were accomplished using the literature procedure (Scheme 1).[22] 1,3-Dimethyl-5,6-diaminouracil (**6**)[23] was allowed to react with the appropriate phenoxyacetic acid (**7**) in the presence of the carbodiimide activating reagent, N-(3-dimethylaminopropyl)-N′-ethylcarbodiimide hydrochloride (EDAC).

The resulting amide intermediate was treated under reflux with aqueous sodium hydroxide to yield the corresponding 8-phenoxymethyltheophylline intermediate (**8**). Without further purification, the crude theophylline was 7*N*-methylated with an excess of iodomethane to yield the target compounds, the 8-phenoxymethylcaffeine derivatives **3a**–**j**. The 8-[(phenylsulfanyl)methyl]caffeine derivatives, **4a**–**i** and **5a**–**e**, were prepared in a similar manner by reacting 1,3-dimethyl-5,6-diaminouracil with an appropriate 2-(phenylsulfanyl)acetic acid (**9**) or 3-(phenylsulfanyl)propanoic acid (**10**), respectively (Scheme 2). After ring closure of the resulting amide, the theophylline intermediate (**11**) was obtained. Methylation of **11** in the presence of iodomethane yielded the target 8-[(phenylsulfanyl)methyl]caffeine derivatives **4a**–**i** and **5a**–**e**. Following crystallization, the structures of all compounds were verified by mass spectrometry, ^{1}H NMR and ^{13}C NMR. In certain instances the phenoxyacetic acids (**7**), 2-(phenylsulfanyl)acetic acids (**9**) and 3-(phenylsulfanyl)propanoic acids (**10**), which were required for the synthesis of **3**–**5**, were not commercially available (Table 1). These reagents were thus synthesized according to literature procedures by reacting the appropriate phenol or thiophenol with chloroacetic acid or 3-chloropropionic acid in the presence of base (Scheme 3).[24,25]

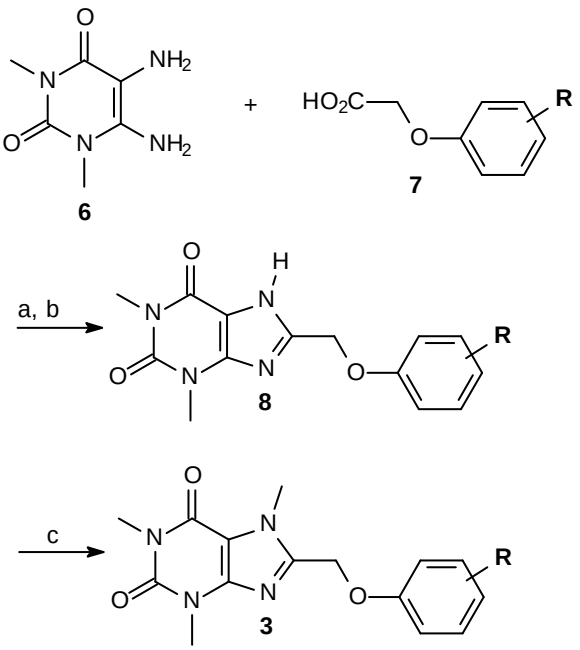

Scheme 1. Synthetic pathway to the 8-phenoxymethylcaffeine derivatives **3**. Reagents and conditions: (a) EDAC dioxane/H_2O, rt; (b) dioxane/NaOH (aq), reflux; (c) CH_3I, K_2CO_3, DMF, 90 °C.

Table 1. The structures of carboxylic acid derivatives 7, 9 and 10.

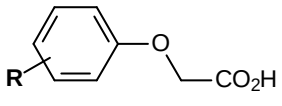

7

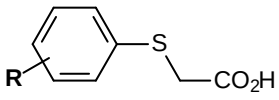

9

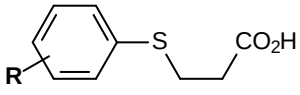

10

	R	mp (° C)	Lit. mp (° C)		R	mp (° C)	Lit. mp (° C)
7a	H	commercially available	(98–100)	**9c**	3-Br	90	86.8–87.6[c]
7b	3-Cl	108–109	108–110[a]	**9d**	3-F	74	73.5–74.2[c]
7c	3-Br	107–108	107–108.8[a]	**9e**	3-CH_3	70	66.8–67.4[c]
7d	3-F	114–115	111–112[a]	**9f**	3-OCH_3	72	62.3–63.5[c]
7e	3-CF_3	92–93	93.5–94.5[b]	**9g**	3-OCH_2CH_3	106	new compd.
7f	3-CH_3	101–105	102–103.5[a]	**9h**	4-Cl	107	107–108[c]
7g	3-OCH_3	117–118	111–118[a]	**9i**	4-Br	117	118–118.5[c]
7h	4-Cl	commercially available	(60–63)	**10a**	H	63	58.5–59.5[d]
7i	4-Br	commercially available	(149–153)	**10b**	3-Cl	83	77–78[e]
7j	4-F	commercially available	(104)	**10c**	3-Br	91	90–91[e]
9a	H	commercially available	(157)	**10d**	4-Cl	88	90–91[e]
9b	3-Cl	86	81.5–82.2[c]	**10e**	4-Br	116	114–115[e]

[a] Value obtained from ref.[37]

[b] Value obtained from ref.[38]

[c] Value obtained from ref.[41]

[d] Value obtained from ref. [40]

[e] Value obtained from ref.[39]

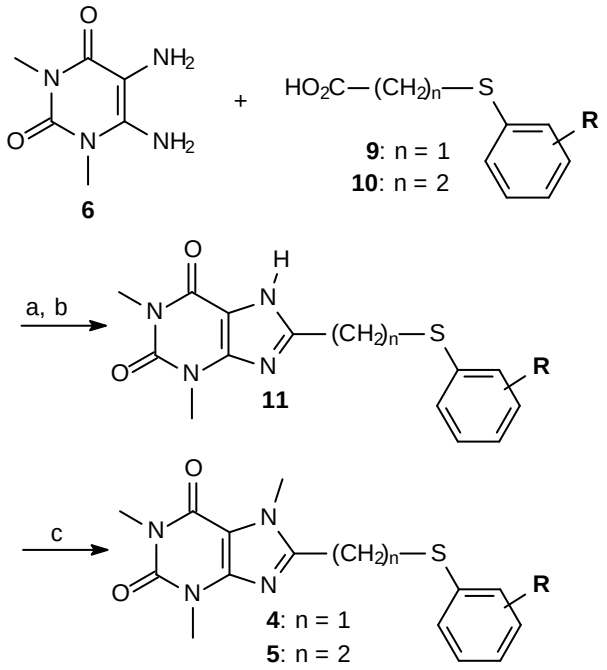

Scheme 2. Synthetic pathway to 8-[(phenylsulfanyl)methyl]caffeines (**4**) and 8-[(phenylsulfanyl)ethyl]caffeines (**5**). Reagents and conditions: (a) EDAC dioxane/H_2O, rt; (b) dioxane/NaOH (aq), reflux; (c) CH_3I, K_2CO_3, DMF, 90 °C.

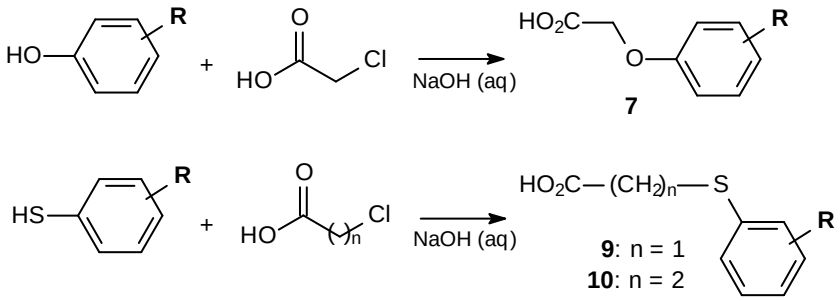

Scheme 3. Synthetic pathway to carboxylic acid derivatives **7**, **9** and **10**.

2.2. Inhibition studies

The inhibitory potencies of the caffeine derivatives, compounds **3**–**5**, towards MAO were examined by employing recombinant human MAO-A and –B as enzyme sources. Kynuramine, a MAO-A/B mixed substrate, served as substrate for the inhibition studies with both enzymes. The determination of MAO catalytic rates in the presence of compounds **4a**–**i** was accomplished by measuring the concentration of 4-hydroxyquinoline, the MAO catalyzed oxidation product of kynuramine, via fluorescence spectrophotometry.[26] 4-Hydroxyquinoline is a fluorescent compound which is readily measured in the presence of

the nonfluorescent kynuramine at excitation and emission wavelengths of 310 nm and 400 nm, respectively. Under these conditions, inhibitors **4a**–**i** do not fluoresce, or quench the fluorescence of 4-hydroxyquinoline. Analogous measurements of 4-hydroxyquinoline concentrations in the presence of inhibitors **3a**–**j** and **5a**–**e** were not possible since these inhibitors fluoresce under the conditions described above, and interfere with the fluorometric determination of 4-hydroxyquinoline at higher inhibitor concentrations. The determination of MAO catalytic rates in the presence of compounds **3a**–**j** and **5a**–**e** was accomplished by measuring the amount of hydrogen peroxide that is produced in the MAO oxidation cycle. In a horseradish peroxidase-coupled reaction, hydrogen peroxide reacts with Ampliflu Red to yield resorufin, a fluorescent compound.[27] Concentration measurement of resorufin may be readily made via fluorescence spectrophotometry at excitation and emission wavelengths of 560 nm and 590 nm, respectively. Under these conditions, inhibitors **3a**–**j** and **5a**–**e** do not fluoresce, or quench the fluorescence of resorufin. The MAO inhibition potencies of the inhibitors are expressed as the IC_{50} values which were estimated from sigmoidal curves of the rate of MAO catalysis versus the logarithm of the inhibitor concentration (Fig. 3).

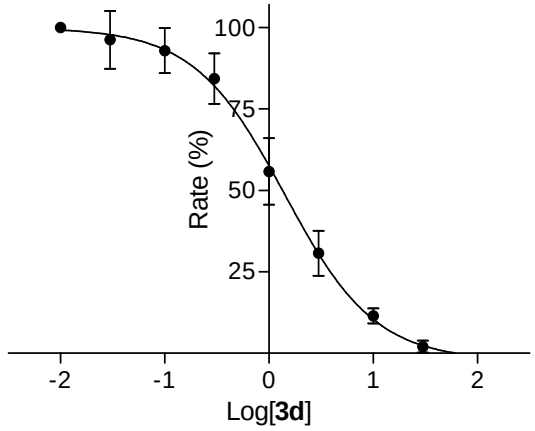

Figure 3. An example sigmoidal dose-response curve of the initial rate of oxidation of kynuramine by recombinant human recombinant human MAO-B vs. the logarithm of concentration of an inhibitor (expressed in μM). These determinations were carried out in duplicate and the values are expressed as the mean ± SD.

2.2.1. IC_{50} values for the inhibition of MAO-B

The MAO inhibition potencies of the caffeine derivatives, compounds **3**–**5**, are presented in tables 2–4. The results show that, among the compounds evaluated, the 8-phenoxymethylcaffeine derivatives, **3a**–**j**, are the most potent inhibitors of MAO-B with IC_{50}

values ranging from 0.148–5.78 μM. The weakest MAO-B inhibitor among the 8-phenoxymethylcaffeine derivatives is the unsubstituted derivative **3a** (IC_{50} = 5.78 μM). Substitution on the *meta* and *para* positions of the phenyl ring with both halogens (Cl, Br and F) and alkyl groups (CF_3, CH_3, OCH_3) leads to enhanced inhibition. With the exception of **3d**, the *meta* fluorine substituted homologue (IC_{50} = 1.61 μM), halogen containing substituents on the phenyl ring yields compounds with IC_{50} values in the submicromolar range. Bromine substitution on the *meta* (**3c**) and *para* (**3i**) positions was found to be particularly appropriate for MAO-B inhibition and yielded the most potent inhibitors of this study with IC_{50} values of 0.148 μM and 0.189 μM, respectively. These compounds are 30–39-fold more potent as MAO-B inhibitors than the unsubstituted homologue **3a**. Compared to halogen substitution, substitution on the *meta* position with the methyl (**3f**, IC_{50} = 1.23 μM) and methoxy (**3g**, IC_{50} = 1.96 μM) groups led to a modest enhancement of the MAO-B inhibition, with these compound being only 3–4-fold more potent than **3a**.

The results of the MAO inhibition studies with the 8-[(phenylsulfanyl)methyl]caffeine derivatives, **4a**–**i**, are presented in table 3. As shown, compounds **4a**–**i** were found to be relatively weak inhibitors of MAO-B with IC_{50} values ranging from 4.05–23.4 μM. As observed as for the 8-phenoxymethylcaffeine derivatives, the unsubstituted homologue, compound **4a** (IC_{50} = 23.4 μM) was the weakest MAO-B inhibitor of this series, and substitution on the *meta* and *para* positions of the phenyl ring leads to enhanced inhibition. Also similar to the results obtained with the 8-phenoxymethylcaffeine derivatives, *meta* (**4c**) and *para* (**4i**) substitution with bromine yielded the most potent MAO-B inhibitors of this series with IC_{50} values of 4.90 μM and 4.05 μM, respectively. Compared to the bromine substituted 8-phenoxymethylcaffeines (**3c** and **3i**), compounds **4c** and **4i** are, however, 21–33-fold weaker as MAO-B inhibitors. This observation leads to the conclusion that phenoxymethylcaffeines are better suited as lead compounds for the design of MAO-B inhibitors than 8-[(phenylsulfanyl)methyl]caffeines. To explore the possibility of improving the MAO inhibition properties of **4a**–**i**, a series of 8-[(phenylsulfanyl)ethyl]caffeine derivatives, **5a**–**e**, were examined as MAO inhibitors. As shown in table 4, compounds **5a**–**e** proved to be weak MAO-B inhibitors, in most instances weaker than the corresponding 8-[(phenylsulfanyl)methyl]caffeine derivatives (**4**). It may thus be concluded that extending the C8 side chain of 8-[(phenylsulfanyl)methyl]caffeine derivatives does not improve their MAO-B inhibitory potencies.

Table 2. The IC_{50} values for the inhibition of recombinant human MAO-A and –B by compounds **3a**–**j**.

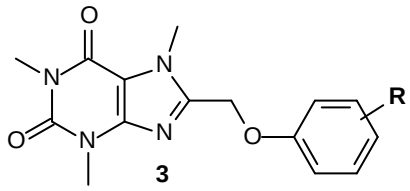

3

		IC_{50} (μM)[a,b]		
	R	MAO-A	MAO-B	SIc
3a	H	21.1 ± 3.23	5.78 ± 0.935	4
3b	3-Cl	No inhibition	0.334 ± 0.010	–
3c	3-Br	34.0 ± 31.5[d]	0.148 ± 0.002	230
3d	3-F	13.2 ± 7.74	1.61 ± 0.723	8
3e	3-CF_3	4.59 ± 1.06	0.641 ± 0.010	7
3f	3-CH_3	18.8 ± 1.52	1.23 ± 0.088	15
3g	3-OCH_3	No inhibition	1.96 ± 0.065	–
3h	4-Cl	20.4 ± 7.27	0.250 ± 0.040	82
3i	4-Br	10.7 ± 2.89	0.189 ± 0.018	57
3j	4-F	8.22 ± 0.336	0.825 ± 0.044	10

[a] All values are expressed as the mean ± SD of duplicate determinations.

[b] The horseradish peroxidase-coupled reaction with Ampliflu Red was used to measure MAO activities.

[c] The selectivity index is the selectivity for the MAO-B isoform and is given as the ratio of IC_{50}(MAO-A)/IC_{50}(MAO-B).

[d] Limited solubility restricts the determination of an accurate IC_{50} value.

Table 3. The IC_{50} values for the inhibition of recombinant human MAO-A and –B by compounds **4a**–**i**.

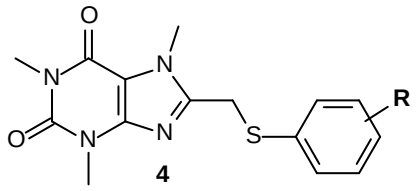

4

		IC_{50} (μM)[a,b]		
	R	MAO-A	MAO-B	SIc
4a	H	66.2± 5.32	23.4 ± 9.83	3
4b	3-Cl	19.4 ± 0.35	6.12 ± 0.45	3
4c	3-Br	23.8 ± 0.95	4.90 ± 1.04	5
4d	3-F	50.1 ± 1.84	22.3 ± 3.82	2
4e	3-CH_3	51.8 ± 4.20	17.9 ± 0.99	3
4f	3-OCH_3	41.3 ± 2.56	8.42 ± 0.10	5
4g	3-OCH_2CH_3	44.7 ± 2.29	18.4 ± 0.70	2
4h	4-Cl	31.6 ± 0.54	6.91 ± 0.65	5
4i	4-Br	20.8 ± 1.62	4.05 ± 0.77	5

[a] All values are expressed as the mean ± SD of triplicate determinations.

[b] MAO activities were determined by measuring 4-hydroxyquinoline formation via fluorescence spectrophotometry.

[c] The selectivity index is the selectivity for the MAO-B isoform and is given as the ratio of IC_{50}(MAO-A)/IC_{50}(MAO-B).

Table 4. The IC_{50} values for the inhibition of recombinant human MAO-A and –B by compounds **5a**–**e**.

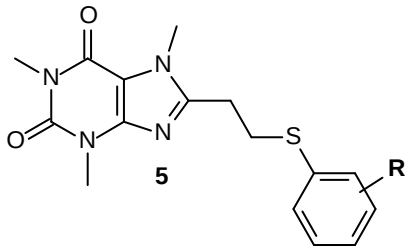

5

		IC_{50} (μM)[a,b]		
	R	MAO-A	MAO-B	SI[c]
5a	H	139 ± 8.82	108 ± 32.7	1.3
5b	3-Cl	No inhibition	5.67 ± 3.55	–
5c	3-Br	372 ± 121	64.1 ± 9.73	6
5d	4-Cl	142 ± 40.6	7.79 ± 0.66	18
5e	4-Br	117 ± 13.7	124 ± 14.2	0.9

[a] All values are expressed as the mean ± SD of triplicate determinations.

[b] The horseradish peroxidase-coupled reaction with Ampliflu Red was used to measure MAO activities.

[c] The selectivity index is the selectivity for the MAO-B isoform and is given as the ratio of IC_{50}(MAO-A)/IC_{50}(MAO-B).

2.2.2. IC_{50} values for the inhibition of MAO-A

As shown in table 2, the 8-phenoxymethylcaffeine derivatives, **3a**–**j**, were relatively weak inhibitors of MAO-A, with the most potent inhibitor, compound **3e**, exhibiting an IC_{50} value of 4.59 μM. All of the 8-phenoxymethylcaffeine derivatives were, however, selective for the MAO-B isoform with selectivity indices ranging from 4–230. The most selective inhibitor, compound **3c**, also is the most potent MAO-B inhibitor of the compounds investigated. It may thus be concluded that **3c** represents a potent MAO-B selective inhibitor. The 8-[(phenylsulfanyl)methyl]caffeine (**4a**–**i**) and 8-[(phenylsulfanyl)ethyl]caffeine (**5a**–**e**) derivatives were similarly found to be weak MAO-A inhibitors with the most potent homologue, compound **4b**, exhibiting an IC_{50} value of 19.4 μM. Interestingly, **5b** exhibited no MAO-A inhibition, thus making it a highly selective MAO-B inhibitor. This structure may therefore serve as a lead in design studies where absolute selectivity is required.

2.2.3. Reversibility of MAO inhibition

Caffeine derived MAO inhibitors have been shown to interact reversibly with the MAO enzymes.[28] This is a desirable property since de novo synthesis is not required for the recovery of enzyme activity. Enzyme activity is recovered when the inhibitor is cleared from the tissues. Since the 8-phenoxymethylcaffeines may represent a promising new class of MAO inhibitors, this study verified that they interact reversibly with MAO-A and –B. For this purpose the time-dependence of MAO inhibition by 2 selected inhibitors was examined. Compounds **3e** and **3c** were selected as representative inhibitors since they were found to be the most potent inhibitors of MAO-A and –B, respectively, among the 8-phenoxymethylcaffeines. These inhibitors were preincubated with MAO-A or –B for time periods of 0, 15, 30 and 60 min. These preincubations were conducted at inhibitor concentrations of approximately twofold their measured IC_{50} values for the inhibition of the respective MAO enzymes. Following these preincubations the reactions were diluted twofold, to yield inhibitor concentrations equal to their IC_{50} values, and the residual MAO catalytic activities were measured. The results of these reversibility studies are shown in Figure 4. When **3e** and **3c** were preincubated with MAO-A and –B, respectively, no time-dependent reductions of the catalytic activities occurred, even following a period of 60 min preincubation with the enzyme. These data are consistent with a reversible interaction of **3e** and **3c** with MAO-A and –B, respectively.

To provide further evidence for the reversible interaction of 8-phenoxymethylcaffeines with MAO, Lineweaver–Burk plots were constructed for the inhibition of MAO-B by compound **3c**. The MAO-B catalytic rates were measured in the absence of inhibitor, and presence of three different concentrations of **3c**. These measurements were carried out using four different concentrations of the substrate, kynuramine (15–90 μM). A set of 4 Lineweaver–Burk plots were constructed from these experiments and is given in Figure 5. The results show that the Lineweaver–Burk plots are linear and intersect at the y-axis. This indicates that the inhibition of MAO-B by **3c** is competitive, and is further support that **3c** is a reversible MAO-B inhibitor.

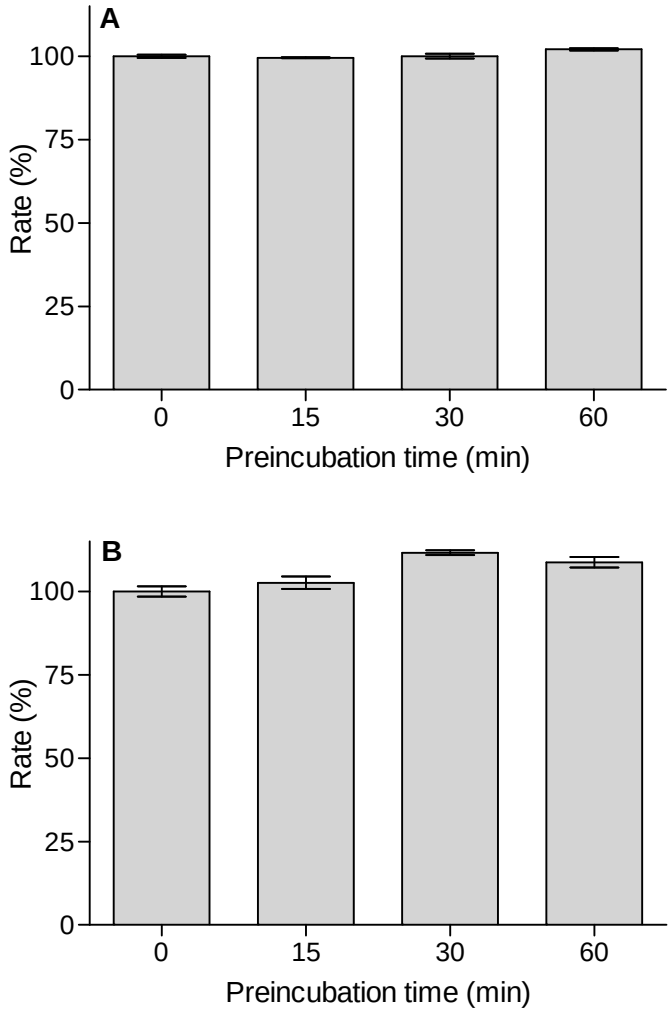

Figure 4. Time-dependant inhibition of recombinant human MAO-A (Panel A) and recombinant human MAO-B (Panel B) by **3e** and **3c**, respectively. The enzymes were preincubated for various periods of time (0–60 min) with **3e** (MAO-A) and **3c** (MAO-B) at inhibitor concentrations of 9.7 μM and 0.3 μM, respectively.

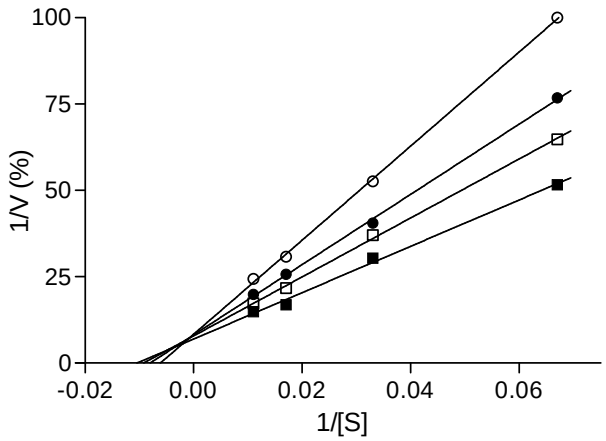

Figure 5. Lineweaver-Burk plots of the recombinant human MAO-B catalyzed oxidation of kynuramine in the absence (filled squares) and presence of various concentrations of **3c**. The concentrations employed for **3c** were 0.0375 μM (open squares), 0.075 μM (filled circles), 0.15 μM (open circles).

2.2.4. Modelling studies

The results of the MAO inhibition studies have shown that **3c** acts as a potent MAO-B inhibitor while its sulfanyl homologue, compound **4c**, is approximately 33-fold less potent as an MAO-B inhibitor. Also, **3c** is a highly selective inhibitor of MAO-B, with a 230-fold selectivity over the MAO-A isoform. To provide additional insight, possible binding orientations of **3c** and **4c** within the MAO active sites were explored. For this purpose, molecular docking with the CDOCKER module of Discovery Studio 3.1 (Accelrys)[29] was carried out. The crystallographic structures of human MAO-A cocrystallized with harmine (PDB entry: 2Z5X)[30] and human MAO-B cocrystallized with 7-(3-chlorobenzyloxy)-4-formylcoumarin (PDB entry: 2V60)[31] served as protein models. These protein models and docking protocol have previously been shown to be appropriate for predicting binding orientations of ligands in the active sites of MAO-A and –B.[32]

The highest ranked solution of **3c** within the MAO-B active site is illustrated in Figure 6. The orientations of the ten best solutions differed by less than 0.08 Å from the highest ranked solution. As shown, the caffeine ring of the inhibitor binds within the substrate cavity of the enzyme, in proximity to the FAD cofactor. In the space directly in front of the FAD cofactor, which is considered to be the polar part of the active site, the C6 carbonyl oxygen of the caffeine ring undergoes potential hydrogen bonding with the phenolic hydrogen of Tyr-435 and a water molecule. Furthermore, the caffeine ring is orientated approximately parallel to the phenyl rings of Tyr-435 and Tyr-398, an orientation that is restricted by the flat shape of

the substrate cavity. This places the caffeine ring within π–π interaction distance to Tyr-398. The C8 phenoxymethyl side chain of **3c** extends into the entrance cavity of MAO-B. Since the entrance cavity constitutes a highly hydrophobic environment, the C8 substituents are expected to be stabilized principally by Van der Waals interactions within this space.[33] An analysis of the interaction energies suggests particular favorable Van der Waals interactions with Ile-199 and Leu-171. Figure 7 illustrates the highest ranked solution of **4c** within the MAO-B active site. In this instance, the orientations of the ten best solutions differed by less than 0.07 Å from the highest ranked solution. Compound **4c** exhibits a similar orientation with respect to the placement of the caffeine ring and C8 side chain to that observed for **3c**. The most notable difference, however, is that the polar functional groups of the caffeine ring of **4c** are not placed within hydrogen bond interaction distance to residues and waters in the substrate cavity. Calculation of the interaction energies show that an unfavorable interaction may exist between the thioether sulfur of **4c** and Tyr-326. This interaction is most likely due to close contact between these moieties. This unfavorable interaction with Tyr-326 and the loss of potential hydrogen bonding may explain the reduced binding affinity of **4c** for the MAO-B active site compared **3c**.

The highest ranked docking orientation of **3c** within the MAO-A active site is presented in Figure 8. Similar to its orientation in MAO-B, compound **3c** binds with the caffeine ring in the proximity of the FAD cofactor while the C8 phenoxymethyl side chain extends towards the entrance of the MAO-A active site. The inhibitor may undergo π–π and π–σ interactions with Tyr-407 and Phe-208, respectively, as well as hydrogen bonding with an active site water molecule. The most notable difference between the binding orientations of **3c** in MAO-A and –B is that, in MAO-A, **3c** binds in a folded conformation, while exhibiting an extended conformation in the MAO-B active site. The folded conformation observed in the MAO-A active site is, to a large degree, imposed by the bulk of the phenyl side chain of Phe-208. This residue may impede the binding of relatively large inhibitors in the MAO-A active site, and, in order to avoid structural overlap with Phe-208, larger inhibitors adopt a folded conformation. In the MAO-B active site, the residue occupying the analogous position to Phe-208 is Ile-199. The side chain of Ile-199, which is comparatively smaller compared to the phenyl ring of Phe-208, is able to rotate from the MAO-B active site cavity, which enables larger inhibitors to bind in an extended conformation in MAO-B.[16] An analysis of the interaction energies suggests that the binding orientation of **3c** in MAO-A imposes an unfavorable interaction between the N7 methyl group of the inhibitor and the side chain of Asn-181. Since the extended conformation results in no unfavorable interactions with the MAO-B active site, the ability of **3c** to bind in an extended conformation to MAO-B may explain its higher binding affinity for MAO-B. Also, the extended conformation may allow for

more and improved productive interactions between the inhibitor and enzyme than the folded inhibitor conformation.

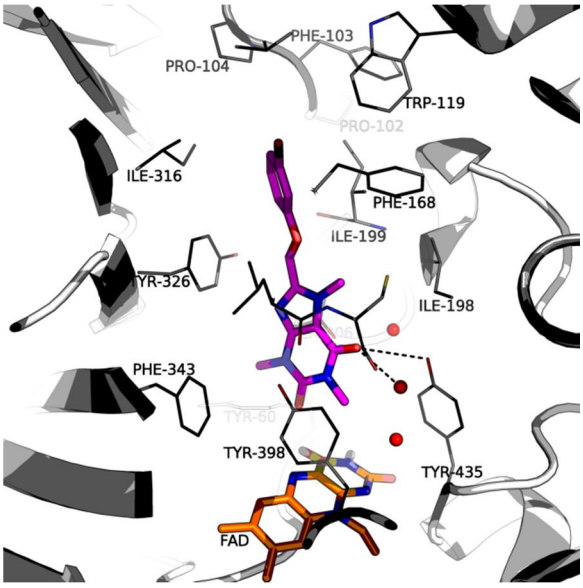

Figure 6. The predicted binding orientation of **3c** within the MAO-B active site.

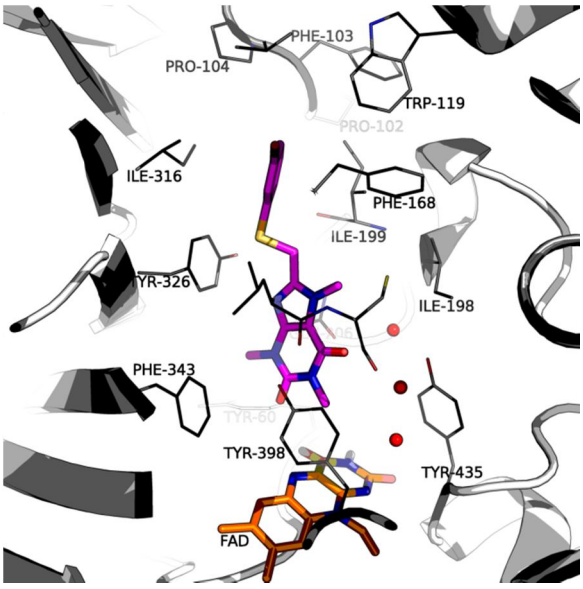

Figure 7. The predicted binding orientation of **4c** within the MAO-B active site.

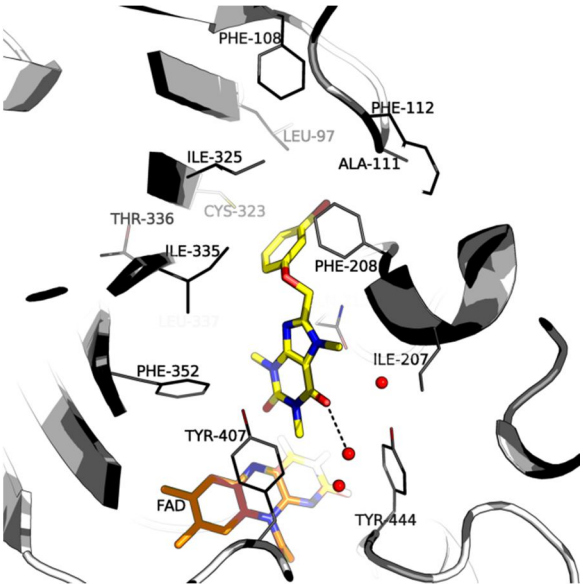

Figure 8. The predicted binding orientation of **3c** within the MAO-A active site.

3. Discussion and conclusion

The present study examines the possibility that series of 8-phenoxymethylcaffeine (**3**) and 8-[(phenylsulfanyl)methyl]caffeine (**4** and **5**) derivatives may act as inhibitors of human MAO. The results demonstrate that the 8-phenoxymethylcaffeines are the most active MAO inhibitors, with 6 compounds exhibiting IC_{50} values in the submicromolar range. The most potent inhibitor, compound **3c**, was also shown to interact reversible and competitively with MAO-B. In contrast, the phenylsulfanyl derivatives **4** and **5** proved to be comparatively weak MAO-B inhibitors. Modelling studies suggest that, while homologues **3c** and **4c** exhibit similar binding orientations in the MAO-B active site, an unfavorable Van der Waals interaction between the thioether sulfur of **4c** and Tyr-326 may explain, in part, the low MAO-B inhibition potency of this inhibitor compared to **3c**. It may therefore be concluded that the 8-phenoxymethylcaffeines, particularly compound **3c**, represent promising lead compounds for the development of reversible MAO-B selective inhibitors. The results obtained with compounds **4** and **5** show that differing substitution on the phenyl ring and modification of the linker between the caffeine and phenyl ring do not improve the MAO inhibitory properties of the 8-[(phenylsulfanyl)methyl]caffeines. Considering these results, it is apparent that 8-[(phenylsulfanyl)methyl]caffeines are not suitable leads for the design of MAO-B inhibitors, and minor structural modifications would not lead to improved inhibitory properties.

Compared with the previously reported 8-benzyloxycaffeines (**1**)[19] the 8-phenoxymethylcaffeines **3** are, however, weaker MAO-B inhibitors. For example, 8-(3-bromobenzyloxy)caffeine, the benzyloxycaffeine homologue of **3c**, inhibits human MAO-B

with an IC_{50} value of 0.068 μM, which is approximately twofold more potent than the inhibition potency of **3c**. This result suggests that, the placement of the ether oxygen in the C8 side chain of caffeine derived inhibitors is an important consideration in the design of MAO-B inhibitors. When comparing the MAO-B inhibition potencies of previously reported 8-(benzylsulfanyl)caffeines (**2**)[20] with the potencies of the 8-[(phenylsulfanyl)methyl]caffeine derivatives **4**, a similar conclusion may be drawn. For example, 8-(benzylsulfanyl)caffeines inhibit human MAO-B with an IC_{50} values as low as 0.167 μM, while the most potent 8-[(phenylsulfanyl)methyl]caffeine derivative examined here, compound **4i**, inhibits MAO-B with an IC_{50} values of 4.05 μM. Therefore, the position of the thioether sulfur in the C8 side chain of caffeine derived inhibitors also has large effects on the MAO-B inhibition potencies. These results demonstrate that, when a heteroatom is introduced into the C8 side chain of caffeine derived structures, substitution directly on C8 of the caffeine ring is likely to lead to the most potent MAO-B inhibition.

Interestingly, compared to the previously reported 8-benzyloxycaffeines (**1**) the 8-phenoxymethylcaffeine (**3**) exhibited weak inhibition potencies towards MAO-A. As mentioned in the Introduction, the ability of 8-benzyloxycaffeines to bind within the MAO-A active site may be attributed to the relatively large degree of rotational freedom of the C8 side chain at the carbon-oxygen ether bond.[19] This rotational freedom presumably enables the inhibitor to adopt the folded conformation required for binding to MAO-A. Although, the 8-phenoxymethylcaffeines also contain a carbon-oxygen ether bond in the C8 side chain, they exhibit weak binding to the MAO-A active site. The position of the ether oxygen in the C8 side chain of caffeine derived inhibitors therefore, in part, determines the affinities of these inhibitor for MAO-A. One potential reason for this observation is that the placement of the ether oxygen distal from the caffeine ring does not allow for the correct measure of flexibility of the C8 side chain for the inhibitor to be accommodated well in the MAO-A binding site. This reduced/modified degree of flexibility may, in part, be accounted for by differences in the resonance of the phenoxy and the oxycaffeinyl systems.

4. Experimental section

4.1. Chemicals and instrumentation

Unless otherwise noted, all starting materials were obtained from Sigma-Aldrich and were used without further purification. 1,3-Dimethyl-5,6-diaminouracil (**6**) was prepared according to the literature procedure.[23] Proton (^{1}H) and carbon (^{13}C) NMR spectra were recorded on a Bruker Avance III 600 spectrometer at frequencies of 600 MHz and 150 MHz, respectively. All NMR measurements were conducted in $CDCl_3$ and the chemical shifts are reported in parts per million (δ) downfield from the signal of tetramethylsilane. Spin multiplicities are

given as s (singlet), brs (broad singlet), d (doublet), dd (doublet of doublets), t (triplet), q (quartet) or m (multiplet). High resolution mass spectra (HRMS) were obtained on a DFS high resolution magnetic sector mass spectrometer (Thermo Electron Corporation) in electron ionization (EI) mode. Melting points (mp) were determined on a Buchi M-545 melting point apparatus and are uncorrected. For fluorescence spectrophotometry, a Varian Cary Eclipse fluorescence spectrophotometer was employed. The following chemical and biological agents were obtained from Sigma-Aldrich: microsomes from insect cells containing recombinant human MAO-A or MAO–B (5 mg/mL), kynuramine.2HBr, Ampliflu Red (10-Acetyl-3,7-dihydroxyphenoxazine), horseradish peroxidase, (R)-deprenyl.HCl, clorgyline.HCl and H_2O_2 (3%).

4.2. Synthesis of 8-phenoxymethylcaffeine derivatives (3a–j)

The syntheses of **3a**–**j** were accomplished using the literature procedure.[22] 1,3-Dimethyl-5,6-diaminouracil[23] (4 mmol) and N-(3-dimethylaminopropyl)-N′-ethylcarbodiimide hydrochloride (EDAC; 5.36 mmol) were dissolved in 42 mL dioxane/H_2O (1:1) and the appropriate phenoxyacetic acid (4 mmol) was added. A thick suspension was obtained and the pH was adjusted to 5–6 with 4 N aqueous HCl. The reaction was stirred for 2 h at room temperature and neutralized with aqueous NaOH (1 N). The precipitate was collected by filtration and subsequently dissolved in 40 mL dioxane/H_2O (1:1). The reaction was heated under reflux for 2 h, cooled to 0 °C and acidified to a pH of 4 with 4 N aqueous HCl. The resulting precipitate, the corresponding 1,3-dimethyl-8-substituted-7*H*-xanthinyl analogue, was collected by filtration, washed with 50 mL H_2O and dried at 50 °C. The 7*H*-xanthinyl analogue was used in the subsequent reaction without further purification. The corresponding 1,3-dimethyl-8-substituted-7*H*-xanthinyl analogue (2 mmol) was dissolved in a minimum amount of DMF (approximately 20 mL) at 90 °C. K_2CO_3 (5 mmol), followed by iodomethane (4 mmol) were added, and the reaction mixture was stirred at 90 °C for 1 h. The reaction progress was followed with TLC employing neutral alumina sheets and ethyl acetate/dichloromethane (1:1) as mobile phase. The insoluble materials were removed by filtration. H_2O (350 ml) was added to the filtrate and the mixture was cooled on ice for 3 hours. The precipitate that formed was collected by filtration and dried overnight at room temperature. The products were recrystallized from methanol/ethyl acetate (7:5).

4.2.1. 8-Phenoxymethylcaffeine (3a)

The title compound was prepared from phenoxyacetic acid in a yield of 73%: mp 197–199 °C (methanol/ethyl acetate 7:5). ^{1}H NMR ($CDCl_3$) δ 3.37 (s, 3H), 3.56 (s, 3H), 4.03 (s, 3H),

5.17 (s, 2H), 6.99 (m, 3H), 7.29 (t, 2H, J = 7.53 Hz); ^{13}C NMR ($CDCl_3$) δ 27.9, 29.7, 32.4, 62.0, 108.7, 114.6, 122.0, 129.7, 147.4, 147.9, 151.6, 155.4, 157.5; EIMS 300; EI-HRMS *m*/*z*: calcd for $C_{15}H_{16}O_3N_4$, 300.1222, found 300.1218.

4.2.2. 8-(3-Chlorophenoxymethyl)caffeine (3b)

The title compound was prepared from 3-chlorophenoxyacetic acid in a yield of 83%: mp 201–203 °C (methanol/ethyl acetate 7:5). ^{1}H NMR ($CDCl_3$) δ 3.38 (s, 3H), 3.56 (s, 3H), 4.02 (s, 3H), 5.15 (s, 2H), 6.87 (dd, 1H, J = 2.6, 8.3 Hz), 6.97 (m, 1H), 7.01 (t, 1H, J = 2.3 Hz), 7.20 (t, 1H, J = 8.3 Hz); ^{13}C NMR ($CDCl_3$) δ 27.9, 29.7, 32.4, 62.1, 108.8, 113.0, 115.4, 122.3, 130.5, 135.1, 147.2, 147.4, 151.5, 155.4, 158.2; EI-HRMS *m*/*z*: calcd for $C_{15}H_{15}O_3N_4Cl$, 334.0833, found 334.0843.

4.2.3. 8-(3-Bromophenoxymethyl)caffeine (3c)

The title compound was prepared from 3-bromophenoxyacetic acid in a yield of 78%: mp 200–204 °C (methanol/ethyl acetate 7:5). ^{1}H NMR ($CDCl_3$) δ 3.36 (s, 3H), 3.55 (s, 3H), 4.01 (s, 3H), 5.14 (s, 2H), 6.91 (d, 1H, J = 7.5 Hz), 7.12 (m, 3H); ^{13}C NMR ($CDCl_3$) δ 28.0, 29.7, 32.4, 62.1, 108.8, 113.5, 118.2, 123.0, 125.2, 130.8, 147.2, 147.4, 151.5, 155.4, 158.2; EI-HRMS *m*/*z*: calcd for $C_{15}H_{15}O_3N_4Br$, 378.0328, found 378.0301.

4.2.4. 8-(3-Fluorophenoxymethyl)caffeine (3d)

The title compound was prepared from 3-fluorophenoxyacetic acid in a yield of 67%: mp 198–201 °C (methanol/ethyl acetate 7:5). ^{1}H NMR ($CDCl_3$) δ 3.36 (s, 3H), 3.55 (s, 3H), 4.02 (s, 3H), 5.15 (s, 2H), 6.71 (m, 2H), 6.76 (dd, 1H, J = 2.3, 8.3 Hz), 7.22 (m, 1H); ^{13}C NMR ($CDCl_3$) δ 28.0, 29.7, 32.4, 62.2, 102.7 (d), 108.8, 108.9 (d), 110.3 (d), 130.5 (d), 147.3 (d), 151.6, 155.4, 158.7 (d), 162.7, 164.3; EI-HRMS *m*/*z*: calcd for $C_{15}H_{15}O_3N_4F$, 318.1128, found 318.1131.

4.2.5. 8-[3-(Trifluoromethyl)phenoxymethyl]caffeine (3e)

The title compound was prepared from 2-[3-(trifluoromethyl)phenoxy]acetic acid in a yield of 52%: mp 172–174 °C (methanol/ethyl acetate 7:5). ^{1}H NMR ($CDCl_3$) δ 3.38 (s, 3H), 3.56 (s, 3H), 4.04 (s, 3H), 5.22 (s, 2H), 7.17 (m, 1H), 7.25 (d, 1H, J = 7.5 Hz), 7.29 (s, 1H), 7.40 (t, 1H, J = 8.3 Hz); ^{13}C NMR ($CDCl_3$) δ 28.0, 29.7, 32.4, 62.1, 108.8, 111.7 (q), 118.2, 118.7 (q), 122.8, 124.6, 130.3, 132.2 (q), 147.0, 147.4, 151.5, 155.4, 157.6; EI-HRMS *m*/*z*: calcd for $C_{16}H_{15}O_3N_4F_3$, 368.1096, found 368.1081.

4.2.6. 8-(3-Methylphenoxymethyl)caffeine (3f)

The title compound was prepared from 3-methylphenoxyacetic acid in a yield of 72%: mp 195–196 °C (methanol/ethyl acetate 7:5). ^{1}H NMR ($CDCl_3$) ^{1}H NMR (Bruker Avance III 600, $CDCl_3$) δ 2.30 (s, 3H), 3.70 (s, 3H), 3.55 (s, 3H), 4.02 (s, 3H), 5.14 (s, 2H), 6.80 (m, 3H), 7.16 (t, 1H, J = 8.3 Hz); ^{13}C NMR ($CDCl_3$) δ 21.4, 27.9, 29.7, 32.4, 61.9, 108.7, 111.3, 115.5, 122.8, 129.4, 139.8, 147.3, 148.0, 151.5, 155.4, 157.5; EI-HRMS *m*/*z*: calcd for $C_{16}H_{18}O_3N_4$, 314.1379, found 314.1386.

4.2.7. 8-(3-Methoxyphenoxymethyl)caffeine (3g)

The title compound was prepared from 3-methoxyphenoxyacetic acid in a yield of 36%: mp 165–167 °C (methanol/ethyl acetate 7:5). ^{1}H NMR ($CDCl_3$) δ 3.36 (s, 3H), 3.54 (s, 3H), 3.75 (s, 3H), 4.01 (s, 3H), 5.14 (s, 2H), 6.53 (m, 2H), 6.56 (m, 1H), 7.17 (t, 1H, J = 8.7 Hz); ^{13}C NMR ($CDCl_3$) δ 27.9, 29.7, 32.4, 55.3, 62.0, 101.2, 106.6, 107.5, 108.7, 130.1, 147.3, 147.8, 151.5, 155.4, 158.7, 160.9; EI-HRMS *m*/*z*: calcd for $C_{16}H_{18}O_4N_4$, 330.1328, found 330.1320.

4.2.8. 8-(4-Chlorophenoxymethyl)caffeine (3h)

The title compound was prepared from 4-chlorophenoxyacetic acid in a yield of 52%: mp 181–183 °C (methanol/ethyl acetate 7:5). ^{1}H NMR ($CDCl_3$) δ 3.36 (s, 3H), 3.54 (s, 3H), 4.01 (s, 3H), 5.13 (s, 2H), 6.91 (d, 2H, J = 8.7 Hz), 7.22 (d, 2H, J = 8.7 Hz); ^{13}C NMR ($CDCl_3$) δ 27.9, 29.7, 32.4, 62.2, 108.7, 116.0, 127.0, 129.6, 147.3, 147.4, 151.5, 155.4, 156.0; EI-HRMS *m*/*z*: calcd for $C_{15}H_{15}O_3N_4Cl$, 334.0833, found 334.0838.

4.2.9. 8-(4-Bromophenoxymethyl)caffeine (3i)

The title compound was prepared from 4-bromophenoxyacetic acid in a yield of 80%: mp 195–197 °C (methanol/ethyl acetate 7:5). ^{1}H NMR ($CDCl_3$) δ 3.35 (s, 3H), 3.53 (s, 3H), 4.00 (s, 3H), 5.13 (s, 2H), 6.86 (d, 2H, J = 9.0 Hz), 7.35 (d, 2H, J = 9.0 Hz); ^{13}C NMR ($CDCl_3$) δ 27.9, 29.7, 32.4, 62.1, 108.7, 114.3, 116.4, 132.5, 147.3, 151.5, 155.3, 156.5; EI-HRMS *m*/*z*: calcd for $C_{15}H_{15}O_3N_4Br$, 378.0328, found 378.0317.

4.2.10. 8-(4-Fluorophenoxymethyl)caffeine (3j)

The title compound was prepared from 4-fluorophenoxyacetic acid in a yield of 79%: mp 212–213 °C (methanol/ethyl acetate 7:5). ^{1}H NMR ($CDCl_3$) δ 3.37 (s, 3H), 3.55 (s, 3H), 4.02 (s, 3H), 5.13 (s, 2H), 6.94 (m, 4H); ^{13}C NMR ($CDCl_3$) δ 27.9, 29.7, 32.4, 62.6, 108.7, 115.8, 115.9, 116.0, 116.2, 147.3, 147.6, 151.5, 153.6, 155.4, 157.1, 158.7; EI-HRMS *m*/*z*: calcd for $C_{15}H_{15}O_3N_4F$, 318.1128, found 318.1114.

4.3. Synthesis of 8-[(phenylsulfanyl)methyl]caffeine (4a–i)

Compounds **4a**–**i** were synthesized from 1,3-dimethyl-5,6-diaminouracil[23] and an appropriate 2-(phenylsulfanyl)acetic acid according to the procedure described above for the syntheses of **3a**–**j**.[22]

4.3.1. 8-[(Phenylsulfanyl)methyl]caffeine (4a)

The title compound was prepared from 2-(phenylsulfanyl)acetic acid in a yield of 74%: mp 154–156 °C (methanol/ethylacetate 7:2). ^{1}H NMR ($CDCl_3$) δ 3.34 (s, 3H), 3.47 (s, 3H), 3.78 (s, 3H), 4.13 (s, 2H), 7.24 (m, 3H), 7.35 (m, 2H); ^{13}C NMR ($CDCl_3$) δ 27.8, 29.6, 30.8, 32.0, 107.9, 128.0, 129.1, 131.9, 133.3, 147.5, 149.4, 151.5, 155.2; EI-HRMS *m*/*z*: calcd for $C_{15}H_{16}N_4O_2S$, 316.0994, found 316.0988.

4.3.2. 8-{[(3-Chlorophenyl)sulfanyl]methyl}caffeine (4b)

The title compound was prepared from 2-[(3-chlorophenyl)sulfanyl]acetic acid in a yield of 56%: mp 174–177 °C (methanol/ethylacetate 7:2). ^{1}H NMR ($CDCl_3$) δ 3.35 (s, 3H), 3.49 (s, 3H), 3.90 (s, 3H), 4.17 (s, 2H), 7.19 (m, 2H), 7.23 (m, 1H), 7.41 (m, 1H); ^{13}C NMR ($CDCl_3$) δ 27.9, 29.6, 30.1, 32.1, 108.1, 127.7, 128.9, 130.1, 130.6, 134.7, 135.5, 147.4, 148.8, 151.5, 155.2; EI-HRMS *m*/*z*: calcd for $C_{15}H_{15}ClN_4O_2S$, 350.0604, found 350.0615.

4.3.3. 8-{[(3-Bromophenyl)sulfanyl]methyl}caffeine (4c)

The title compound was prepared from 2-[(3-bromophenyl)sulfanyl]acetic acid in a yield of 75%: mp 151–152 °C (methanol/ethylacetate 7:2). ^{1}H NMR ($CDCl_3$) δ, 3.35 (s, 3H), 3.49 (s, 3H), 3.89 (s, 3H), 4.16 (s, 2H), 7.12 (t, 1H, J = 7.9 Hz), 7.27 (m, 1H), 7.34 (m, 1H), 7.56 (m, 1H); ^{13}C NMR ($CDCl_3$) δ 27.9, 29.6, 30.1, 32.1, 108.1, 122.8, 129.4, 130.3, 130.6, 133.4, 135.8, 147.4, 148.8, 151.5, 155.2; EI-HRMS *m*/*z*: calcd for $C_{15}H_{15}BrN_4O_2S$, 394.0099, found 394.0100.

4.3.4. 8-{[(3-Flourophenyl)sulfanyl]methyl}caffeine (4d)

The title compound was prepared from 2-[(3-flourophenyl)sulfanyl]acetic acid in a yield of 30%: mp 155–156 °C (methanol/ethylacetate 7:2). ^{1}H NMR ($CDCl_3$) δ, 3.45 (s, 3H), 3.48 (s, 3H), 3.89 (s, 3H), 4.18 (s, 2H), 6.92 (m, 1H), 7.13 (m, 2H), 7.22 (m, 1H); ^{13}C NMR ($CDCl_3$) δ; 27.9, 29.6, 30.1, 32.1, 108.1, 114.5. 114.6, 117.5, 117.6, 126.3, 130.3, 130.4, 135.8, 135.9, 147.4, 148.8, 151.5, 155.2, 161.8, 163.4; EI-HRMS *m*/*z*: calcd for $C_{15}H_{15}FN_4O_2S$, 334.0900, found 334.0893.

4.3.5. 8-{[(3-Methylphenyl)sulfanyl]methyl}caffeine (4e)

The title compound was prepared from 2-[(3-methylphenyl)sulfanyl]acetic acid in a yield of 37%: mp 124–126°C (methanol/ethylacetate 7:2). ^{1}H NMR ($CDCl_3$) δ, 2.32 (s, 3H), 3.39 (s, 3H), 3.53 (s, 3H) 3.85 (s, 3H), 4.18 (s, 2H), 7.09 (brs, 1H), 7.19 (m, 2H), 7.24 (m, 1H); ^{13}C NMR ($CDCl_3$) δ; 21.2, 27.8, 29.6, 30.7, 32.0, 107.9, 128.6, 128.7, 128.9, 132.3, 133.1, 139.0, 147.5, 149.5, 151.5, 155.2; EI-HRMS *m*/*z*: calcd for $C_{16}H_{18}N_4O_2S$, 330.1150, found 330.1157.

4.3.6. 8-{[(3-Methoxyphenyl)sulfanyl]methyl}caffeine (4f)

The title compound was prepared from 2-[(3-methoxyphenyl)sulfanyl]acetic acid in a yield of 41%: mp 161–165 °C (methanol/ethylacetate 7:2). ^{1}H NMR ($CDCl_3$) δ; 3.36 (s, 3H), 3.50 (s, 3H), 3.75 (s, 3H), 3.84 (s, 3H), 4.16 (s, 2H), 6.78 (dd, 1H, J = 1.9, 7.9 Hz), 6.93 (m, 2H), 7.17 (t, 1H, J = 7.9 Hz); ^{13}C NMR ($CDCl_3$) δ; 27.9, 29.7, 30.5, 32.1, 55.3, 108.0, 113.6, 116.5, 123.3, 130.0, 134.8, 147.5, 149.4, 151.5, 155.2, 159.9; EI-HRMS *m*/*z*: calcd for $C_{16}H_{18}N_4O_3S$, 346.1100, found 346.1091.

4.3.7. 8-{[(3-Ethoxyphenyl)sulfanyl]methyl}caffeine (4g)

The title compound was prepared from 2-[(3-ethoxyphenyl)sulfanyl]acetic acid in a yield of 55%: mp 147–149 °C (methanol/ethylacetate 7:2). ^{1}H NMR ($CDCl_3$) δ 1.35 (t, 3H, J = 6.8 Hz), 3.34 (s, 3H), 3.48 (s, 3H), 3.82 (s, 3H), 3.95 (q, 2H, J = 6.8 Hz), 4.15 (s, 2H), 6.75 (d, 1H, J = 8.3 Hz), 6.91 (m, 2H), 7.14 (t, 1H, J = 7.5 Hz); ^{13}C NMR ($CDCl_3$) δ 14.7, 27.8, 29.6, 30.5, 32.0, 63.5, 108.0, 114.1, 117.1, 123.2, 129.9, 134.7, 147.5, 149.5, 151.5, 155.2, 159.2; EI-HRMS *m*/*z*: calcd for $C_{17}H_{20}N_4O_3S$, 360.1256, found 360.1261.

4.3.8. 8-{[(4-Chlorophenyl)sulfanyl]methyl}caffeine (4h)

The title compound was prepared from 2-[(4-chlorophenyl)sulfanyl]acetic acid in a yield of 59%: mp 149–150 °C (methanol/ethylacetate 7:2). ^{1}H NMR ($CDCl_3$) δ, 3.34 (s, 3H), 3.46 (s, 3H), 3.86 (s, 3H), 4.12 (s, 2H), 7.23 (d, 2H, J = 7.5 Hz), 7.29 (d, 2H, J = 7.5 Hz); ^{13}C NMR ($CDCl_3$) δ; 27.9, 29.6, 30.8, 32.1, 108.0, 129.3, 131.8, 133.0, 134.1, 147.4, 149.0, 151.4, 155.2; EI-HRMS *m*/*z*: calcd for $C_{15}H_{15}ClN_4O_2S$, 350.0604, found 350.0597.

4.3.9. 8-{[(4-Bromophenyl)sulfanyl]methyl}caffeine (4i)

The title compound was prepared from 2-[(4-bromophenyl)sulfanyl]acetic acid in a yield of 73%: mp 160–164 °C (methanol/ethylacetate 7:2). ^{1}H NMR ($CDCl_3$) δ, 3.39 (s, 3H), 3.51 (s, 3H), 3.92 (s, 3H), 4.17 (s, 2H), 7.27 (d, 2H, J = 7.5 Hz), 7.42 (d, 2H, J = 7.5 Hz); ^{13}C NMR

($CDCl_3$) *δ*; 27.9, 29.6, 30.6, 32.1, 108.0, 122.1, 132.2, 132.5, 133.0, 147.4, 149.0, 151.4, 155.2; EI-HRMS *m*/*z*: calcd for $C_{15}H_{15}BrN_4O_2S$, 394.0099, found 394.0092.

4.4. Synthesis of 8-[(phenylsulfanyl)ethyl]caffeine derivatives (5a–e)

Compounds **5a**–**e** were synthesized from 1,3-dimethyl-5,6-diaminouracil[23] and an appropriate 3-(phenylsulfanyl)propanoic acid according to the procedure described above for the syntheses of **3a**–**j**.[22]

4.4.1. 8-[(Phenylsulfanyl)ethyl]caffeine (5a)

The title compound was prepared from 3-(phenylsulfanyl)propanoic acid in a yield of 45%: mp 143–145 °C (methanol/ethylacetate 7:2). ^{1}H NMR ($CDCl_3$) *δ*, 3.00 (t, 2H, J = 7.2 Hz), 3.35 (s, 3H), 3.35 (t, 2H, J = 7.2 Hz), 3.50 (s, 3H), 3.79 (s, 3H), 7.15 (m, 1H), 7.24 (m, 2H), 7.31 (m, 2H); ^{13}C NMR ($CDCl_3$) *δ*; 26.9, 27.8, 29.6, 31.7, 31.8, 107.3, 126.6, 129.0, 129.7, 134.7, 147.9, 151.6, 151.9, 155.2; EI-HRMS *m*/*z*: calcd for $C_{16}H_{18}N_4O_2S$, 330.1150, found 330.1148.

4.4.2. 8-{[(3-Chlorophenyl)sulfanyl]ethyl}caffeine (5b)

The title compound was prepared from 3-[(3-chlorophenyl)sulfanyl]propanoic acid in a yield of 3%: mp 181–183 °C (methanol/ethylacetate 7:2). ^{1}H NMR ($CDCl_3$) *δ*, 3.04 (t, 2H, J = 6.8 Hz), 3.37 (s, 3H), 3.39 (t, 2H, J = 6.8 Hz); 3.52 (s, 3H), 3.84 (s, 3H), 7.12 (m, 1H), 7.18 (m, 2H); 7.24 (m, 1H); ^{13}C NMR ($CDCl_3$) *δ*; 26.9, 27.8, 29.7, 31.6, 31.8, 107.3, 126.5, 127.4, 128.7, 130.0, 134.7, 137.0, 147.8, 151.5, 155.2; EI-HRMS *m*/*z*: calcd for $C_{16}H_{17}ClN_4O_2S$, 364.0761, found 364.0743.

4.4.3. 8-{[(3-Bromophenyl)sulfanyl]ethyl}caffeine (5c)

The title compound was prepared from 3-[(3-bromophenyl)sulfanyl]propanoic acid 2-{[(3-bromophenyl)methyl]sulfanyl}acetic acid in a yield of 61%: mp 175–177 °C (methanol/ethylacetate 7:2). ^{1}H NMR ($CDCl_3$) *δ*, 2.90 (t, 2H, J = 6.4); 3.23 (s, 3H); 3.25 (t, 2H, J = 6.4 Hz); 3.38 (s, 3H), 3.70 (s, 3H), 6.97 (t, 1H, J = 7.5 Hz); 7.09 (d, 1H, J = 7.5 Hz); 7.13 (d, 1H, J = 6.8 Hz), 7.24 (s, 1H); ^{13}C NMR ($CDCl_3$) *δ*; 27.0, 27.8, 29.7, 31.7, 31.7, 107.3, 122.8, 127.9, 129.4, 130.2, 131.6, 137.3, 147.8, 151.5, 151.5, 155.1; EI-HRMS *m*/*z*: calcd for $C_{16}H_{17}BrN_4O_2S$, 408.0256, found 408.0255.

4.4.4. 8-{[(4-Chlorophenyl)sulfanyl]ethyl}caffeine (5d)

The title compound was prepared from 3-[(4-chlorophenyl)sulfanyl]propanoic acid in a yield of 23%: mp 148–150 °C (methanol/ethylacetate 7:2). ^{1}H NMR ($CDCl_3$) δ, 2.99 (t, 2H, J = 6.8 Hz); 3.34 (t, 2H, J = 6.8 Hz), 3.36 (s, 3H), 3.50 (s, 3H), 3.82 (s, 3H), 7.20 (d, 2H, J = 8.3 Hz); 7.23 (d, 2H, J = 8.3 Hz); ^{13}C NMR ($CDCl_3$) δ 26.9, 27.9, 29.6, 31.8, 32.1, 107.3, 129.1, 131.1, 132.7, 133.3, 147.9, 151.6, 151.6, 155.2; EI-HRMS *m*/*z*: calcd for $C_{16}H_{17}ClN_4O_2S$, 364.0761, found 364.0755.

4.4.5. 8-{[(4-Bromophenyl)sulfanyl]ethyl}caffeine (5e)

The title compound was prepared from 3-[(4-bromophenyl)sulfanyl]propanoic acid in a yield of 26%: mp 159–161 °C (methanol/ethylacetate 7:2). ^{1}H NMR ($CDCl_3$) δ, 3.00 (t, 2H, J = 6.8 Hz), 3.34 (t, 2H, J = 6.8 Hz), 3.35 (s, 3H), 3.49 (s, 3H), 3.81 (s, 3H), 7.15 (d, 2H, J = 8.3 Hz), 7.34 (d, 2H, J = 8.3 Hz); ^{13}C NMR ($CDCl_3$) δ 26.9, 27.8, 29.6, 31.7, 31.9, 107.2, 120.4, 131.2, 131.9, 133.9, 147.8, 151.5, 151.5, 155.2; EI-HRMS *m*/*z*: calcd for $C_{16}H_{17}BrN_4O_2S$, 408.0256, found 408.0255.

4.5. Synthesis of carboxylic acid derivatives (7, 9 and 10)

When not commercially available, the phenoxyacetic acids (**7**), 2-(phenylsulfanyl)acetic acids (**9**) and 3-(phenylsulfanyl)propanoic acids (**10**) required for the synthesis of **3**–**5** were synthesized according to literature procedures.[24,25] The experimentally determined as well as literature melting points of these acids are given in table 1. The physical data of compound **9g**, previously unknown, is given below.

*Phenoxyacetic acids (**7**)*: An appropriately substituted phenol (50 mmol) was added to a solution of NaOH (187.5 mmol) in 15 mL of H_2O. Chloroacetic acid (85 mmol) was added slowly at to the resulting solution at 40 °C and the reaction mixture was heated to 85 °C. Stirring was continued for 2 h, the reaction was cooled to room temperature and 100 mL H_2O was added. The reaction was filtered and the filtrate was acidified with concentrated HCl to pH 1–2. The brown oil fraction which formed was extracted to diethylether (2 × 50 ml). The ether fraction, in turn, was extracted with an aqueous solution of 5% Na_2CO_3 (2 × 37.5 ml). The combined Na_2CO_3 fractions were acidified to pH 1–2 with concentrated HCl and the resulting precipitate was collected by filtration and oven dried to obtain the required acids.[24]

*2-(Phenylsulfanyl)acetic acids (**9**) and 3-(phenylsulfanyl)propanoic acids (**10**)*: An appropriate thiophenol (10 mmol) was dissolved in ethanol (5 mL) and a solution of NaOH (10 mmol) in H_2O (3 mL) was added. In a separate flask, chloroacetic acid or 3-chloropropionic acid (11 mmol) was dissolved in H_2O (3 mL) and Na_2CO_3 (5.5 mmol) was added. The resulting solution was added to the thiophenol containing reaction and the reaction was allowed to stir

at room temperature for 3 h. The reaction was subsequently heated under reflux for 1 h, cooled to room temperature and acidified with 2 N HCl to pH 2. H_2O (25 mL) was added and the brown oil fraction was extracted to diethylether (50 mL). The ether fraction was extracted with an aqueous solution of 5% Na_2CO_3 (25 ml). The Na_2CO_3 fraction was acidified to pH 2 with concentrated HCl and the resulting precipitate was collected by filtration and oven dried to obtain the required acids.[25]

2-[(3-Ethoxyphenyl)sulfanyl]acetic acid (**9g**): Yield 85%: mp 106 °C. ^{1}H NMR ($CDCl_3$) δ 1.38 (t, 3H, J = 7.2 Hz), 3.37 (s, 2H), 3.99 (q, 2H, J = 7.2 Hz), 6.75 (dd, 1H, J = 2.3, 8.3 Hz), 6.92–6.95 (m, 2H), 7.17 (t, 1H, J = 8.3 Hz); ^{13}C NMR ($CDCl_3$) δ 14.7, 36.2, 63.5, 113.6, 115.5, 121.6, 130.0, 135.6, 159.3, 174.3.

4.6. Determination of IC_{50} values

Microsomes from baculovirus infected insect cells expressing either recombinant human MAO-A or MAO–B (5 mg/mL) were obtained from Sigma-Aldrich, pre-aliquoted and stored at –70 °C. All enzymatic reactions were carried out to a final volume of 500 µL in 2 mL microcentrifuge tubes. Potassium phosphate buffer (100 mM, pH 7.4, made isotonic with KCl) served as reaction solvent.

*IC_{50} measurements of **4a–i***: The reactions contained the MAO-A/B mixed substrate, kynuramine (45 µM and 30 µM for MAO-A and –B, respectively), and various concentrations of the test inhibitor (0.003–100 µM). Stock solutions of the test inhibitors were prepared in DMSO and added to the reactions to yield a final concentration equal to 4% (v/v) DMSO. The reactions were initiated with the addition of MAO-A or –B (0.0075 mg/mL) and incubated at 37 °C for 20 min in a water bath. The reactions were subsequently terminated with the addition of 400 µL NaOH (2 N). After the addition of distilled water (1000 µL), the concentrations of the MAO generated 4-hydroxyquinoline were measured by fluorescence spectrophotometry (λ_{ex} = 310 nm, λ_{em} = 400 nm).[26] Quantitative estimations of 4-hydroxyquinoline concentrations were made via a linear calibration curve, which was constructed from solutions of 4-hydroxyquinoline (0.047–1.5 µM) in potassium phosphate buffer. To each standard solution (500 µL), 4% DMSO as co-solvent, 400 µL NaOH (2 N) and 1000 µL distilled water was added. The initial rate of kynuramine oxidation was graphed versus the logarithm of the inhibitor concentration to yield sigmoidal dose–response curves. For each curve, at least 6 different inhibitor concentrations spanning at least 3 orders of magnitude were used. The IC_{50} values were determined by fitting the sigmoidal curves to the one site competition model incorporated into the Prism 5 software package (GraphPad). All experiments were carried out in triplicate and the IC_{50} values are expressed as mean ± standard deviation (SD).[19]

*IC_{50} measurements of **3a**–**j** and **5a**–**e***: The reactions contained kynuramine (45 μM and 30 μM for MAO-A and –B, respectively), various concentrations of the test inhibitor (0.003–100 μM), horseradish peroxidase (1 unit/mL) and Ampliflu Red (200 μM). Stock solutions of the test inhibitors were prepared in DMSO and added to the reactions to yield a final concentration of 4% (v/v) DMSO. The reactions were initiated with the addition of MAO-A or –B (0.0075 mg/mL), incubated at 37 °C for 20 min in a water bath and terminated with the addition of 10 μL (R)-deprenyl (5 mM) for MAO-B and 10 μL clorgyline (5 mM) for MAO-A. Distilled water (1400 μL) was added to each reaction and the concentrations of resorufin in the reactions were determined by fluorescence spectrophotometry (λ_{ex} = 560 nm, λ_{em} = 590 nm).[27] Quantitative estimations of resorufin were made by means of a linear calibration curve, which was constructed from solutions of H_2O_2 (0.05–1.6 μM). Each calibration standard was prepared to a final volume of 500 μL in potassium phosphate buffer and also contained horseradish peroxidase (1 unit/mL), Ampliflu Red (200 μM), 4% DMSO as co-solvent, 10 μL (R)-deprenyl (5 mM) for MAO-B and 10 μL clorgyline (5 mM) for MAO-A. Distilled water (1400 μL) was added to each standard. The IC_{50} values were determined as described above.

4.7. Time-dependence of inhibition

The time-dependencies of the inhibition of MAO-A and –B by selected inhibitors, compounds **3e** and **3c**, were examined. Recombinant human MAO-A and –B (0.03 mg/mL) were preincubated with compounds **3e** and **3c**, respectively for various periods of time (0, 15, 30, 60 min) at 37 ºC. Potassium phosphate buffer (100 mM, pH 7.4, made isotonic with KCl) served as reaction solvent and the concentrations of inhibitors **3e** (9.7 μM) and **3c** (0.3 μM) were approximately twofold the measured IC_{50} value for the inhibition of MAO-A and –B, respectively. The preincubated reactions were subsequently diluted twofold by the addition of kynuramine to yield final kynuramine concentrations of 45 μM and 30 μM for MAO-A and –B, respectively. After dilution, the final concentrations of the **3e** and **3c** were approximately equal to the IC_{50} values and the final MAO concentration was 0.015 mg/mL. The reactions, which were carried out in 2 mL microcentrifuge tubes to a volume of 500 μL, were incubated for a further 15 min at 37 °C and terminated with the addition of 400 μL NaOH (2 N). After the addition of 1000 μL distilled water, the rates of the MAO generated of 4-hydroxyquinoline were measured spectrophotometrically as described above. All measurements were carried out in triplicate and are expressed as mean ± SD.[34,35]

4.8. Lineweaver-Burk plots

Since the caffeine derivatives examined here exhibit selective MAO-B inhibition, the mode of MAO-B inhibition by a selected inhibitor, compound **3c**, was investigated. For this inhibitor,

a set consisting of 4 Lineweaver–Burk plots were constructed. One plot was constructed in the absence of inhibitor. To construct the remaining 3 plots, the concentrations selected for inhibitor **3c** were 0.0375–0.15 μM. Kynuramine at concentrations of 15–90 μM served as substrate and recombinant human MAO-B were used at a concentration of 0.015 mg/mL. The initial the rates of the MAO generated of 4-hydroxyquinoline were measured spectrophotometrically as described above. Linear regression analysis was performed using the Prism 5 software package.[34]

4.9. Molecular docking studies

Docking of selected inhibitors was accomplished with the Windows based Discovery Studio 3.1 software package (Accelrys Inc., San Diego, CA, USA)[29]. The crystallographic models of MAO-A (PDB code, 2Z5X)[30] and MAO-B (PDB code, 2V60)[31] were acquired from the Brookhaven Protein Data Bank. The pKa values and protonation states of the ionizable amino acids were calculated at pH 7.4 and hydrogen atoms were added accordingly to the models. When necessary, the valences of the FAD cofactors (oxidized state) and cocrystallized ligands were corrected and the enzyme models were typed with the Momany and Rone CHARMm forcefield. A fixed atom constraint was applied to the backbone of the enzyme models and the energies of the models were minimized using the Smart Minimizer protocol. For this purpose the maximum steps were set to 50000 and the implicit generalized Born solvation model with molecular volume was used. The cocrystallized ligands present in the active sites and the crystal water molecules were subsequently removed from the models and the binding sites were identified from the existing enzyme cavities. For the purpose of the docking procedure, the backbone constraint was also removed from the models. The following active site waters are considered conserved and were retained for the docking calculations: In the MAO-B active site, HOH 1159, 1166 and 1309 in the A-chain of 2V60;[31] In the MAO-A active site, HOH 710, 718 and 739 of 2Z5X. The structures of the selected inhibitors were constructed within Discovery Studio. Hydrogen atoms were added to the inhibitors and starting geometries of the structures were computed using a Dreiding-like forcefield (5000 iterations). Atom potential types and partial charges were assigned with the MMFF forcefield and the inhibitors were docked into the MAO models with the CDOCKER protocol. Allowance was made for the generation of 10 random ligand conformations, a heating target temperature of 700 K. The full potential was used for CDOCKER and in situ ligand minimization of the docking solutions was finally carried out using the Smart Minimizer algorithm. Unless otherwise specified, all the application modules within Discovery Studio were set to their default values. The illustrations were prepared with PyMOL.[36]

Acknowledgements

The NMR spectra were recorded by André Joubert of the SASOL Centre for Chemistry, North-West University while the MS spectra were recorded by Marelize Ferreira of the Mass Spectrometry Service, University of the Witwatersrand. This work was supported by grants from the National Research Foundation and the Medical Research Council, South Africa.

References

1. Youdim, M. B. H.; Bakhle, Y. S. *Br. J. Pharmacol*. **2006**, *147*, S287.
2. Edmondson, D. E.; Mattevi, A.; Binda, C.; Li, M.; Hubálek, F. *Curr. Med. Chem*. **2004**, *11*, 1983.
3. Binda, C.; Newton-Vinson, P.; Hubálek, F.; Edmondson, D. E.; Mattevi, A. *Nat. Struct. Biol.* **2002**, *9*, 22.
4. Youdim, M. B. H.; Edmondson, D.; Tipton, K. F. *Nat. Rev. Neurosci*. **2006**, *7*, 295.
5. Boulton, A. A. *Prog. Neuropsychopharmacol. Biol. Psychiatry*. **1991**, *15*, 139.
6. Lasbennes, F.; Sercombe, R.; Seylaz, J. J. *Cereb. Blood Flow. Metab*. **1983**, *3*, 521.
7. Da Prada, M.; Zürcher, G.; Würthrich, I.; Haefely, W. E. *J. Neural Tansm*. **1988**, *26* (suppl), 33.
8. Shih, J. C.; Chen, K.; Ridd, M. J.; *Annu. Rev. Neurosci*. **1999**, *22*, 197.
9. Zisook, S. E. *Psychosomatics*. **1985**, *26*, 240.
10. Birkmayer, W.; Riederer, P.; Ambrozi, L.; Youdim, M. B. *Lancet*, **1977**, *309*, 439.
11. Finberg, J. P.; Wang, J.; Bankiewich, K.; Harvey-White, J; Kopin, I. J.; Goldstein, D. S. *J. Neural Transm. Suppl*. **1998**, *52*, 279.
12. Collins, G. G. S.; Sandler, M.; Williams, E. D.; Youdim, M. B. H. *Nature*. **1970**, *225*, 817.
13. Kalaria, R. N.; Mitchell, M. J.; Harik, S. I. *Brain* **1988**, *111*, 1441.
14. Nicotra, A.; Pierucci, F.; Parvez, H.; Senatori, O. *Neurotoxicology*. **2004**, *25*, 155.
15. Fowler, J. S.; Volkow, N. D.; Wang, G. J.; Logan, J.; Pappas, N.; Shea, C.; MacGregor, R. *Neurobiol. Aging*. **1997**, *18*, 431.
16. Edmondson, D. E.; Binda, C.; Wang, J.; Upadhyay, A. K.; Mattevi, A. *Biochemistry*, **2009**, *48*, 4220.
17. Menazza, S.; Blaauw, B.; Tiepolo, T.; Toniolo, L.; Braghetta, P.; Spolaore, B.; Reggiani, C.; Di Lisa, F.; Bonaldo, P.; Canton, M. *Hum Mol Genet*. **2010**, *19*, 4207
18. Trouche, E.; Mias, C.; Seguelas, M. H.; Ordener, C.; Cussac, D.; Parini, A. *Stem Cells Dev*. **2010**, *19*, 1571.

19. Strydom, B.; Malan, S. F.; Castagnoli, N.; Bergh, J. J.; Petzer, J. P. *Bioorg. Med. Chem*. **2010**, *18*, 1018.
20. Booysen, H. P.; Moraal, C.; Terre'Blanche, G.; Petzer, A.; Bergh, J. J.; Petzer, J. P. *Bioorg Med Chem*. **2011**, *19*, 7507.
21. Di Monte, D. A.; DeLanney, L. E.; Irwin, I.; Royland, J. E.; Chan, P.; Jakowec, M. W.; Langston, J. W. *Brain. Res*. **1996**, *738*, 53.
22. Suzuki, F.; Shimada, J.; Shiozaki, S.; Ichikawa, S.; Ishii, A.; Nakamura, J.; Nonaka, H.; Kobayashi, H.; Fuse, E. *J. Med. Chem*. **1993**, *36*, 2508.
23. Blicke, F. F.; Godt, H. C. Jr. *J. Am. Chem. Soc*. **1954**, *76*, 2798.
24. Zhao, G.; Yu, T.; Wang, R.; Wang, X.; Jing, Y. *Bioorg. Med. Chem*. **2005**, *13*, 4056.
25. Wang, T.; Zhang, Y. -H; Kong, X. -W.; Lai, Y. -S.; Li, H.; Chen, Y, -P.; Peng, S. -X. *Chem. Biodivers*. **2009**, *6*, 466.
26. Novaroli, L.; Reist, M.; Favre, E.; Carotti, A.; Catto, M.; Carrupt, P. A. *Bioorg. Med. Chem*. **2005**, *13*, 6212.
27. Zhou, M.; Panchuk-Voloshina, N. *Anal. Biochem*. **1997**, *253*, 169.
28. Strydom, B.; Bergh, J. J.; Petzer, J. P. *Eur. J. Med. Chem*. **2011**, *46*, 3474.
29. http://accelrys.com/products/discovery-studio/
30. Son, S. –Y.; Ma, J.; Kondou, Y.; Yoshimura, M.; Yamashita, E.; Tsukihara, T. *Proc. Natl. Acad. Sci. U.S.A*. **2008**, *105*, 5739.
31. Binda, C.; Wang, J.; Pisani, L.; Caccia, C.; Carotti, A.; Salvati, P.; Edmondson, D. E.; Mattevi, A. *J. Med. Chem*. **2007**, *50*, 5848.
32. Legoabe, L. J.; Petzer, A.; Petzer, J. P. *Eur. J. Med. Chem*. **2012**, *49*, 343.
33. Novaroli, L.; Daina, A.; Favre, E.; Bravo, J.; Carotti, A.; Leonetti, F.; Catto, M.; Carrupt, P. A.; Reist, M. *J. Med. Chem*. **2006**, *49*, 6264.
34. Manley-King, C. I.; Bergh, J. J.; Petzer, J. P. *Bioorg. Med. Chem*. **2011**, *19*, 261.
35. Petzer, A.; Harvey, B. H.; Wegener, G.; Petzer, J. P. Toxicol. Appl. Pharm. **2012**, *258*, 403
36. DeLano, W. L. The PyMOL Molecular Graphics System. DeLano Scientific, San Carlos, USA, 2002.
37. Hayes, N. V.; Branch, G. E. K. *J. Am. Chem. Soc*. **1943**, *65*, 1555.
38. Newman, M.; Fones, W.; Renoll, M. *J. Am. Chem. Soc*. **1947**, *69*, 718.
39. Pasto, D. J.; McMillan, D.; Murphy, T. *J. Org. Chem*. **1965**, *30*, 2688.
40. Ahn, Y.; Cohen, T. *J. Org. Chem*. **1994**, *59*, 3142.
41. Degani, I.; Fochi, R.; Spunta, G. *Bollettino Scientifico della Facolta di Chimica Industriale di Bologna*, **1966**, *24*, 75.

ACKNOWLEDGEMENTS

- First of all I would like to thank my Lord and Saviour, Jesus Christ for sustaining me. I too, like Job can bodly say “For I know my Redeemer liveth”.
- I would also like to thank my family for all their support.
- Prof. Jacques Petzer, thank you for all your guidance and patience. I was priviledged to have you as a mentor. May the Lord bless you abundantly.
- To Prof. Bergh (co-supervisor), thank you for your assistance, it did not go unnoticed.
- A heartfelt thank you to André Joubert of the SASOL Centre for Chemistry, North-West University for the NMR spectra and Marelize Ferreira of the Mass Spectrometry Service, University of the Witwatersrand for the MS spectra.
- This work was supported by grants from the National Research Foundation.